1982

Diagonally pretensioned lattice frame.

Arunachalam. Mohan
University of Windsor

CANADIAN THESES ON MICROFICHE

I.S.B.N.

THESES CANADIENNES SUR MICROFICHE

National Library of Canada
Collections Development Branch

Canadian Theses on
Microfiche Service

Ottawa, Canada
K1A 0N4

Bibliothèque nationale du Canada
Direction du développement des collections

Service des thèses canadiennes
sur microfiche

NOTICE

The quality of this microfiche is heavily dependent upon the quality of the original thesis submitted for microfilming. Every effort has been made to ensure the highest quality of reproduction possible.

If pages are missing, contact the university which granted the degree.

Some pages may have indistinct print especially if the original pages were typed with a poor typewriter ribbon or if the university sent us a poor photocopy.

Previously copyrighted materials (journal articles, published tests, etc.) are not filmed.

Reproduction in full or in part of this film is governed by the Canadian Copyright Act, R.S.C. 1970, c. C-30. Please read the authorization forms which accompany this thesis.

AVIS

La qualité de cette microfiche dépend grandement de la qualité de la thèse soumise au microfilmage. Nous avons tout fait pour assurer une qualité supérieure de reproduction.

S'il manque des pages, veuillez communiquer avec l'université qui a conféré le grade.

La qualité d'impression de certaines pages peut laisser à désirer, surtout si les pages originales ont été dactylographiées à l'aide d'un ruban usé ou si l'université nous a fait parvenir une photocopie de mauvaise qualité.

Les documents qui font déjà l'objet d'un droit d'auteur (articles de revue, examens publiés, etc.) ne sont pas microfilmés.

La reproduction, même partielle, de ce microfilm est soumise à la Loi canadienne sur le droit d'auteur, SRC 1970, c. C-30. Veuillez prendre connaissance des formules d'autorisation qui accompagnent cette thèse.

THIS DISSERTATION
HAS BEEN MICROFILMED
EXACTLY AS RECEIVED

LA THÈSE A ÉTÉ
MICROFILMÉE TELLE QUE
NOUS L'AVONS REÇUE

NL-339 (r. 82/08)

Canada

DIAGONALLY PRETENSIONED LATTICE FRAME

by

© Arunachalam Mohan

A Thesis
submitted to the Faculty of Graduate Studies
through the Department of
Civil Engineering in Partial Fulfillment of the
requirements for the Degree of Master of
Applied Science at the University of Windsor

Windsor, Ontario, Canada

1981

Arunachalam Mohan 1981

DEDICATION

To My Mother

Sundarambal

ABSTRACT

DIAGONALLY PRETENSIONED LATTICE FRAME

by

Arunachalam Mohan

The buckling strength of a lattice frame could be increased several times by reinforcing the frame with pretensioned diagonal members. The magnitude of the initial pretension in the diagonals affects the critical load of the frame. This thesis deals with the stability analysis and the effect of initial pretension on the critical load of lattice frames. A geometric analysis has been done to derive the expression for calculating the minimum effective and the optimum pretensions. The stability analysis and the geometric analysis have been programmed in FORTRAN IV Language and have been run on an IBM/3031 Computer. A numerical example frame has been used to study the effect of various parameters like crossarm length, size and the modulus of elasticity of the diagonals on the critical load, the buckling modes and the efficiency of the frame. A rational design method is also suggested for the design of these lattice frames.

A plane lattice frame was used for the experimental study of its behaviour. The experimental buckling loads are compared with the theoretical loads. The experimental result confirms the buckling strength increase in the frame, when the diagonal members are pretensioned. Both the theoretical and the experimental results indicate the great influence of the initial pretension in the diagonals on the buckling load.

ACKNOWLEDGEMENTS

The author wishes to express his sincere gratitude to his advisor Dr. M.C. Temple, for his encouragement, assistance and valuable suggestions throughout the preparation of this thesis. The support of John S. Ellis is also gratefully acknowledged.

Thanks are due to:

the Computer Center at the University of Windsor for running computer programs;

the structural engineering staff members for their valuable advice;

the technicians of the Civil Engineering laboratory for their assistance in the preparation of the model.

TABLE OF CONTENTS

LIST OF ILLUSTRATIONS

LIST OF TABLES

LIST OF ABBREVIATIONS

English Letters

A = cross-sectional area

A_b = cross-sectional area of ring beam

A_c = cross-sectional area of vertical member

A_{ca} = cross-sectional area of crossarm

A_d = cross-sectional area of diagonal member

C = constant of proportionality in Eq. 3.15

E = modulus of elasticity

E_{ac} = modulus of elasticity of column material discussed in Section 5.3(2)

E_b = modulus of elasticity of ring beam material

E_{bc} = modulus of elasticity of column material discussed in Section 5.3(2)

E_c = modulus of elasticity of vertical member material

E_{ca} = modulus of elasticity of crossarm material

E_d = modulus of plasticity of diagonal member material

E_e = equivalent modulus of elasticity of diagonal member

F_f = final axial compressive force in crossarm

F_i = initial axial compressive force in crossarm

F_r = additional horizontal force in crossarm caused by a small lateral deflection

$\{F\}$ = load vector at the node

G_b = modulus of rigidity of ringbeam material

I = moment of inertia of cross-section

I_{ac} = cross-sectional moment of inertia of column discussed in Section 5.3(2)

I_b = cross-sectional moment of inertia of ringbeam

I_{bc} = cross-sectional moment of inertia of column discussed in Section 5.3(2)

I_c = cross-sectional moment of inertia of vertical member

I_{ca} = cross-sectional moment of inertia of crossarm

$[I_m]$ = unit matrix

k = effective length factor

k_a = effective length factor of columns discussed in Section 5.3

k_B = effective length factor of vertical member in a battened frame

k_b = effective length factor of columns discussed in Section 5.3

$k_{B,L}$ = effective length factor of vertical member in a battened or lattice frame

K_c = axial stiffness of vertical member

K_{ca} = axial stiffness of crossarm

K_d = axial stiffness of diagonal member

k_L = effective length factor of vertical member in lattice frame

$[K]$ = master stiffness matrix

$[K_E]$ = master elastic stiffness matrix

$[K_G]$ = master geometric stiffness matrix

$[K_G^*]$ = master geometric stiffness matrix for unit load

$[\overline{K}_E]$ = elastic stiffness matrix in local coordinate system

$[\overline{K}_G]$ = geometric stiffness matrix in local coordinate system

L = length

ℓ = length of vertical member

ℓ_{ad} = actual length of rods used in diagonal

ℓ_b = length of column discussed in Section 5.3(1)

ℓ_{ca} = length of crossarm

ℓ_d = length of diagonal

P = axial load in column

P_a = externally applied load on vertical member

P_{a4}, P_{b4}, P_{c4}
P_{d4}, P_{e4}, P_{f4} } = critical loads of columns discussed in Section 4.3.1

P_{a8}, P_{b8}, P_{c8}
P_{d8}, P_{e8}, P_{f8} } = critical loads of columns discussed in Eq. 8.1

P_{a9}, P_{b9}, P_{c9}
P_{d9}, P_{e9}, P_{f9} } = critical loads of columns discussed in Eq. 8.2

P_B = critical load of battened frame

$P_{B,L}$ = critical load of a battened or lattice frame

P_E = Euler load of a column having a length equal to the vertical member

P_f = final axial force in the vertical member

P_i = initial axial force in the vertical member

P_{in} = initial load when geometric stiffness matrix is calculated

P_L = critical load of lattice frame

$P_{L,max}$ = maximum critical load of lattice frame

P^* = relative magnitudes of applied loads taken as unity

P_{100} = critical load of basic frame shown in Fig. 4.9

R = restraining moment

R_b = mean radius of ring beam

R_r = rotational restraint at crossarm level

S_{comb} = combined axial stiffness of diagonal member

T_b = tensile force applied to ring beam

T_f = final tension in diagonal member

$T_{f\ell}$ = tension in shortened diagonal

T_{fr} = tension in elongated diagonal

T_i = initial pretension in diagonal

T_{max} = maximum possible pretension in diagonal

T_{min} = minimum effective pretension in diagonal

T_{opt} = optimum pretension in diagonal

T_1, T_2, T_3
T_4, T_5, T_6 } = tension in the corresponding diagonal member numbered as in Fig. 7.1

u_1 = displacement along x axis at node 1

u_2 = displacement along x axis at node 2

v_1 = displacement along y axis at node 1

v_2 = displacement along y axis at node 2

W = total weight of frame

W_{batt} = total weight of battened frame

W_{latt} = total weight of lattice frame

W_{100} = total weight of basic frame shown in Fig. 4.9

Greek Letters

α = angle between diagnonal member and vertical member

γ = $1/\lambda$.

Δ_c = shortening of vertical member due to external load

Δ_{ca} = elongation of crossarm due to applied load

Δ_{ci} = shortening of vertical member due to initial pretension

Δ_{d} = shortening of diagonal member

Δ_{di} = elongation of actual length of rod due to axial tension

Δ_{dt} = total elongation of diagonal member (addition of elongation of rod and deflection of ring beam)

$\Delta_{\ell ca}$ = axial shortening of crossarm due to initial pretension

Δ_{m} = deflection of frame at crossarm level (end panel)

Δ_{rb} = deflection of ring beam

$\{\Delta\}$ = vector of nodal displacements

θ = angle between crossarm and diagonal member

θ_a, θ_b = rotation of vertical member with respect to vertical line

θ_1 = rotation of member at node 1

θ_2 = rotation of member at node 2

λ = eigen value

σ = allowable fiber stress

ϕ = diameter of rod used for diagonal

CHAPTER 1

INTRODUCTION

1.1 General

A lattice frame is a frame consisting of various vertical, horizontal and diagonal members used to resist axial and transverse loads. The horizontal members are referred to as crossarms. A typical lattice frame and its components are shown in Fig. 1.1. Depending upon the number of segments, frames are classified under various names. For example a frame with two segments is referred to as a two segment frame and a frame with three segments as a three segment frame. In the similar manner other frames are classified, under various names, depending upon the number of segments. Two, three and four segment frames are shown in Figs. 1.1 and 1.2. The diagonal members resist the translational movement and the crossarms resist the rotation at the level of the crossarms. The connections between vertical and horizontal members are rigid, while the connections between the diagonal and vertical members are assumed to be hinged.

Some frames will not have any diagonals. They are referred to as battened frames. If the frames have pretensioned diagonals then, they are referred to as lattice frames. A restraint against lateral movement is created by the vertical members in the battened frame. An additional lateral restraint is also created by the horizontal components of diagonal tensile force in the lattice frame. Hence the total lateral restraint force in a lattice frame is greater than the lateral restraint force in a battened frame. When the diagonals are not pretensioned, the

diagonals will be effective only when large deflection occurs. These forces act as lateral restraints to postpone the buckling and this results in increasing the critical load of a lattice frame. (This is discussed in detail in the subsequent chapters). In this thesis diagonally pretensioned ideal lattice frames are referred to simply as lattice frames. The magnitude of the critical load of a battened frame is affected by various other parameters like crossarm length, cross-sectional area, etc. Introduction of pretensioned diagonals increases the overall weight of a battened frame and the critical load. If all the members are proportioned carefully, the maximum possible critical load may be achieved with the minimum material weight. (Other factors that influence the cost are neglected). These lattice frames will have a minimum profile area. Due to this factor the forces developed by wind and bomb blasts will have minimum effect on lattice frames. Lattice frames are suitable for masts for ships, offshore structures, antenna towers, etc.

In practice the three-dimensional frames are widely used. A three-dimensional frame is shown in Fig. 1.3. Discontinuous lines show the pretensioned diagonals on the back faces. Like other columns and frames the support conditions may be varied for lattice frames. A two-dimensional frame is preferred for the laboratory studies, since they are easy to build and to monitor while performing experiments. Two-dimensional frames are braced in one plane and hence they can buckle only in the plane perpendicular to the braced plane.

An accurate analysis which will predict the behaviour of the frame is necessary to design it efficiently. A through analysis on the behaviour of battened and lattice frames has been conducted in the subsequent chapters.

1.2 Previous Method of Study

A lattice frame behaves similar to a stayed column. Considerable research has been conducted on the analysis of both ideal and real stayed columns (Ref. 1-15). The following methods of solution were used in all of this research;

(1) The classical method of solving differential equations,

(2) The stability function method,

(3) Finite element method, and

(4) Substitute column method.

Among all the methods the finite element method is the most flexible and is also a non-iterative method. Thus the finite element method of solution is used in this study.

In most of the previous studies of stayed columns it was assumed that a very small amount of tension is left in the stays just prior to buckling. The maximum buckling load was determined without considering the initial pretension. All of these assumptions are also valid for diagonally tensioned frames. Hafez (5) has derived a linear relationship between the initial pretension and the critical load as shown in Fig. 1.4. The upper limit in Zone I is bounded by the Euler load while in Zone II it is the maximum critical load. No research has been performed to predict the relationship between initial pretension

and the critical load or to study the behaviour of lattice frames theoretically. Only an experimental investigation was carried out by Ellis (4) to find out the experimental buckling load of these frames. Thus it is necessary to review the method of solution applicable to stayed columns and to modify it to make it suitable for the lattice frames.

1.3 The System and Scope of Work

A theoretical analysis and an experimental investigation applicable to the frames are necessary. The frame under investigation is a two legged diagonally pretensioned ideal lattice frame (Referred to simply as a lattice frame). The purpose of this research is as follows:

(1) To establish a relationship between the initial pretension in the diagonals and the critical load.

(2) To study the change in behaviour of a lattice frame when various parameters such as crossarm length, size of members etc. are varied, and to compare it with a battened frame.

(3) To compare the theoretical solutions with experimental results, and

(4) To develop a rational method for the design of these lattice frames.

CHAPTER 2

REIVEW OF PREVIOUS RESEARCH

2.1 General

Considerable research has been conducted on the stayed columns with hinged and rigidly connected crossarms. Some of the researchers have verified their theoretical work by experiments and others have not. The previous research covers both ideal and real stayed columns. Research on the lattice frames started only recently. All the previous research work both on the stayed column and the frames has been outlined in this Chapter.

2.2 Stayed Column

In 1963 Chu and Berge (1) studied the behaviour of a slender pin-ended column stayed with tension ties arranged in equilateral rosettes around the column and bearing on several intermediate supports along the hogging frames. The columns and crossarms are joined with ideal hinges. The column is assumed to be an ideal column. It was proved that the maximum critical load would be a fourfold increase in the buckling strength over the Euler load. If there is no more tension remaining in the ties at the time of buckling the critical load will be reduced accordingly. Any increase in the number of symmetrically placed intermediate frames did not affect the strength increase. All the theoretical results were verified with experiments.

In 1967 Mauch and Felton (8) developed an analytical foundation for the rational design of stayed columns. The structural index (i.e. P/L^2) has been used, in which P is the applied axial load on the column and L is the length of the column. This index can be considered as a measure

of load intensity. Their analysis indicated that at low values of structural index columns supported by tension ties offer potential savings of up to 50% of the weight of optimum simple columns. At low values of structural index the optimum stress for simple tubular columns is well below the elastic limit of most structural materials.

In 1970 a design-build-test (3) project was performed by final year Civil Engineering undergraduates at the Royal Military College of Canada. The crossarms were rigidly connected to the column and not hinged as in Chu and Berg's study. The stays were pretensioned, so that just prior to buckling their tensile force goes to zero. They showed an increase in experimental buckling load of seven times the Euler load. No theoretical analysis was performed.

In 1971 Pearson (9) examined the behaviour of a pin-edged single-crossarm stayed column with a high slenderness ratio when loaded to its buckling point. In that study the variation in buckling strength of the column with the variation in stay slopes and pretension forces were examined experimentally. The results of the tests indicated that the buckling strength varies considerably with variations in crossarm length, stay slope and stay tension. No theoretical work was performed.

In 1972 Clarke (2) conducted an experimental study to verify Pearsons conclusions. The results showed that there was no simple relationship between the buckling load and the pretension or the slopes of the stays.

In the same year McCaffrey performed some experiments on the same stayed columns. The experiments indicated a strength increase between

34 to 45 times that of the Euler critical load.

In 1975 Smith, McCaffrey and Ellis (10) published a paper on the stayed column. An analytical solution was developed to predict the critical load of a pin-ended single-crossarm stayed column associated with two modes of buckling. Studies are also performed on influence of various parameters on the buckling load. A differential calculus approach was used in their work.

In 1976 Temple (12) developed an analytical solution to predict the critical loads and the corresponding buckling shape for single, double and triple crossarm stayed columns, by employing the stability function method and an eigen-value approach.

In the same year, Khosla (7) developed an analytical method using the finite element approach to determine both the buckling load of the column and the various buckled shapes. This method is an extremely simple and flexible method. This approach can be used for any type of stayed column with small modifications. No experimental work was performed.

In 1977 Hathout (6) extended the previous work of Temple and Khosla to study the buckling behaviour of a three-dimensional stayed column. He employed two methods to conduct the analytical study. They are the stability function approach and the finite element approach. The effect of different parameters on the buckling load of the stayed column were demonstrated. The studies were also conducted for various support conditions. Finally the efficiency of the column based on the weight per unit buckling load was calculated. The results indicated that a higher buckling load

doesn't necessarily mean higher efficiency of the column. Only theoretical studies were performed.

In the same year Hafez (5) derived the complete relationship between the minimum and optimum pretensions and the buckling load. He also studied the effect of various parameters like crossarm length and stay properties on buckling strength of the column. The same finite element approach developed by Khosla was used to get the theoretical buckling load. To justify the analytical results experiments were done on an ideal pin-ended single-crossarm stayed column. Experimental results showed good agreement with theoretical values.

Later in 1977 Williams and Howson (14) published a paper on concise buckling analysis of stayed columns. A substitute column approach was used. Only an analytical study was performed.

In 1980 Wong (15) conducted research on a real stayed column with some initial imperfections. The effect of initial imperfections on initial pretensions and buckling load was investigated. A computer program was developed with an incremental iterative approach to calculate the buckling load and the deflections of a real stayed column. Theoretical results showed good agreement with the experimental results.

2.3 Lattice Frames

In 1980 Ellis (4) published a paper on diagonally pretensioned lattice frames based on an experimental study. The experiments were conducted on two and three-dimensional frames. Diagonals were arranged in two forms, an intersecting and an offsetting arrangement. Experiments

showed an increase in buckling load of three to four times for intersecting diagonals and up to 5 times for offset diagonals, over a battened frame. Not much analytical work was performed.

CHAPTER 3

ANALYTICAL STUDY OF DIAGONALLY PRETENSIONED LATTICE FRAMES

3.1 General

As mentioned in the previous chapters, a lattice frame is a structure with rigid crossarms and pretensioned diagonals, subjected to any type of loading. In this thesis only vertical loads are being considered. The buckling load of a lattice frame is several times higher than the buckling load of a similar battened frame. The increase in buckling load depends upon various parameters like, material properties, initial pretension in the diagonals, geometry of the frame and end conditions. The frame under consideration is symmetrical about both the x and y axis.

Considering small displacements, an increase in the axial load of a lattice frame will reduce the tension in the diagonals, due to the axial shortening. At a certain load the tension in the diagonals goes to zero. Well below the critical load the tension in the diagonals provide lateral restraints at the crossarm levels. These lateral restraints increase the critical load. If the tension in the diagonals reaches a zero value, lateral restaints offered by the diagonals disappear. At the critical load the frame buckles either by the reduction in diagonal tension or by the buckling of vertical members as individual columns. At the critical load a state of unstable equilibrium is reached and the frame buckles. The frame buckles in one of two modes, Mode I or Mode II. The magnitudes of the translational and rotational restraints offered by

the diagonals and the crossarms respectively, decides the mode of failure. If the area of the diagonal member and the length of the crossarm are very small, the created rotational restraint will be large and the translational restraint will be small. Thus Mode I buckling occurs by a translational movement at the crossarm levels. On the other hand, if the area of the diagonal member and the length of the crossarm are quite large, the translational restraint becomes large and the rotational restraint will be small. It initiates Mode II buckling, by rotation of the vertical members at the crossarm levels. (The above two explanations are given in detail in Chapter 4). If the initial pretension is equal to the optimum pretension then the lateral restraint created by the horizontal component of the tensile force in the diagonals will remain effective until the maximum critical load of the lattice frame is reached. Thus to make the frame withstand the maximum critical load, it is necessary to have the initial diagonal pretension equal to the optimum pretension. If the initial pretension is greater than the optimum pretension, then the vertical component of the pretension force itself acts as a part of the axial load on the vertical members and reduces the external load carrying capacity of the frame. Thus it is necessary to know the minimum effective and the optimum pretension values. This chapter deals with some definitions and the relationship between the critical load and the initial pretensions.

3.2 Basic Assumptions

The following assumptions are made in this study:

(1) The lattice frame considered here is perfectly symmetrical and axially loaded in both legs.

(2) The lattice frame is an ideal frame (i.e. there is no initial imperfection or crookedness).

(3) The connections between the vertical and horizontal members are perfectly rigid, while the connections between the diagonals and the other members are assumed to be ideal hinges.

(4) Axial loads are applied equally on both vertical legs of the frame.

(5) Axial deformations in all the diagonals are equal.

(6) The critical load is identified by considering the neutral equilibrium and the magnitude of the load is calculated by the finite element method.

(7) The critical load is reached when the tension in the diagonals goes to zero for the lattice frames with initial pretension less than or equal to optimum pretension.

(8) The axial deformations of all the members have been neglected when computing the buckling load, but have been considered while studying the tension in the diagonals.

3.3 Definitions

The following are the definitions of some of the terms used in this chapter:

(1) Battened frame critical load: It is the critical load of a battened frame (i.e. The critical load of a frame without any diagonal member). It is similar to the Euler load of the core of a stayed column.

(2) Lattice frame critical load: It is the critical load of a lattice frame. (i.e. The critical load of a frame with pretensioned diagonals). It is similar to the critical load of a stayed column.

(3) Minimum effective pretension: It is the minimum initial pretension in the diagonals which remains effective until the load on the frame is equal to the critical load of a similar battened frame. If the initial pretension is equal to or less than the minimum effective pretension, then at a certain load well below or equal to the battened frame critical load, the diagonals become slack and the lattice frame will behave like a battened frame. Thus the critical load will be equal to the battened frame critical load.

(4) Optimum pretension: It is the initial pretension in the diagonals which disappears just after the load on the frame is equal to the maximum critical load of the lattice frame. All diagonals remain effective until this loading is reached.

(5) Maximum possible pretension: It is the initial pretension in the diagonals which gives vertical components large enough to cause buckling without any additional load on the frame.

(6) Residual tension: When the initial pretension in the diagonals is larger than the optimum pretension, the tension in the diagonals does not go to zero at the instant of buckling. The tension which remains in the diagonals during buckling is the residual tension. Since the initial pretension in practical situations is kept at a value equal to or less than the optimum pretension, the maximum possible pretension and residual pre-

tension are of no practical significance.

3.4 Geometric Analysis

A two-dimensional lattice frame can be supported either at both ends of each vertical leg or at one end of vertical legs. (see Figs. 4.7(a) and (c)). For the geometric analysis a frame hinged at both ends of each vertical leg is considered. When a lattice frame is loaded, axial shortening of the vertical and diagonal members occurs. Due to axial shortening the tension in the diagonal members decreases. As explained earlier, the lateral restraint created by the components of the tensile forces at the crossarm levels disappears at the time of buckling. If the initial pretension in the diagonals is equal to the minimum effective pretension, the tension in the diagonals disappears at the load equal to the battened frame critical load. Thus there will be no lateral restraint to prevent the buckling if the load is increased beyond the battened frame critical load. On the other hand, if the initial pretension is greater than the minimum effective pretension, the tension in the diagonals remains effective even when the load is greater than the battened frame critical load. Obviously the critical load of such a lattice frame will be greater than the battened frame critical load and will be equal to a load at which the diagonal tension reaches a zero value. Minimum effective and optimum pretensions are calculated from battened and lattice frame critical loads respectively as explained in the next section.

3.4.1 Relationship Between Initial Pretension and Buckling Load

Any lattice frame with more than one segment could be used to derive the relationship. It is assumed that all the segments deform

equally. Just for convenience an end panel was used for the derivation.

Fig. 3.1 shows the forces acting in the left half portion of a three segment lattice frame. Forces in an end and interior joints are shown separately in Fig. 3.2. Referring to Fig. 3.2 the relationship between axial force (P_i) caused by initial pretension (T_i) can be written as follows:

$$P_i = T_i \cos\alpha \qquad (3.1)$$

where α = the angle between the vertical and the diagonal members. Once the external load (P_a) is applied to the vertical member the total axial force (P_f) becomes:

$$P_f = P_a + T_f \cos\alpha \qquad (3.2)$$

where T_f = the tension in the diagonals after the application of the load.

Due to the axial force caused by the initial pretension, the vertical member shortens by an amount Δ_{ci} and which can be written as follows:

$$\Delta_{ci} = \frac{T_i \, \ell \cos\alpha}{A_c E_c} = \frac{T_i \cos\alpha}{K_c} \qquad (3.3)$$

where $K_c = \frac{A_c E_c}{\ell}$, the axial stiffness of the vertical member ; A_c = the cross-sectional area of the vertical member; E_c = the modulus of elasticity

of the vertical member; and ℓ = the length of one segment.

The crossarms are subjected to a compressive force (F_i) caused by the initial pretension in the diagonals. F_i causes an axial shortening of $\Delta\ell_{ca}$. F_i and $\Delta\ell_{ca}$ may be written as:

$$F_i = 2T_i \sin\alpha \tag{3.4}$$

$$\Delta\ell_{ca} = \frac{2T_i \ell_{ca} \sin\alpha}{A_{ca} \ell_{ca}} = \frac{2T_i \sin\alpha}{K_{ca}} \tag{3.5}$$

where $K_{ca} = \frac{A_{ca} E_{ca}}{\ell_{ca}}$, the axial stiffness of the crossarm; A_{ca} = the cross-sectional area of the crossarm; E_{ca} = the modulus of elasticity of the crossarm; and ℓ_{ca} = the length of the crossarm.

When the frame is subjected to an external load the tension in the diagonals will be reduced to T_f. Axial shortening of the diagonals causes this reduction in diagonal tension. The change in diagonal tension will cause the axial force in the crossarm to change to F_f. Assuming that α does not change, F_f could be calculated from:

$$F_f = 2T_f \sin\alpha \tag{3.6}$$

Due to the externally applied load (P_a) the vertical members will shorten by an amount Δ_c, which is:

$$\Delta_c = \frac{\ell (P_f - P_i)}{A_c E_c} = \frac{P_f - P_i}{K_c} \tag{3.7}$$

Substituting for P_f and P_i from Eqs. 3.1 and 3.2 in 3.7 Δ_c can be written as:

$$\Delta_c = \frac{P_a - (T_i - T_f)\cos\alpha}{K_c} \tag{3.8}$$

The change in tension in the diagonals will cause a change in axial force in the crossarm. So the crossarm will elongate by an amount Δ_{ca} which can be determined by:

$$\Delta_{ca} = \frac{(F_i - F_f)\ell_{ca}}{A_{ca} E_{ca}} = \frac{(F_i - F_f)}{K_{ca}} \tag{3.9}$$

Substituting for F_i and F_f from Eqs. 3.4 and 3.6 into Eq. 3.9, Δ_{ca} can be written as:

$$\Delta_{ca} = \frac{2(T_i - T_f)\sin\alpha}{K_{ca}} \tag{3.10}$$

The reduction in tension in the diagonals will cause a reduction in the length of the diagonals by an amount Δ_d. Δ_d is:

$$\Delta_d = \frac{(T_i - T_f)}{A_d E_d}\ell_d = \frac{T_i - T_f}{K_d} \tag{3.11}$$

where $K_d = \frac{A_d E_d}{\ell_d}$, the axial stiffness of the diagonal; A_d = the cross-sectional area of the diagonal; E_d = the modulus of elasticity of the diagonal; and ℓ_d = the length of the diagonal.

After the application of the external load (P_a), the change in the length of the diagonal can be written in terms of the change in length of the vertical member and the crossarm. (Assuming deformations are very small). Referring to Fig. 3.3 (just for convenience it is shown in the figure that the support moves relative to the crossarm level in the vertical direction) Δ_d can be written as:

$$\Delta_d = \Delta_c \cos\alpha - \frac{\Delta_{ca}}{2} \sin\alpha \quad * \qquad (3.12)$$

As the ends of the crossarms are partially prevented from elongation by the vertical legs, the real axial deformation in the crossarms will be slightly smaller than Δ_{ca} used in Eq. 3.12. But the magnitude of change in crossarm length itself is very small. Thus the difference between the actual change in crossarm length and Δ_{ca} used in Eq. 3.12 is neglected. Thus the approximate Δ_{ca} value is used in equation 3.12. Substituting the values of Δ_d, Δ_c, Δ_{ca} from Eqs. 3.8, 3.10 and 3.11 into Eq. 3.12 yields:

$$\frac{T_i - T_f}{K_d} = \frac{[P_a - (T_i - T_f)\cos\alpha]}{K_c} \cos\alpha - \frac{(T_i - T_f)}{K_{ca}} \sin^2\alpha \qquad (3.13)$$

---

* If the intermediate panel is selected to derive the Eq. 3.12, Δ_d can be written as follows:

$$\Delta_d = \Delta_c \cos\alpha - \Delta_{ca} \sin\alpha \qquad (3.12)^{**}$$

since the axial stiffness of crossarm (K_{ca}) is very high compared to the axial stiffness of diagonal member (K_d), the difference in eqs. (3.12) and (3.12)** will be very small. Hence it is reasonable to have Eq. 3.12 as the expression even for other panels.

By rearranging the terms in Eq. 3.13, the change in diagonal tension may be expressed as follows:

$$T_i - T_f = \frac{P_a \cos\alpha}{K_c\left[\frac{1}{K_d} + \frac{\sin^2\alpha}{K_{ca}} + \frac{\cos^2\alpha}{K_c}\right]} \tag{3.14}$$

or

$$T_i - T_f = P_a C \tag{3.15}$$

where

$$C = \frac{\cos\alpha}{K_c\left[\frac{1}{K_d} + \frac{\sin^2\alpha}{K_{ca}} + \frac{\cos^2\alpha}{K_c}\right]}$$

Eq. 3.15 shows that the relationship between the external load and the tension in the diagonals is linear.

The minimum effective and optimum pretensions are calculated as follows. At the critical load the final tension (T_f) in the diagonals should disappear. Thus substituting $T_f = 0$, Eq. 3.15 can be written as follows:

$$T_i = P_a C \tag{3.16}$$

Substituting $T_i = T_{min}$ or T_{opt} and the corresponding critical load Eq. 3.16 can be written as follows:

$$T_{min} = 1/2\ P_B\ C \tag{3.17}$$

$$T_{opt} = 1/2\ P_{L,\ max}\ C \tag{3.18}$$

where P_B = the battened frame critical load; and $P_{L,max}$ = the maximum critical load of the lattice frame. P_B and $P_{L,max}$ are calculated using the computer program explained in Chapter 4. All the above equations are valid for battened and lattice frames with any number of segments. (greater than one)

Fig. 1.4 illustrates the relationship between the buckling load and the diagonal pretension. Zone I is the region where the initial pretension is less than or equal to the minimum effective pretension. Zone II is the region where the initial pretension is between the minimum effective and optimum pretensions. Zone III is the region where the initial pretension is greater than the optimum pretension. Zone II is the only zone of practical importance.

CHAPTER 4

EFFECT OF VARIOUS PARAMETERS ON A DIAGONALLY PRETENSIONED LATTICE FRAME

4.1 General

As explained in the previous chapters it is necessary to make a through investigation of the various parameters that affect the behaviour of a structure. The buckling load of a lattice frame is greatly affected by the length of the crossarms, size and the modulus of elasticity of the diagnals. An improper proportioning of the members may result in an increase of the total weight of the frame which may be directly proportional to the cost. Sometimes a lattice frame can carry only a slightly higher load than a battened frame. In order to have that slight increase in the load, it may be necessary to increase the material weight of the lattice frame considerably. If the material required per unit buckling load of the lattice frame is higher than the material required per unit buckling load of the battened frame, the lattice frame will be uneconomical to build. (All the other factors that influence the cost of the frame are neglected). Hence, an analysis of the frames has been done to aid an efficient and minimum weight design. This chapter deals with the principle of the battened and the lattice frames, and the effect of the following parameters on the critical loads and the efficiencies;

(1) The support conditions (hinged, fixed or free)

(2) The length of the crossarm (ℓ_{ca})

(3) The size of the diagonals (ϕ)

(4) The modulus of elasticity of the diagonals (E_d)

(5) The initial pretension in the diagonals (T_i)

4.2 Basis for Comparison

The load carrying capacity of a simple Euler column is directly proportional to its moment of inertia and inversely proportional to the square of the effective length, while the modulus of elasticity is kept constant. When crossarms and stays are added to the Euler column it becomes a stayed column and the buckling strength increases. The strength of a stayed column can be compared to the strength of the Euler column to determine the increase in buckling strength of the stayed column. The strength of the Euler column is independent of all the parameters of a stayed column, except the effective length and the moment of inertia (modulus of elasticity is assumed to be constant). For example, any change in the crossarm length will not have any effect on the strength of the Euler column. When the load carrying capacity is considered, the buckling strength of a lattice frame can be compared to the strength of a similar battened frame. Unlike the Euler column, the buckling strength of a battened frame will not remain the same with a change in the crossarm length. Thus the buckling strength of a lattice frame should be compared to the strength of a battened frame, which has the same crossarm length as the lattice frame. (Cross-sectional and material properties, and the segment length should also be the same). Whenever the term 'a battened frame similar to the lattice frame' is used in this report, it means that the segment length, crossarm length, cross-sectional properties of the crossarms and verticals, and the support conditions for both the lattice and battened frames are identical.

4.3 Principle of Tensioned Stuctures

4.3.1 Stayed Column

An ideal pin-ended axially loaded column is shown in Fig. 4.1 (a). The column fails by Mode I buckling. When a lateral restraint is introduced at mid-height of the column it buckles by Mode II shape. (Fig. 4.1 (b)). If two lateral restaints are introduced to the column, then it buckles by Mode III shape (Fig. 4.1(c)). The translational movement is completely arrested (at the nodes) for the columns shown in Figs. 4.1 (b) and (c). When the cross-sectional and material properties are the same for the three columns discussed above, the following expression is valid.

$$P_{a4} < P_{b4} < P_{c4} \qquad (4.1)$$

where P_{a4}, P_{b4} and P_{c4} = the critical loads of the columns shown in Figs. 4.1 (a), (b) and (c) respectively. Thus it can be concluded that the load carrying capacity of a column may be increased by introducing restraint at intermediate points along the column. (Assuming the stress in the core of the column remains within the elastic limit.)

A column which has a partial lateral restraint at mid-height buckles as shown in Fig. 4.1 (d). Fig. 4.1 (e) shows the buckling shape of a column restrained completely in the lateral direction and restrained partially from rotation, at mid-height. If both the lateral and the rotational restraints appliedto the column are partial, it buckles as shown in Fig. 4.1 (f). The following expression is valid, when all the columns have the same cross-

sectional, material properties and length.

$$P_{a4} < P_{d4} < P_{f4} < P_{e4} \tag{4.2}$$

where P_{a4}, P_{d4}, P_{e4} and P_{f4} = the critical loads of the columns shown in Figs. 4.1 (a), (d), (e) and (f) respectively.

When a stayed column fails by Mode I buckling, it is similar to the buckling shape shown in Fig. 4.1 (f) and when the Mode II buckling occurs with the stayed columns it is similar to the buckling shape shown in Fig. 4.1 (e). A stayed column and its buckling shapes are shown in Fig. 4.2. The stays and the crossarms are responsible for the translational and the rotational restraints. The magnitude of the lateral and the rotational restraints depends upon the cross-sectional properties of the stay and the length of the crossarm. A stayed column can buckle in one of the two modes as shown in Figs. 4.2 (b) and (c) (only the right half of the stayed column is shown). If the translational restraint is smaller than the translational restraint required to maintain Mode II buckling, the buckling occurs by a translational displacement at the crossarm level (Mode I buckling). When the translational restraint required to maintain the Mode II buckling is smaller than the translational restraint present in the frame (or the rotational restraint is smaller than the rotational restraint required to maintain the Mode I buckling), buckling occurs by rotation of column at crossarm level (Mode II buckling).

Any type of structure subjected to a vertical load will have a number of possible modes. Of all these modes, the one corresponds

to the minimum load governs the buckling of that structure. The same explanation is also valid to any type of stayed column. Fig. 4.3 illustrates the plot of critical (or buckling) load versus a stayed column parameter. For example (Refer to Fig. 4.3) if the length of the crossarm and the critical load of a stayed column are chosen in the horizontal and vertical axes respectively, depending upon the individual magnitude of the translational and the rotational restraints, the respective curve (Mode I or Mode II curves) will govern the buckling failure. At one point the Mode I and the Mode II curves intersect. At the point of intersection the buckling changes from Mode I to Mode II.

4.3.2 Frames

4.3.2.1 Battened Frames

A battened frame subjected to vertical loading is shown in Fig. 4.4 (a). The frame fails by Mode I buckling as shown in Fig. 4.4 (b). The principle of the behavior of the frame can be explained by considering a real battened frame. As the load on the real battened frame increases, the lateral deflection also increases. The deflection causes a bending in the crossarms. Thus the crossarms provide restraints against rotation. If the crossarm is quite long, the rotational restraint offered will be small and vice versa. The lateral restraint created by the vertical members will be relatively small. Hence the only possible failure mode is Mode I buckling. The same argument is valid also for an ideal battened frame (lateral deflection will not occur prior to buckling). An equivalent system with moment springs is shown in Fig. 4.4 (c).

4.3.2.2 Lattice Frames

A diagonally pretensioned lattice frame and its modes of buckling are shown in Fig. 4.5. The pretensioned diagonals resist the lateral movement and the crossarms resist the rotation at the joints. Like a stayed column, if the translational restraint present in the frame is smaller than the translational restraint required to maintain Mode II buckling, the frame fails by Mode I buckling (see Fig. 4.5 (b)) and if the rotational restraint present in the frame is smaller than the rotational restraint required to maintain Mode I buckling, the frame fails by Mode II buckling (see Fig. 4.5 (c)). A large translational restraint can be created by a large diameter (ϕ) or a high modulus of elasticity (E_d) of the diagonal or a long crossarm. A large rotational restraint can be created by a short crossarm length or a large moment of inertia or a high modulus of elasticity of the crossarm. If the frame is in the Mode II buckling zone, any further increase in the translational restraint will not increase the critical load. Because the translational restraint already present in the frame is sufficient to maintain Mode II buckling. Hence to increase the critical load of a frame, which is in the Mode II buckling zone, it is necessary to increase the rotational restraint. When the frame is in the Mode I buckling zone any further increase in the translational restraint will be helpful in increasing the critical load. At the same time an increase in the rotational restraint either may or may not increase the critical load. For example, a battened frame which does not have any considerable translational restraint usually buckles by Mode I buckling. When the crossarm length is large,

there will be some rotation and lateral displacement of the vertical member at the crossarm level. Any reduction in the crossarm length will increase the rotational restraint and will reduce the rotation of the vertical member at the crossarm level. If this rotation is completely prevented by the crossarm, then any further increase in the rotational restraint at the crossarm level will not be useful in increasing the critical load. Until this stage is reached any increase in the rotational restraint will increase the critical load irrespective of the buckling modes. An equivalent system to the lattice frame is shown in Fig. 4.5 (d).

Two types of diagonal arrangements are possible with the lattice frames. They are the intersecting and the offset arrangements. Both types of diagonal arrangements are shown in Fig. 4.6. Among the offset arrangement two types are possible. They are the offset along the crossarm and the offset along the verticals. (Figs. 4.6 (b) and (c) respectively). The intersecting diagonals will not create any rotational restraint at the crossarm level as they are capable of creating only translational restraint. The offset diagonals are capable of creating both rotational and translational restraints at the crossarm level. An equivalent system to a lattice frame with offset diagonals is shown in Fig. 4.6 (d). Ellis (4) has experimentally demonstrated that the buckling load of a lattice frame with offset diagonals is greater than the lattice frame buckling load with intersecting diagonals. The investigation in this report however is limited only to the intersecting arrangement.

4.4 Effect of End Support Condition

The buckling strength and the mode of failure of a column is greatly influenced by the end support conditions (hinged, fixed, etc.). Depending upon the supports the effective length factor (k) will vary. Different types of end support conditions also will vary the buckling strength and the modes of failure of a lattice frame. The effect of various end support conditions on the behavior of a lattice frame is discussed in this section.

(1) Frame with four hinged supports:

A lattice frame with four hinged supports is free to rotate at the ends. If the translational restraint at the crossarm level is relatively small, the frame will exhibit a failure shape referred to as Mode I failure (see Fig. 4.5 (b)). When the translational restraint at the crossarm level is large, the frame will fail by Mode II buckling (see Fig. 4.5 (c)). The rotation of the vertical member at the crossarm level depends upon the magnitude of the rotational restraint at the crossarm level.

(2) Frame with four rigid supports:

No rotation or displacement is allowed at the ends, if the frame has four rigid supports. Lattice frames with rigid supports will have the highest buckling strength. Two modes of buckling are possible with these frames. They are Mode III (see Fig. 4.7 (a)) and Mode IV (see Fig. 4.7 (b)).

(3) Frame with rigid bottom supports and a free top edge:

A lattice frame with rigid bottom supports and a free top edge is called a cantilever frame. No rotational or translational movement is

allowed at the bottom supports, while both types of movements are allowed at the top supports. Two failure modes are possible with these end supports. Mode V failure (see Fig. 4.7 (c)) is initiated by a relatively small translational restraint and Mode VI failure (see Fig. 4.7 (d)) is initiated by a relatively large translational restraint. For Mode VI failure no lateral displacement occurs at the top edge even though this movement is not restrainted.

(4) Frame with hinged-bottom supports and a free top edge:

A lattice frame with a free top edge and hinged bottom supports has two possible modes of failure. They are Mode VII (Fig. 4.7 (e)) and Mode VIII (Fig. 4.7 (f)). Rotations and lateral displacements are allowed at the top edge, while only rotation is allowed at the bottom supports. When Mode VIII failure occurs there is no lateral displacement at the top edge even though there is no support at that location.

(5) Frame with rigid bottom supports and hinged top supports:

A lattice frame with rigid bottom supports and hinged top supports also has two modes of failure. They are Mode IX (see Fig. 4.7 (g)) and Mode X (see Fig. 4.7 (h)). At the bottom supports no rotation or lateral movement is allowed and at the top supports only rotation is allowed.

Although different types of end support conditions are possible with lattice frames, for simplicity a frame with four hinged supports will be considered in this study.

4.5 Effect of Crossarm Length

The buckling strength of a frame and the modes of buckling are

greatly influenced by the crossarm length. For battened frames, rotational restraint is influenced by the crossarm length and for lattice frames, both lateral and the rotational restraints are influenced by the crossarm length (Refer Eqs. 4.7 and 4.8). Some researchers have used columns with hinged crossarms (1). In this study crossarms with rigid end connections are used because they are more rigid than the crossarms with hinged ends. The influence of the crossarm length of spaced stayed columns on the translational and the rotational restraints were studied mathematically by Hathout (6). The mathematical expressions used in that study can easily be modified for the lattice frames.

Referring to Fig. 4.8 the change in the diagonal length (Δ_d) due to a deflection Δ_m (although no lateral deflection occurs with an ideal lattice frame prior to the buckling, a small deflection is introduced to demonstrate the magnitude of the lateral restraint force) introduced at the crossarm level can be written as follows:

$$\Delta_d = \Delta_m \cos\theta \qquad (4.3)$$

where θ = angle between the diagonal and the crossarm. The deflection causes an extension of the stay which results in an additional force in the stay. The extra stay force results in an additional horizontal force at the level of the crossarm (F_r). The additional force can be calculated as follows (assuming the change in θ is negligible).

$$F_r = 2(T_{fr}-T_{f\ell})\cos\theta$$

$$= 2[(T_{fr}-T_i) + (T_i-T_{f\ell})]\cos\theta$$

since $(T_{fr}-T_i)$ and $(T_i-T_{f\ell})$ are the change in the diagonal tension and $(T_{fr}-T_i)$, $(T_i-T_{f\ell}) = \Delta_d K_d$, F_r can be written as:

$$F_r = 4\Delta_d K_d \cos\theta \tag{4.4}$$

where T_{fr} = tension in the elongated diagonal; $T_{f\ell}$ = tension in the shortened diagonal; T_i = initial pretension in the diagonals; and $K_d = \frac{A_d E_d}{\ell_d}$, axial stiffness of the diagonal. Substitution of Eq. 4.3 in Eq. 4.4 yields:

$$F_r = 4\Delta_m K_d \cos^2\theta$$

and

$$F_r = 4\Delta_m \frac{A_d E_d}{\ell_d} \cos^2\theta \tag{4.5}$$

If the modulus of elasticity and the cross-sectional area are constants, Eq. 4.5 becomes;

$$\frac{F_r}{\Delta_m} \propto \frac{\cos^2\theta}{\ell_d} \tag{4.6}$$

Substitution of $\cos\theta$ in terms of the member lengths in Eq. 4.6 yields;

$$\frac{F_r}{\Delta_m} \propto \frac{\ell_{ca}^2}{\ell_d^3} \propto \frac{\ell_{ca}^2}{(\ell^2+\ell_{ca}^2)^{3/2}} \tag{4.7}$$

where ℓ = the length of the segment. From Eq. 4.7 it is clear that for a constant value of deflection (Δ_m), an increase in the crossarm length (ℓ_{ca}) will cause an increase in the lateral restraint force (F_r). When the lateral restraint force is very large, there will not be any lateral movement at the crossarm level and the buckling occurs by the rotation of the vertical members at the crossarm level (called Mode II buckling).

The bending stiffness ($\frac{E_{ca} I_{ca}}{\ell_{ca}}$) of the crossarm has to be considered to examine the variation in the rotational restraint. The rotational restraint (R_r) at the crossarm level can be expressed as follows:

$$R_r \propto \frac{E_{ca} I_{ca}}{\ell_{ca}} \tag{4.8}$$

when the modulus of elasticity (E_{ca}) and the moment of inertia (I_{ca}) of the crossarm remains constant, an increase in the crossarm length will decrease the magnitude of the rotational restraint. If the length of the crossarm is very small, the rotational restraint created by the crossarm will be very large and the buckling of the frame will occur by the translational displacement of the frame at the crossarm level (called Mode I buckling). Later in this chapter a frame will be used in an example to explain this effect.

4.6 Effect of the Diagonal Size

In a lattice frame, the ends of the diagonal members are hinged to the joints. The size of the diagonal member (ϕ) will affect the buckling strength and the modes of buckling, because it is directly related to the lateral restraint of the frame at the crossarm level. Assuming that the

modulus of elasticity, length of the crossarm, the angle (θ) and the deflection (Δ_m) remain constant, Eq. 4.5 can be written as:

$$F_r \propto A_d \propto \phi^2 \tag{4.9}$$

From the above equation it is clear that an increase in the size of the diagonal, will increase the lateral restraint force at the crossarm level. When the size is large Mode II buckling will possibly occur. This parameter (ϕ) has no effect on the ideal stayed column prior to buckling, as there is no deflection prior to buckling. A numerical example will be used to demonstrate this effect in the later portion of this chapter.

4.7 Effect of the Modulus of Elasticity of the Diagonals

The variation in the modulus of elasticity of the diagonals will affect the buckling strength and the modes of buckling of a lattice frame. Eq. 4.5 can be written as follows if the size of the diagonal, length of the crossarm, the angle θ and the deflection (Δ_m) are taken as constants.

$$F_r \propto E_d \tag{4.10}$$

The increase in the modulus of elasticity will have an effect similar to the increase in the size of the diagonals, on the lateral restraint force. When the modulus of elasticity of the diagonal is large, the frame is likely to fail by Mode II buckling. This parameter has no effect on an ideal lattice frame prior to buckling because no deflection occurs before the buckling. An

example frame will be used to explain this effect in the later portion of this chapter.

4.8 Effect of Various Parameters on Efficiency

The previous sections of this chapter have demonstrated the influence of the crossarm length, the size and the modulus of elasticity of the diagonals, on the buckling strength of an ideal lattice frame. These explanations, however, do not give any insight into the strength of the lattice frame relative to its total weight.(In this study it is assumed that the weight is the major factor which influences the cost. Other factors, which affect the cost are neglected). To accomplish this, the term efficiency is introduced. The efficiency of a structure is defined as the magnitude of the critical or the buckling load resisted by a unit weight of the material. The total weight of a lattice frame includes the weight of the vertical members, crossarms and the diagonals. Any additional weight contributed to the connections has been neglected. An increase in the buckling or the critical load does not necessarily mean an increase in the efficiency of a frame. Efficiency will be useful in proportioning a frame (selection of suitable crossarm length, size of the members, modulus of elasticity, etc.) in such a manner to use the minimum possible weight of material. This section deals with the various factors that affect the efficiency of a lattice frame.

(1) The Crossarm Length:

An increase in the crossarm length will increase the translational restraint at the crossarm level and at the same time the overall weight of

the material will also increase. Similarly a reduction in the crossarm length will cause an increase in the rotational restraint at the crossarm level and a reduction to the overall weight of the material of the lattice frame. The magnitudes of the restraints (translational and rotational) determines the magnitude of the critical load of a lattice frame. The combined effect of the buckling load and the overall weight of the frame decides the magnitude of the efficiency. When the crossarm length is large the buckling load will be small and the total weight of the lattice frame will be large. Thus the combined effect will result in a small efficiency. As the crossarm length is reduced the overall weight of the lattice frame also will be reduced. As the length of the crossarm is reduced, one of the three things will happen to the critical load, as follows: (1) A reduction in the critical load, (2) No change in the critical load or (3) An increase in the critical load. When a reduction in critical load occurs, depending upon the rate of reduction in the critical load and the rate of reduction in the total weight of the frame, an increase or decrease in the efficiency will occur. When the critical load remains constant with a reduction in the crossarm length, the combined effect of the constant critical load and the reduced overall weight will result in an increase in the efficiency. If the critical load increases with a reduction in the crossarm length, the combined effect of the increased load and the reduced overall weight of the frame will cause an increase in the efficiency.

(2) The Size of the Diagonal:

An increase in the size of the diagonals (ϕ) will increase the

overall weight of the frame. It will cause either an increase or no change in the critical load of a lattice frame. Depending upon the rate of increase in the weight and the rate of increase in the critical load, the increase or the decrease in the efficiency will occur. As the size of the diagonal is increased the combined effect of the increased overall weight and the constant critical load will reduce the efficiency of the frame.

(3) The Modulus of Elasticity of the Diagonal:

The increase in the modulus of elasticity of the diagonals will not have any effect on the overall weight of the frame. The increased modulus of elasticity either will increase the critical load or will not cause any change in the critical load. Thus the combined effect will either increase or will not cause any change in the efficiencies.

(4) The End Support Conditions:

Any change in the end support conditions will not have any impact on the weight of the frame and the critical load will either be increased or decreased. Thus an increase and a decrease in the critical load will decide the increase and the decrease of the efficiency respectively.

All the above discussed parameters, except the end support conditions, are explained with a numerical example in the following sections of this chapter.

4.9 Calculation of the Efficiency of a Lattice Frame

It is always convenient to have a basic structure which is assumed to be hundred percent efficient. The efficiencies of all the other structures

can be calculated with respect to that basic structure in terms of the percentages. The efficiencies calculated on this basis will be easier for comparison. The efficiency of the basic structure should be independent of the various parameters (like change in crossarm length, size of the diagonals, etc.). It is reasonable to have a Euler column as the basic structure for a stayed column analysis, because the critical load of the Euler column is independent of the crossarm length, size and the modulus of elasticity of the diagonals. Hence the efficiency of the Euler column is also constant. (Assuming that there is no change in the cross-sectional properties of the core of the column). In a similar manner, the lattice frame analysis also requires a basic structure. A battened frame similar to a lattice frame (see Section 4.2 for the explanation of the term 'battened frame similar to the lattice frame') will not be convenient to be considered as a basic structure for the efficiency calculations since the efficiency of a battened frame is a dependent variable of the crossarm length. Thus a structure as shown in Fig. 4.9 is assumed to be a basic structure (for calculation) for a two-dimensional three-segment lattice frame efficiency calculation. The structure showed in Fig. 4.9 is indpendent of the crossarm length, size and the modulus of elasticity of the diagonals. The sectional area of the leg is equal to the sectional area of the vertical member in the lattice frame.

The following expression is used to calculate the efficiency of the frame.

$$\% \text{ Efficiency} = \left[\frac{W_{100} \times P_{B,L}}{P_{100} \times W}\right] \times 100\% \qquad (4.11)$$

where P_{100} = the critical load of the basic frame; W_{100} = the total weight of the basic frame; $P_{B,L}$ = the critical load of the frame under consideration; and W = the total weight of the frame under consideration. Eq. 4.11 is included in the computer program discussed in the following chapter and using that program the efficiency is calculated.

4.10 Numerical Example

In this section a two-dimensional three-segment ideal pin-ended lattice frame is used to explain the effect of varying the parameters (like crossarm length, size of the diagonal, etc.) on the buckling load, minimum effective and optimum pretensions and the modes of buckling. The height of the frame is 72 in., consisting of three segments 24 in. each. The vertical members and the crossarms are of 1.0 in. diameter (solid circular sections). The diagonal sizes (ϕ) are varied between 0.1875 in. and 0.875 in. diameter rods. The modulus of elasticity of the vertical members and the crossarms are of 29600 ksi and the values of the modulus of elasticity of the diagonals (E_d) are varied from 9400 ksi to 29600 ksi. The ratio of the segment length to the crossarm length (ℓ/ℓ_{ca}) is varied from 1 to 10. The ends of the crossarms are rigidly connected to the joints and the ends of the diagonals are assumed to be ideal hinges. Throughout the discussion it is assumed that the stresses in the members remain elastic at the instant of buckling.

4.10.1 Effect of the Crossarm Length

The variation of the critical load and the initial pretensions (minimum effective and optimum pretensions) with the variation in the

crossarm length (represented in terms of the ratio ℓ to ℓ_{ca}) is illustrated in Figs. 4.10 to 4.25. These figures reveal that the critical load of a battened frame changes with the change in the ratio of ℓ to ℓ_{ca}. This is due to the fact that a change in the crossarm length will change the rotational restraint applied at the crossarm level. When the crossarm length is large, even a small change in the ℓ to ℓ_{ca} ratio can change considerably the critical load of the battened frame and at the small crossarm lengths, even a large change in the ℓ to ℓ_{ca} ratio does not make any significant change in the critical load. These figures also reveal that the initial pretensions vary with the variation in the corresponding critical loads. For example, the minimum effective pretension increases with an increase in the battened frame critical load and the optimum pretension increases or decreases, depending upon the increase or the decrease in the maximum critical load of the lattice frame. The initial pretensions are the functions of the critical loads and the constant C (Refer to Eqs. 3.15 to 3.18). The term C does not change greatly with a change in the crossarm length at large ratios of ℓ to ℓ_{ca}. At small ratios of ℓ to ℓ_{ca} the term C decreases gradually with an increase in the crossarm length. The slope of the minimum effective pretension curve remains almost equal to the battened frame critical load curve at large ratios of ℓ to ℓ_{ca}, and the slopes are not equal at small ratios of ℓ to ℓ_{ca}. This is due to the fact that the product of the critical load and the term C controls the value of initial pretensions. Battened frames always fail by Mode I buckling because those frames don't have enough lateral restraint to initiate Mode II buckling.

Fig. 4.10 illustrates the plot of critical load and the initial pretensions versus the ratio of ℓ to ℓ_{ca} with a small size of the diagonal (0.1875 in.) and a modulus of elasticity equal to 29600 ksi. The maximum critical load of the lattice frame increases with the increase in the ratios of ℓ to ℓ_{ca} and reaches a maximum value at the ratio of ℓ to ℓ_{ca} equal to four. After that the maximum critical load decreases with an increase in the ratio of ℓ to ℓ_{ca}. In the increasing portion of the critical load curve the failure is governed by the Mode II buckling and in the decreasing portion of the critical load curve the failure is governed by the Mode I buckling. When the length of the crossarm is large (at small ratios of ℓ to ℓ_{ca}) the restraint against the lateral movement will be large and the restraint against the rotation will be small. Thus the failure occurs by the rotation of the vertical member at the level of the crossarm (Mode II buckling). At large ratios of ℓ to ℓ_{ca} the translational restraint will be small and the rotational restraint will be large, thus failure occurs by the lateral movement of the frame at the crossarm level. The optimum pretension will also increase when the critical load increases, and will decrease when the critical load decreases. The above effect is due to the fact that the optimum pretension is a function of the maximum critical load of the lattice frame and the term C (Refer Eq. 3.15). The optimum pretension varies with the maximum critical load and C. The maximum possible critical load of the lattice frame and the maximum optimum pretension lie at the intersection of Mode I and Mode II curves.

Figs. 4.10 to 4.13 illustrate the effect of the crossarm length

on the critical load and the initial pretensions with various diagonal sizes (ϕ) at a constant modulus of elasticity of the diagonal equal to 29600 ksi. These figures reveal that as the size of the diagonal increases, the maximum possible critical load occurs at greater ratios of ℓ to ℓ_{ca}. The critical load versus the ratio of ℓ to ℓ_{ca} shown in Figs. 4.10 to 4.13 are also shown in Fig. 4.14. This figure reveals that the increase in the diagonal size increases the maximum possible critical load. The increase in the size of the diagonal increases the lateral restraint. Thus the intersection point of Mode I and Mode II buckling curve occurs at greater ratios of ℓ to ℓ_{ca} and at a larger critical load. For example, the intersection point lies at the ℓ to ℓ_{ca} ratio of 4 for a diagonal size of 0.1875 in. If the ℓ to ℓ_{ca} ratio of the frame is increased beyond 4, the magnitude of the rotational restraint at the crossarm level will increase and the magnitude of the translational restraint will decrease. The required magnitude of the translational restraint to maintain Mode II buckling will be higher than the magnitude of the translational restraint created by an 0.1875 in.diagonal beyond the ℓ to ℓ_{ca} ratio of 4. Hence the failure is changed from Mode II to Mode I. To maintain the Mode II buckling beyond the ℓ to ℓ_{ca} ratio of 4 it is necessary to increase the translational restraint. The translational restraint can be increased by increasing the size or the modulus of elasticity of the diagonal or the length of the crossarm. Hence the intersection point (of Mode I and II curves) at a diagonal size of 0.3125 in. lies at a higher ℓ to ℓ_{ca} ratio than 4. As the size of the diagonal is increased to 0.875 in.

the translational restraint created at the crossarm level is so large that the lattice frame fails by Mode II buckling even at an ℓ to ℓ_{ca} ratio of 10. The maximum possible critical load increases by approximately 13% as the size of the diagonal is increased from 0.1875 in. to 0.3125 in.

Fig. 4.15 is a plot of the initial pretensions versus the ratio of ℓ to ℓ_{ca} for various values of diagonal sizes. At a constant value of the ℓ to ℓ_{ca} ratio an increase in the size of the diagonal increases the initial pretensions. This is due to the fact that an increase in the diagonal size (ϕ) increases the axial stiffness of the diagonal (K_d) and consequently the term C (Eq. 3.15). Thus the initial pretensions are increased with an increase in the size of the diagonal irrespective of the critical load. For example at the ℓ to ℓ_{ca} ratio of 6 the critical load of the lattice frame varies by 64% (see Fig. 4.14) and the optimum pretension varies by 330% for the variation of the diagonal size, from 0.1875 in. to 0.3125 in. At the same ℓ to ℓ_{ca} ratio of six with the same change in the size of the diagonal (0.1875 in. to 0.3125 in) causes an increase of 165% in the minimum effective pretension value.

Figs. 4.16 to 4.19 illustrate the plot of the critical load and the initial pretensions versus the ratio of ℓ to ℓ_{ca} when the modulus of elasticity is kept constant at 19500 ksi and the diagonal size is varied. Figs. 4.20 to 4.23 also illustrate the plot of the critical load and the initial pretensions versus the ratios of ℓ to ℓ_{ca} when the modulus of elasticity is kept constant at 9400 ksi and the diagonal size is varied. These figures show that all the previous observations (Figs. 4.10 to 4.15) are

also valid for a modulus of elasticity smaller than 29600 ksi. Fig. 4.24 illustrates the variation in the critical load with the variation in the ratios of ℓ to ℓ_{ca} for various values of modulus of elasticity at a diagonal size of 0.1875 in. As the modulus of elasticity of the diagonal increases, the maximum possible critical load occurs at a larger ratio of ℓ to ℓ_{ca}. The reason for the above fact is also similar to the one given for Fig. 4.14. For example, at a modulus of elasticity of 19500 ksi the maximum possible critical load occurs at an ℓ to ℓ_{ca} ratio of three and at 29600 ksi the critical load occurs at an ℓ to ℓ_{ca} ratio of four. Fig. 4.25 illustrates the plot of the initial pretensions versus the ratio of ℓ to ℓ_{ca} at a diagonal size of 0.1875 in. The optimum pretension occurs at the same ℓ to ℓ_{ca} in which the corresponding maximum possible critical load occurs, irrespective of the modulus of elasticity. Figs. 4.24 and 4.25 reveal that when the modulus of elasticity is increased it will cause a small increase in the critical load and a corresponding large increase in the initial pretensions. This is again due to the term C in Eq. 3.15. For example, at an ℓ to ℓ_{ca} ratio of six a change in the modulus of elasticity from 9400 ksi to 19500 ksi will cause a 21% increase in the maximum critical load and 150% increase in the optimum pretension.

4.10.2 Effect of the Size of Diagonal

Figs. 4.26 to 4.29 illustrate the critical load and the initial pretensions as a function of the diagonal size. These figures reveal that the battened frame critical load remains unchanged with the diagonal size as the frame is independent of the diagonals. Hence the battened frame critical load remains unchanged at a constant ℓ to ℓ_{ca} ratio irrespective

of the diagonal sizes. The minimum effective and the optimum pretensions of the diagonals increase with an increase in the diagonal size, even without any change in the corresponding critical load. This is due to the fact that an increase in the diagonal size will cause an increase in the axial stiffness (K_d) and consequently an increase in the magnitude of the term C (Ref. Eq. 3.15).

Fig. 4.26 shows the plot of the critical load versus the diagonal size. The ratio of ℓ to ℓ_{ca} is kept constant at five and the modulus of elasticity of the diagonal is varied from 9400 ksi to 29600 ksi. When the size of the diagonal is small the critical load increases with the increase in the diagonal size. Beyond a certain diagonal size, the critical load remains constant even with an increase in the diagonal size. For example, the critical load increases steadily when the diagonal size is increased from 0.1875 in. to 0.5 in. (E = 9400 ksi). If the diagonal size is increased beyond 0.5 in., the critical load remains constant irrespective of the change in the diagonal size. It can be explained as follows. As the size of the diagonal increases, the lateral restraint also will increase. When the lattice frame is in the Mode I failure zone, any increase in the translational restraint will cause an increase in the critical load. Once the buckling changes from Mode I to Mode II any further increase in the translational restraint will not make any difference in the critical load. Between the diagonal sizes of 0.1875 in. and 0.5 in. the failure occurs by Mode I buckling and after 0.5 in. it occurs by Mode II buckling (E = 9400 ksi). For a modulus of elasticity of 9400 ksi the intersection of the Mode I and the

Mode II curves occur at a diagonal size of 0.5 in. As the modulus of elasticity is increased, the intersection of Mode I and Mode II curves occur at a smaller diagonal size. It is due to the fact that an increase in the modulus of elasticity increases the lateral restraint and the Mode II buckling occurs at a smaller diagonal size.

Fig. 4.27 indicates the variation in the initial pretensions with the variation in the diagonal size. The ratio of ℓ to ℓ_{ca} is kept constant at five and the diagonal modulus of elasticity is varied from 9400 ksi to 29600 ksi. As the diagonal size is increased the minimum effective pretension increases slowly and the optimum pretension increases quite rapidly. The critical load corresponds to the minimum effective pretension remains constant as the term C changes uniformly with a uniform change in the size of the diagonal (Refer to Eq. 3.17). Consequently, the minimum effective pretension, which is a function of the critical load and the term C also varies uniformly and slowly. On the other hand, as the diagonal size increases the critical load corresponds to the optimum pretension (Refer to Eq. 3.18) increases quite fast and reaches a constant value, which is several times higher than the battened frame critical load. The term C increases slowly and uniformly with a variation in the diagonal size. Hence the optimum pretension which is a function of the corresponding critical load and the term C varies at a faster rate than the minimum effective pretension. At small sizes of the diagonals the change in the optimum and the minimum effective pretensions are also small and at large sizes of the diagonals the change in the optimum and the minimum pretensions are also

large as the modulus of elasticity is varied.

Fig. 4.28 shows the plot of the buckling load versus the size of the diagonals for an ℓ to ℓ_{ca} ratio of ten. From the figure it is clear that the critical load increases with an increase in the size of the diagonal. As the diagonal size is varied from 0.1875 in. to 0.875 in. the critical load increases by approximately 140%, at a modulus of elasticity of 9400 ksi. The entire portion of the critical load curve remains in the Mode I failure region. Hence an increase in the diagonal size increases the critical load (explained in section 4.3.2.2). As the modulus of elasticity is increased from 19500 to 29600 ksi the critical load also increases upto a diagonal size which is equal to a value slightly smaller than 0.875 in. The critical load increases for all the diagonal sizes when the modulus of elasticity is increased from 9400 ksi.

Comparing Fig. 4.26 and 4.28 it is clear that small diagonal sizes will have higher critical loads at small ratios of ℓ to ℓ_{ca} than at large ratios of ℓ to ℓ_{ca}. Similarly, large diagonal sizes will have higher critical loads at large ratios of ℓ to ℓ_{ca} than at small ratios of ℓ to ℓ_{ca}.

The plot of the initial pretensions versus the diagonal size is shown in the Fig. 4.29 for an ℓ to ℓ_{ca} ratio equal to ten. All the observations made for Fig. 4.27 are also valid for this figure. Comparing Figs. 4.27 and 4.29 it is clear that with a small diagonal size the initial pretensions are higher at small ℓ to ℓ_{ca} ratios than at larger ℓ to ℓ_{ca} ratios and vice versa. This effect is only due to the magnitude of the

corresponding critical load. At small diagonal sizes a change in the modulus of elasticity will not have a great change in the initial pretension values and at large diagonal sizes even a small change in the modulus of elasticity will cause a large change in the initial pretensions. The variation in the term C (Eq. 3.15) and the corresponding critical load are the cause of all the above variations.

4.10.3 Effect of Modulus of Elasticity of Diagonal

The plot of the critical load and the initial pretensions versus the values of the modulus of elasticity of the diagonals are shown in Figs. 4.30 to 4.33. From the above figures, it is apparent that the critical load of a battened frame remains unaffected with the modulus of elasticity of the diagonals because, a battened frame is independent of the diagonals. The minimum effective and the optimum pretensions of the diagonals increase with an increase in the modulus of elasticity, even at a constant critical load. The above effect can be explained as follows. Any variation in the modulus of elasticity will vary the axial stiffness of the diagonal member (K_d) and the change in the axial stiffness will affect the magnitude of the term C in Eq. 3.15. Consequently, the initial pretensions are also affected. For example, when the critical load corresponds to the minimum effective pretension remains constant (Refer to Eq. 3.17), the variation in the term C controls the variation of the minimum effective pretension. Hence the minimum effective pretension changes with a change in the modulus of elasticity.

Fig. 4.30 illustrates the critical load as a function of the modulus of elasticity. The ratio of ℓ to ℓ_{ca} is five and the size of the diagonal

is varied from 0.1875 in. to 0.875 in. If the modulus of elasticity and the size of the diagonals are relatively large, any change in the modulus of elasticity will have only a small change or will not have any change on the critical load. For example, when the size of the diagonal is 0.3125 in., and the modulus of elasticity is varied from 19500 ksi to 29600 ksi the critical load remains the same. When the size of the diagonal is relatively small, any change in the modulus of elasticity will have a considerable influence on the critical load of the lattic frame. For example, when the diagonal size is 0.1875 in. and the modulus of elasticity is varied from 19500 ksi to 29600 ksi, the critical load is increased by 26%. The reason for the above effect can be explained as follows: An increase in the modulus of elasticity of the diagonals will cause an increase in the translational restraint at the crossarm level. If the failure of the frame is in the Mode I region, the increase in the translational restraint will increase the critical load. When the frame has a relatively small diagonal size, the frame usually fails by Mode I buckling. Hence an increase in the translational restraint will increase the critical load. When the frame is in the Mode II failure region any increase in the translational restraint will not increase the critical load. If the size of the diagonal is very large the frame usually fails by Mode II buckling. Hence any increase in the translational restraint by increasing the modulus of elasticity will not increase the critical load. The entire portion of the curve corresponding to 0.1875 in. diagonal lies in the Mode I buckling region and the curve corresponding to 0.5 in. and 0.875 in. falls in the

Mode II buckling zone. The intersection point of the Mode I and Mode II curves corresponding to 0.3125 in. diagonal size coincides with a modulus of elasticity equal to 19500 ksi.

Fig. 4.31 shows the plot of initial pretensions versus the modulus of elasticity of the diagonal for an ℓ to ℓ_{ca} ratio of five while the diagonal size is varied from 0.1875 in. to 0.875 in. The minimum effective and the optimum pretensions increase with the increase in the modulus of elasticity. As the modulus of elasticity increases, the increase in the minimum effective pretension value is quite slow compared to the increase in the optimum pretension. The anticipated reason for this effect can be explained as follows. The minimum effective and the optimum pretensions are the functions of the corresponding critical loads and the term C Hence depending upon these two variables the initial pretensions are controlled. At relatively small values of modulus of elasticity the initial pretensions increase at a slower rate than the initial pretensions at large values of modulus of elasticity with an increase in the size of the diagonal. These initial pretension curves increase rapidly irrespective of the mode of buckling. The optimum pretension corresponding to a diagonal size of 0.875 in. is very large. This is again due to the corresponding critical load and the term C

Fig. 4.32 represents the effect of the modulus of elasticity on the critical load with an ℓ to ℓ_{ca} of ten. All the general observations made for Fig. 4.30 are also valid to this figure. It is apparent from the figure that as the modulus of elasticity increases the critical load also increases

but at a slower rate with a small diagonal size than with a large diagonal size (when the frame lies in the Mode I buckling zone). This is due to the fact that as the diagonal size and the modulus of elasticity increases the translational restraint also increases. Depending upon the magnitude of the translational restraint the increase in the critical load will occur. Comparing Figs. 4.30 and 4.32 it can be concluded that at large ℓ to ℓ_{ca} ratios the critical load corresponding to a large diagonal size will be greater than the corresponding critical load at relatively small ℓ to ℓ_{ca} ratios. For example, the critical load is 150 kips at an ℓ to ℓ_{ca} ratio of ten (E = 19500 ksi and ϕ = 0.875 in.) and the critical load is 120 kips at the ℓ to ℓ_{ca} ratio of five (E = 19500 ksi and ϕ = 0.875in.). Similarly, small and medium size diagonals will give large critical loads at small and medium ℓ to ℓ_{ca} ratios.

Fig. 4.33 indicates the plot of initial pretensions versus modulus of elasticity for an ℓ to ℓ_{ca} ratio of ten. Comparing Figs. 4.31 and 4.33 it can be concluded that all the observations made with long crossarms are also valid with short crossarms. At small diagonal sizes the increase in the initial pretensions are not great with an increase in the modulus of elasticity. For example, at a diagonal size of 0.1875 in. the increase in the minimum effective and the optimum pretensions are less than 500 lbs as the modulus of elasticity is changed from 9400 ksi to 29600 ksi. As explained earlier the minimum effective and the optimum pretensions are the functions of the term C (Eq. 3.15) and the corresponding critical load. The change in the initial pretension is appreciable with larger diagonal sizes. For example,

when the modulus of elasticity is changed from 9400 ksi to 29600 ksi at a diagonal size of 0.875 in., the minimum effective pretension increases by 5600 lbs and the optimum pretension increases by 20000 lbs. The initial pretensions increase continuously in both the Mode I and Mode II regions.

4.11 Effect of Various Parameters on Efficiency

The effect of various parameters like the crossarm length, size and modulus of elasticity of the diagonal on the efficiency are discussed with a numerical example in this section. The example frame is the same as the one used in the previous sections.

4.11.1 Effect of Crossarm Length

Figs. 4.34 to 4.37 indicate the influence of the crossarm length on the efficiency. These figures indicate that the efficiency of a battened frame increases with the reduction in the crossarm length. This is due to the fact that the critical load of a battened frame increases with the reduction in the length of the crossarm, and the overall weight of the frame decreases with a reduction in the crossarm length. As explained earlier, the combined effect of these factors (critical load and the total weight of the frame) increases the efficiency of a battened frame. The critical load and the total weight of the battened frame changes at a much faster rate at long crossarm lengths than at short crossarm lengths. Hence the efficiency increases at a faster rate with small ℓ to ℓ_{ca} ratios than at large ℓ to ℓ_{ca} ratios.

Fig. 4.34 shows the plot of efficiency versus the crossarm length

for a small size of the diagonal (0.1875 in.). As the ℓ to ℓ_{ca} ratio increases the efficiency also increases. It reaches a maximum value and then starts decreasing with a further increase in the ℓ to ℓ_{ca} ratio. The shape of the efficiency curve is also similar to the critical load curve. As explained earlier, the weight of the frame continously decreases with the increase in the ℓ to ℓ_{ca} ratio. The influence of the weight on the efficiency is smaller than the influence of the critical load on the efficiency at small diagonal sizes. Hence the efficiency curve is more or less similar to the critical load curve. The efficiency and the critical load reach a maximum value at the same ℓ to ℓ_{ca} ratio. For example, at the maximum critical load the efficiency of the lattice frame (E = 29500 ksi) is 1700% (max at ℓ to ℓ_{ca} = 4). The efficiency of the battened frame at the same ℓ to ℓ_{ca} ratio is 650%. The maximum efficiency lies at the intersection of Mode I and Mode II curves. The maximum possible efficiency of a battened frame is only 750% and it occurs at an ℓ to ℓ_{ca} ratio of ten. Figs. 4.35 to 4.37 illustrate the efficiency versus ℓ to ℓ_{ca} ratio for various values of diagonal sizes. From these figures it is clear that the maximum efficiency occurs at a relatively large ℓ to ℓ_{ca} ratio as the diagonal size increases. In the increasing portion of the efficiency curve the failure is controlled by the Mode II buckling and in the decreasing portion of the efficiency curve the failure is controlled by the Mode I buckling. As the modulus of elasticity of the diagonal increases the efficiency also increases at small crossarm lengths and remains unchanged at large crossarm lengths.

4.11.2 Effect of Diagonal Size

The effect of the diagonal size on the efficiency is illustrated

in Figs. 4.38 and 4.39. Fig. 4.38 is valid at the ℓ to ℓ_{ca} ratio of five. As stated earlier an increase in the diagonal size increases the total weight of the frame. When the diagonal size increases the buckling load either increases or remains the same. The weight and the critical load control the efficiency of the frame. For example, considering a modulus of elasticity equal to 29600 ksi the efficiency increases between the diagonal sizes of 0.1875 in. and 0.3125 in. It will start decreasing after 0.3125 in. Comparing Figs. 4.26 and 4.38 it can be concluded that in the increasing portion of the critical load curve (between 0.1875 in. and 0.3125 in.) the efficiency also increases and in the portion where the critical load shows no change, the efficiency decreases. This effect can be explained as follows. The effect of the critical load on the efficiency is more than the effect of the weight on the efficiency in the increasing portion of the efficiency curve (0.1875 in. to 0.3125 in.). The effect of the weight on the efficiency increases and the effect of the critical load remains constant beyond the diagonal size of 0.3125 in. Hence, the efficiency decreases beyond the diagonal size of 0.3125 in. The maximum efficiency occurs at a diagonal size of 0.3125 in. and it is equal to 1800%. The battened frame critical load remains constant at 690%, since any change in the diagonal size will have no effect on the critical load and on the weight of the battened frame. The maximum efficiency of the lattice frame occurs at the intersection of the Mode I and Mode II curves. Fig. 4.39 illustrates the plot of the efficiency versus the diagonal size at a large value of the ℓ to ℓ_{ca} ratio (equal to ten). From Figs. 4.38 and 4.39 it is clear that the maximum efficiency occurs at a relatively large diagonal size as the ℓ

to ℓ_{ca} ratio increases. For small values of modulus of elasticity (9400 ksi) the efficiency increases uniformly at a large ℓ to ℓ_{ca} ratio. In Fig. 4.28 the maximum possible critical load occurs at a diagonal size of 0.875 in. (at E = 29600 ksi). In Fig. 4.39 the maximum efficiency occurs at a diagonal size of 0.5 in. (E = 29600 ksi). From the Figs. 4.28 and 4.39 it is clear that at a modulus of elasticity of the diagonal, equal to 29600 ksi, the maximum possible critical load and the maximum efficiency occurs at different values of the diagonal size. The reason for this fact can be explained as follows. At an ℓ to ℓ_{ca} ratio of ten, the maximum possible critical load occurs with a diagonal size of 0.875 in. The weight of the frame with a 0.875 in. diagonal is considerably more (40%) than the weight of the frame with an 0.5 in. diagonal. When the size of the diagonal is changed from 0.5 in. to 0.875 in. the change in the critical load is relatively small. Hence the weight per unit critical load of a frame with 0.875 in. diagonal increases and the efficiency decreases. From these two figures it is clear that an increase in the buckling strength does not necessarily mean an increase in the efficiency. For the values of the modulus of elasticity other than 29600 ksi, the maximum efficiency and the maximum critical load occurs at about the same diagonal size.

4.11.3 Effect of Modulus of Elasticity of Diagonals

Figs. 4.40 and 4.41 illustrate the effect of the modulus of elasticity of the diagonals on the efficiency for two ratios ℓ to ℓ_{ca}, five and ten. The variation in the modulus of elasticity has no effect on weight.

Thus the only factor which controls the efficiency is the critical load. Comparing Figs. 4.30 with 4.40 and 4.32 with 4.41, it can be concluded that the efficiency curves are similar to the critical load curves for all the sizes of diagonals. For example, at an ℓ to ℓ_{ca} ratio of five the critical load and the efficiency remain constant for diagonal sizes of 0.5 in. and 0.875 in. and all the values of the modulus of elasticity. At a diagonal size of 0.3125 in. the critical load and the efficiency increase uniformly when the modulus of elasticity values are 9400 ksi and 19500 ksi but remain constant for values of the modulus of elasticity between 19500 ksi and 29600 ksi. The efficiency and the critical load vary uniformly at a diagonal size of 0.1875 in. (for E = 9400 ksi to 29600 ksi). From Figs. 4.40 and 4.41 it is reasonable to conclude that the efficiency of a frame with 0.875 in. diagonal will be relatively small at an ℓ to ℓ_{ca} ratio of five. At the same ℓ to ℓ_{ca} ratio, 0.3125 in. diagonals govern the maximum efficiency between the values of modulus of elasticity of 15000 ksi and 29600 ksi. The 0.5 in. diagonals govern the maximum efficiency below the modulus of elasticity of 15000 ksi. When the ℓ to ℓ_{ca} ratio is ten, the maximum efficiency is governed by a 0.875 in. diagonal between the values of the modulus of elasticity of 9400 ksi and 22500 ksi. For the modulus of elasticity values greater than 22500 ksi, 0.5 in. diagonals govern the maximum efficiency. The efficiency of all the diagonal sizes between 0.1875 in. and 0.5 in. increases steadily with the modulus of elasticity.

4.12 Maximum Efficiency

Fig. 4.42 illustrates the effect of the diagonal size on the maximum efficiency. As the modulus of elasticity of the diagonal increases, the maximum efficiency also increases. The maximum efficiency increases at small diagonal sizes and decreases at large diagonal sizes. The maximum efficiency occurs at relatively small values of the ℓ to ℓ_{ca} ratio with small diagonal sizes and occurs at relatively large ℓ to ℓ_{ca} ratios with large diagonal sizes. The maximum possible efficiency occurs between the diagonal sizes of 0.3125 in. and 0.5 in. The maximum efficiency of the battened frame remains unchanged as it is independent of the diagonals.

CHAPTER 5

RATIONAL DESIGN OF DIAGONALLY PRETENSIONED LATTICE FRAMES

5.1 General

An efficient design is necessary to proportion the members of any structure and to make use of the material to the maximum possible capacity. All the flexural and the column members are designed in such a manner that stresses are close to the allowable limit, when they are loaded to their maximum capacity. For compression members the buckling effects have to be considered in addition to direct compression. Depending upon the effective length and the cross-sectional properties the column can be classified as one of the following three types. They are the short, intermediate and the long columns. The short columns fail by yielding of the material by direct compression while the long columns fail by buckling. The intermediate columns fail by yielding due to direct compression and buckling. When the lateral restraints are introduced to a column at intermediate heights, the effective length will be reduced and its buckling strength will increase. In case of frame, the lateral and rotational restraints are applied at the crossarm levels by the diagonals and the crossarms. An increase in the number of segments will increase the number of diagonals and the crossarms required. Consequently, the buckling strength of the frame also will be increased. The increase in the size of the diagonal will increase the lateral restraint on the frame. As explained earlier, this increase in lateral restraint either may or may not cause an increase in the buckling strength of the frame while the increase in the diagonal

size will always increase the total weight of the frame. If the allowable direct compressive load on the frame (load the frame can carry when the buckling effects are neglected) is smaller than the buckling (or critical) load of the frame then, there will be no use in increasing the buckling strength of the frame by increasing the number of segments or by increasing the size of the diagonals. Instead of that if the number of crossarms and the size of the diagonals are reduced to have the buckling strength of the frame close to the maximum direct compressive load itself then, the overall weight of the frame will be reduced. Hence, it is necessary to proportion the members properly by considering the allowable direct compressive load, buckling (or critical) load and the efficiency of the frame.

5.2 Theory of Compression Members

The buckling strength of a column is greatly influenced by its effective length. When the column has two pin-ended supports, the effective length of the column will be equal to its length, and if the ends of the column are fixed, the effective length of the column will be reduced to half of its length. Hence, depending upon the end restraints, the effective length of the column will vary and consequently the buckling strength also will vary. A general equation for the critical load (P_{cr}) of a column may be written as follows:

$$P_{cr} = \frac{\pi^2 EI}{(k\ell)^2} \qquad (5.1)$$

where E = the modulus of elasticity of the material of the column; I = the

moment of inertia of the section of the column; ℓ = the length of the column; and k = the effective length factor equal to 1.0 when the supports are hinged and 0.5 when they are fixed.

Eq. 5.1 reveals that an increase in the k value will decrease the critical load and vice versa. Hence the effective length factor (k) will be useful in determining the maximum buckling strength of the column. As the k value decreases, the buckling strength of the column will increase. Thus while designing the column (which has the option of various support conditions) it is advisable to select the dimensions and the support conditions in such a manner to get the minimum possible k value. The vertical members of a lattice frame act as individual columns with the segmental length as the length and with flexible end supports (rotational and translational restraints vary the flexibility of support). The magnitude of the restraints created at the supports of vertical member (joints are the supporting points for vertical member) depends greatly upon the crossarms and the diagonals. The effective length factor k for the vertical member can be calculated using Eq. 5.1. Due to the different support conditions (at joints) the effective length of vertical member in each panel will be different and hence the k value also will be different. To calculate the individual k value of all vertical members it is necessary to have the corresponding axial load. The axial load is assumed to be the same throughout the length of the leg. Hence the k value is also assumed to be equal for all the vertical members. If the crossarms and the diagonals are chosen in such a manner to get the maximum possible buckling load, then the k value will be minimum. Once the minimum possible K

value is achieved, the dimensions of the frame has to be readjusted to get the maximum possible efficiency.

As explained earlier there are two possible modes of failure (Mode I and Mode II). Fig. 5.1(a) shows the buckled shape of a column with hinges and two restraining moments at the ends. This column corresponds to a vertical member in a lattice frame where Mode II buckling occurs. Depending upon the magnitude of the moment, the effective length factor (k) of the column will vary from 1.0 to 0.5. Figs. 5.1(b) corresponds to a column with one end hinged and the other end free to displace. The restraining moments are applied to both ends. This column is the same as a vertical member in the end segment of the lattice frame when the Mode I buckling occurs. Fig. 5.1(c) is similar to the vertical member in the middle segment of a lattice frame when Mode I buckling occurs. An equivalent column for a vertical member in the end segment is shown in Fig. 5.1(d). A partial translational restraint is created at the top end by the diagonal members and rotational restraints are provided at the ends by the crossarms. The effective length factor of this frame will be equal to or smaller than 1.0. A relatively long crossarm will create a small rotational restraint and a small crossarm will create a large rotational restraint.

For a simple column, knowing the support conditions (hinged, fixed, free etc.) the k value can be assumed and the corresponding buckling loads may be calculated. In the case of a frame, the critical load can be calculated using the finite element approach described in Chapter 6 and

the k value is not known.

The k value of the vertical member can be calculated using the calculated critical load as follows.

The Euler load (P_E) of a column equal to the length of the vertical member is,

$$P_E = \frac{\pi^2 E_c I_c}{(k\ell)^2} \qquad k = 1.0 \qquad (5.2)$$

The critical load of the frame is as follows:

$$P_{B,L}/2 = \frac{\pi^2 E_c I_c}{(k_{B,L}\ \ell)^2} \qquad (5.3)$$

where the suffix B refers to the battened frame and suffix L refers to the lattice frame; P = the total load on the frame; and P/2 is the critical load carried by each leg. Substituting Eq. 5.2 into Eq. 5.3 yields,

$$P_{B,L}/2 = \frac{P_E}{k^2_{B,L}}$$

and hence,

$$k_{B,L} = \left(\frac{2\ P_E}{P_{B,L}}\right)^{1/2} \qquad (5.4)$$

The critical loads (P_B or P_L) are calculated using the computer program explained in Chapter 6. If the k value is equal to 0.5, the critical load on the vertical member and consequently the critical load on the frame cannot be increased simply by varying the crossarms and the diagonals

(rotational and translational restraints). The only possible way to increase the critical load is to vary the cross-sectional properties of the vertical member.

5.3 Effect of Various Parameters on the k Value

The various parameters that affect the k value and are discussed in this section are:

(1) length of segment: when the length of the vertical segment is quite large, the critical load of the frame will be small and the k value also will be relatively small (see Ref. (13)). For example, if an axially loaded real column of length ℓ_a and with restraining moments R creates a rotation θ_a at the supports (Fig. 5.1(a)), the corresponding effective length factor will be k_a. If the length of the column is changed from ℓ_a to ℓ_b (assume $\ell_b > \ell_a$) at the constant restraining moment R, then the created rotation θ_b which will be smaller than θ_a. Hence the corresponding effective length factor k_b will be smaller than k_a.

(2) cross-sectional properties of vertical member: An increase in the moment of inertia or the modulus of elasticity of the vertical member will increase the critical load and the k value, at a constant length and constant restraining moments at the ends (see reference (13)). For example, if an axially loaded real column of length ℓ_a, modulus of elasticity E_{ac} and cross-sectional moment of inertia I_{ac} having restraining moments R at the ends creates a rotation θ_a at the supports (Fig. 5.1(a)), the corresponding effective length factor will be k_a. If the moment of inertia and the modulus of elasticity are increased to I_{bc} and E_{bc} respectively

at a constant restraining moment R, then the created rotation θ_b will be greater than θ_a and hence the corresponding effective length factor k_b will be greater than k_a.

(3) length of crossarm: As the length of the crossarm increases, the restraining moments at the ends of the vertical member will be relatively small and hence there will be an increase in rotation at the ends and the effective length factor (see reference (13)).

(4) size of diagonal: An increase in the size of the diagonal will increase the translational restraint. If this increase in the translational restraint increases the critical load, the corresponding k value will decrease. Otherwise the corresponding k value will not change.

5.4 General Procedure for the Design of Members

A general design procedure is discussed in this section. The following are the given parameters: Load, height of the frame, possible minimum crossarm length, possible minimum segment length and the support condition. The following are the required quantities: The cross-sectional details of the members, number of segments, length of crossarm, size of the diagonal member, initial pretensions and the efficiency of the frame.

5.4.1 Design

(1) The area of cross-section of verticals and crossarms:

The minimum area (A) required to resist the axial compression is

$$A = \frac{P_L}{2\sigma} \tag{5.5}$$

where P_L = the total load carried by the lattice frame; and σ = the allowable

stress.

(2) Number of Segments:

From the calculated value of area (Eq. 5.5) the available moment of inertia (I_c) is selected. The section may be either a solid circular section or a tubular section. A k value is selected between 0.5 and 1.0. According to the theory of columns it is possible to achieve a k value of 0.5. But computer results have indicated that it is difficult to achieve a k value below 0.55. Hence a k value of 0.6 is selected to start the calculations. The above selected values are substituted in Eq. 5.3 which is in a modified form is,

$$\ell = \left(\frac{\pi^2 E_c I_c}{\frac{P_L}{2} k^2} \right)^{1/2} \qquad (5.6)$$

where ℓ = the segment length.

The total number of segments are given by:

$$\text{Total number of segments} = \frac{\text{Total height of the frame}}{\ell}$$

Any fractional number of segments is rounded up to the closest higher integer value.

(3) Selection of diagonal size:

There is no direct theoretical method to select the diagonal size. The diagonal size depends on the crossarm length. The crossarm length which corresponds to the maximum efficiency is unknwon. Thus a few trials are required to select the size of the diagonal members. Once the selection process to determine the diagonal size has been completed,

the actual k value of the proportioned frame is checked with the value assumed in Eq. 5.6. If the actual k value from the computer analysis is smaller than or equal to the assumed k value, the frame can carry the specified load (P_L) and it is considered to be safe.

5.4.2 Numerical Example

The design procedure is discussed with a numerical example in this section.

The following quantities are given:

(1) The total load on the frame = 100 Kips.

(2) Height of the frame = 72 in.

(3) Allowable stress in the material = 65 ksi.

(4) Minimum possible crossarm length = 5 in.

(5) Minimum possible segment length = 6 in.

(6) Support condition, all the four ends hinged.

(7) Modulus of elasticity = 29600 ksi.

(1) The minimum cross-sectional area of verticals and crossarms can be calculated using Eq. 5.5 as follows.

$$A = \frac{P_L}{2\sigma} = \frac{100}{2x65} = 0.769 \text{ in.} \qquad (5.7)$$

A solid circular section of 1.0 in. diameter has been selected. Area and the moment of inertia of the selected section are 0.785 in. and $0.049 in.^4$ respectively.

(2) The number of segments can be calculated as follows.

Using Eq. 5.6

$$\ell = \left(\frac{\pi^2 E_c I_c}{\frac{P_L}{2} k^2} \right)^{1/2}$$

Assuming k = 0.6

$$\ell = \left(\frac{\pi^2 \times 29600 \times 0.049}{50 \times (0.6)^2} \right)^{\frac{1}{2}} = 28"$$

Thus,

$$\text{Number of segments} = \frac{72}{28} = 2.57$$

Three segments of 24 in. each are suitable. The maximum k value required to achieve this load is given by

$$k = \left(\frac{\pi^2 E_c I_c}{P_L/2 \, \ell^2} \right)^{1/2}$$

$$= \left(\frac{\pi^2 \times 29600 \times 0.049}{50 \times (24)^2} \right)^{1/2} = 0.70$$

So if the computer analysis (explained in Chapter 6) gives a value of k below 0.7 the structure will be safe.

(3) The selection of the diagonal size and crossarm length can be performed as follows.

The length of the crossarms and diagonal sizes will be changed accordingly to achieve the maximum efficiency and the required load. As

per the initial data the minimum possible crossarm length is 5 in. Hence the possible ℓ to ℓ_{ca} ratio is given by, $\frac{24}{5} = 4.8$. Hence, ℓ to ℓ_{ca} ratio of four will be o.k.

Four diagonal sizes were chosen in a random manner and the corresponding computer outputs are given in Tables 5.1 to 5.6.

These tables clearly indicate that when the ℓ to ℓ_{ca} ratio increases the efficiency also increases and the maximum efficiency occurs with a relatively large diagonal size. The cross-sectional area of the vertical member is capable of carrying only a load of 50 kips. A further increase in the load will cause yielding due to direct axial compression. Considering the Tables 5.1 to 5.4 the maximum efficiency occurs at an ℓ to ℓ_{ca} ratio of 4 and with a diagonal size of 0.1875 in. The corresponding critical load is 113.9 kips (total load). Although the critical load in each leg is more than 50 kips. this diagonal size of 0.1875 in. will be suitable, since it gives the maximum efficiency. The actual k value calculated from the computer analysis is equal to 0.66 which is smaller than 0.7. Hence, the frame is safe.

The dimensions of the members are as follows.

(1) The size of the verticals and crossarms = 1.0 in. solid circular section.

(2) The segment length = 24 in.

(3) Crossarm length = 6 in.

(4) The size of the diagonal = 0.1875 in.

Suppose that the minimum possible crossarm length is 4 in. instead of 5 in., then some more aspects have to be considered in selecting the diag-

onal size and the crossarm length.

Comparing the six Tables 5.1 to 5.6 it can be concluded that a maximum efficiency (1940%) occurs at an ℓ to ℓ_{ca} ratio of six and with a diagonal size of 0.3125 in. The critical load of the frame is 130 kips. But according to Eq. 5.7 the maximum allowable load is only 100 kips. A frame with an ℓ to ℓ_{ca} of ratio six and a 0.3125 in. diagonal will weigh 39.0 lbs. Referring to Table 5.5 (ℓ to ℓ_{ca} ratio = 5) the efficiency of a frame with 0.3125 in. diagonal is 1800% and the corresponding critical load of the frame is 122 kips. This is also higher than 100 kips. Table 5.4 (ℓ to ℓ_{ca} ratio = 4) indicates that at a diagonal size of 0.1875 in. the buckling load of the frame is 114 lbs. Total weight of the frame is 38.8 lbs., which is slightly less than the frame first mentioned (39.0 lbs). Hence the diagonal size of 0.1875" and the crossarm length of 6" will be suitable even though the efficiency is smaller than the frame at the ℓ to ℓ_{ca} ratio of 6. The difference in weight of the above two frames may be small for this design. It may be considerable for other designs. Thus it is better to select a minimum weight frame.

5.5 Limitations of the Design Method

The design method explained in this Chapter is an efficient method. Unfortunately it has a few limitations as listed below.

(1) The design method does not include the local buckling effects when thin walled sections are used.

(2) The cross-sectional properties of the vertical members and the crossarms must be equal.

(3) The design procedure will not handle the frames of unequal segment length.

CHAPTER 6

COMPUTER SOLUTION

6.1 General

It is necessary to have a computer program to perform the calculations (like the buckling load, initial pretensions etc.) to predict the behaviour of a frame. The program should be capable of providing enough details with a minimum input, and should use a minimum computer time. A computer program, based on the finite element approach outlined by Khosla (7) and the geometric analysis explained in Chapter 3, was written. The computer program requires a minimum of data such as the co-ordinates, member properties, etc. It provides the complete details of information on the frame, such as the buckling load, buckling shapes, initial pretensions, weight and the efficiency of the frame. Using the output of the program, the complete relationship between the buckling load and the initial pretensions can be obtained with a minimum effort. As it is, the program is applicable for any frame with members of circular cross-section. After a slight modification the program can be used for any other cross-section. It is also suitable for frames with any number of segments. It can provide the output for a number of frames (with different crossarm lengths and diagonal sizes) simultaneously.

The same program can be used to calculate the battened frame critical load in a single run. After a slight modification, it can be used for a three-dimensional frame. This Chapter deals with the theoretical background and the body of the program.

6.2 Finite Element Method of Buckling Analysis (Ref. (7))

As in the finite element method of buckling anlysis, the

structure is divided into a number of small linear elements. These elements are assumed to be interconnected at a discrete number of nodal points. The minimization of the total potential energy will always result in a stiffness relationship as given by

$$[K]\ \{\Delta\} = \{F\} \tag{6.1}$$

Where $[K]$ = the stiffness matrix of the complete structure; $\{\Delta\}$ = the displacement vector; and $\{F\}$ = the force vector at the nodes.

Because of the presence of large deflections encountered in the buckling problems, strain displacement equations containing nonlinear terms must be included in the stiffness matrix. Including appropriate nonlinear terms in the strain displacement relationship, results in a stiffness matrix $[K]$, which is the sum of two parts as follows:

$$[K] = [K_E] + [K_G] \tag{6.2}$$

where $[K_E]$ = the elastic stiffness matrix; and $[K_G]$ = the geometric stiffness matrix or the initial stiffness matrix. The elastic stiffness matrix is independent of the load level. The geometric stiffness matrix, however, depends not only on the geometry but also on the initial internal forces existing in the member at the start of each loading step. This matrix represents the effect of the axial load on the flextural stiffness. The derivation of the geometric stiffness matrix is given in Ref. (7). Elements of the elastic and the geometric stiffness matrices in local coordinate

system are given in Eqs. 6.3 and 6.4.

$$[\bar{K}_E] = \begin{array}{c} \begin{matrix} u_1 & v_1 & \theta_1 & u_2 & v_2 & \theta_2 \end{matrix} \\ \begin{bmatrix} \frac{AE}{L} & 0 & 0 & -\frac{AE}{L} & 0 & 0 \\ & \frac{12EI}{L^3} & \frac{6EI}{L^2} & 0 & -\frac{12EI}{L^3} & \frac{6EI}{L^2} \\ & & \frac{4EI}{L} & 0 & -\frac{6EI}{L^2} & \frac{2EI}{L} \\ & & & \frac{AE}{L} & 0 & 0 \\ & & & & \frac{12EI}{L^3} & -\frac{6EI}{L^2} \\ & & & & & \frac{4EI}{L} \end{bmatrix} \end{array} \quad \text{(symmetrical)} \qquad (6.3)$$

$$[\bar{K}_G] = P_{in} \begin{array}{c} \begin{matrix} u_1 & v_1 & \theta_1 & u_2 & v_2 & \theta_2 \end{matrix} \\ \begin{bmatrix} 0 & 0 & 0 & 0 & 0 & 0 \\ & \frac{6}{5L} & \frac{1}{10} & 0 & -\frac{6}{5L} & \frac{1}{10} \\ & & \frac{2L}{15} & 0 & -\frac{1}{10} & -\frac{L}{30} \\ & & & 0 & 0 & 0 \\ & & & & \frac{6}{5L} & -\frac{1}{10} \\ & & & & & \frac{2L}{15} \end{bmatrix} \end{array} \quad \text{(symmetrical)} \qquad (6.4)$$

where E = the modulus of elasticity of the element; A = the cross-sectional area of the element; I = the moment of inertia; L = the length of the element; $[\overline{K}_E]$ = the elemental elastic stiffness matrix in the local coordinate system; $[\overline{K}_G]$ = the elemental geometric stiffness matrix in local coordinate system; and P_{in} = the initial loading at which the geometric stiffness matrix is calculated.

As a first step in calculating the critical load, $[K_E]$ is assembled for all the elements, while $[K_G]$ is assembled only for elements with a significant axial load (i.e. elements of the vertical members). Then the master elastic and the master geometric stiffness matrices are assembled for the possible nodal displacements.

The axial load (P) in the column can be written as follows:

$$P = \lambda P^* \tag{6.5}$$

where λ = a constant; and P^* = the relative magnitude of the applied loads, which is taken as unity. Since the geometric stiffness matrix is proportional to the internal forces at the start of the loading step, $[K_G]$ can be written as follows:

$$[K_G] = \lambda [K_G^*] \tag{6.6}$$

where $[K_G^*]$ = geometric stiffness matrix for the unit value of applied forces (i.e. $\lambda = 1$).

Thus Eq. 6.1 can be written as follows:

$$[K_E + \lambda K_G^*] \{\Delta\} = \{F\} \tag{6.7}$$

At the critical load the stiffness of the structure becomes zero and no external disturbances are required to displace the structure. Thus Eq. 6.7 yields:

$$[K_E + \lambda K_G^*] \{\Delta\} = \{0\} \tag{6.8}$$

At the critical load $\{\Delta\}$ cannot be equal to zero. Thus the determinant of the other term in Eq. 6.8 should be equal to zero. Hence,

$$|K_E + \lambda K_G^*| = 0 \tag{6.9}$$

The lowest value of λ multiplied by P^* gives the critical load for the column. This is a typical eigen value problem. When P^* is chosen as unity, the smallest value of λ is the first buckling load, the second smallest value is the second buckling load, etc. The eigenvectors associated with the loads represent the relative value of displacements in the buckling shapes.

Rearranging Eq. 6.9,

$$|\gamma [I_m] + [K_E]^{-1} [K_G^*]| = 0 \tag{6.10}$$

where $\gamma = 1/\lambda$; and $[I_m]$ = a unit matrix. $[K_G^*]$ is a singular matrix and its inversion is not possible. Thus the terms are arranged as shown in Eq. 6.10 which involves no inversion of $[K_G^*]$.

Subroutine NROOT, from the IBM system/3031 Scientific Subroutine Package (11), calculates the eigenvalues of the matrix $[K_E]^{-1}$ $[K_G^*]$ which are γ. To obtain the desired eigenvalues λ, the values of γ are simply inverted. For example, to get a smallest value of λ the largest value of γ is inverted.

6.3 Equations to Calculate the Various Parameters

The equations used in the computer program to calculate the initial pretensions, effective length factor and the efficiency are listed below. From Eqs. 3.17 and 3.18 the minimum effective and the optimum pretensions can be written as:

$$T_{min} = \frac{1}{2} P_B C$$

$$T_{opt} = \frac{1}{2} P_{L,max} C$$

where

$$C = \frac{\cos\alpha}{K_c\left[\frac{1}{K_a} + \frac{\sin^2\alpha}{K_{ca}} + \frac{\cos^2\alpha}{K_c}\right]}$$

From Eq. 5.4 the effective length factor can be written as:

$$k_B = \left[\frac{\pi^2 EI}{\frac{1}{2} P_B \ell^2}\right]^{1/2}$$

$$k_L = \left[\frac{\pi^2 EI}{\frac{1}{2} P_L \ell^2}\right]^{1/2}$$

The efficiency, from Eq. 4.11 can be written as follows:

$$\text{Efficiency} = \left[\frac{W_{100} \times P_{B,L}}{P_{100} \times W}\right] \times 100\%$$

6.4 Description of the Computer Program

The computer program, consisting of approximately 400 cards, was written in Fortran IV and run on an IBM/3031 computer. It consists of a few subroutines with a main program. The program is discussed in detail in the following sections. A listing of the computer program is given in Appendix.

6.4.1 Main Program

The various steps in the program are given below.

(1) Input data: Required data are:

(a) Number of elements (M)

(b) Number of nodes (N)

(c) Number of degrees of freedom (NDF)

(d) Number of elements with significant axial load (NKG)

(e) Number of elements that can resist bending (NBS)

(f) Output print code to control the quantity of output (NPRC) (1,2,3,4)

(g) Nodal connectivity table (MN)

(h) Variable correlation table (IVC)

(i) Coordinates of the nodes (CNO)

(j) Starting ℓ/ℓ_{ca} ratio (LRS)*

(k) Finishing ℓ/ℓ_{ca} ratio (LRF)*

(l) Number of different diagonal sizes (NSD)*

(m) Number of elements in each vertical member (NE)

(n) Number of segments in the frame (NSE)

(o) Inner diameter of the members with bending stiffness (BDI)*

(p) Outer diameter of the members with bending stiffness (BDO)*

(q) Modulus of elasticity of the members with bending stiffness (EBS)*

(r) Modulus of elasticity of the diagonal members (EST)*

(s) Size of the diagonal members (SD)*

* Explained at the end of this section

(2) Call the subroutine DAF and form all the required data.

(3) Calculate the following member properties:

(a) Moment of inertia (MI)

(b) Cross-sectional area (AA)

(c) Length of the element (LGTH)

(d) Direction cosines (DL1, DL2, DM1, DM2)

(e) Segmental slenderness ratio (ELOR)

(4) Print the input data and the member properties.

(5) Set up the master elastic (GLK1) and the master geometric (GLK2) stiffness matrices through the subroutines ELKM and GEOKM.

(6) Calculate the eigenvalues γ and the corresponding eigenvectors through the subroutines ARRAY and NROOT.

(7) Print the buckling loads and the mode shapes.

(8) Calculate the following quantities:

  (a) The minimum effective and the optimum pretensions.

  (b) The effective length factor.

  (c) The total weight of the frame.

  (d) The efficiency of the frame.

(9) Print the calculated values in step 8.

(10) End of the program.

Explanation of some of the input data:

This program can provide the output for frames with different crossarm lengths (the segment length of all the frames are equal) and different diagonal sizes simultaneously in a single run. Input of the starting and the finishing ℓ/ℓ_{ca} ratios (input step (j) and (k)) can provide the complete information about the crossarm lengths. For example, if the output is required for various frames with ℓ/ℓ_{ca} ratios ranging from one to ten, the coordinates read in Step (i) of the input data should correspond to an ℓ/ℓ_{ca} ratio of one (irrespective of the starting ℓ/ℓ_{ca} ratio, in Step (j)) and in the input Steps (j) and (k) the values should be one and ten respectively. As the first step the program will check whether the calculated value of ℓ/ℓ_{ca} ratio from the given coordinates (Step (i)) is equal to the starting ℓ/ℓ_{ca} ratio (Step (j)) or not (using the subroutine

DAF). If equal the program will calculate the first set of output, taking the given coordinates (Step (i)) as the coordinates of the frame. If not using the subroutine DAF the x-coordinates will be modified (without changing the y-coordinates) to get the ℓ/ℓ_{ca} ratio equal to the value given in the input step (j). Its value is one for this example. Then the complete output is calculated with the modified coordinates. The coordinates are checked for the second time and they are modified to have the ℓ/ℓ_{ca} ratio equal to the value next of that one given in Step (j). Its value is two for this example. Then the second set of output is calculated with the new modified coordinates. In the similar manner outputs are calculated for all the frames. The program is terminated after the output is calculated for the ℓ/ℓ_{ca} ratio given in Step (k) and it is equal to ten in this example. Thus by varying the starting and the finishing ℓ/ℓ_{ca} ratios (input (j) and (k)) the complete output of all the frames can be calculated. Also for each and every ℓ/ℓ_{ca} ratio a set of various diagonal sizes can be used (maximum fifteen in a set). The total number of diagonal sizes is specified in the input Step (l). In this program it is not necessary to give the cross-sectional and the material properies of each and every element. The elements are divided into two sets. They are the elements which can resist the bending and which cannot resist any bending. The elements of the vertical members and the crossarms are the rigid elements. They can resist bending. Diagonal members cannot resist any bending. It will be sufficient if two sets of the member sizes and the values of modulus of elasticity are included in the input (refer input Steps(o), (p), (q), (r) and (s), one set for the verticals

and the crossarms and the other set for diagonals). The subroutine DAF will distribute the above two sets of information properly to the respective elements. Thus very few lines will be sufficient to provide all the informations about the cross-sectional and the material properties of the elements.

6.4.2 Subroutines

The subroutines used in this program are listed as follows:

DAF - Forms a set of input data from the given information.

ELKM - Calculates the master elastic stiffness matrix

GEOKM- Calculates the master geometric stiffness matrix

ARRAY - Changes the master elastic and the geometric stiffness matrices in a vector form to use them in the subroutine NROOT

NROOT - Calculates the eigenvalues and the eigenvectors.

6.5 Limitations of the Computer Program

The few limitations of the above computer program are listed below:

(1) The members must have circular cross-sections. Modifications are necessary to handle other cross-sections.

(2) Properties of the vertical and the horizontal members should be equal and they should be uniform throughout the length.

(3) The program is applicable only for a two-dimensional frame.

(4) It is necessary to number the elements as shown in Fig. 6.1.

CHAPTER 7

EXPERIMENTAL SETUP AND PROCEDURE

7.1 General

A model of the diagonally pretensioned lattice frame was constructed for an experimental investigation and for comparison to the theoretical results. Experiments were performed for various initial pretensions. The same model was used for investigations on both battened and lattice frames. This chapter deals with the experimental set-up and the experimental procedure.

7.2 The Model of Lattice Frame

7.2.1 Reason to Choose the Type of Model:

A two-dimensional three-segment frame as shown in Fig. 7.1 was selected for the experimental investigation. There is no specific reason for selecting this number of segements. The laboratory conditions determined the number of segments. All four supports were hinged. A three-dimensional model is a more practical frame than a two-dimensional model. A two-dimensional model was selected instead of a three-dimensional model because a two-dimensional frame has the following advantages over a three-dimensional model.

(1) The model is easier to build, since it involves less labour and material.

(2) The deflected shape is confined to one plane. Hence it is easy to identify the buckling of the model.

(3) The deflections could be measured easily and accurately.

7.2.2 Description of Components

The vertical and the horizontal members were of solid circular

cross-sections instead of tubular sections. Solid sections are cheaper, easy to machine and to weld.

7.2.2.1 Rigid members:

The verticals and the crossarms were made from 0.625 in. diameter solid circular mild steel bars. Material properties of these bars were found from a tension test. The modulus of elasticity and the yield stress were found to be 29350 ksi and 66 ksi respectively. The ends of all the members were carefully machined to exact dimensions and then welded together. The dimensions of the members are shown in Fig. 7.1. It is not possible to align the centerlines of the crossarms next to the supports with the axes of the hinges. Thus they were positioned a few inches above the hinges. A small hole was drilled in all the four supporting ends of the frame to accommodate a safety pin as shown in Fig. 7.2(b). The purpose of these pins are explained in Section 7.2.2.3. The supporting faces of the vertical legs were carefully machined to have the bottom faces in one horizontal plane and the top face in another horizontal plane. If there is any difference in levels of these faces it will cause an unequal distribution of loads to the two legs of the frame. During the welding process extra care was taken to avoid overheating of the joints which could cause some bending in the members at the location of the joints. This bending would result in large initial imperfections. At various locations small plates were clamped to the vertical leg to be used in the measurement of deflections.

7.2.2.2 Diagonal members:

There were six diagonal members made from 0.1875 in diameter

rods. The modulus of elasticity and the yield stress were 29350 ksi and 68 ksi respectively. The diagonals were cut at about the middle of the length to accommodate ring beam load cells. These load cells were used to measure the tension in the diagonals. The connection between the diagonals and the ring beams are shown in Fig. 7.3. The nuts were tightened to introduce the pretension to the diagonals. The ends of the diagonls were welded to the joints as shown in Fig. 7.4. These connections should be hinged, but since the size of the diagonals was very small they are so flexible they can be considered to be pinned even though it was a welded joint. The maximum allowable tension in the diagonals was 1800 lbs. During the experiment the diagonals were stressed to only 600 lbs. Thus the load in the diagonals was well below the yield stress.

7.2.2.3 Supports:

The top and the bottom supports are shown in Figs. 7.5 to 7.8. All the supports were made with knife edges. Knife edges allow rotations in only one plane and the friction at the contact surfaces will be minimal. The knife edges are shown in Fig. 7.2(b). The small rocker shown in Fig. 7.2(b) was resting on the knife edge. The load was transferred from the vertical leg to the rocker and then to the knife edges. A safety pin was placed between the leg and the rocker to avoid slip of the leg while loading the frame. The rocker and the knife edge arrangement was placed inside a 1.5 in. diameter hole in a solid block of steel as shown in Fig. 7.2(b). The solid block was welded to an adjustable base plate which was bolted to the bottom base block as shown in Fig. 7.2(a). The base block was supported by a loading jack.

The base block was guided by a frame (Fig. 7.6) to avoid twisting. The top support was arranged in the similar manner and is shown in Figs. 7.7 and 7.8. The top base block was attached to a flat load cell which was fixed to a top supporting frame.

7.2.2.4 Lateral supports:

The lateral supports were necessary to confine the buckling of the frame to one plane. A good lateral support takes care of the following aspects.

(1) It will not allow the frame to buckle in more than one plane.

(2) The friction at the contact surfaces between the vertical members and support will be minimal.

The contact surfaces were greased to reduce friction. Four lateral supports were used as shown in Figs. 7.9 to 7.11.

7.2.3 Dimension of the model frame:

The dimensions of the frame are shown in Fig. 7.1. The crossarms were 12 in. long and the total height of the lattice frame was 72 in. The maximum theoretical load the frame can carry was 14.6 kips.

7.3 Experimental Equipment

As explained earlier, ring beam load cells were used to determine the tension in the diagonals. The dimensions of the ring beam load cells are shown in Fig. 7.3. It is an aluminum ring with two holes in it into which the diagonals are inserted. It was kept in position by two nuts. To increase the level of pretension in the diagonal the nuts were tightened. The magnitude of the applied tension was determined by measuring the strains with two strain gages as shown in Fig. 7.3. The maximum capacity of the

ring beam load cell when subjected to tension was 1860 lbs. Six ring beam load cells were used, one in each of the six diagonals. Each load cell was calibrated in a separate tension test. The calibration readings showed a linear relationship between the tension and the strain readings.

7.3.2 Flat load cell:

To determine the load on the frame a flat load cell was used. The load cell was bolted to the top supporting frame as shown in Fig. 7.8. The top base block was bolted to the load cell. The magnitude of the load was measured by means of a strain indicator. The load cell was calibrated prior to the tests. The capacity of the load cell was 50.0 kips and the maximum load during the experiment was expected to be only 14.6 kips. Hence it was well below the capacity of the load cell.

7.3.3 Hydraulic jack:

A hand operated hydraulic jack was used to apply the load from the bottom portion of the base block. It is shown in Fig. 7.12. The maximum capcity of the jack was 50 kips. The load from the jack is transferred to the column through the base block.

7.3.4 Miscellaneous:

A transit was used to align the frame and to measure the initial imperfections. Twelve dial gages were used with two of them used to monitor the deflection in the lateral supports (see Fig. 7.10 and 7.13). An automatic strain indicator was used to measure the strain gage readings.

7.4 Testing Procedure

The various steps involved in the testing procedure are listed below.

(1) The frame was aligned in its position with the aid of the transit.

(2) The ring beams were removed and the dial gages were positioned as required. The set-up was to test the frame without the effect of the diagonals (similar to the battened frame).

(3) The load was applied in 1.0 kip increments initially. The increments were reduced to 0.5 kip as the load approached the buckling load.

(4) The strain gages on the top and the bottom of the legs were monitored to determine whether or not the load was being equally applied to both legs.

(5) At each and every loading step the deflections and the strain gage readings were recorded.

(6) As the buckling load was approached, the deflections increased suddenly with a small increment of load. The load corresponding to this increased deflection was the buckling load.

(7) The deflection readings were carefully monitored to avoid excessive deflection, which would cause yielding of the vertical legs.

(8) Once the buckling load was reached, the load was reduced in increments to check the deflection readings and to ensure that the vertical legs had not yielded.

(9) The ring beam load cells were attached to the diagonals to test the frame as a diagonally pretensioned lattice frame.

(10) The nuts in the ring beams were tightened gradually to introduce the required level of pretension in the diagonals. Extra care was taken while introducing the pretension to minimize the lateral deflection due to the pretension in the diagonals.

(11) The loading procedure was the same as in step (3). At each loading step the strain gage readings in the ring beams were also recorded along with the other readings.

(12) Once the buckling load was identified, as in step 6, the load was released in increments to recheck the readings.

(13) In a similar manner the readings were also taken for various initial pretensions.

The results recorded in these tests will be discussed in Chapter 8.

CHAPTER 8

ANALYSIS OF EXPERIMENTAL RESULTS

8.1 General

A series of experiments were conducted to compare the theoretical and the experimental results. A model frame was used for the experimental study. The frames used in the theoretical analysis were assumed to be ideal and perfect (without any imperfections) while the model frame used in the experiments contained some initial imperfections. Since there is no facility to include the imperfections in the computer program (see Chapter 6) the theoretical results were calculated for an ideal model frame. Prior to the experiments, the geometric and the material properties of the model frame were used to predict the theoretical critical loads, initial pretensions and the buckling modes. Experiments were conducted on frames with and without diagonals. The initial diagonal pretensions were varied between 50 to 600 lbs. A set of readings were taken in every step of the experiment. Several plots showing the relationship between load and deflection, and between load and diagonal tension were drawn for each set of the experimental readings. In this chapter the analytical results of the battened and the lattice frames are compared with the experimentally obtained results.

8.2 Experimental Errors

Whenever an experiment is performed, the experimental results will be influenced by some form of errors. The following are the anticipated errors during the experimental study of the frame.

(1) Although the distribution of the load was monitored carefully by the strain gages, there could have been some possibility for unequal

distribution of the load to the two legs.

(2) There could have been some friction between the frame and the lateral supports.

(3) Although the welding was done carefully, the material and the cross-sectional properties of the frame could have been different for a small section close to the joints.

(4) The experimental buckling load is determined only from the sudden increase of the deflection of the frame. Hence the true buckling load will be close to the observed one.

8.8 Equivalent Modulus of Elasticity

In order to determine the magnitude of tension during the experiment, aluminium ring beam load cells were connected to the diagonals. Due to the introduction of these load cells in the diagonals, the stiffness of the diagonals will vary slightly from the stiffness of the diagonals which don't have any load cells. The term, equivalent modulus of elasticity, is used to denote the stiffness of a diagonal with a ring beam load cell. The equivalent modulus of elasticity is used in place of the modulus of elasticity of the diagonals in the computer program. The equivalent modulus of elasticity can be taken as follows.

Using the strength of materials approach Hafez (5) has derived the following expression to calculate the deflection (Δ_{rb}) of a ring beam subjected to a tensile force (T_b). Δ_{rb} can be written as:

$$\Delta_{rb} = \frac{\pi T_b R_b}{4E_b A_b} + \frac{\pi T_b R_b}{4G_b A_b} + \frac{T_b R_b^3}{4E_b I_b}\left(\pi - \frac{\pi}{8}\right) \tag{8.1}$$

where E_b = the modulus of elasticity of the ring beam; A_b = the cross-sectional area of the ring beam; I_b = the moment of inertia of the ring beam; and R_b = the mean radius of the ring beam.

The axial elongation (Δ_{di}) of the diagonal member due to a tension T_b in the diagonal can be written as follows:

$$\Delta_{di} = \frac{T_b \ell_{ad}}{E_d A_d} \tag{8.2}$$

where ℓ_{ad} = the actual length of the rods used in the diagonal; A_d = the cross-sectional area of the diagonal member; and E_d = the modulus of elasticity of the diagonal member. The total increase in the length (Δ_{dt}) of the diagonal member is,

$$\Delta_{dt} = \Delta_{di} + \Delta_{rb} \tag{8.3}$$

Thus, the combined axial stiffness (S_{comb}) of the diagonal member is given by:

$$S_{comb} = \frac{T_b}{\Delta_{dt}} \tag{8.4}$$

Using Eq. 8.4 the equivalent modulus of elasticity (E_e) may be written as:

$$E_e = \frac{S_{comb} \ell_d}{A_d} \tag{8.5}$$

8.4 Comparison of Ideal and Model Frames

The buckling load predicted by the computer program is applicable only to the ideal frames. All the frames used in the practical situation will be real frames. The critical load of an ideal frame can be used, however as an approximate value to the buckling load of a real frame. Depending upon the initial imperfections in the model frame the experimental buckling load will deviate from the calculated ideal frame buckling load. Although the measured initial imperfections were not used anywhere in this thesis, they were measured just to get an idea of the shape of the frame prior to loading. The following are true for the ideal lattice frames. The lateral deflection will increase indefinitely only at the instant of buckling and there is no deflection prior to buckling. At the instant of buckling the tension in all the diagonals will be reduced to zero.

The following aspects are true with the experimental frame. The lateral defelction of an experimental frame will also increase indefinitely at the instant of buckling and in fact the buckling load is identified only by the indefinite increase of the deflection during the experiment. The load just prior to buckling is assumed to be the buckling load of the frame. The experimental frame will start deflecting as soon as it is loaded. The initial imperfections will be magnified. The tension in all the diagonals will not disappear when the experimental frame buckles. Since the deflection starts with the frame prior to the buckling load, the tension in one set of the diagonals will decrease faster than the other set (explained later in this chapter). The tension in

each diagonal is controlled by the axial deformation of the members and the deflection at the nodal points. The experimental results are discussed in the following sections.

8.5 Comparison of the Theoretical and Experimental Results

The critical load, minimum effective pretension and the optimum pretension were calculated for an ideal pin-ended three-segment lattice frame. The experimental buckling load, deflections and the tension in the diagonals obtained from the model frame are discussed together with the available theoretical results.

8.5.1 Buckling Load

Fig. 8.1 illustrates the deflection of the battened frame model with load (when the ring beam load cells are removed from the diagonals the diagonals become discontinuous and the frame behaves like a battened frame). The theoretical critical load is also shown in the figure. As mentioned earlier the experimental buckling load of a frame is determined only from the relatively large increase in the deflection at a constant load. From the experiment the buckling load can be taken as approximately 6.25 kips and the theoretical critical load is 6.68 kips. The experimental buckling load is 6% lower than the theoretical load. The initial imperfections present in the frame prior to the buckling might have caused this 6% difference. The theoretical predictions indicate that the frame will fail by Mode I buckling. From the buckled shape shown in the figure it is apparent that the experimental battened frame also fails by a shape similar to the Mode I buckling.

Figs. 8.2 to 8.4 illustrate the plots of load versus deflection

when the pretension is smaller than the minimum effective pretension (230 lbs). The theoretical buckling load of the lattice frame remains the same as the battened frame critical load and equal to 6.68 kips. These figures reveal that the experimental buckling load is greater than 6.68 kips. When the initial pretension is 50 lbs the experimental buckling load is equal to 7.5 kips which is 12% more than the predicted value. As the initial pretension increases the difference in the buckling load also increases. For example, at an initial pretension value of 100 lbs the buckling load is 8 kips and it is 19% greater than 6.68 kips. The buckling shape is somewhat similar to the predicted Mode I buckling. The anticipated reason for this increase in load has been discussed in a later portion of this section. The load-deflection plot shown in Fig. 8.5 corresponds to the minimum effective pretension. The experimental buckling load is 34% greater than the predicted 6.68 kips.

Figs. 8.5 to 8.9 show the load-deflection plots corresponding to the initial pretensions between the minimum effective pretension (230 lbs) and 400 lbs. At the initial pretension of 260 lbs the experimental buckling load (9.3 kips) is 24% greater than the predicted value. When the diagonal pretension is 230 lbs. the failure is governed by Mode I buckling and the failure is governed by Mode II buckling when the diagonal pretension is 500 lbs. Hence the point of bifurcation will be at one value of initial pretension inbetween the minimum effective and the optimum pretensions. The mode of failure for the experimental frame when the initial pretensions are inbetween 260 and 400 lbs is somewhat similar to Mode II buckling. As the diagonal pretension increases beyond 260 lbs the difference between the

experimental and the theoretical buckling load becomes relatively small. For example, at the initial pretension of 350 lbs the experimental buckling load is only 10% greater than the theoretical value (Fig. 8.8). The buckling shape is also more close to Mode II buckling.

Figs. 8.9 to 8.11 illustrate the plot of load versus deflection when the initial pretension is between 400 and 500 lbs. In this region the experimental buckling load is smaller than the predicted load. For example, when the pretension is 450 lbs the experimental buckling load (12.4 kips) is 5% smaller than the predicted values. As the diagonal pretension increases this difference also increases. Figs. 8.12 and 8.13 correspond to the plot of load-deflection when the initial pretension is greater than the optimum tension. When the initial pretension is greater than 500 lbs, the difference between the theoretical and the experimental buckling loads remains constant at 14%. Fig. 8.14 illustrates the plot of theoretical and experimental buckling loads versus initial pretension. In some of the figures discussed above, the buckled shape of one leg of the frame is similar to Mode I buckling and the other leg is similar to Mode II buckling. These things would have happened probably due to the unequal imperfections in the legs.

There is a considerable difference between the theoretical and the experimental buckling loads. Usually the experimental buckling load will be affected considerably by the initial imperfections present. The buckling loads of the model frame used in the experimental study are greater than the predicted loads for some values of initial pretensions, and they are smaller for some other values of initial pretensions. The possible

reason for this difference may be explained as follows. Six types of buckling shapes are shown in Fig. 8.15. Fig. (a) is similar to Mode I failure and the buckling shapes shown in Fig. (b) and (c) are high energy mode failures. Usually the shapes shown in Fig. 8.15(b) and (c) will not occur unless some external restraint (anywhere along the length) or some initial imperfections are present. As soon as the model frame is subjected to an increment of load it will start deflecting due to the initial imperfections present in the frame. Prior to the loading the net horizontal force on the crossarms will be zero. Once the load is introduced on the frame the deflections may cause unsymmetrical displacements and rotations at the nodes (due to the initial imperfections). These unsymmetrical displacements and rotations will vary the tension in the diagonals unsymmetrically. The deflections caused by the first increment of load will act as the imperfections for the following increment of loading. In a similar manner the deflection will continue to increase until the buckling of the real (or model) lattice frame occurs. Unless this nonlinear variation in the deflections and the joint coordinates in each increment of loading is included in the theoretical analysis there will be some difference between the theoretical and the experimental buckling loads. Using the buckled shapes it is possible to determine the relative magnitude of the theoretical and the experimental loads to some extent. The following expression is valid with Fig. 8.15.

$$P_{b8}, P_{c8}, P_{d8}, P_{f8} > P_{a8} \qquad (8.6)$$

where P_{a8}, P_{b8}, P_{c8}, P_{d8}, P_{e8} and P_{f8} are the corresponding buckling loads of Figs. 8.15 (a), (b), (c) (d), (e), (f). The theoretical buckling occurs by Mode I when the diagonal pretension is 230 lbs (minimum effective pretension) and the buckling occurs by Mode II, when the initial pretension is 500 lbs.(optimum pretension). Thus the point of bifurcation occurs at some intermediate values of the initial pretension. It is not possible to predict this point of bifurcation theoretically. From the modes of buckling the bifurcation point may be determined approximately as follows. If a column fails by Mode I buckling instead of Mode II buckling (theoretically predicted buckling shape) the buckling load will be smaller than the predicted buckling load and if the column fails by Mode II buckling instead of Mode I buckling (theoretically predicted buckling shape) the buckling load will be greater than the predicted buckling load. Hence from the difference in the buckling loads (positive or negative) the mode shapes can be determined approximately. The same procedure can be applied to determine the point of bifurcation between the initial pretensions 230 lbs and 500 lbs. Below the initial pretension of 400 lbs the experimental buckling loads are greater than the theoretical loads and above 400 lbs they are smaller than the theoretical loads. Hence around 400 lbs the bifurcation occurs (Mode I to Mode II change). Since the effect of the initial imperfections and the nonlinear variation in the deflection on the buckling loads are not known, the exact value of the initial pretension at which the bifurcation occurs cannot be determined. Figs. 8.1 to 8.9 reveal that at an initial pretension value below 400 lbs the model frame fails by one of the modes shown in Figs. 8.15 (except Fig. 8.15(d)) while the theoretical failure is similar to the one shown in Fig. 8.15(a). Hence from Eq. 8.6 it is clear that

the experimental buckling load is greater than the theoretical load. This increase in experimental buckling load may be due to the initial imperfections and the unsymmetrical variation in the coordinates (while the load is applied).

Similarly, the following expression is valid with the Fig. 8.15:

$$P_{d9} > P_{a9}, P_{b9}, P_{c9}, P_{e9}, P_{f9} \qquad (8.7)$$

in which P_{a9}, P_{b9}, P_{c9}, P_{d9}, P_{e9} and P_{f9} correspond to the buckling loads of the Figs. 8.15 (a) to (f). When the initial pretension is above 400 lbs the experimental buckling occurs in one of the modes shown in Figs. 8.15 (a), (b), (c), (e), (f), while the theoretical buckling occurs by buckling mode shown in Fig. 8.15(d). Hence according to Eq. 8.7 the experimental buckling load is smaller than the theoretical load. This decrease in experimental buckling load may be due to the initial imperfections and the unsymmetrical variation of nodal coordinates (while the load is applied).

8.5.2 Deflections

The deflections at several points were recorded during the experiment. When the Mode I buckling occurs with a symmetrical real frame, the deflection at the mid-height of the frame will be greater than the deflection at other locations and when the Mode II buckling occurs there is no deflection at the crossarm levels while the deflections are equal at the mid-point of all the segments. Since the computer program used

in this study is applicable only for the ideal frames, it is not possible to calculate the deflections using the computer program.

Fig. 8.1 illustrates the plot of load versus deflection of the battened frame model. The predicted mode of failure is by Mode I buckling. The buckled shape of the frame is also shown in the same figure (for the sake of convenience the deflected points in the buckled shape figure are joined by straight lines instead of a curve). The deflection at 1/3 height (from the top support) is greater than the deflection at other sections of the battened frame. Three deflection curves are shown in the figure (1/6 height, 1/3 height and 1/2 height). The deflections used in this plot are measured from the left leg of the frame. A few trial experiments have showed that the deflection at the 1/3 height is relatively large for battened frames and it is quite large at 1/6 height of the left leg (from top support) for lattice frames. Hence 1/3 height deflection is used to identify the buckling of the battened frame and 1/6 height deflection is used to identify the lattice frame buckling load when carrying out the experiment. For battened frames the deflections at 1/6 height, 1/3 height and 1/2 height increases uniformly . The deflection of the battened frame just prior to the buckling is approximately 0.045 in.

Figs. 8.2 to 8.5 also illustrate the load-deflection curves. The diagonal pretensions are varied between 50 lbs and 230 lbs. (minimum effective pretension). From Fig. 8.2 (pretension = 50 lbs) it is clear that the deflection at the 1/6 height is greater than the deflection at mid-height. The mid-height deflection just prior to buckling is reduced to one-fourth of the corresponding deflection of the battened frame. From

the buckled shape shown, it is clear that the deflection in both legs are not similar, one leg deflects more than the other. When the diagonal pretension is between 100 lbs and 230 lbs (Figs. 8.3 to 8.5) the mid-height deflection slowly increases at the initial stages of loading and it decreases at the latter stages of loading. The 1/6 height deflections are smaller than the corresponding deflections of the battened frame. Figs. 8.6 to 8.11 represent the plot of load versus deflection for the value of initial pretension between the minimum effective and the optimum pretensions. These figures also show that the buckled shape of both legs are not similar. As the initial pretension reaches a value close to the optimum pretension the 1/6 height deflection just prior to buckling is almost equal to the battened frame deflection in the corresponding location. The deflection of the lattice frame for a diagonal pretension value greater than the optimum pretension are shown in Figs. 8.12 and 8.13. The observations made with regard to previous figures are also valid to these figures.

8.5.3 Diagonal Tension

As mentioned in the previous sections when a lattice frame is loaded the diagonal tension in one set of the diagonals will increase and in the other set of the diagonals it will decrease. Referring to Fig. 7.1, it can be concluded that when the frame deflects to the right side, the tension in the diagonals 2 and 5 will increase and the tension in the diagonals 1 and 6 will decrease. The tension in the diagonals 3 and 4 will decrease equally if the displacements and the deformations of the vertical members in the mid-segment are equal. If not the increase or the decrease in the tension will be decided accordingly.

The tension in the diagonals of a real frame is influenced by two factors. They are, (1) the deflections in the frame, and (2) the axial deformations of the member. The combined effect of these two factors will decide the change of tension in the diagonals. Well below the buckling load the influence of the axial shortening will be more than the influence of the deflection on the tension in the diagonals. Hence the tension in all the diagonals will decrease with the increase of the load. The rate of decrease in the diagonal tension will be less in the diagonals which resist the deflection (diagonals 1 and 6) than in the other diagonals (diagonals 2 and 5). The rate of tension change will be almost linear. Close to the buckling load the influence of the deflection on the diagonal tension will be more than the influence of the axial shortening of the members. Hence, the tension in the diagonals which resist the deflection will start increasing suddenly. In the other set of diagonals the tension either will disappear (if the initial pretension is less than or equal to the optimum pretension) or some tension will remain (if the initial pretension is greater than the optimum pretension). The experimental results are similar to what has been described above. Figs. 8.16 to 8.27 show the experimental load-diagonal tension curves for initial pretensions from 50 lbs to 600 lbs. Six curves are shown in each figure. The curves in the dotted lines indicate the tension in the diagonals which resist the deflection and the solid lines represent the tension in the other diagonals. Fig. 8.22 to 8.25 indicate that at the time of buckling a small amount of residual tension is left over in the diagonals which do not resist the deflection, even when the initial pretension is smaller than the optimum pretension. This is probably due to

the unsymmetrical displacements of the nodes.

CHAPTER 9

CONCLUSIONS AND RECOMMENDATIONS

9.1 General

This thesis dealt with the behaviour of a two-dimensional lattice frame (diagonally pretensioned) subjected to vertical loads. An analysis was initiated to determine the relationship between the buckling load of the frame and the initial pretension. The theoretical critical loads were predicted using a computer program. The effect of various parameters like crossarm length, size and the modulus of elasticity of diagonals on the critical load and the behaviour of the frame were studied. All these investigations were conducted on a three-segment frame. A procedure was suggested for the design of ideal lattice frames. An experimental investigation was conducted to compare the theoretical and the experimental results.

9.2 Conclusion

The conclusions obtained from this study are listed as follows:

(1) The maximum critical load of a diagonally pretensioned lattice frame (simply referred to as a lattice frame) is several times greater than the critical load of a similar battened frame.

(2) The relationship between the critical load and the initial pretension is linear between the minimum effective pretension and the optimum pretension and between the optimum pretension and the maximum possible pretension.

(3) If the initial pretension is smaller than the minimum effective pretension, the lattice frame critical load will be equal to the critical load of the battened frame and when it is equal to the optimum

pretension, the critical load will be equal to the maximum critical load of the lattice frame. The lattice frame cannot carry any external load if the initial pretension is equal to the maximum possible pretension.

(4) When the initial diagonal tension is between the minimum effective and the optimum pretensions the critical load will increase with an increase in the initial pretension and if it is between the optimum and the maximum pretensions the critical load will decrease with an increase in the initial pretension.

(5) The battened frames will have a small restraint against translation, due to the absence of the diagonal members. The critical load of a battened frame will increase with the decrease in the crossarm length. The failure of a battened frame is governed by the Mode I buckling irrespective of the length of the crossarm.

(6) The critical load of a lattice frame is influenced by various parameters like the crossarm length, size and the modulus of elasticity of the diagonals. If the crossarm length is relatively long it will create a small rotational restraint and vice versa. When the size and the modulus of elasticity of the diagonals and the crossarm length are relatively large, the created translational restraint will also be large. Mode I buckling governs the failure of a lattice frame when the translational restraint is relatively small and the Mode II buckling governs the failure of a lattice frame when the translational restraint is relatively large.

(7) The minimum effective pretension depends partly upon the

critical load of the battened frame and the optimum pretension depends partly upon the maximum critical load of the lattice frame. An increase in the corresponding critical loads will increase the minimum effective and the optimum pretensions. The increase in the size and the modulus of elasticity of the diagonal will increase the initial pretensions irrespective of the corresponding critical loads.

(8) The efficiency of the lattice frame is controlled by the following two factors. They are, the critical load and the total weight of the frame. An increase in the crossarm length either will increase or will decrease the critical load of a lattice frame. But the over all weight of the frame will decrease with the decrease in the crossarm length and vice versa. In the increasing portion of the critical load-crossarm length curve efficiency also will increase and in the decreasing portion, the efficiency also will decrease. The decrease in the crossarm length will increase the efficiency of a battened frame and vice versa.

(9) An increase in the diagonal size will increase the total weight of the lattice frame. If the increase in the diagonal size causes a relatively large increase in the critical load and a relatively small increase in the total weight, the efficiency will increase and if the critical load remains constant the efficiency will decrease. The change in the modulus of elasticity of the diagonal will not have any impact on the total weight of the frame. If the change in the modulus of elasticity increases the critical load, then the efficiency will also increase and if the critical load remains constant, the efficiency of the lattice frame will

also remain constant.

(10) An increase in the critical load does not necessarily mean an increase in the efficiency.

(11) An increase in the number of segments of a frame will increase the critical load of the frame and the increase or the decrease in the efficiency depends upon the relative change in the total weight.

(12) The effective length factor (k) is a useful factor to check the maximum capacity of a frame. According to the theory of columns it is possible to achieve a minimum value equal to 0.5. The computer analysis of a lattice frame shows that it is practically not possible to achieve a k value below 0.55

(13) It is possible to use the computer program to design a lattice frame efficiently.

(14) The experimental results have showed that there is a difference between the theoretical and the experimental buckling loads ranging from 0 to 34%. At large values of the initial pretensions the experimental buckling load is smaller and at small values of initial pretensions the experimental buckling load is larger than the theoretical loads. The initial imperfections and the unsymmetrical displacements of the nodes while loading might have caused the above differences.

9.3 Suggestions for Further Research

In this study a limited investigation was made to the ideal lattice frames subjected to vertical loads. Due to the imperfections present in the model frame a considerable difference has occurred between the theoretical and the experimental buckling loads. The study of the

following aspects will be useful in this research area.

(1) A nonlinear analysis of the frames which includes the initial imperfections.

(2) The effect of offset diagonals in a lattice frame.

(3) The behaviour of the structure for other forms of loads (like lateral loads).

(4) A three-dimensional analysis of a lattice frame .

(5) The use of the crossarms (in the frames) having the sectional and the material properties other than the vertical member.

(6) In elastic buckling behaviour of the lattice frame.

ILLUSTRATIONS

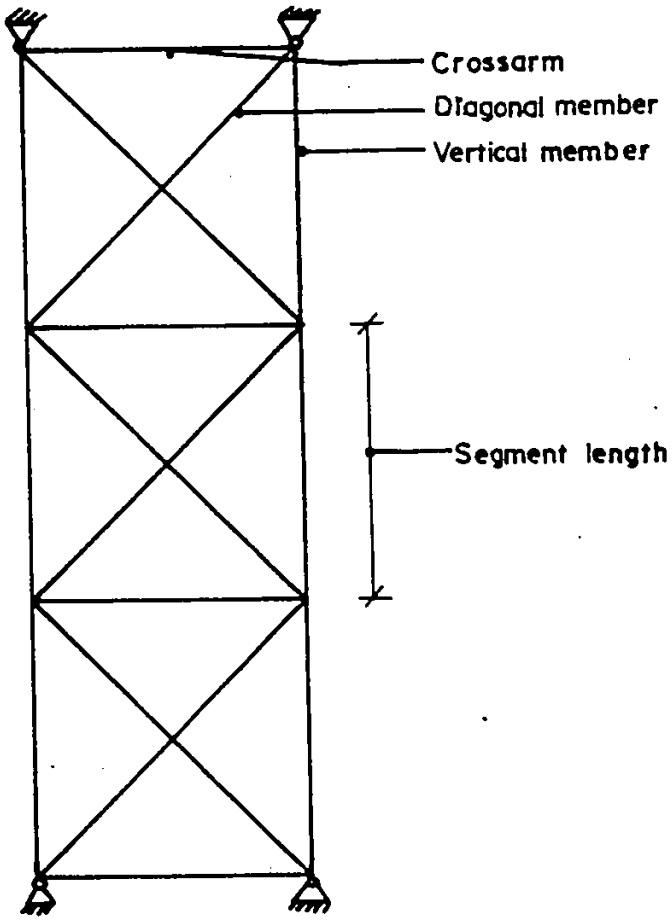

Fig. 1.1 Components of Lattice Frame

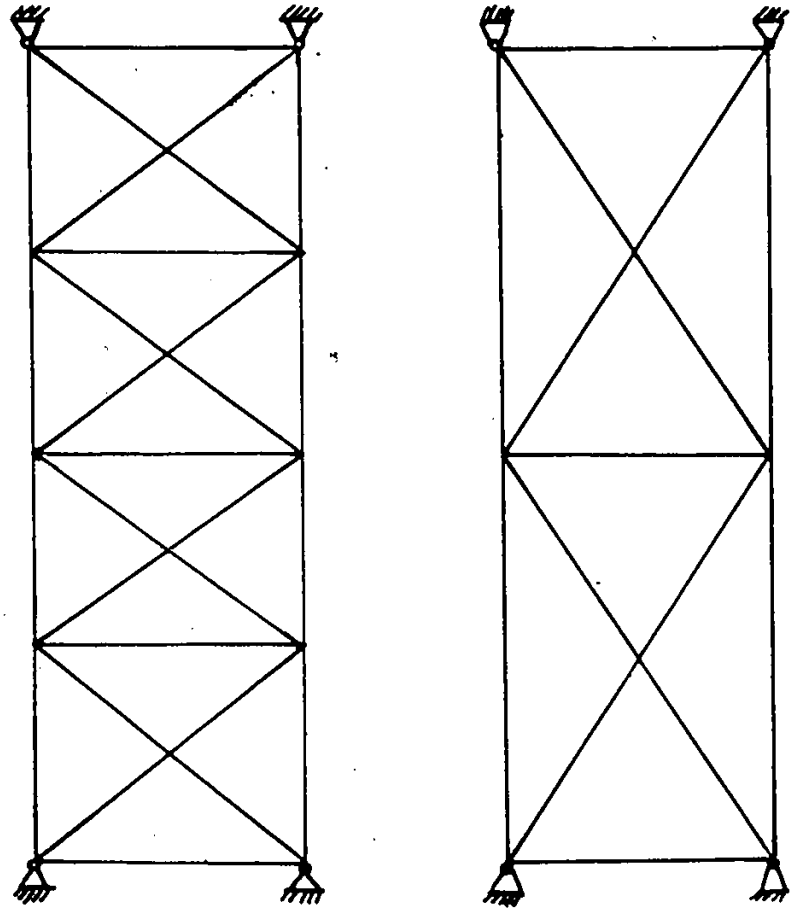

(a) (b)

Four Segment Lattice Frame Two Segment Lattice Frame

Fig. 1.2

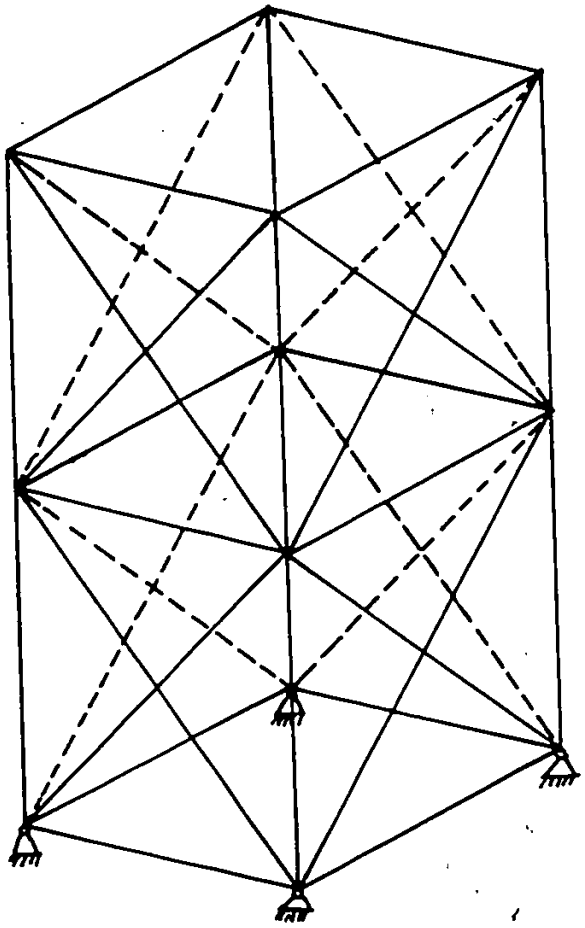

Fig. 1.3 Three-Dimensional Pretensioned Structure

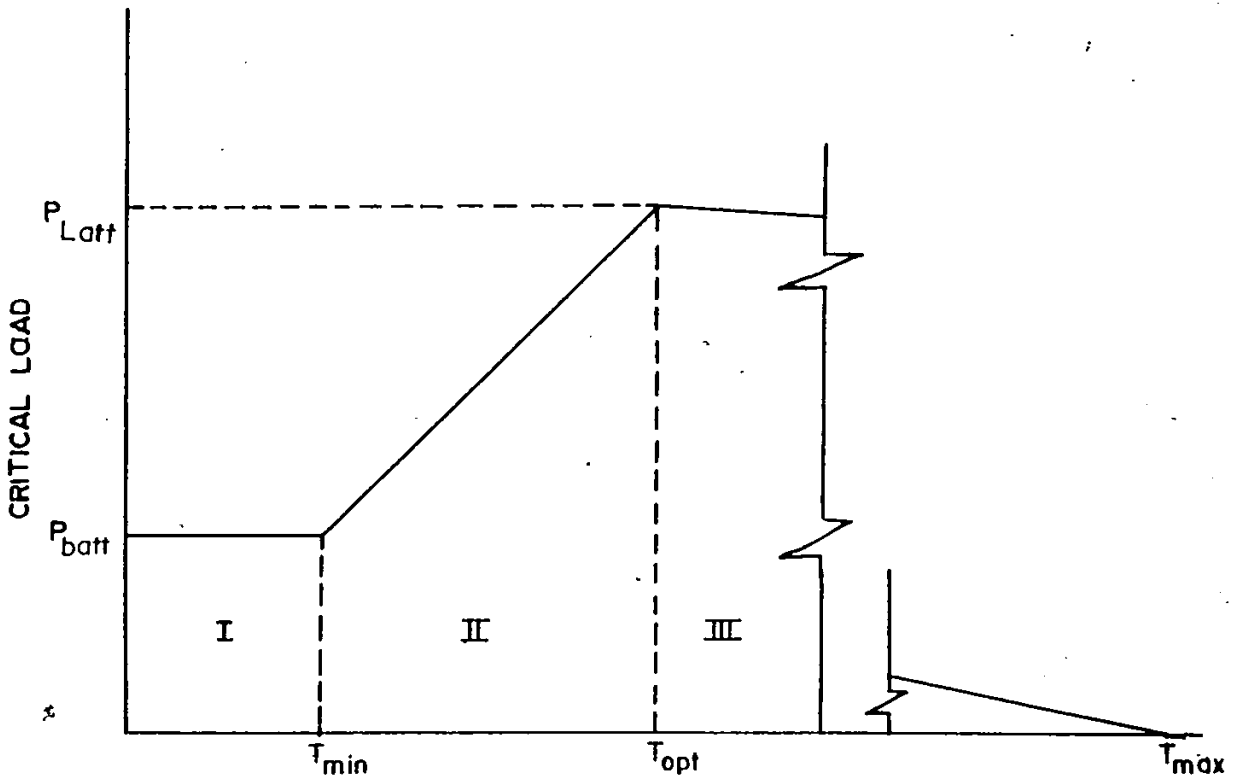

Fig. 1.4 Relationship Between Critical Load and Initial Pretension

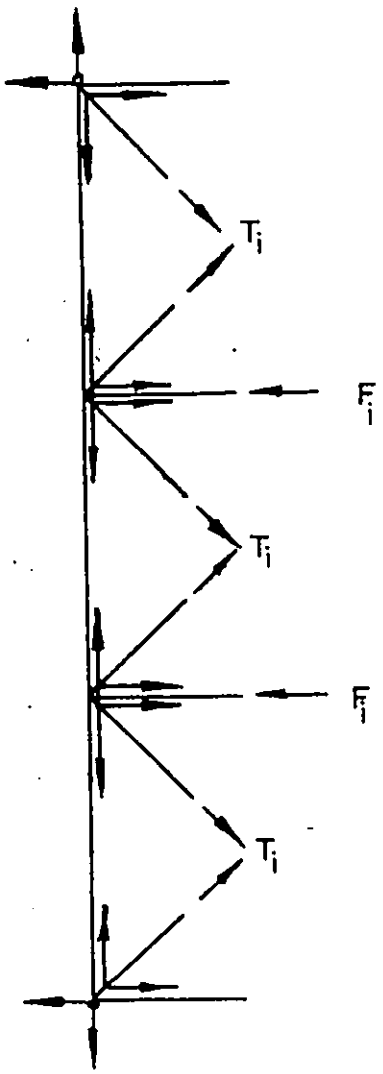

Fig. 3.1 Forces in the Members of Lattice Frame Prior to Loading

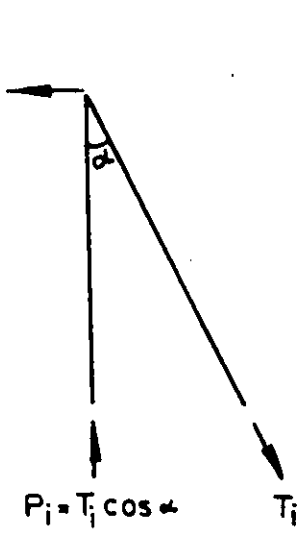

(a) Initial Condition at the End of Vertical Member.

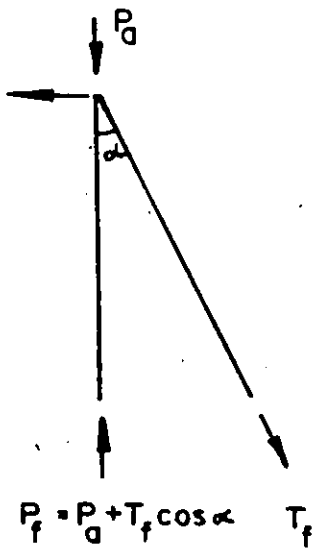

(b) Final condition at the End of Vertical Member.

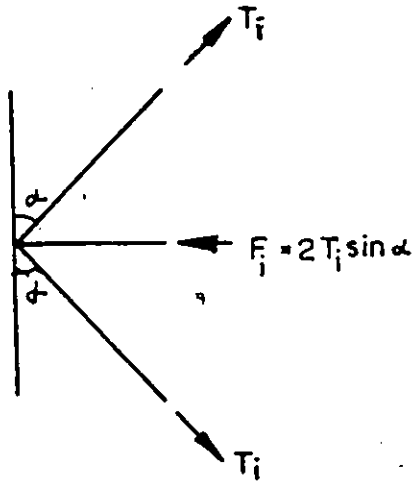

(c) Initial Condition at the End of Crossarm.

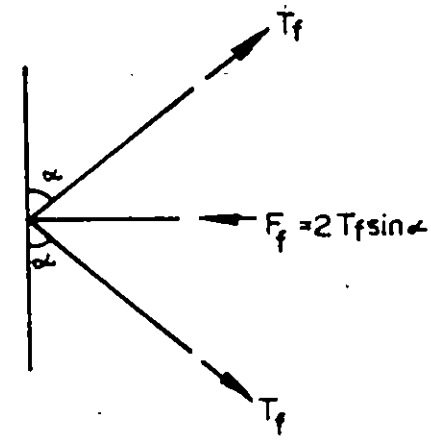

(d) Final Condition at the End of Crossarm.

Fig. 3.2 Free Body Diagram of Forces in Diagonally Pretensioned Lattice Frame.

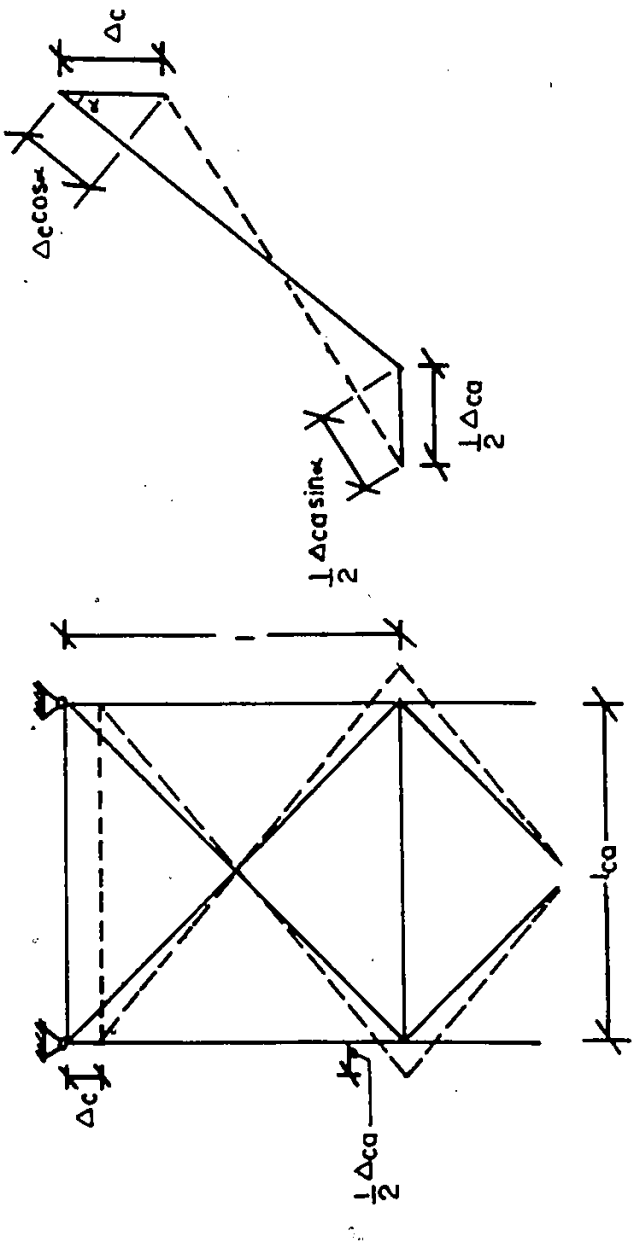

Fig. 3.3 Change in Length of Members.

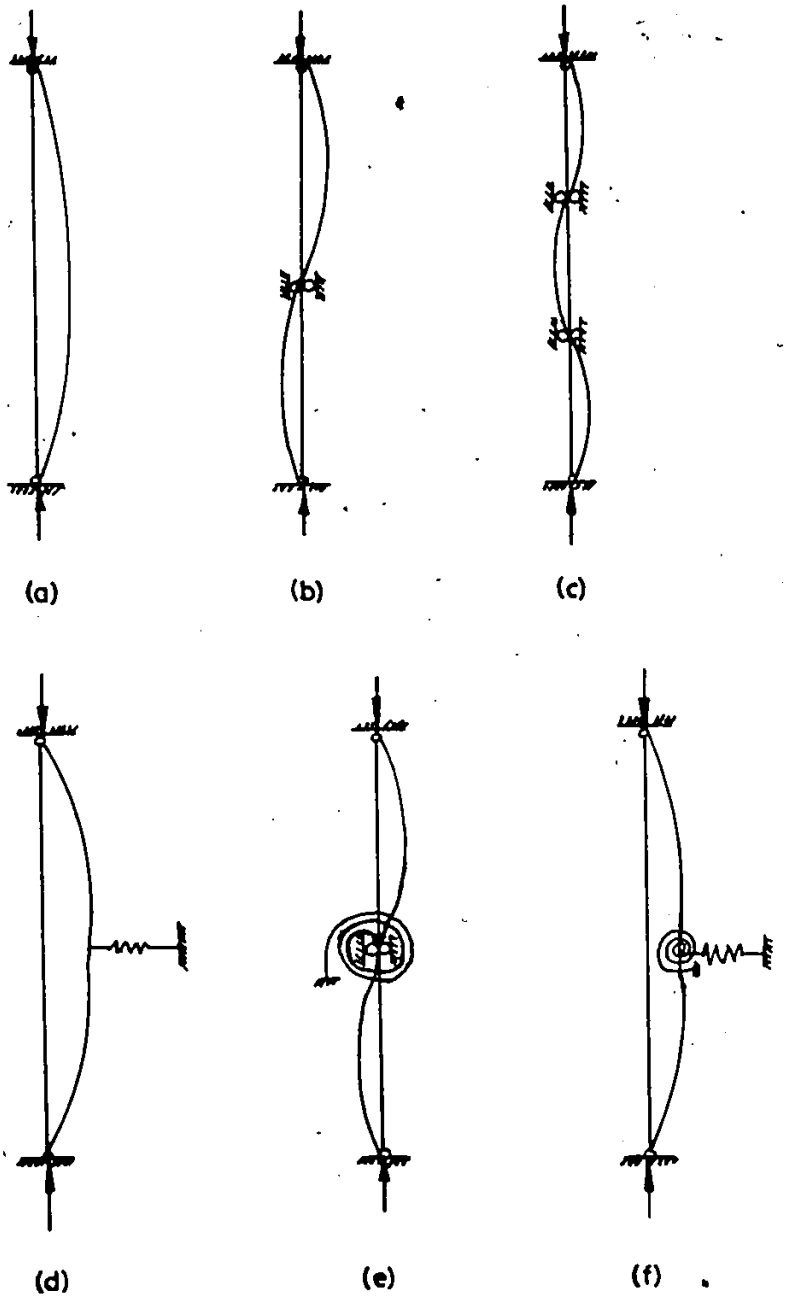

Fig. 4.1 Columns with Various Types of Restraints.

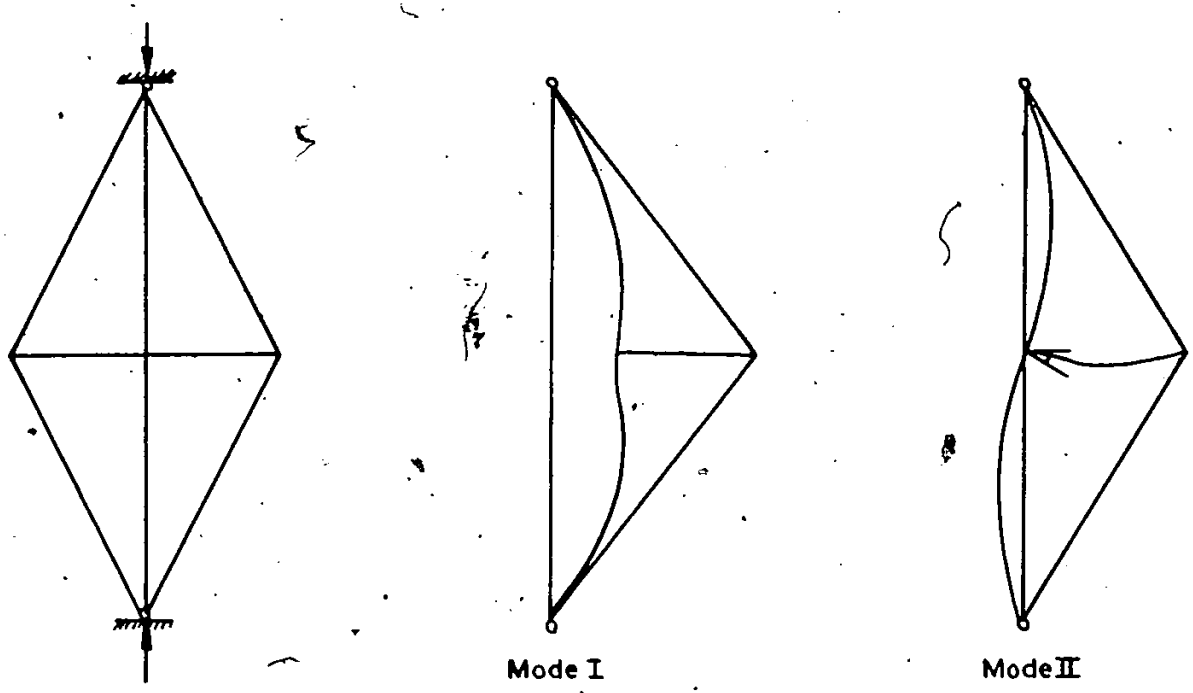

Fig. 4.2 Buckling Modes of Pin-Ended Stayed Column.

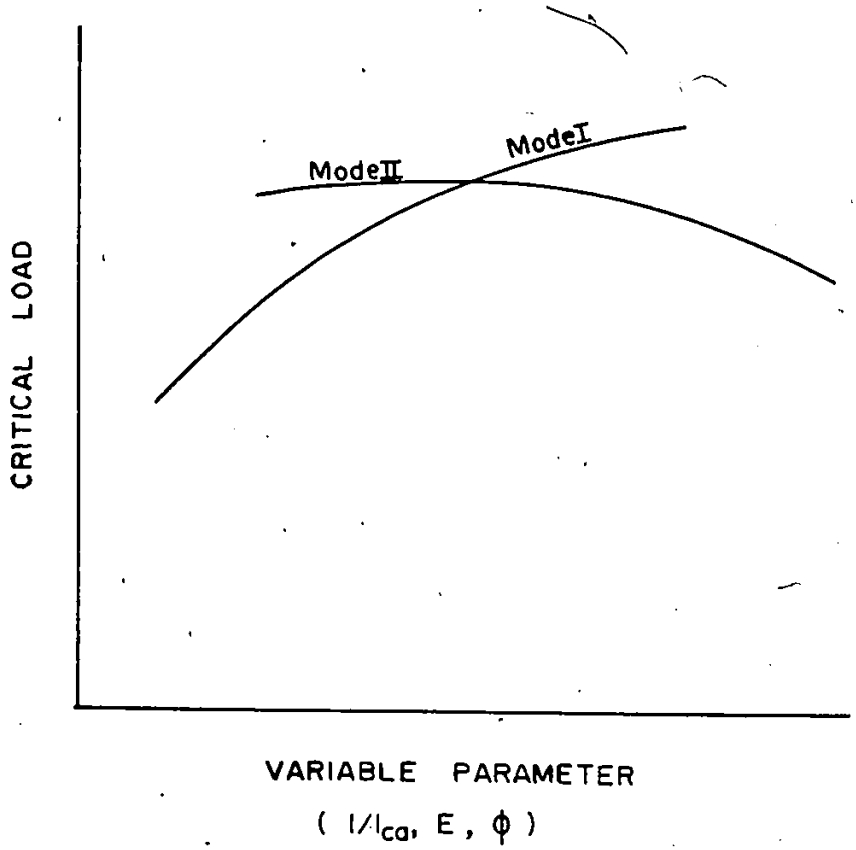

Fig. 4.3 Load Versus a Variable Parameter.

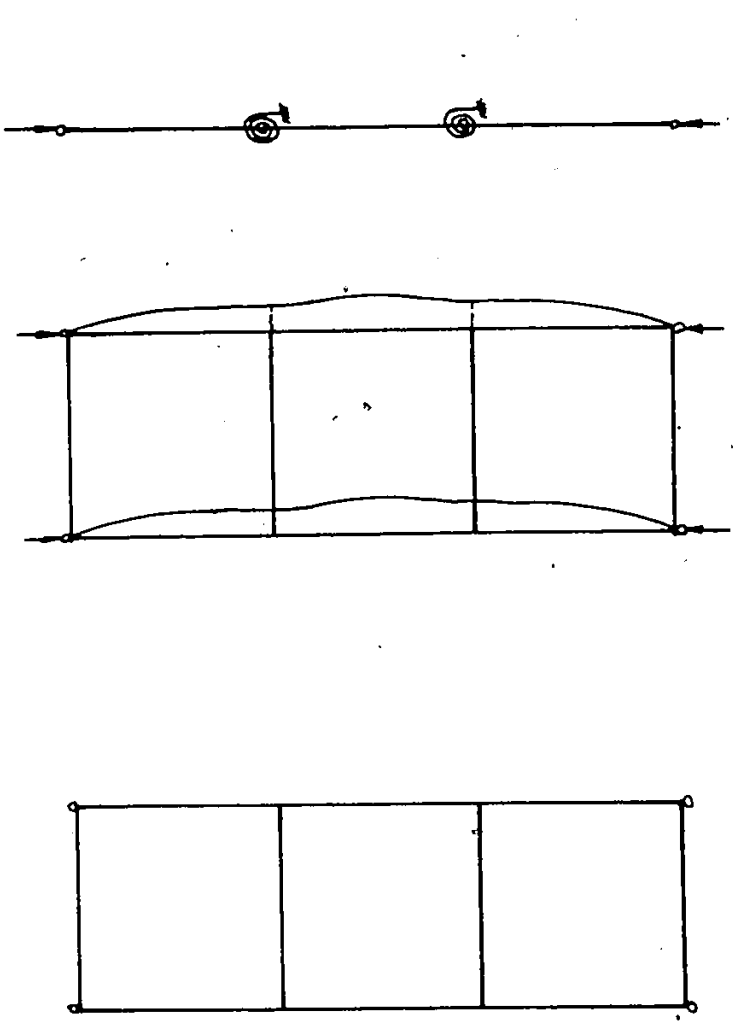

Fig. 4.4 Buckling Mode of Battened Frame.

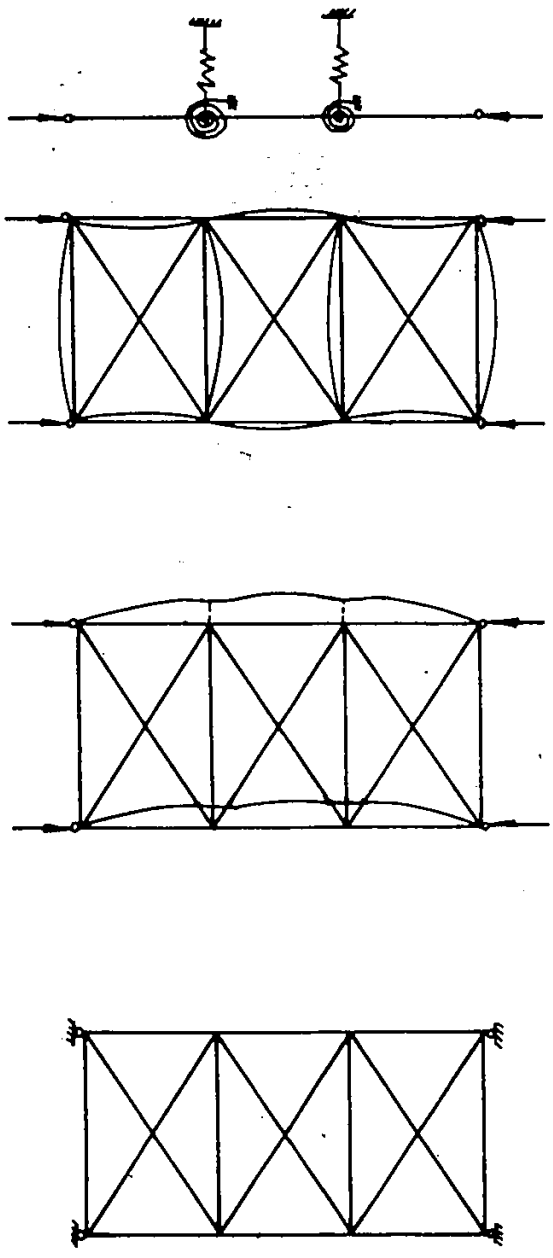

Fig. 4.5 Buckling Modes of Lattice Frame.

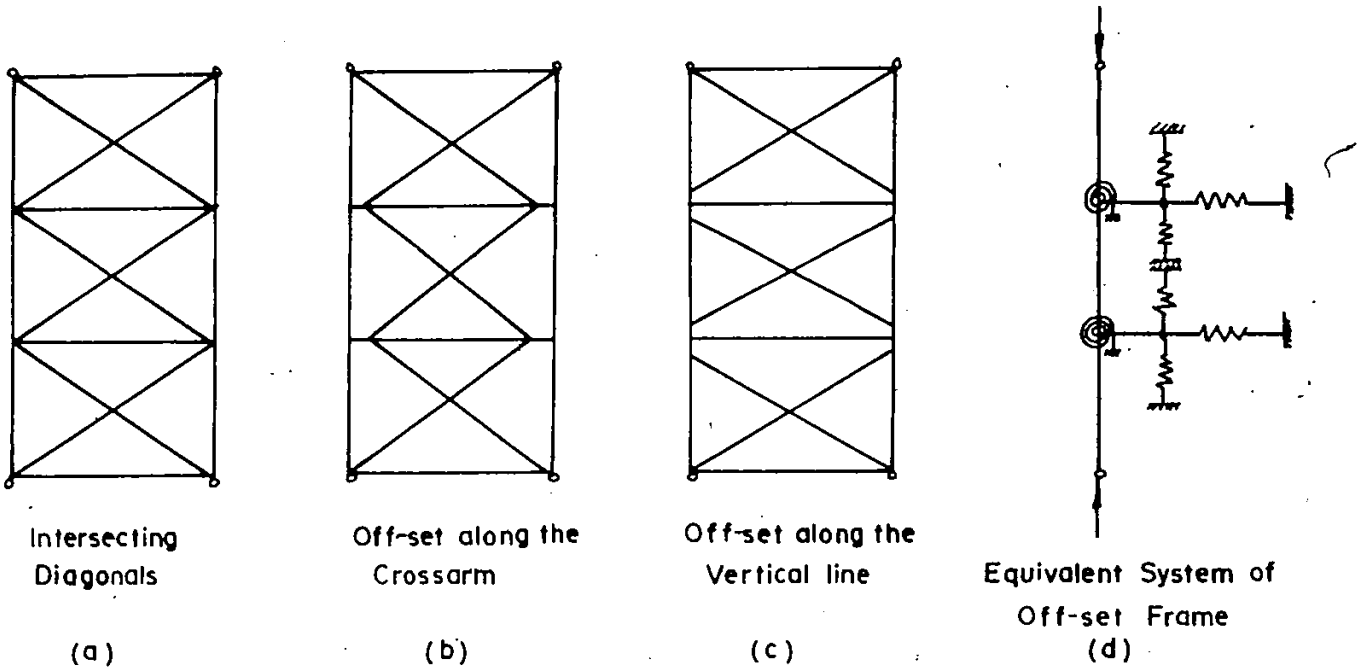

Fig. 4.6 Various Arrangements of Diagonals in Lattice Frame.

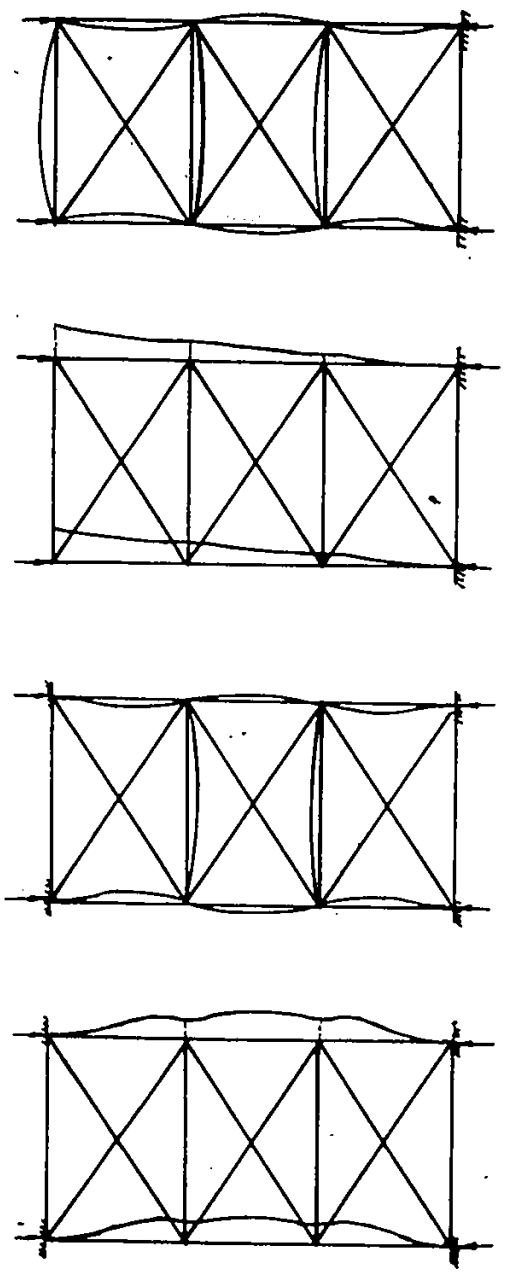

Fig. 4.7 Buckling Modes of Lattice Frame With Various End Conditions.

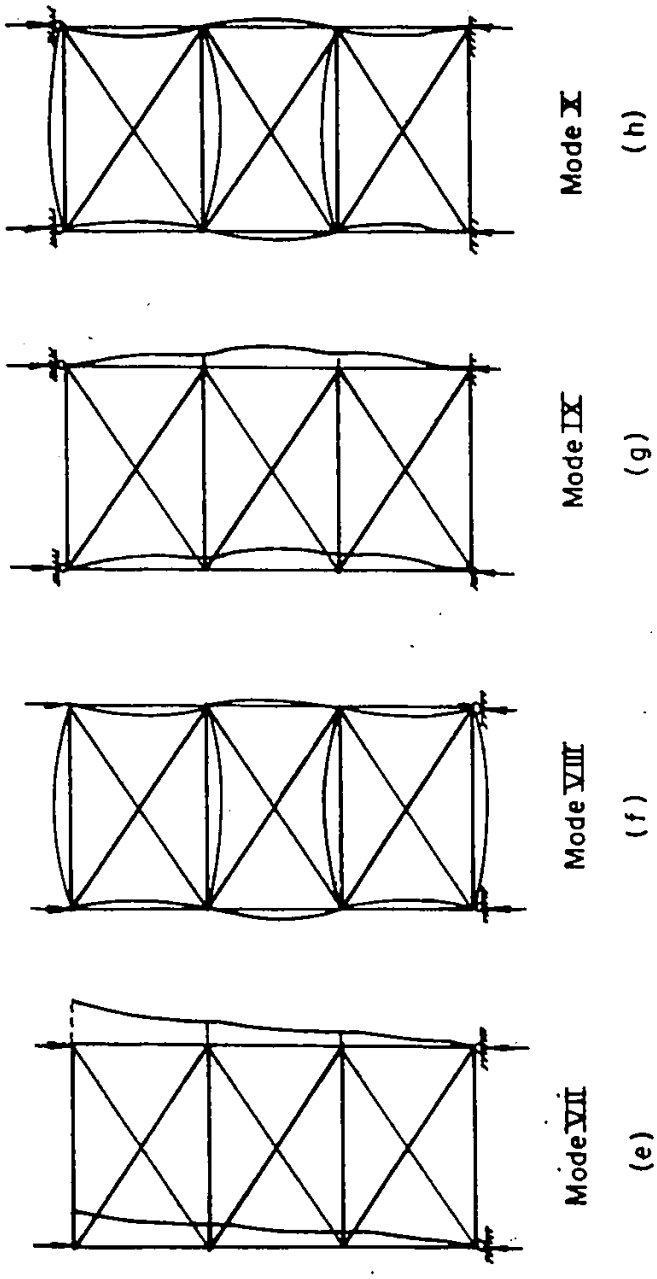

Fig. 4.7 Buckling Modes of Lattice Frame With Various End Conditions.

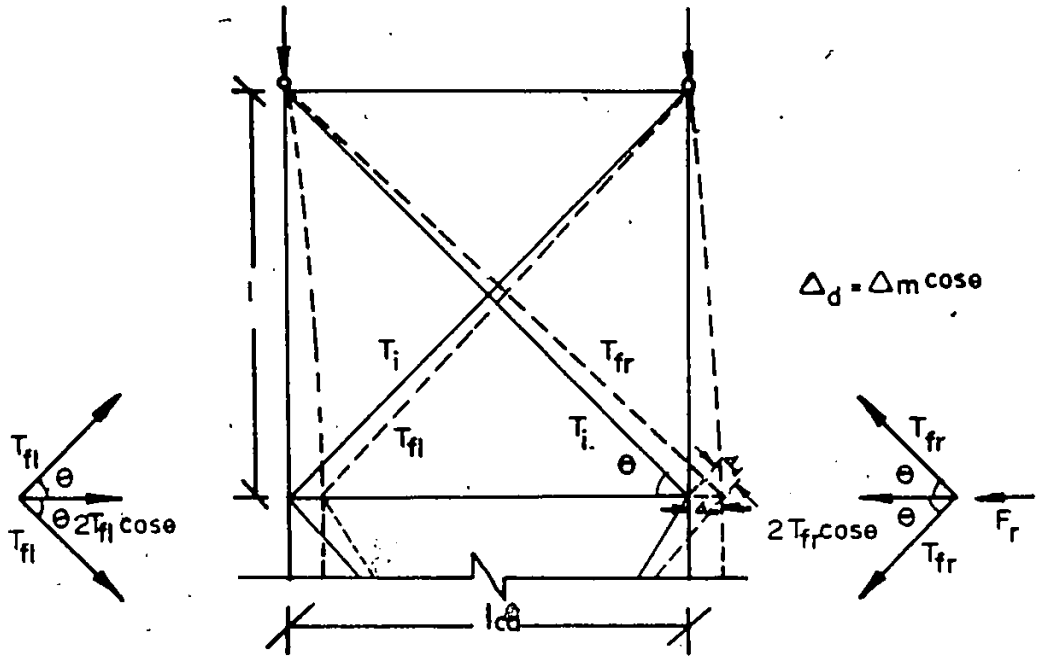

Fig. 4.8 Lateral Restraint Force in Lattice Frame.

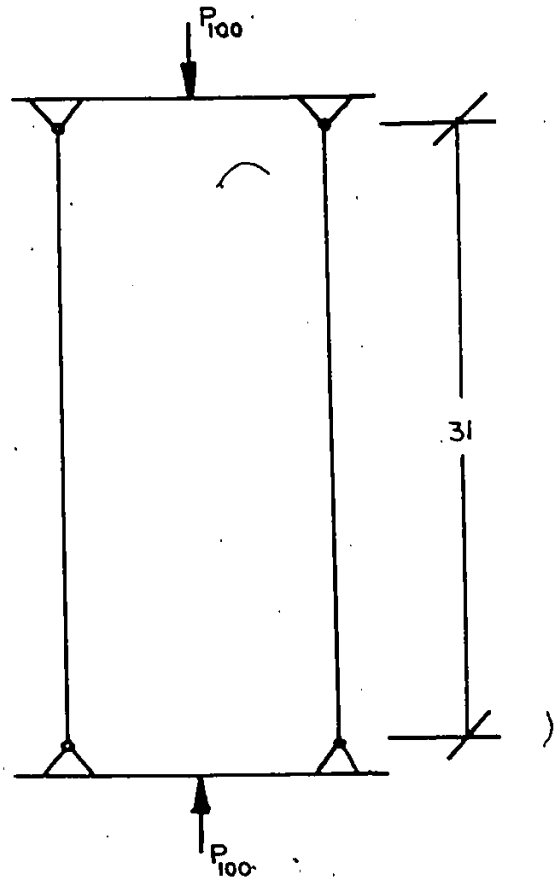

Fig. 4.9 Reference Frame for Efficiency Calculation.

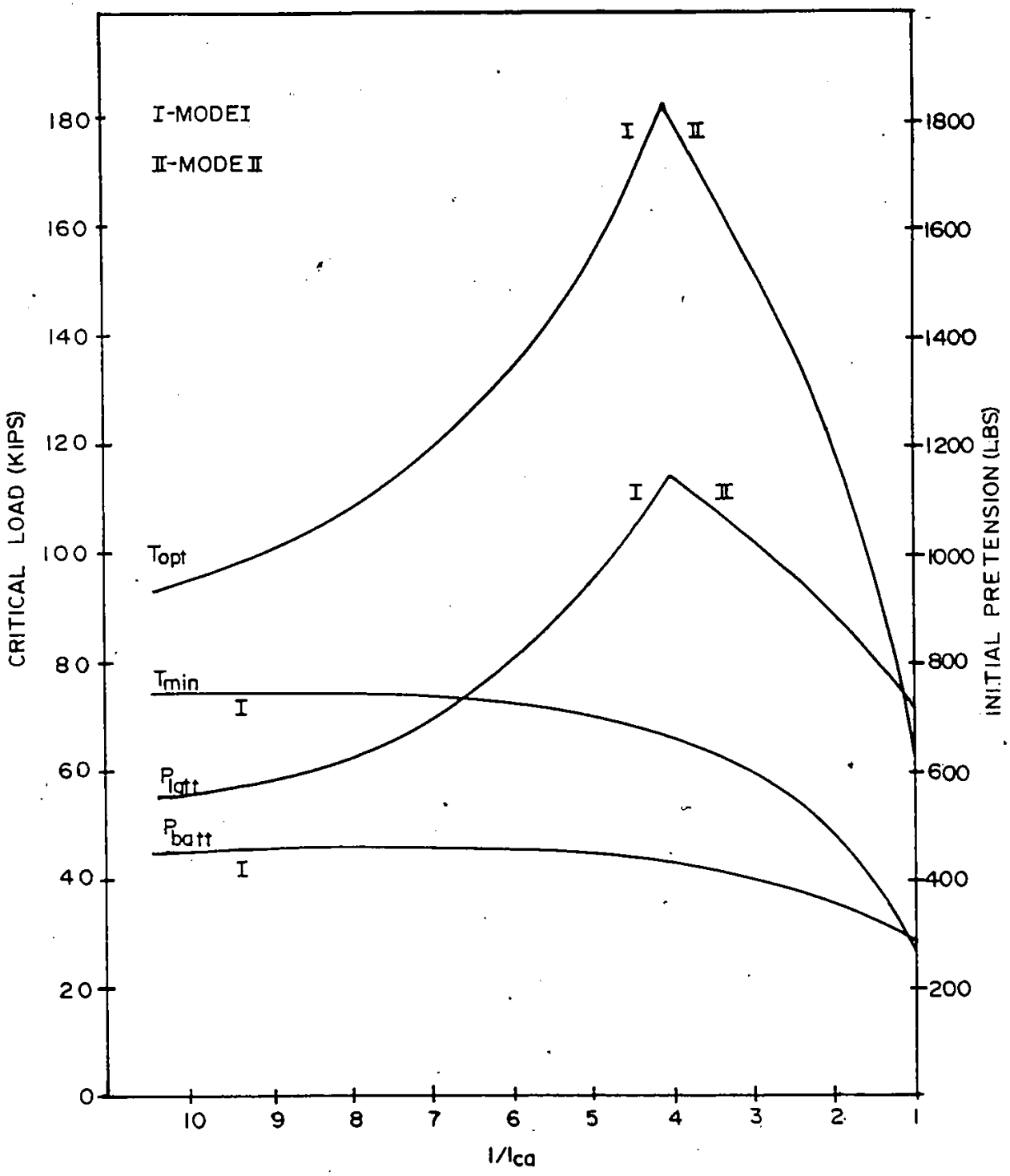

Fig. 4.10 Effect of Crossarm Length for a Diagonal Size of 0.1875 in. and Modulus of Elasticity of 29600 ksi.

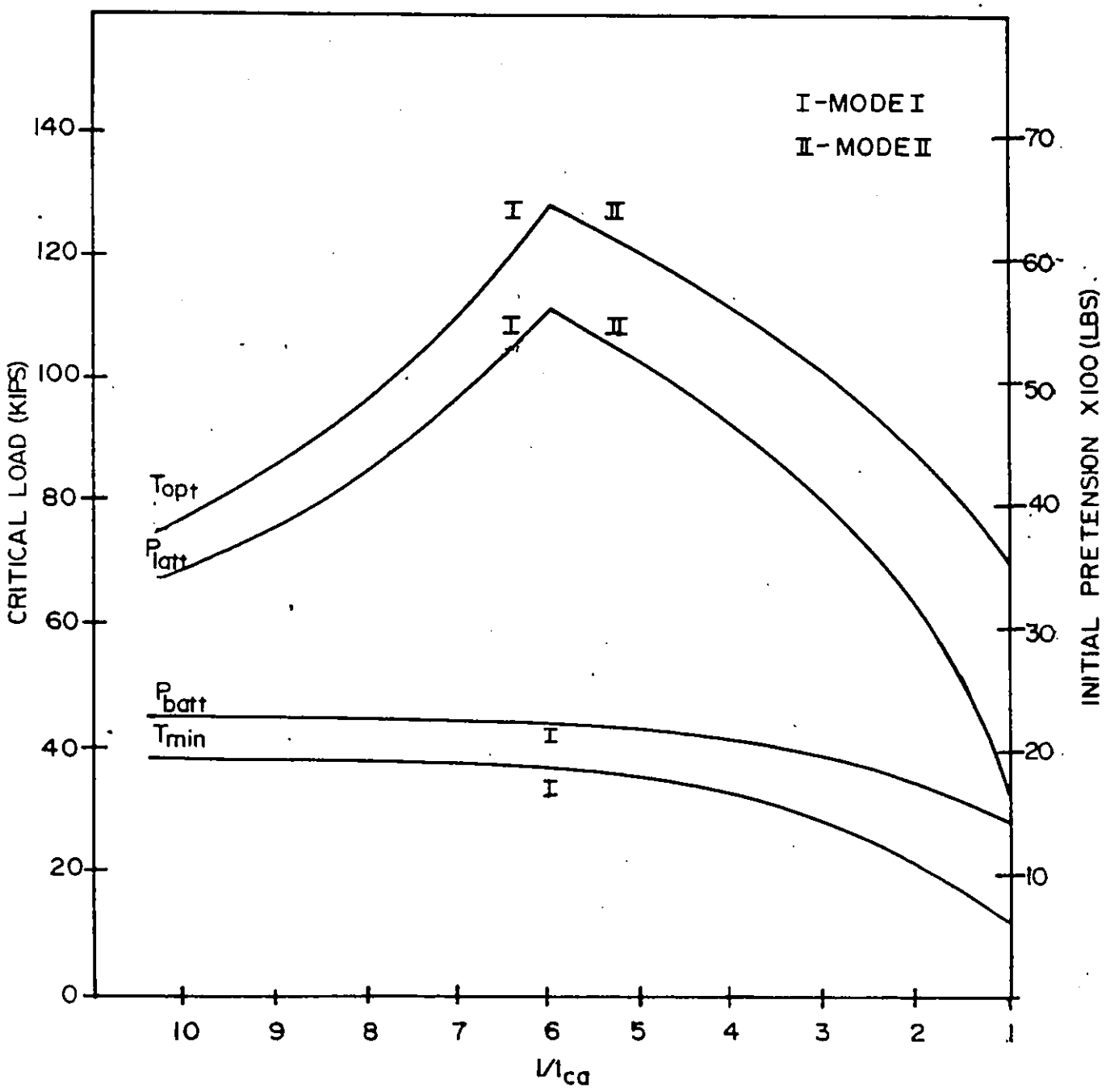

Fig. 4.11 Effect of Crossarm Length for a Diagonal Size of 0.3125 in. and Modulus of Elasticity of 29600 ksi.

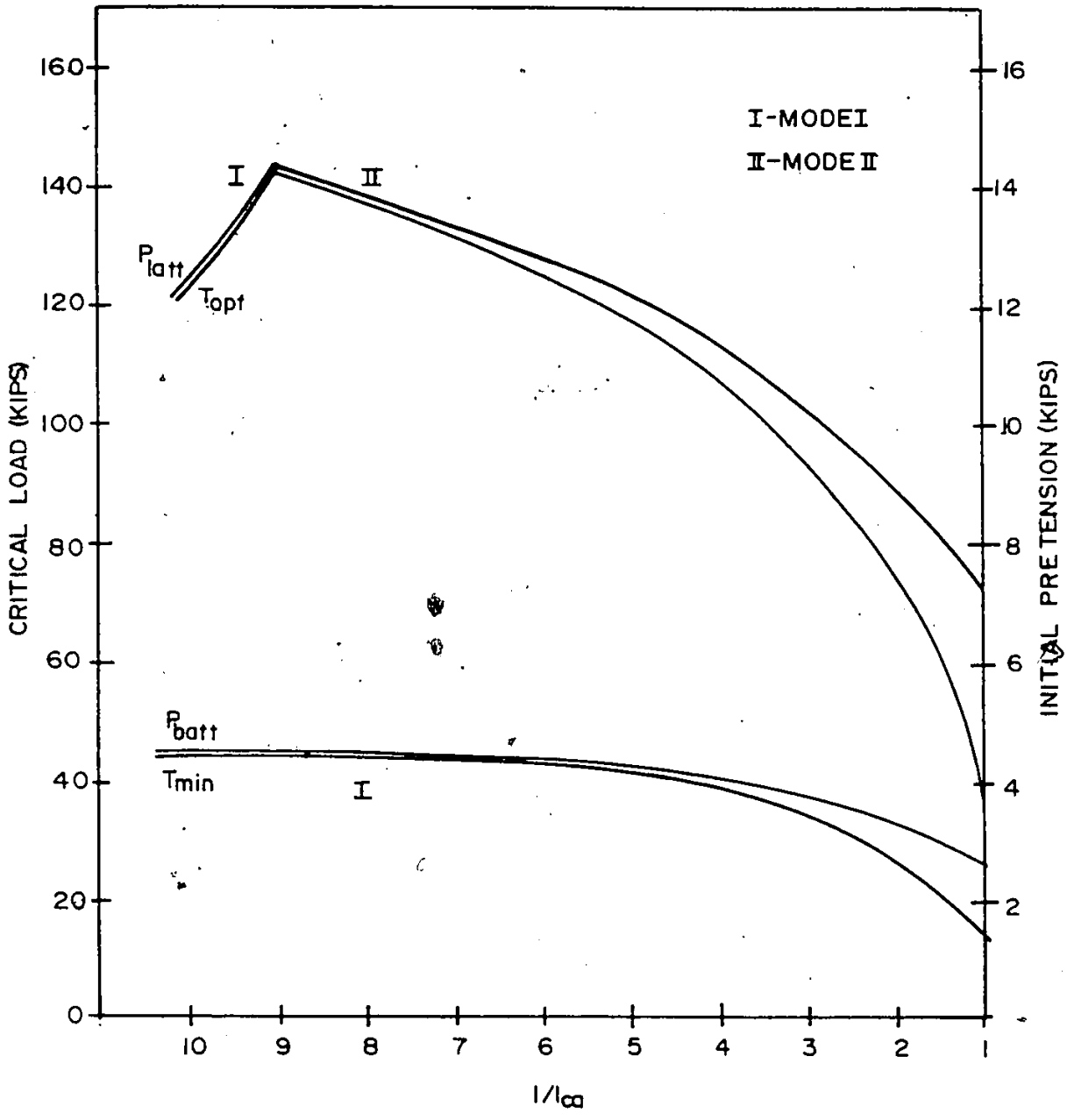

Fig. 4.12 Effect of Crossarm Length for a Diagonal size of 0.5 in. and Modulus of Elasticity of 29600 ksi.

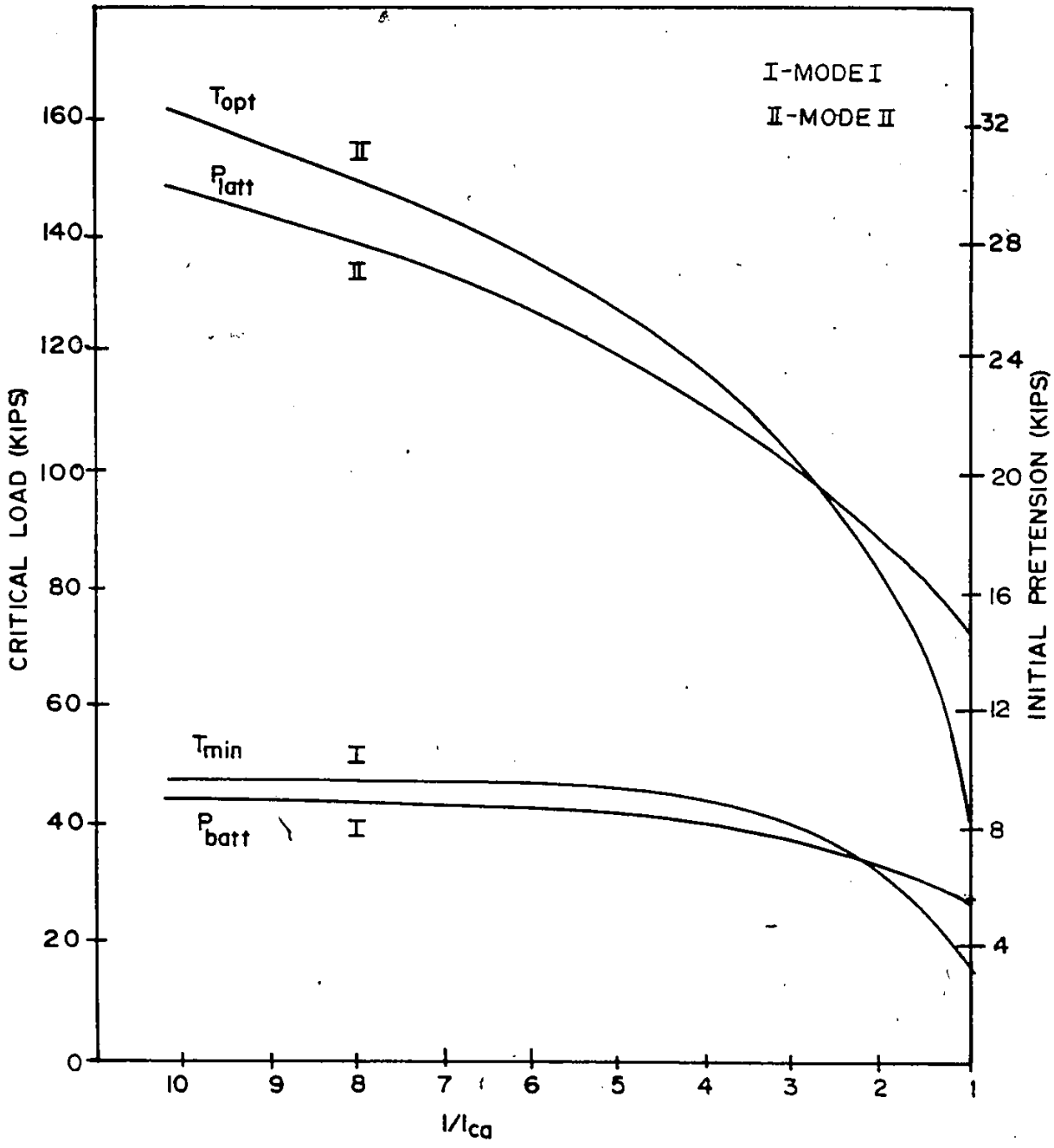

Fig. 4.13 Effect of Crossarm Length for a Diagonal Size of 0.875 in. and Modulus of Elasticity of 29600 ksi.

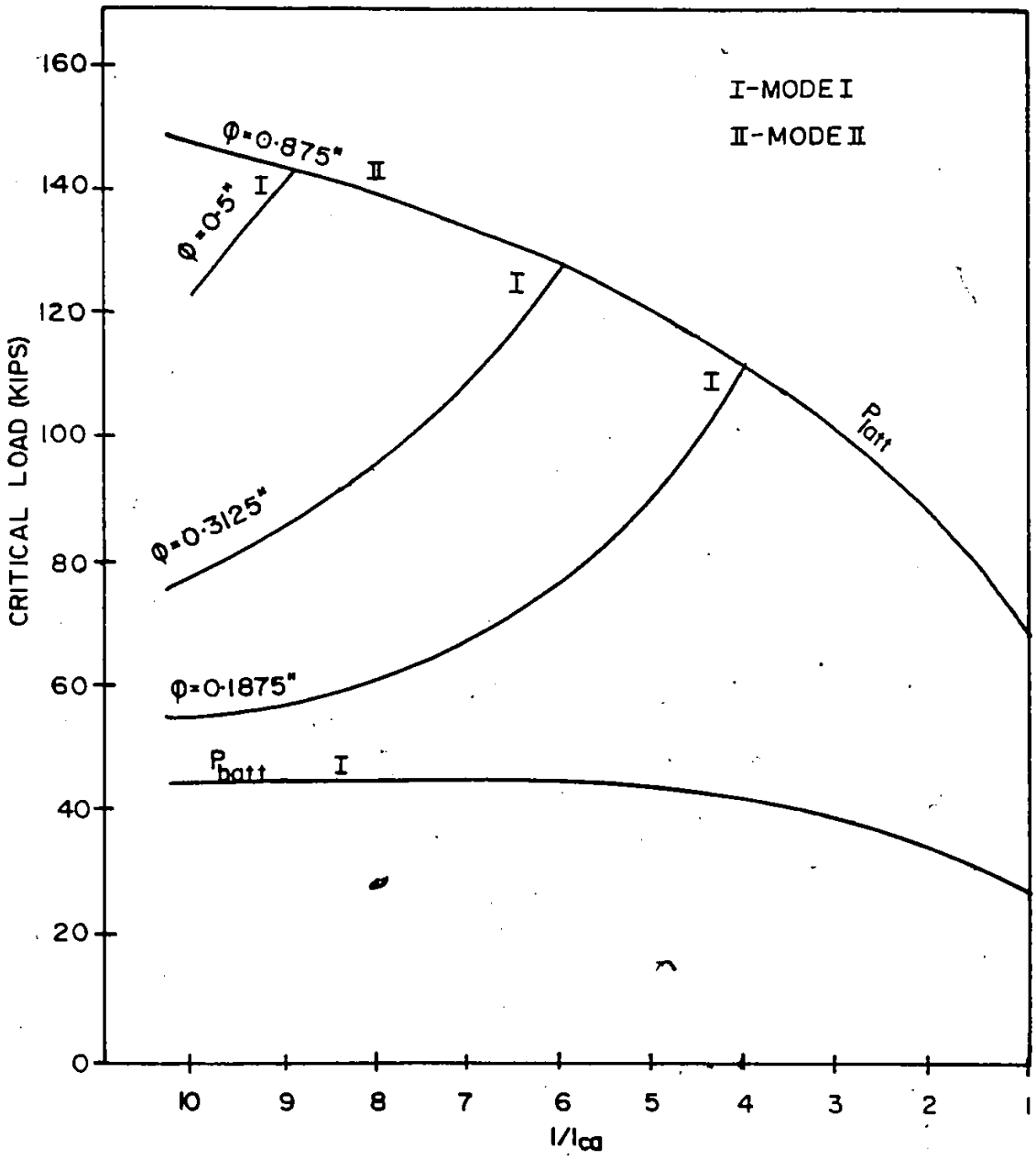

Fig. 4.14 Effect of Crossarm Length on Critial load for a Modulus of Elasticity of 29600 ksi.

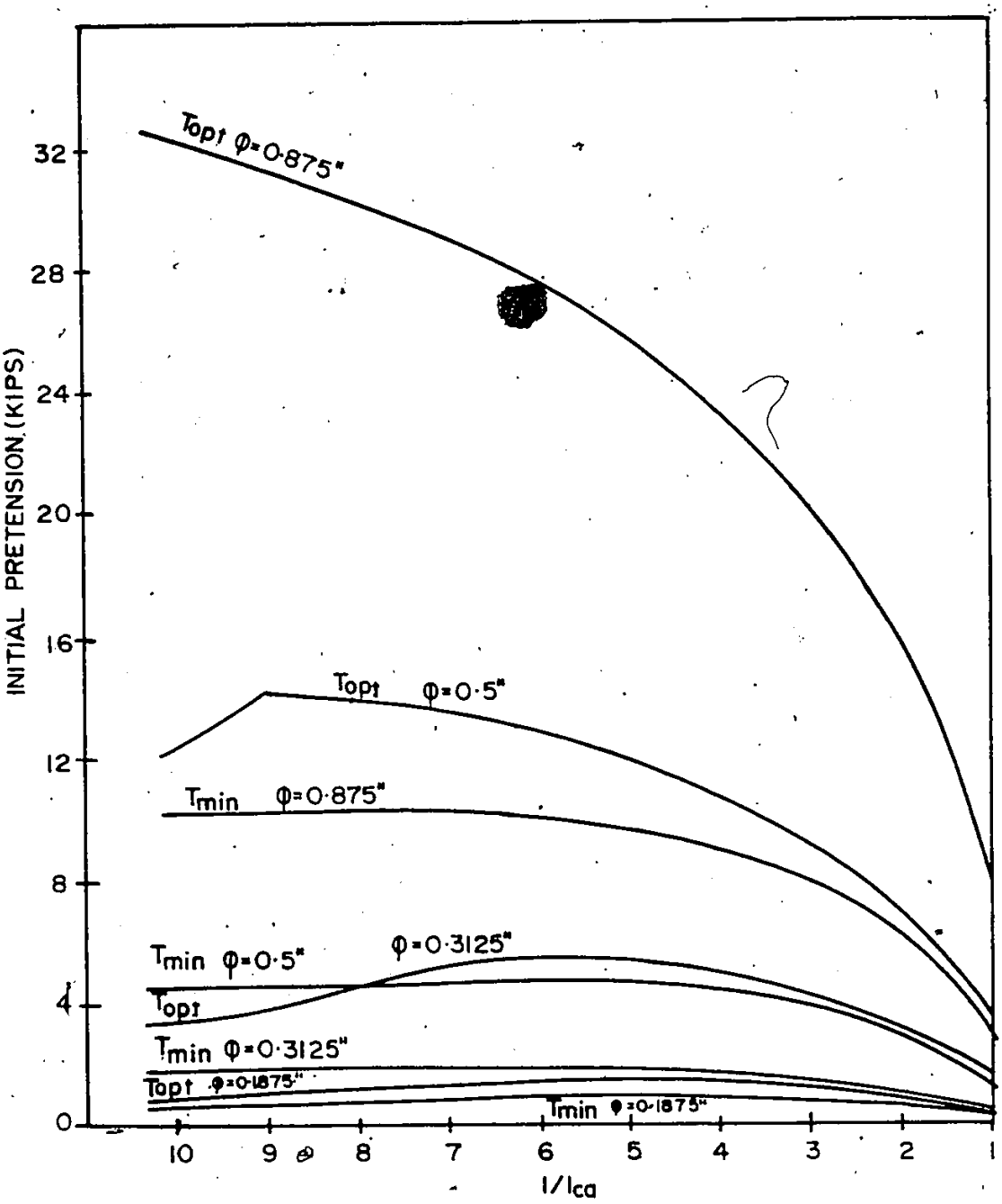

Fig. 4.15 Effect of Crossarm Length on Initial Pretension for a Modulus of Elasticity of 29600 ksi.

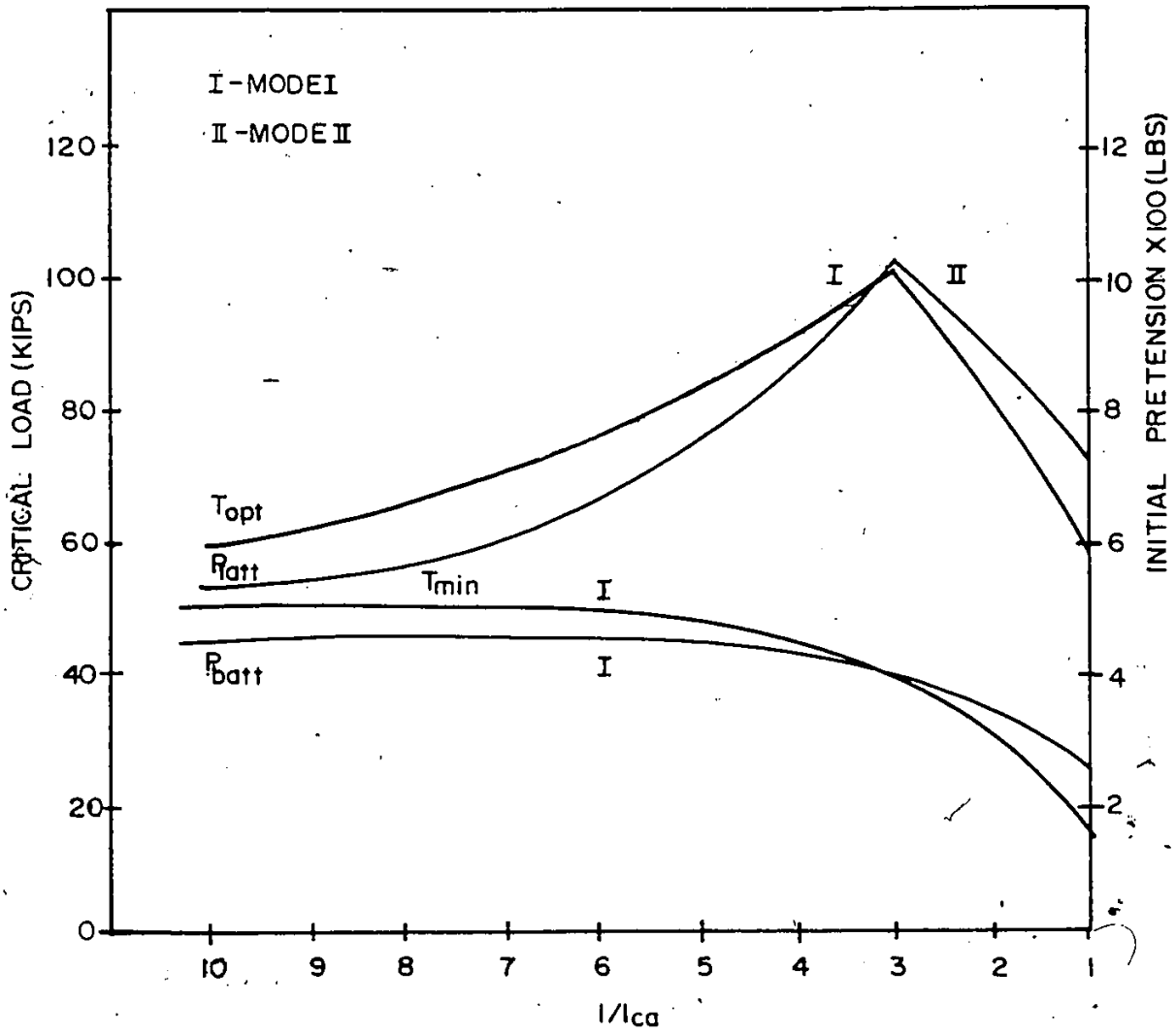

Fig. 4.16 Effect of Crossarm Length for a Diagonal Size of 0.1875 in. and Modulus of Elasticity of 19500 ksi.

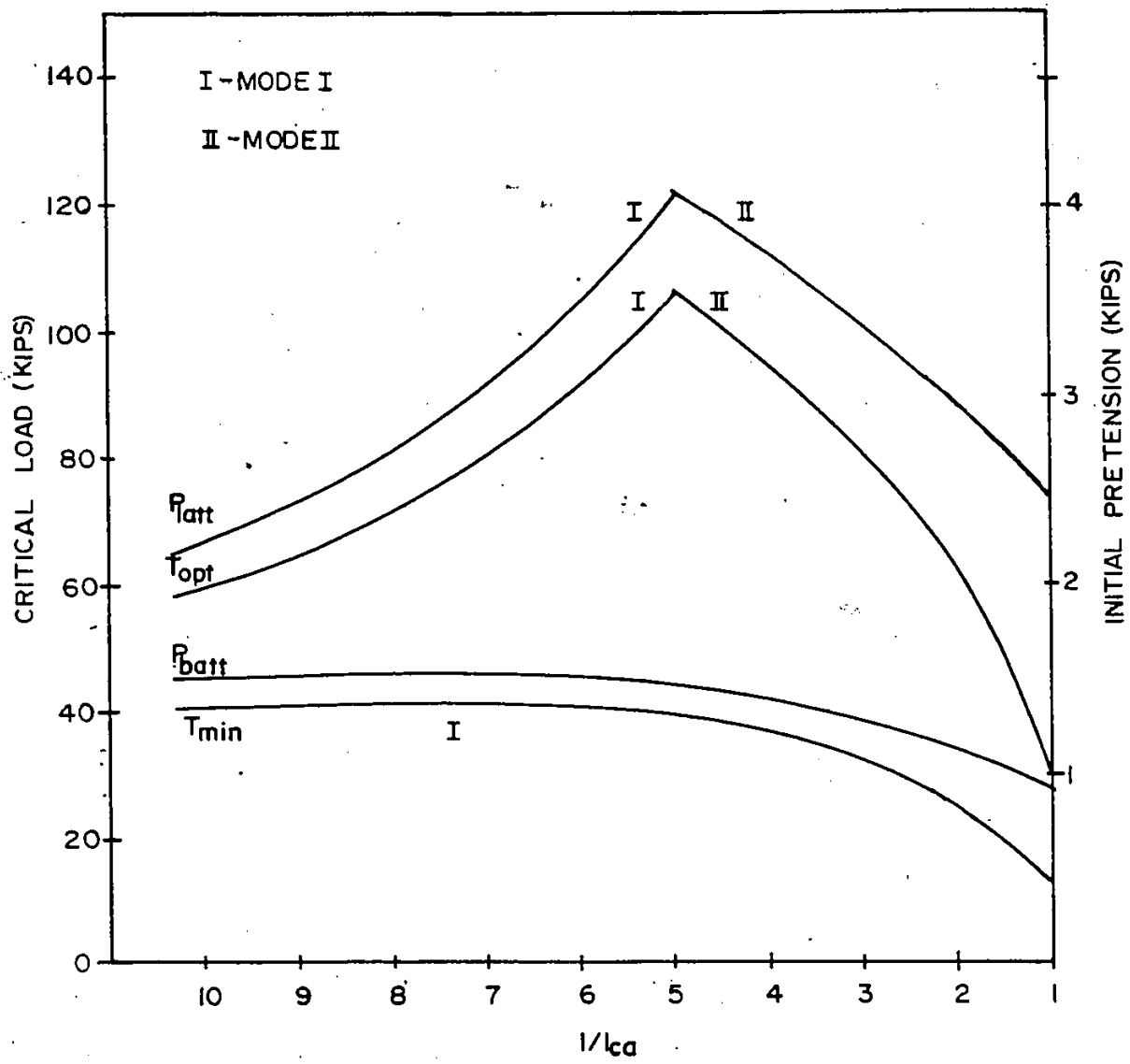

Fig. 4.17 Effect of Crossarm Length for a Diagonal Size of 0.3125 in. and Modulus of Elasticity of 19500 ksi.

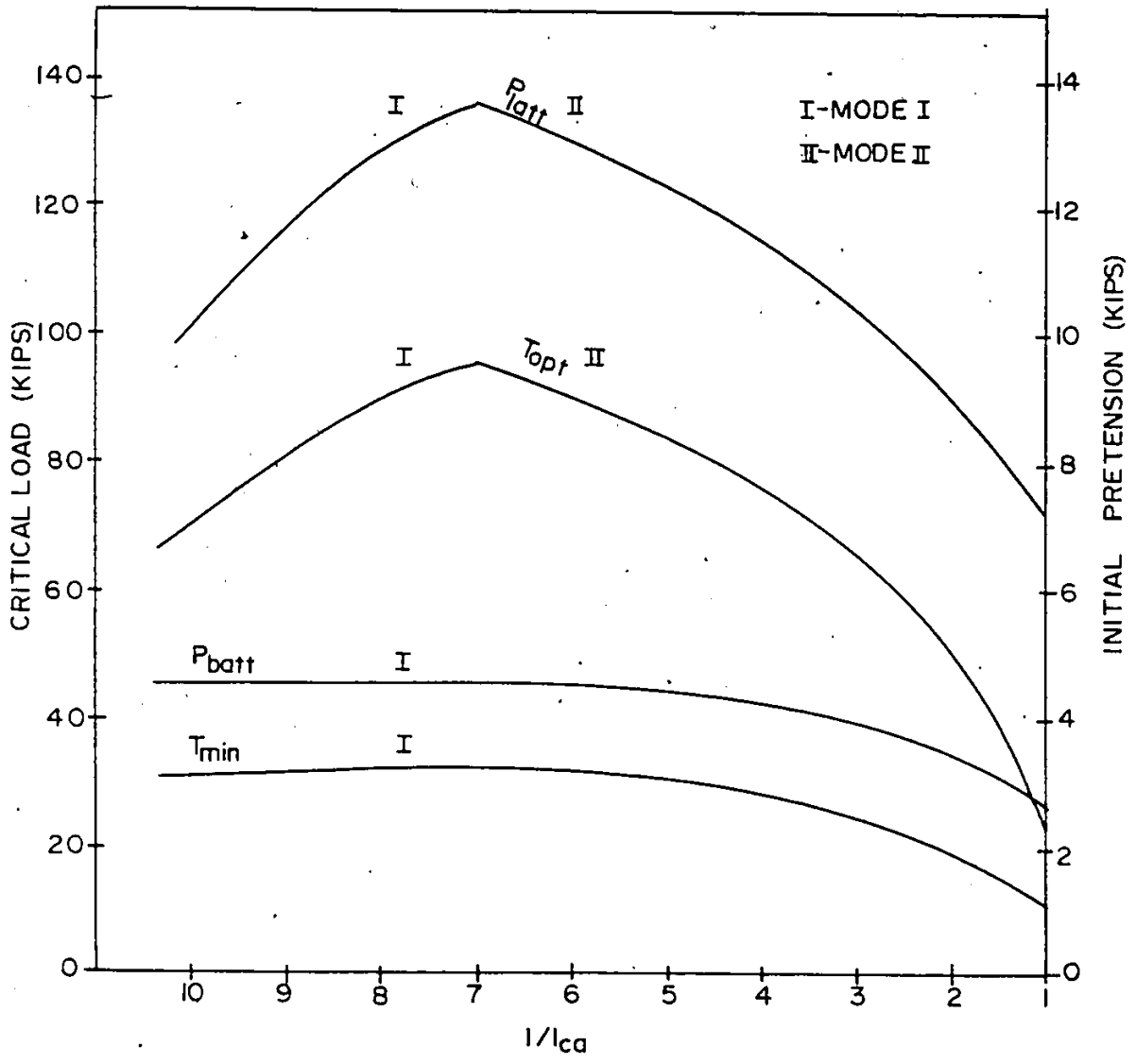

Fig. 4.T8 Effect of Crossarm Length for a Diagonal Size of 0.5 in. and Modulus of Elasticity of 19500 ksi.

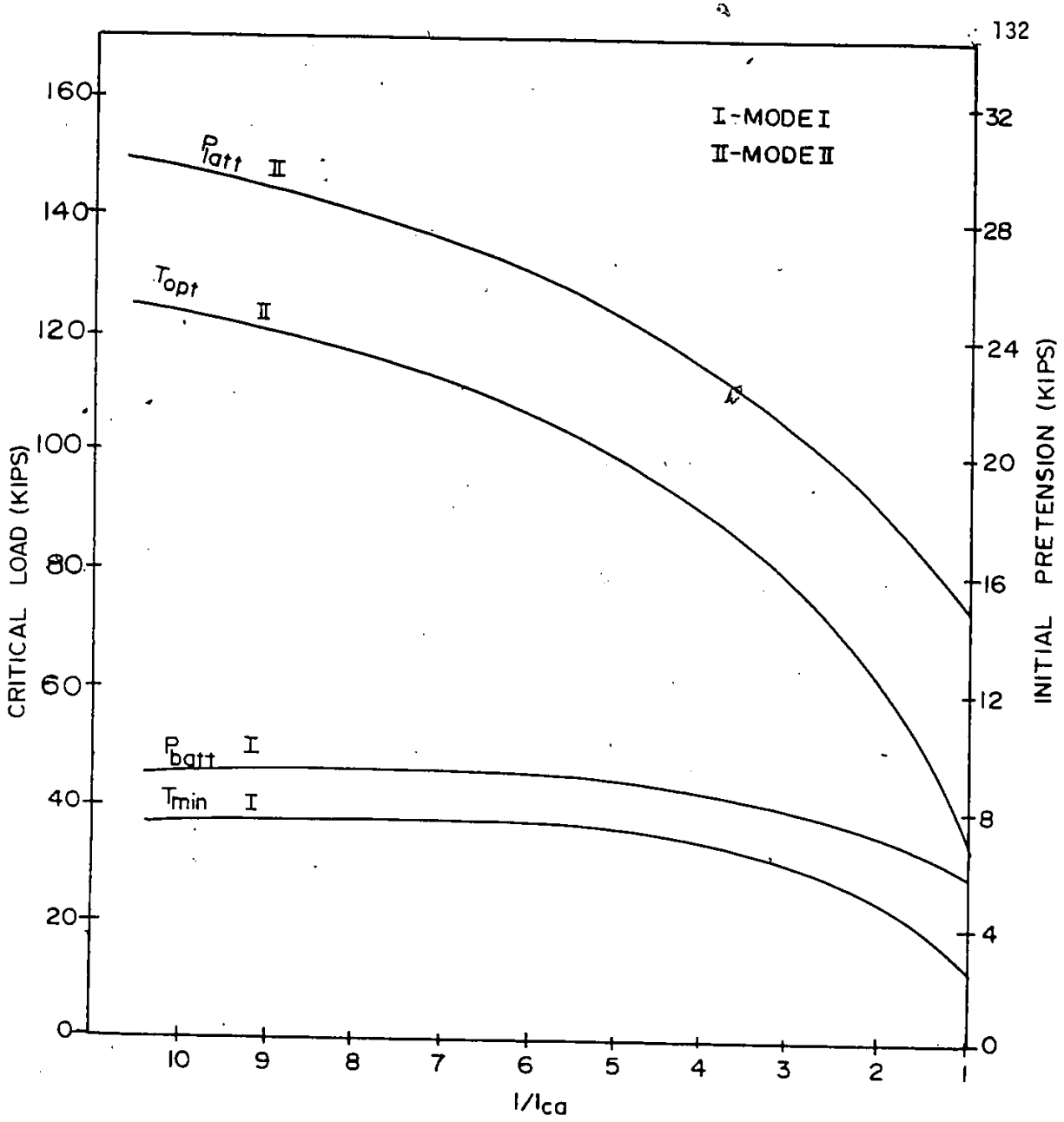

Fig. 4.19 Effect of Crossarm Length for a Diagonal Size of 0.875 in. and Modulus of Elasticity of 19500 ksi.

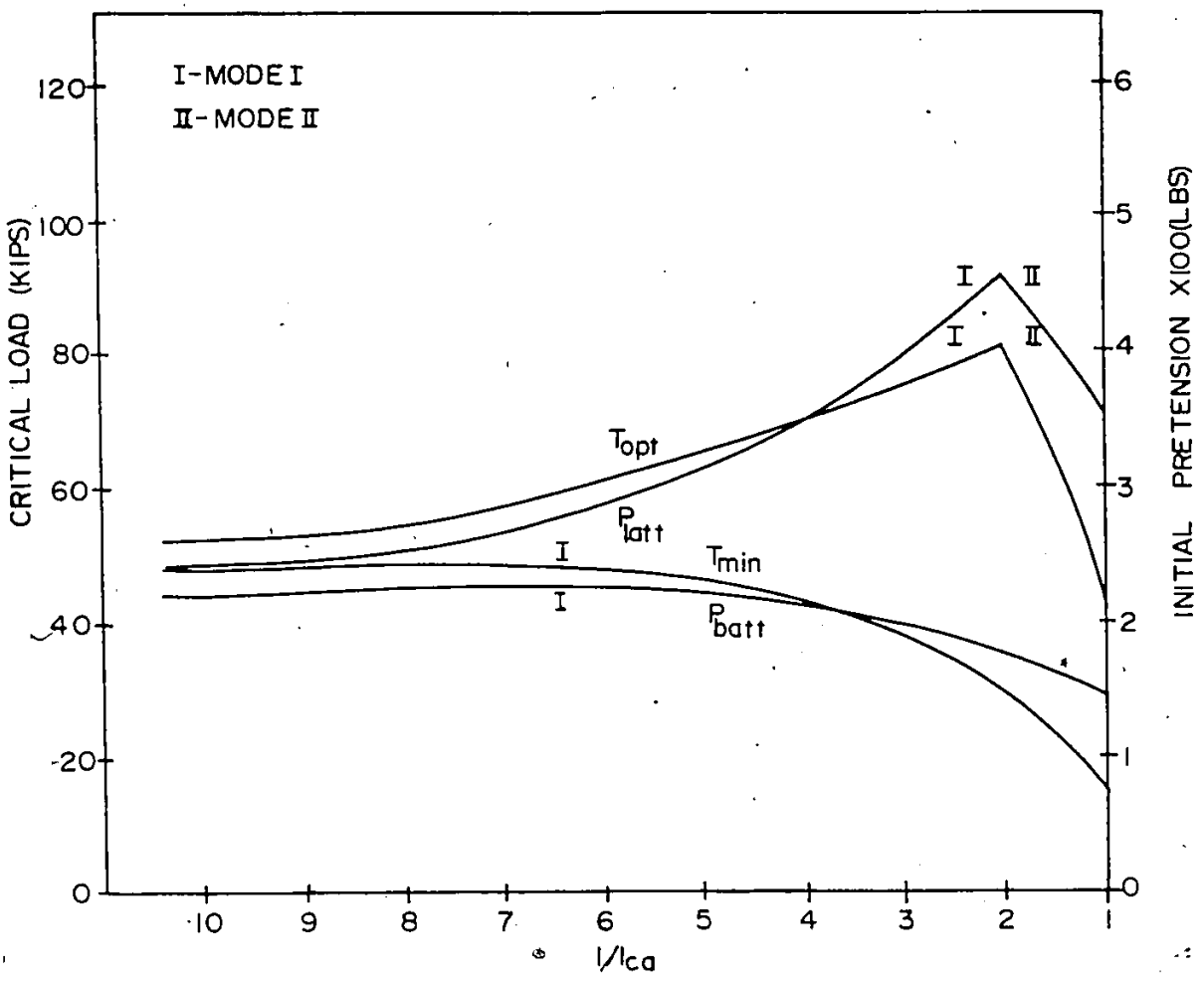

Fig. 4.20 Effect of Crossarm Length for a Diagonal Size of 0.1875 in. and Modulus of Elasticity of 9400 ksi.

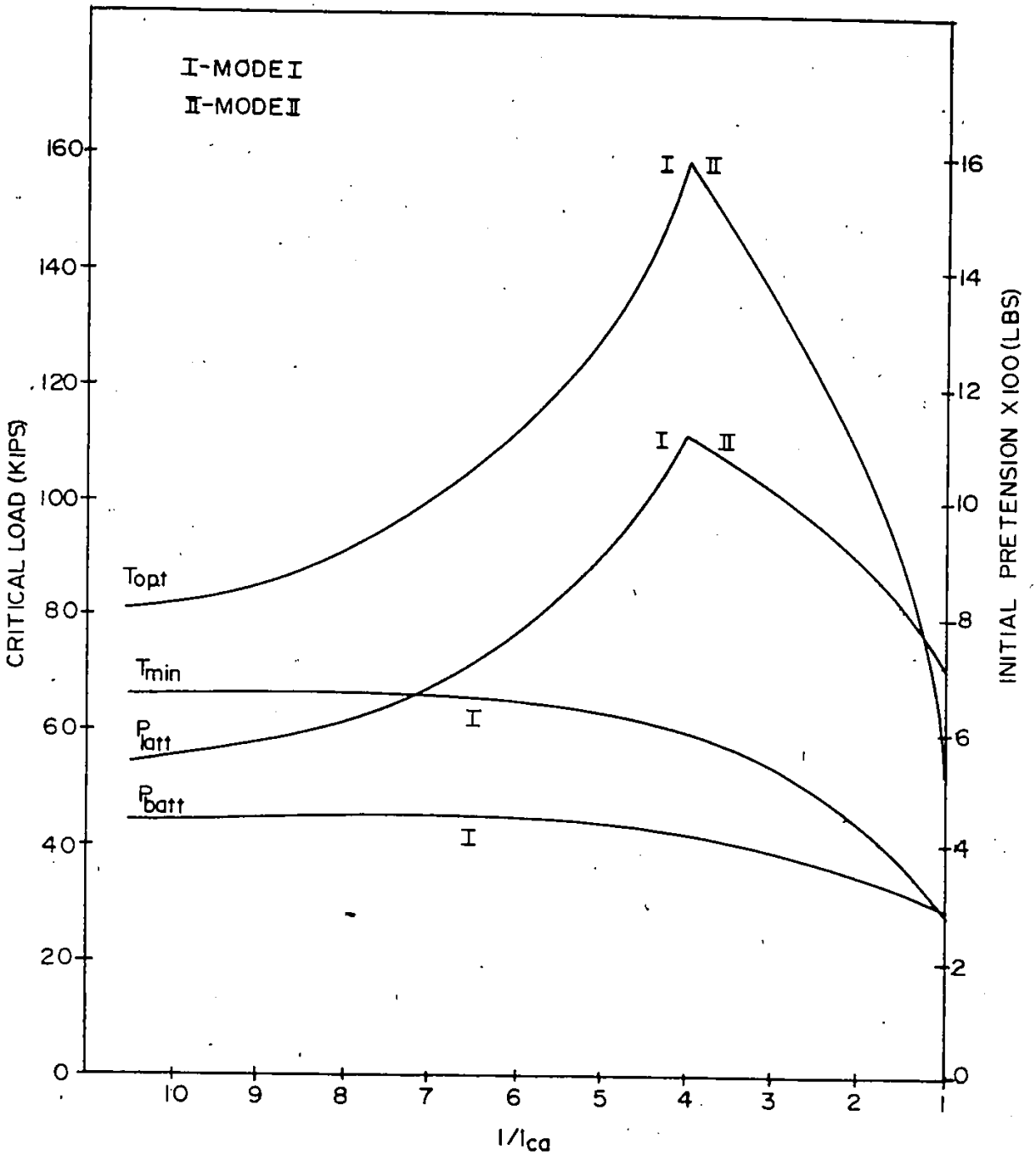

Fig. 4.21 Effect of Crossarm Length for a Diagonal Size Of 0.3125 in. and Modulus of Elasticity of 9400 ksi.

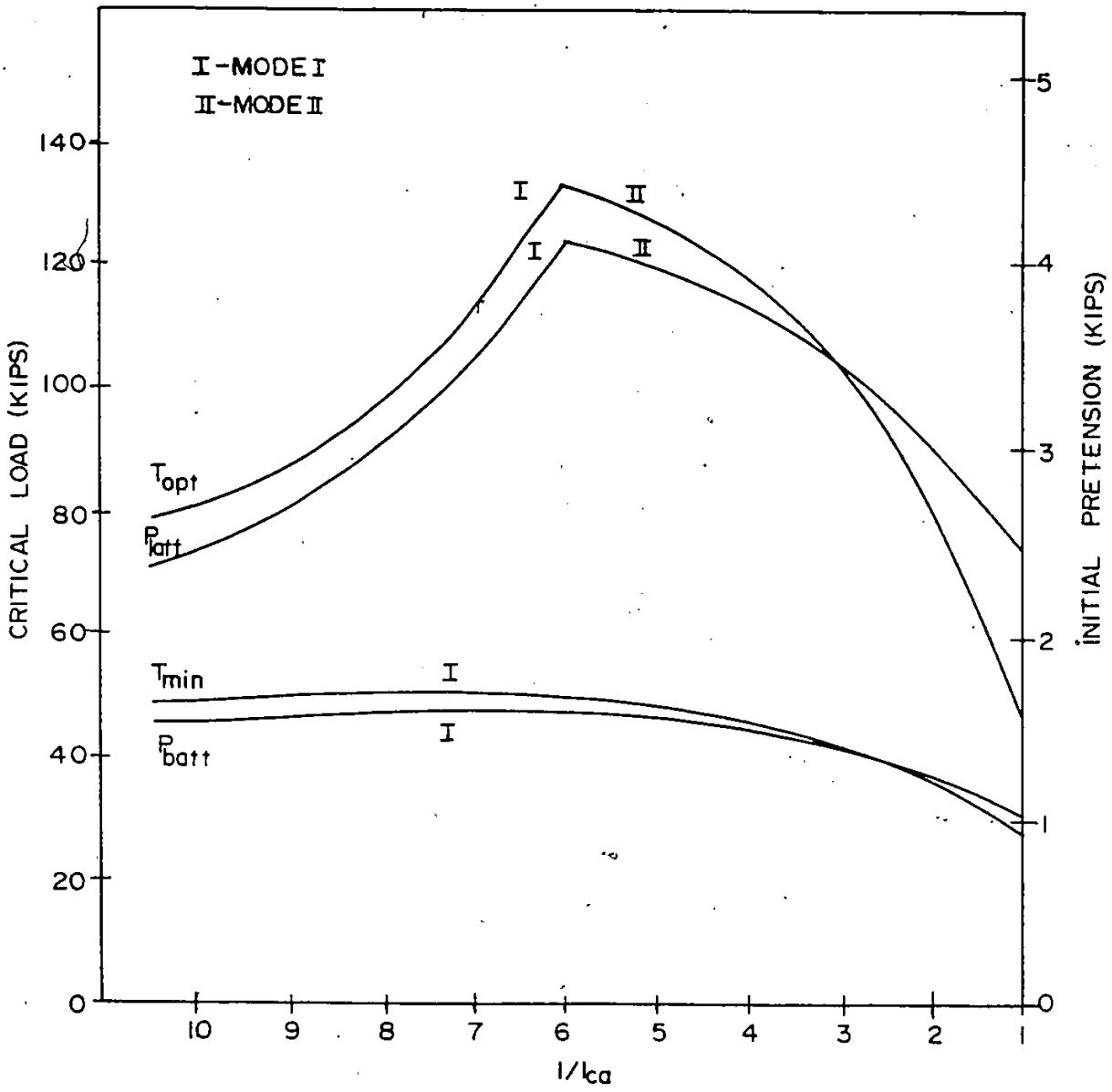

Fig. 4.22 Effect of Crossarm Length for a Diagonal Size of 0.5 in. and Modulus of Elasticity of 9400 ksi.

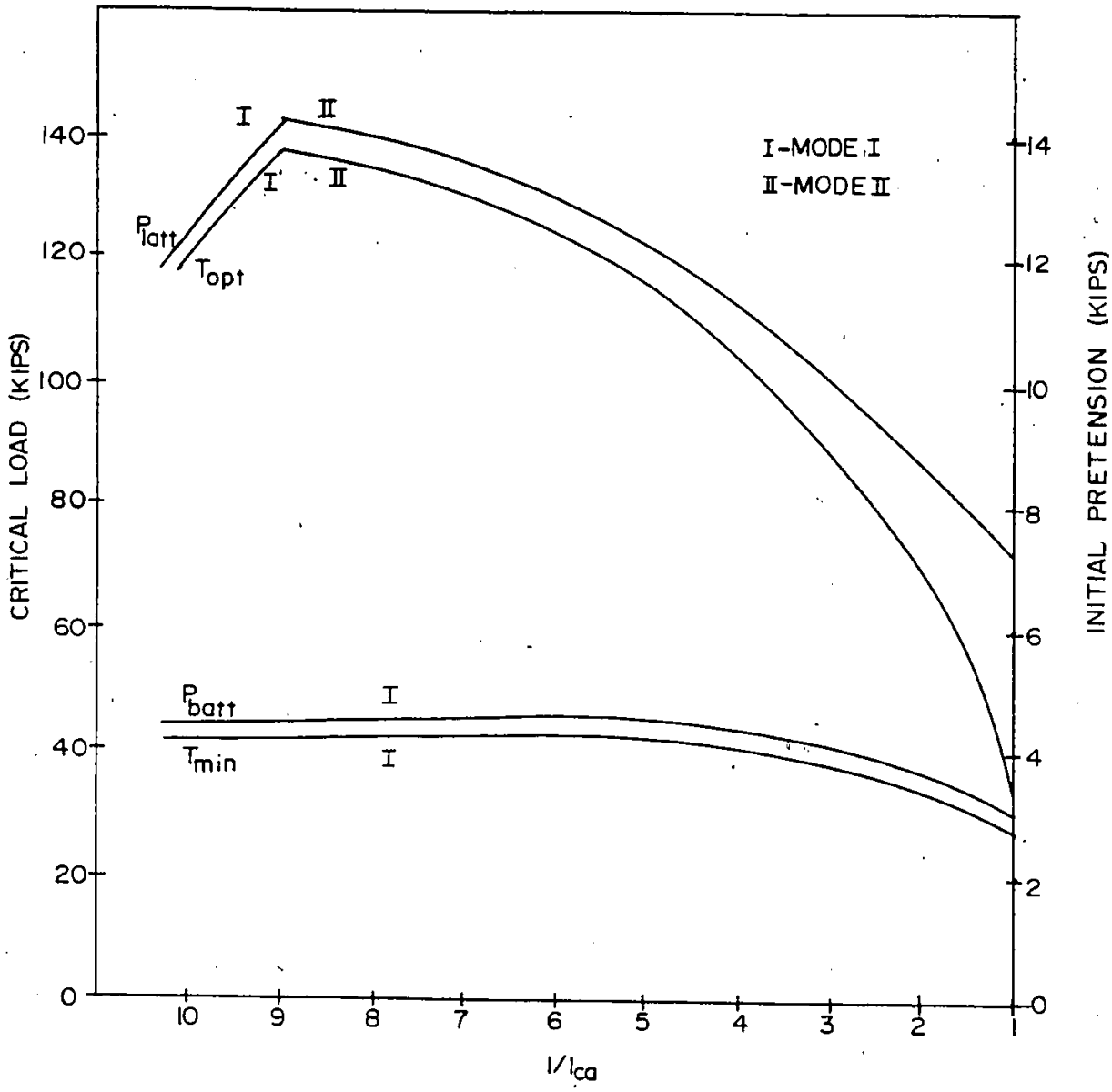

Fig. 4.23 Effect of Crossarm Length for a Diagonal Size of 0.875 in. and Modulus of Elasticity of 9400 ksi.

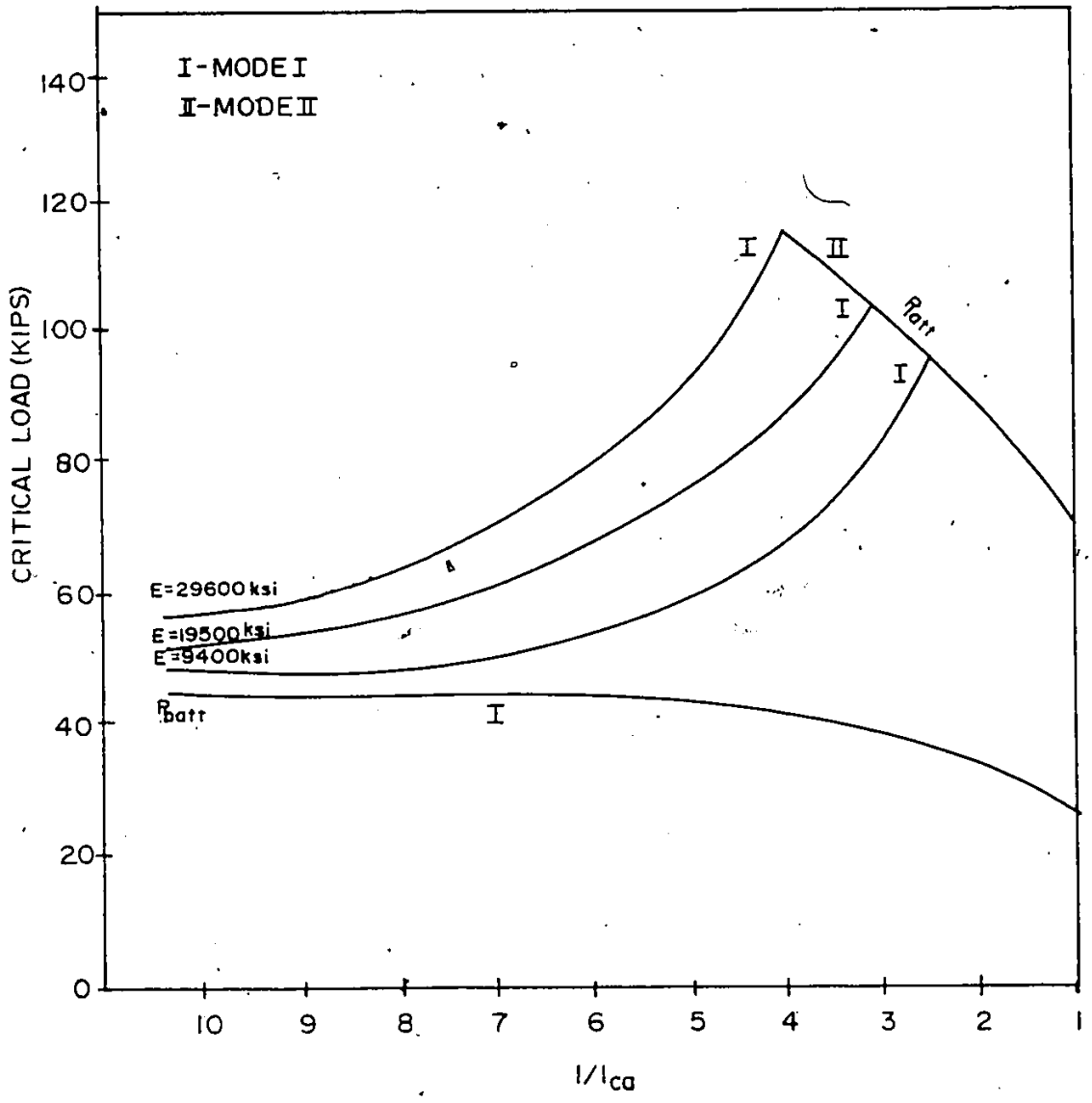

Fig. 4.24 Effect of Crossarm Length on Critical load for a Diagonal Size of 0.1875 in.

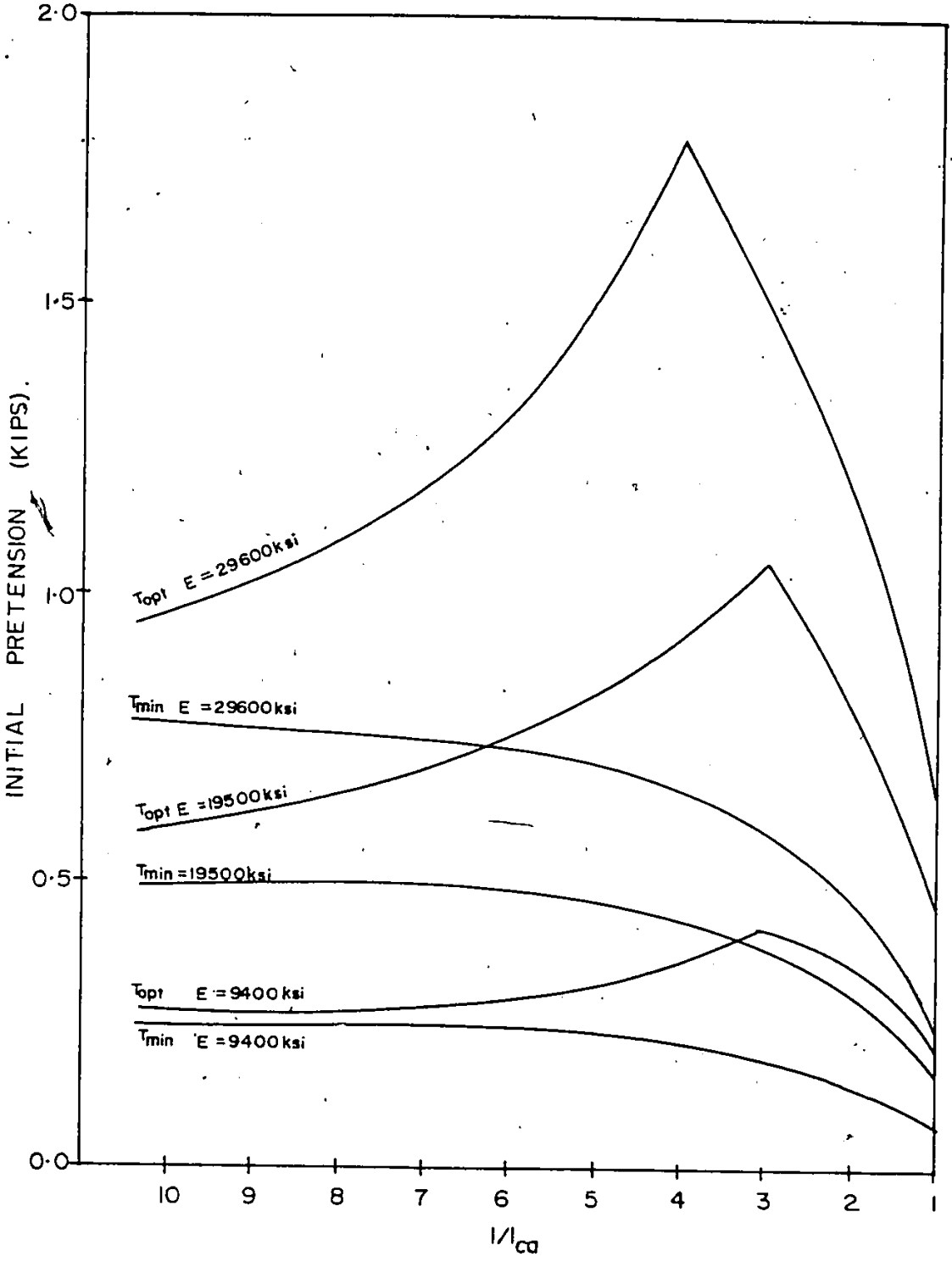

Fig. 4.25 Effect of Crossarm Length on Initial Pretension for a Diagonal Size of 0.1875 in.

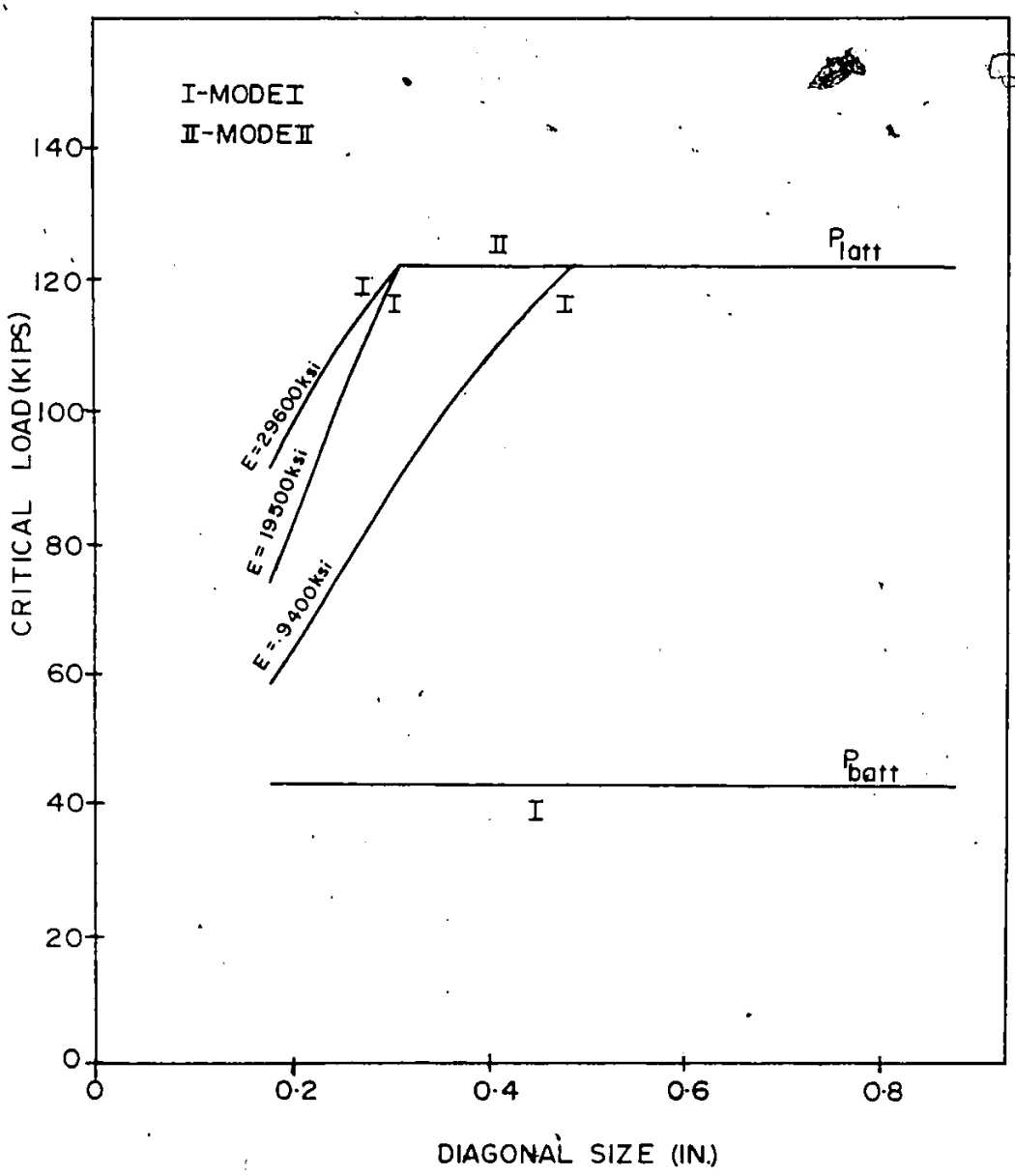

Fig. 4.26 Effect of Diagonal Size on Critical Load for an l/l_{ca} Ratio of five.

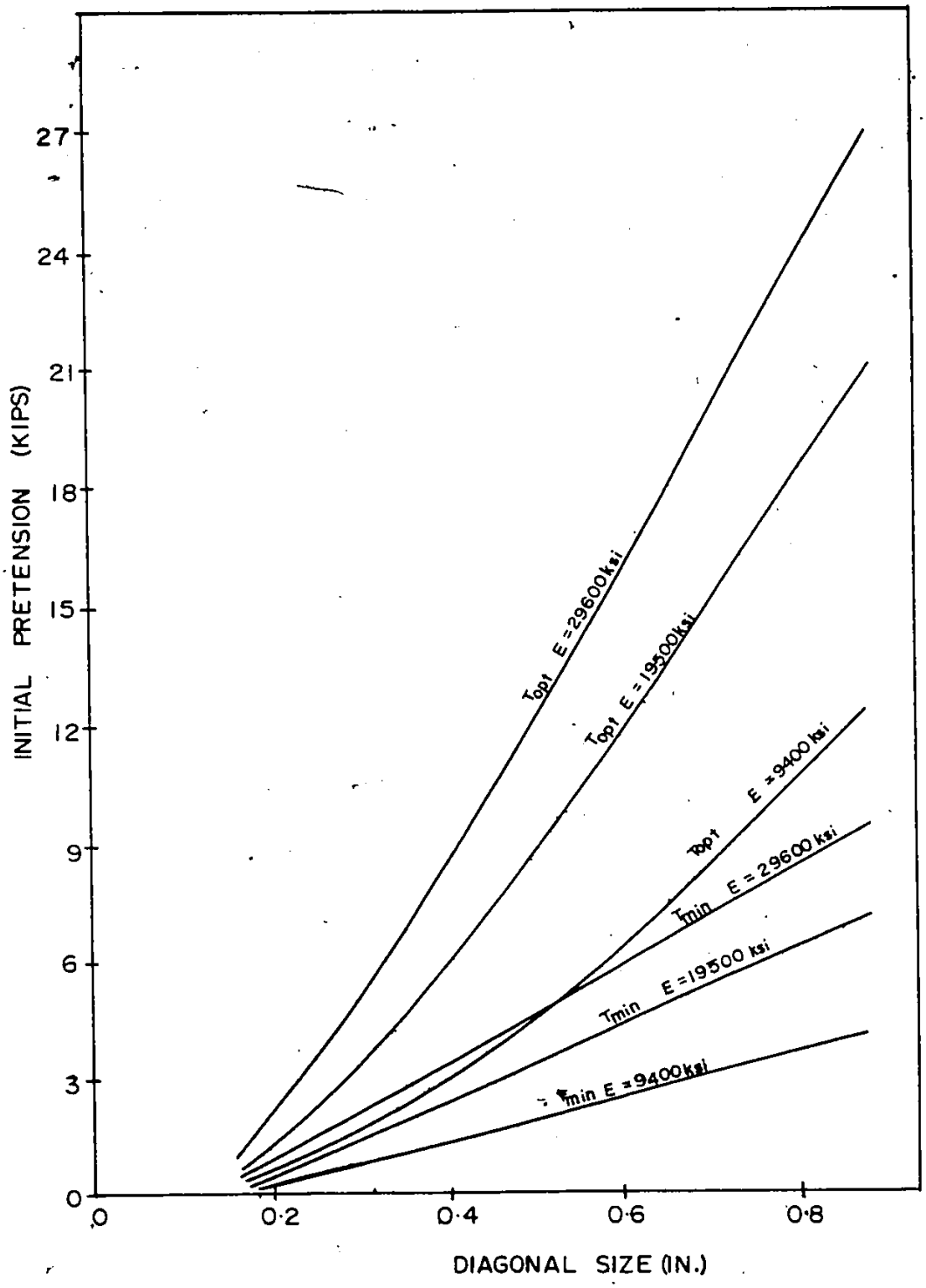

Fig. 4.27 Effect of Diagonal Size on Initial Pretension for an l/l_{ca} Ratio of five.

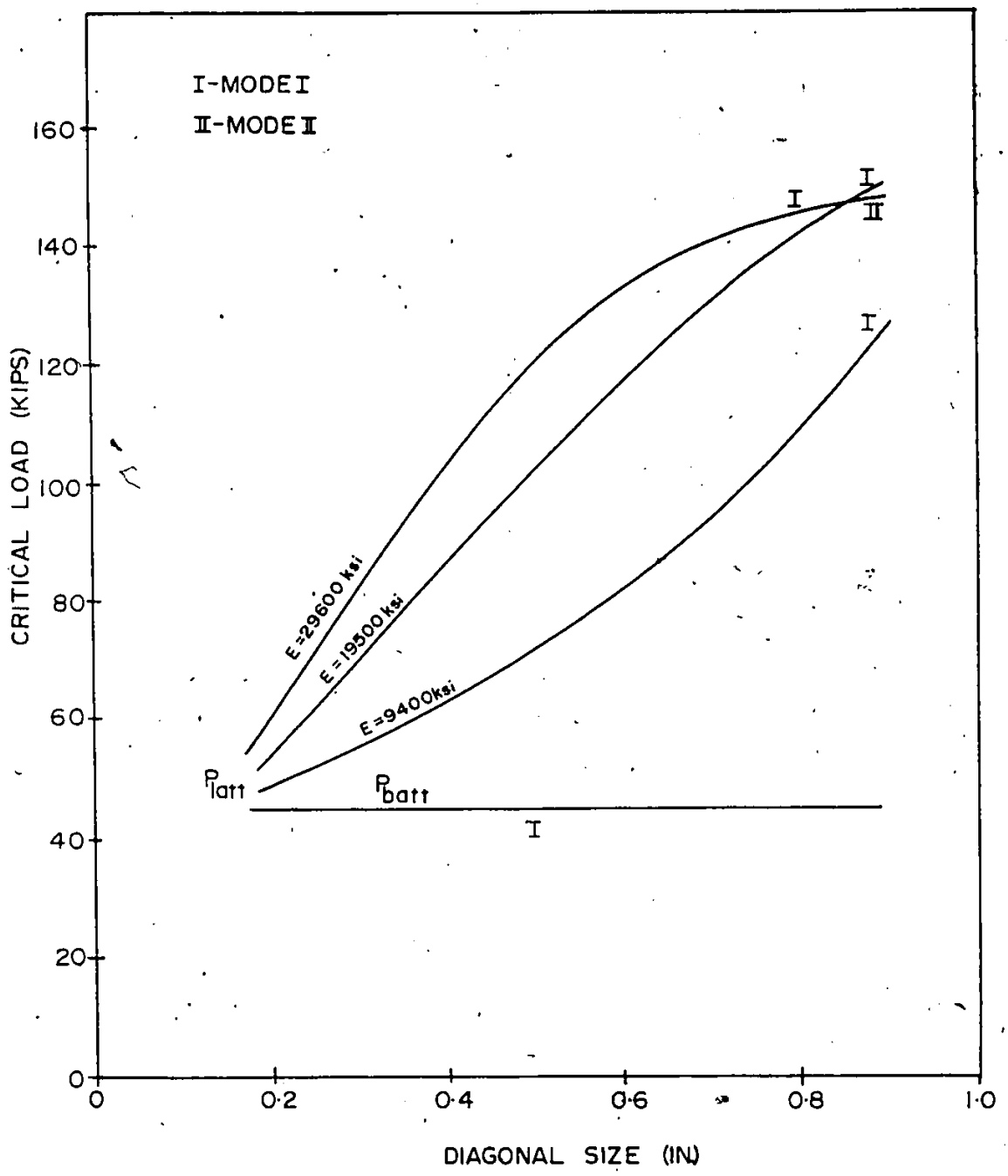

Fig. 4.28 Effect of Diagonal Size on Critical Load for an l/l_{ca} Ratio of ten.

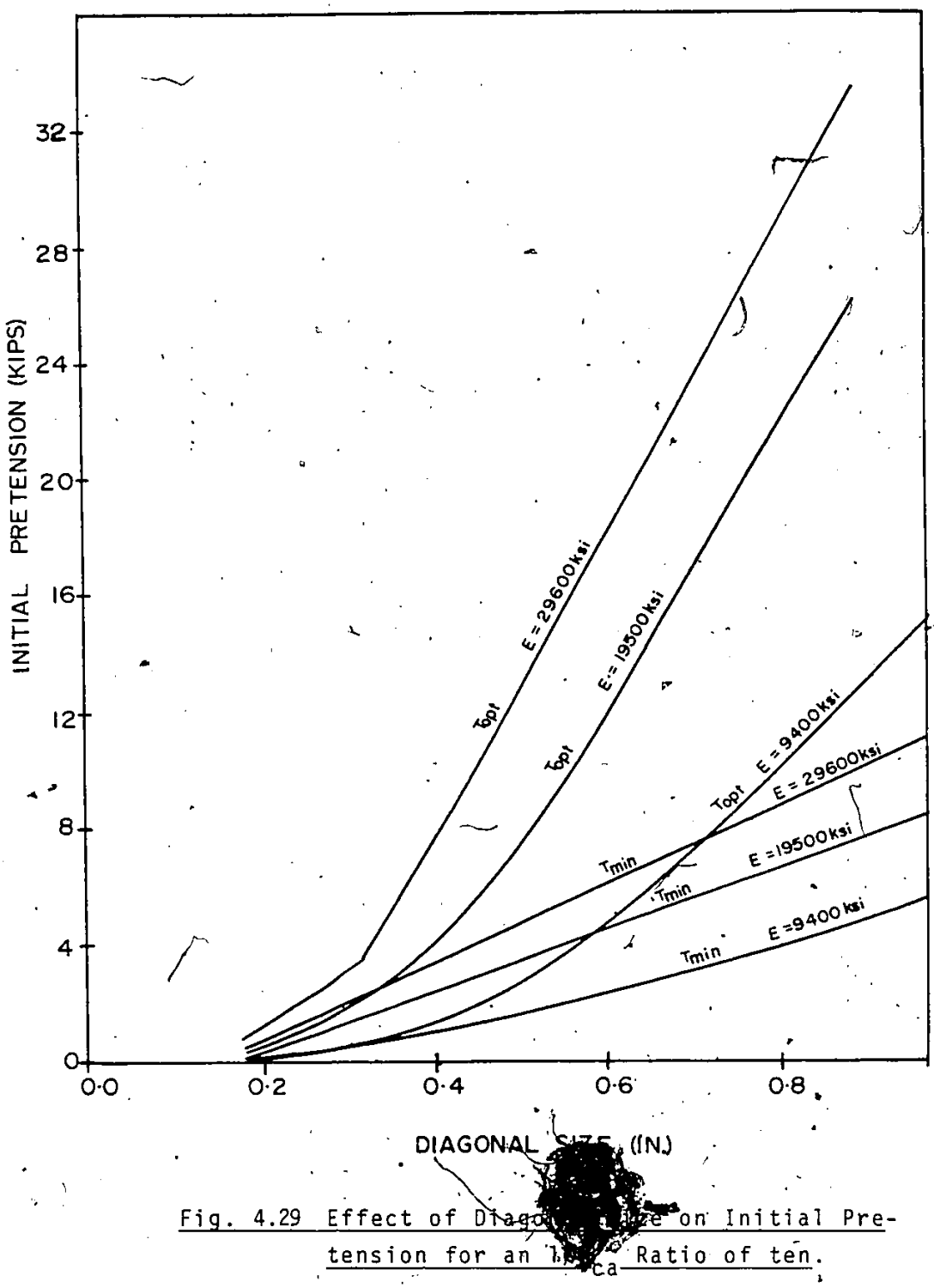

Fig. 4.29 Effect of Diagonal Size on Initial Pretension for an L/a Ratio of ten.

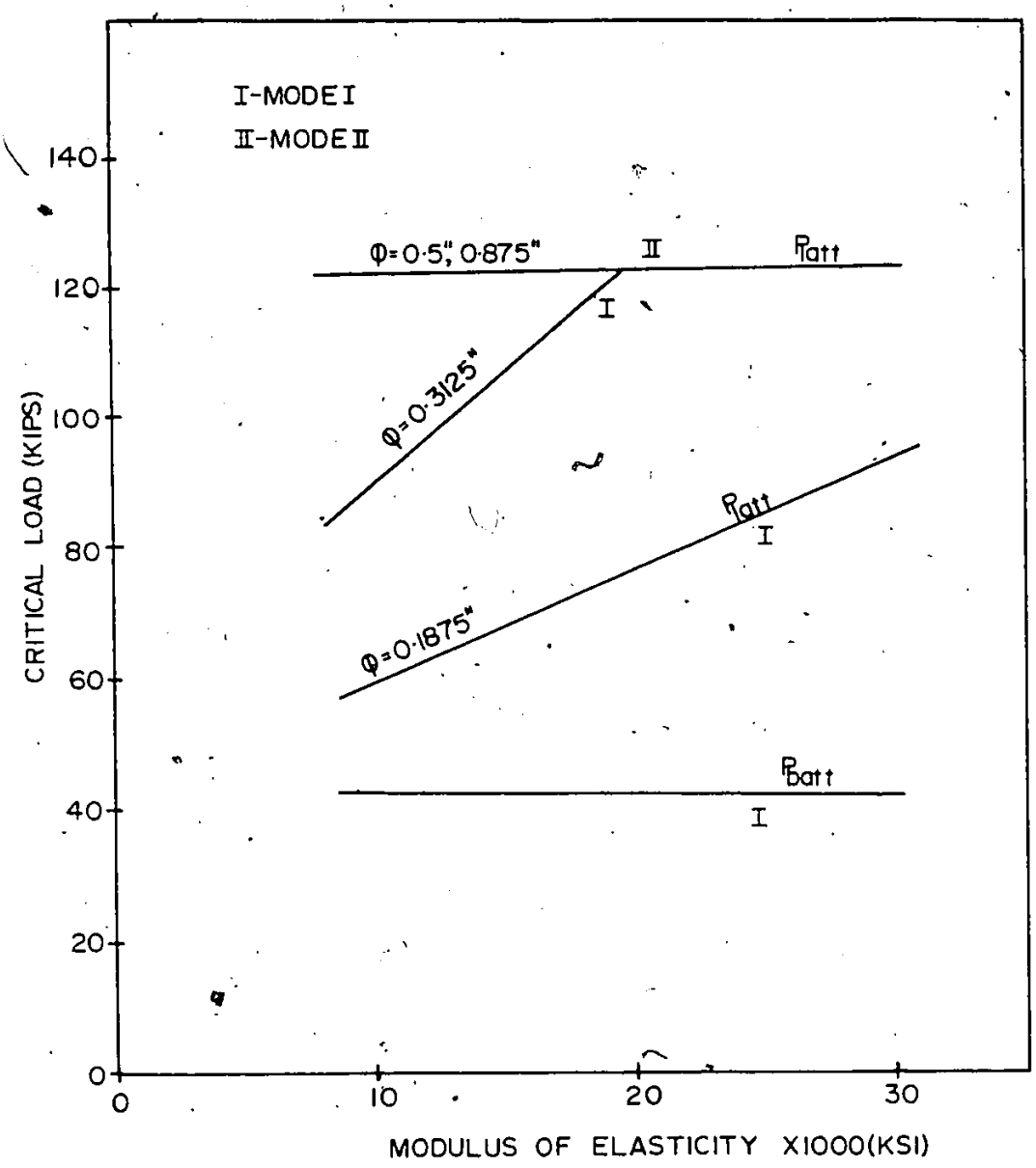

Fig. 4.30 Effect of Modulus of Elasticity of Diagonal on Critical Load for an l/l_{ca} Ratio of Five.

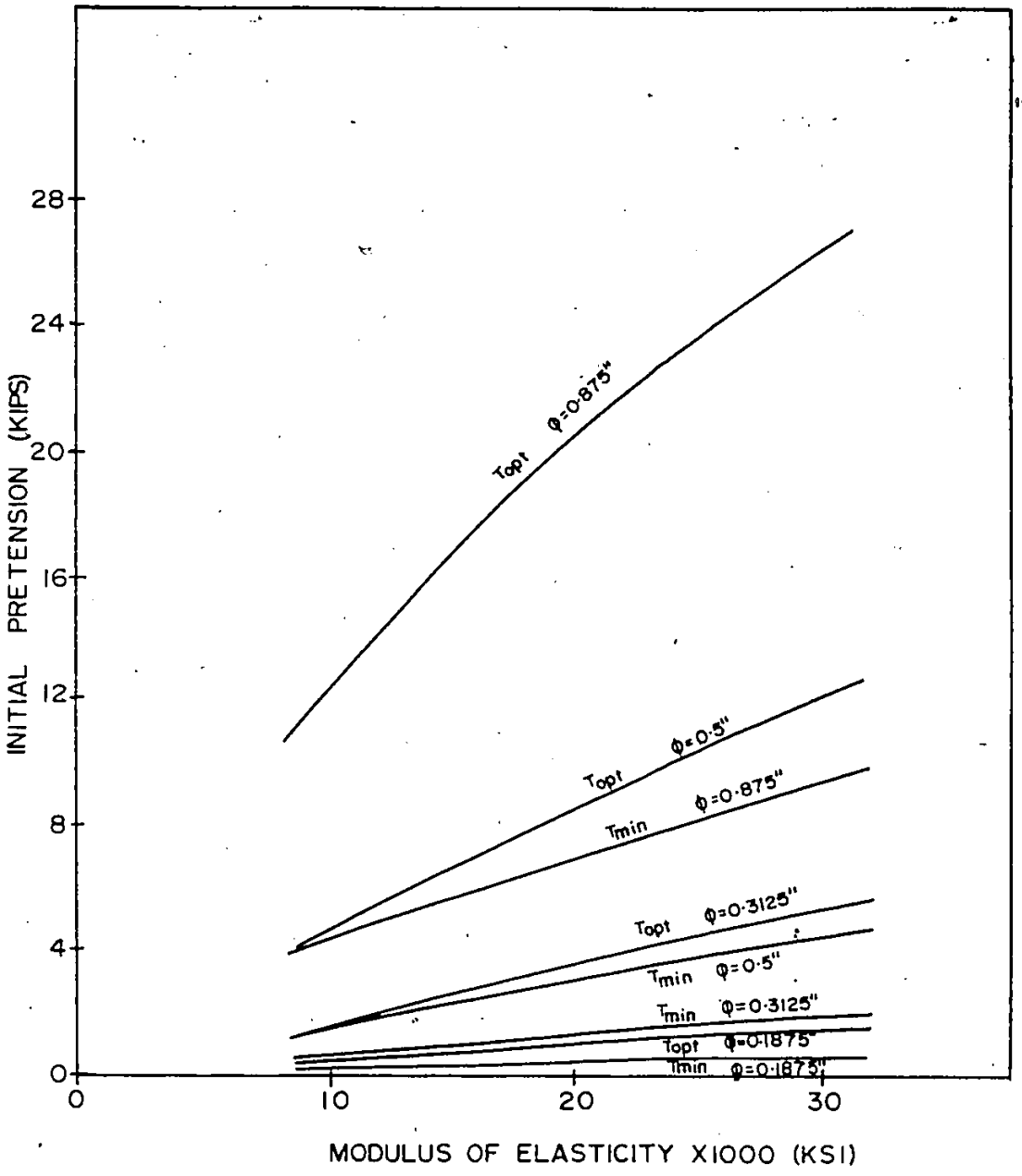

Fig. 4.31 Effect of Modulus of Elasticity of Diagonal on Initial Pretension for an l/l_{ca} Ratio of five

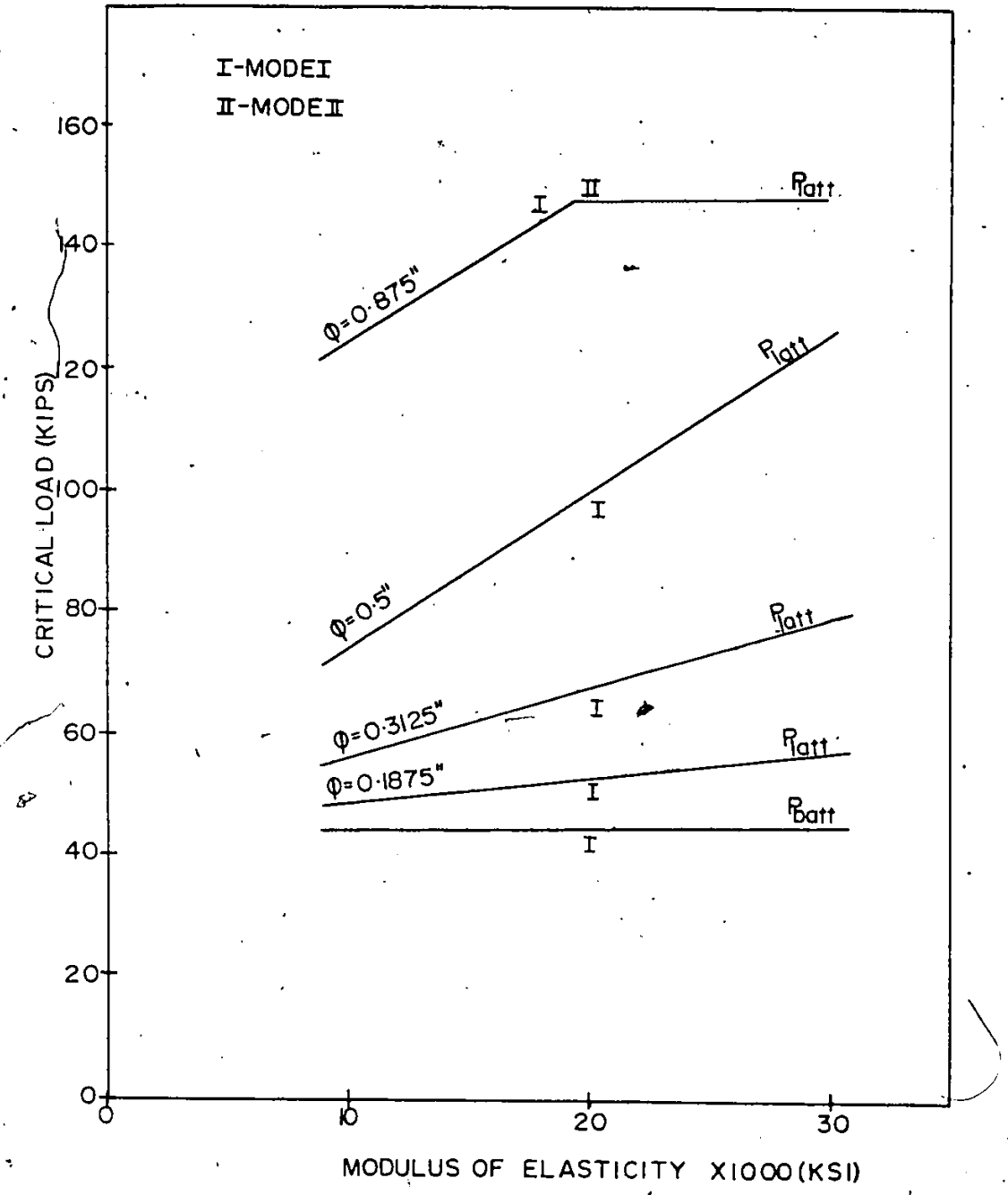

Fig. 4.32 Effect of Modulus of Elasticity of Diagonal on Critical Load for an l/l_{ca} Ratio of ten.

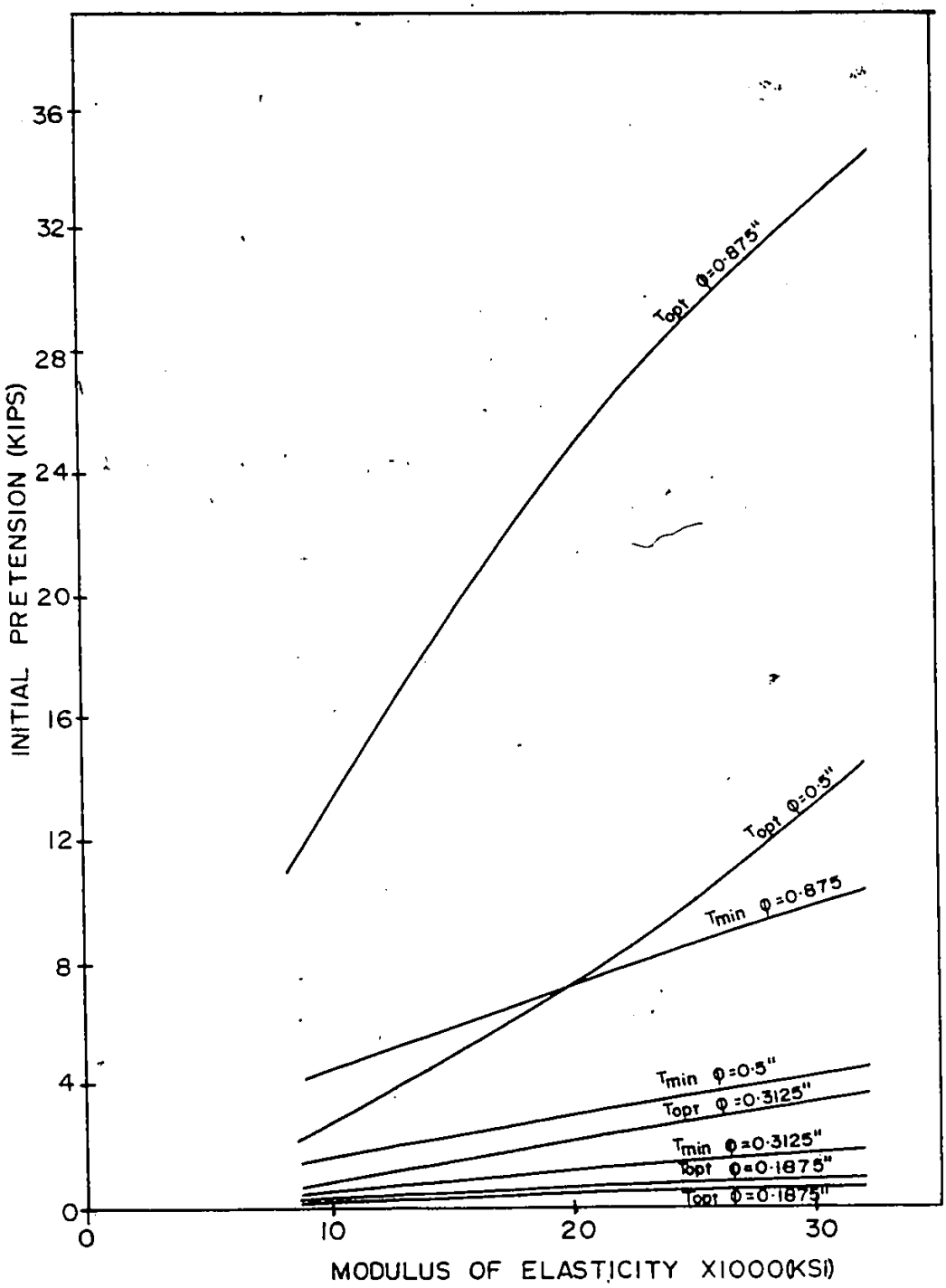

Fig. 4.33 Effect of Modulus of Elasticity of Diagonal on Initial Pretension for an l/l_{ca} Ratio of ten.

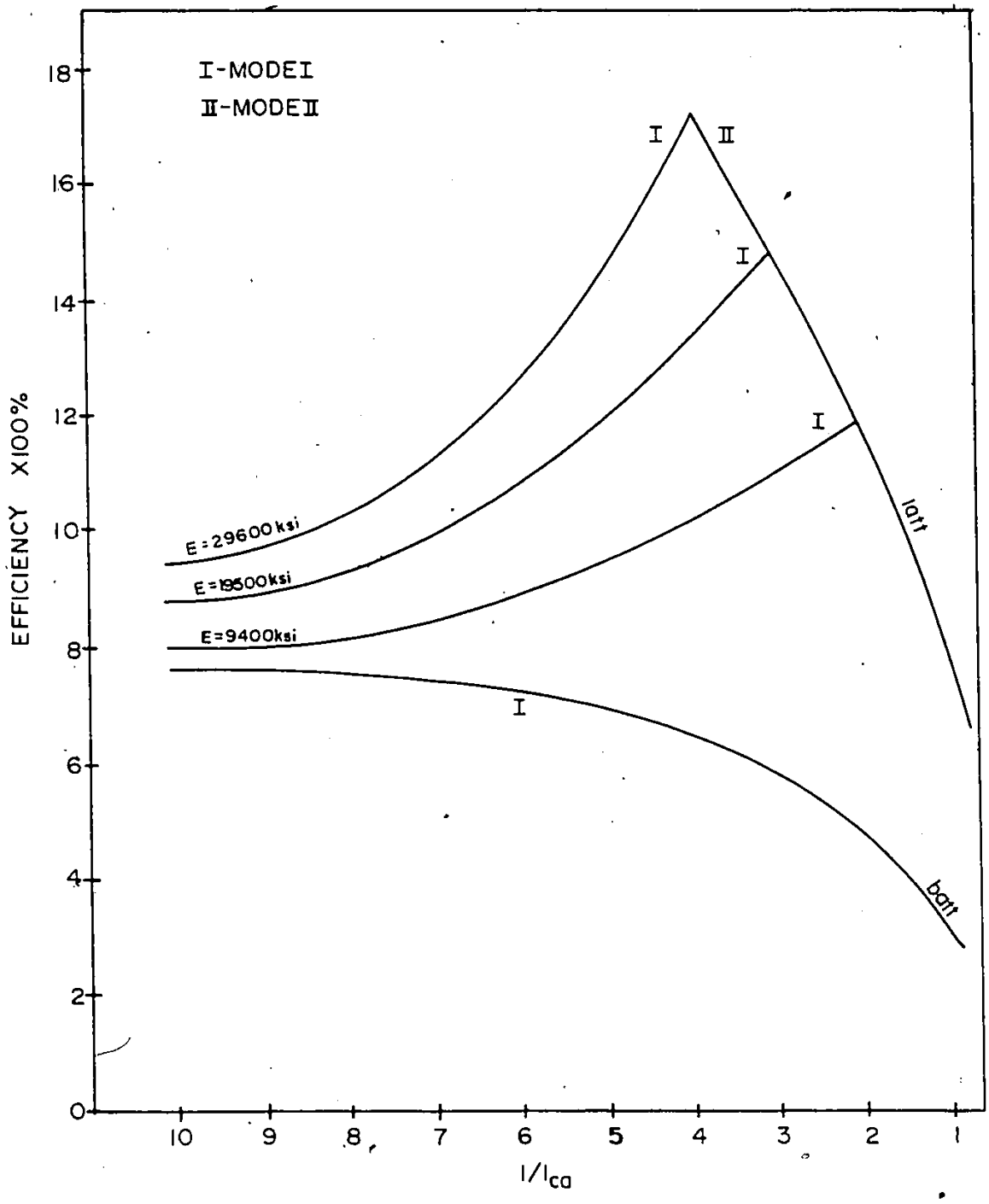

Fig. 4.34 Effect of Crossarm Length on Efficiency for a Diagonal Size of 0.1875 in.

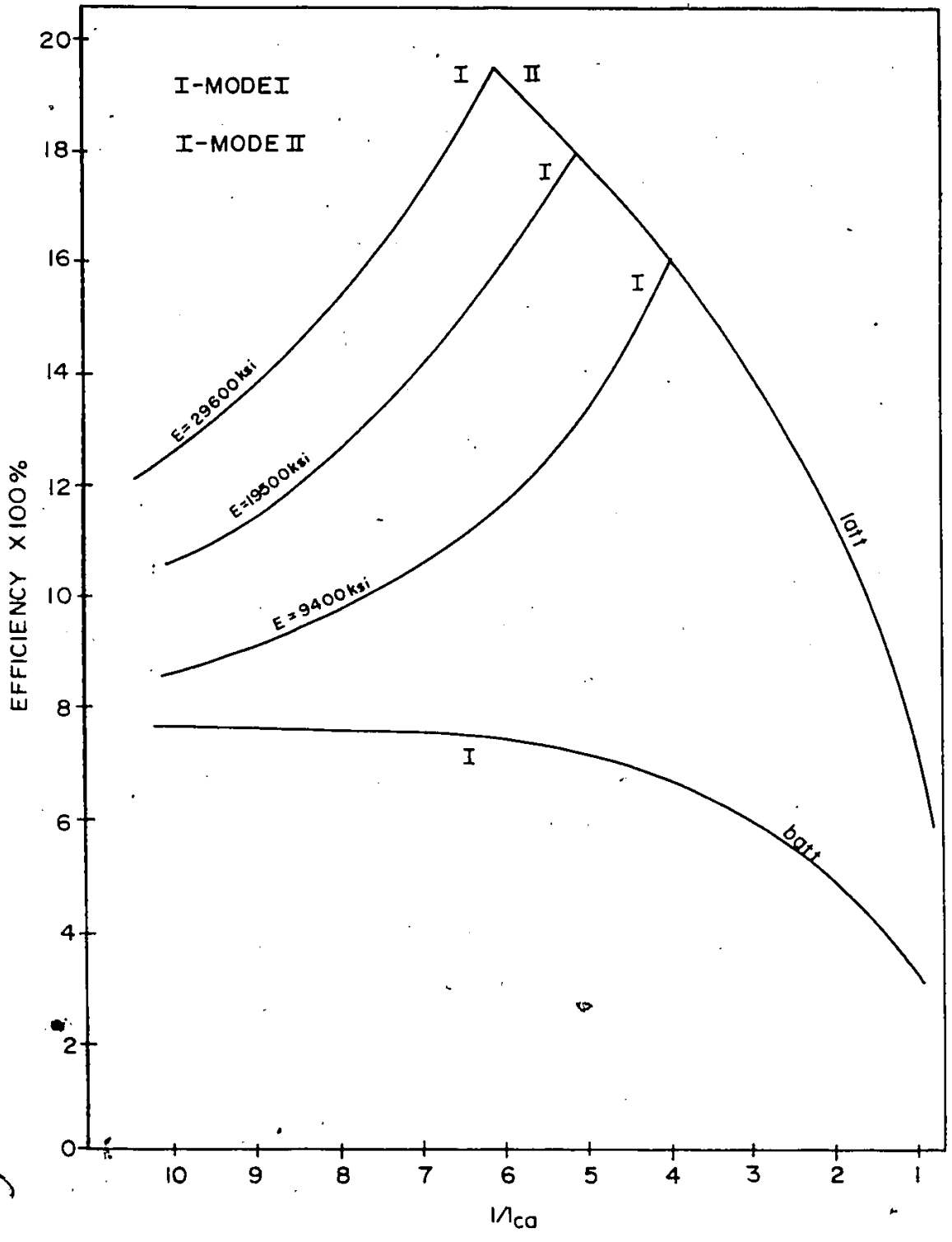

Fig. 4.35 Effect of Crossarm Length on Efficiency for a Diagonal Size of 0.3125 in.

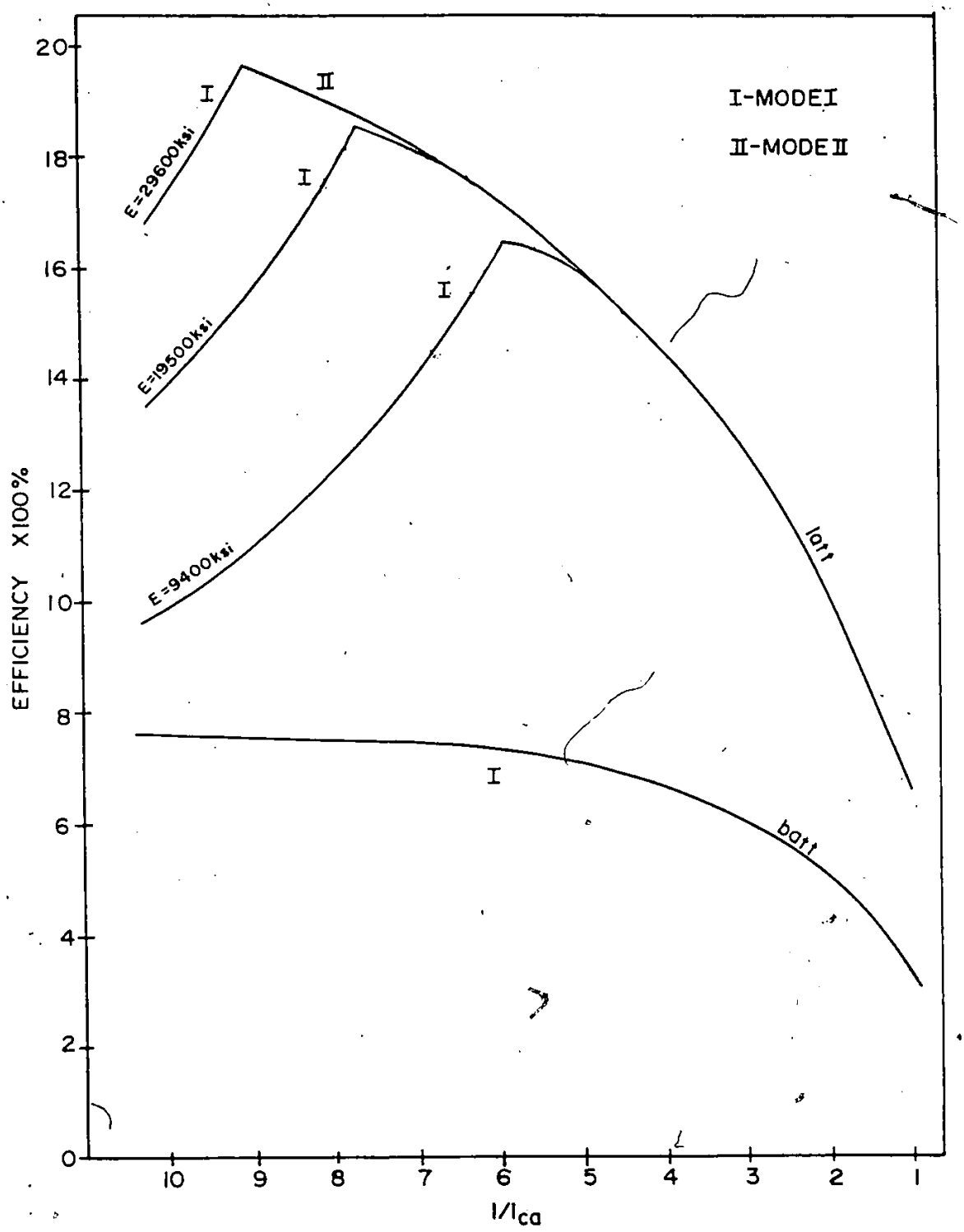

Fig. 4.36 Effect of Crossarm Length on Efficiency for a Diagonal Size of 0.5 in.

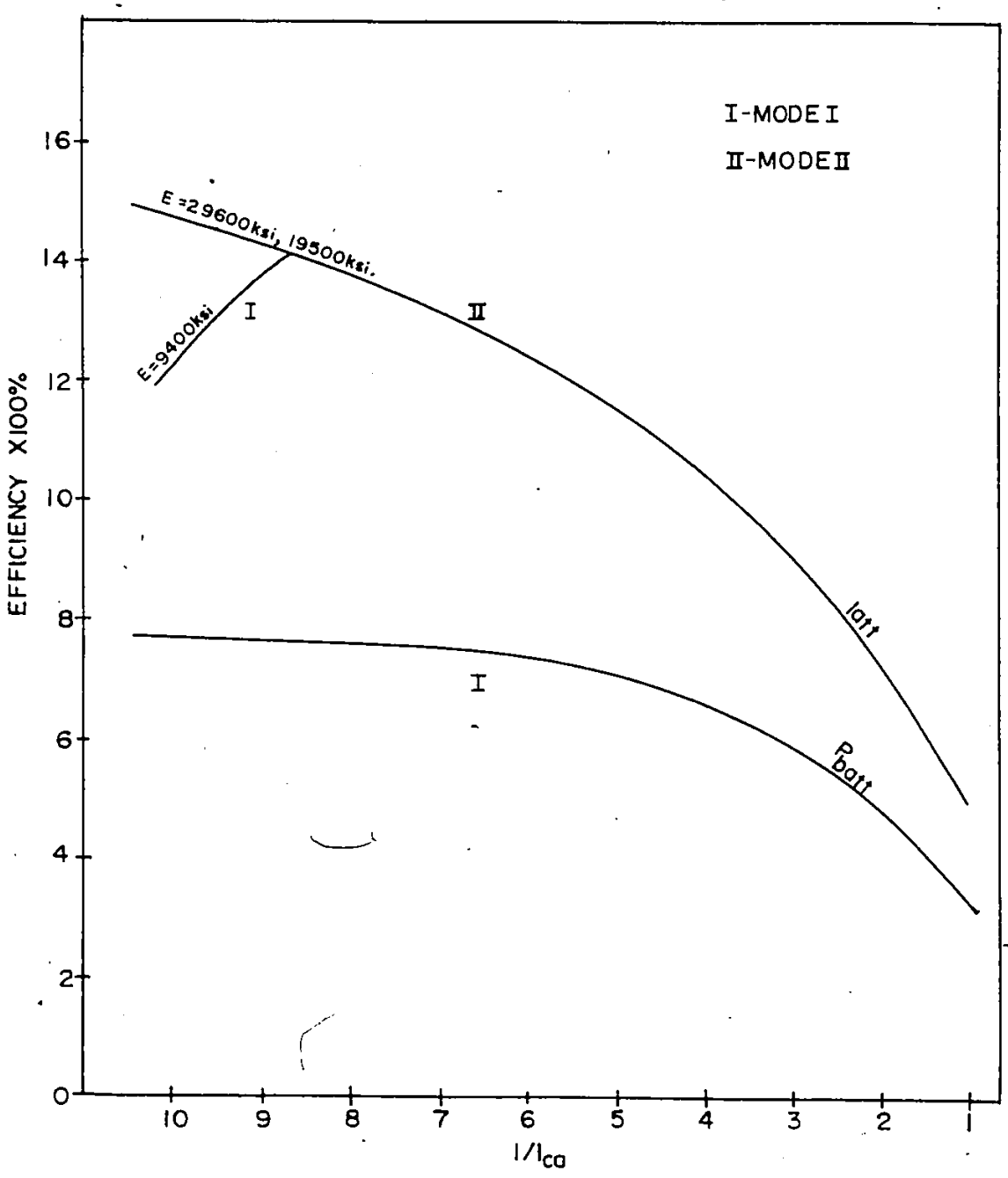

Fig. 4.37 Effect of Crossarm Length on Efficiency for a Diagonal Size of 0.875 in.

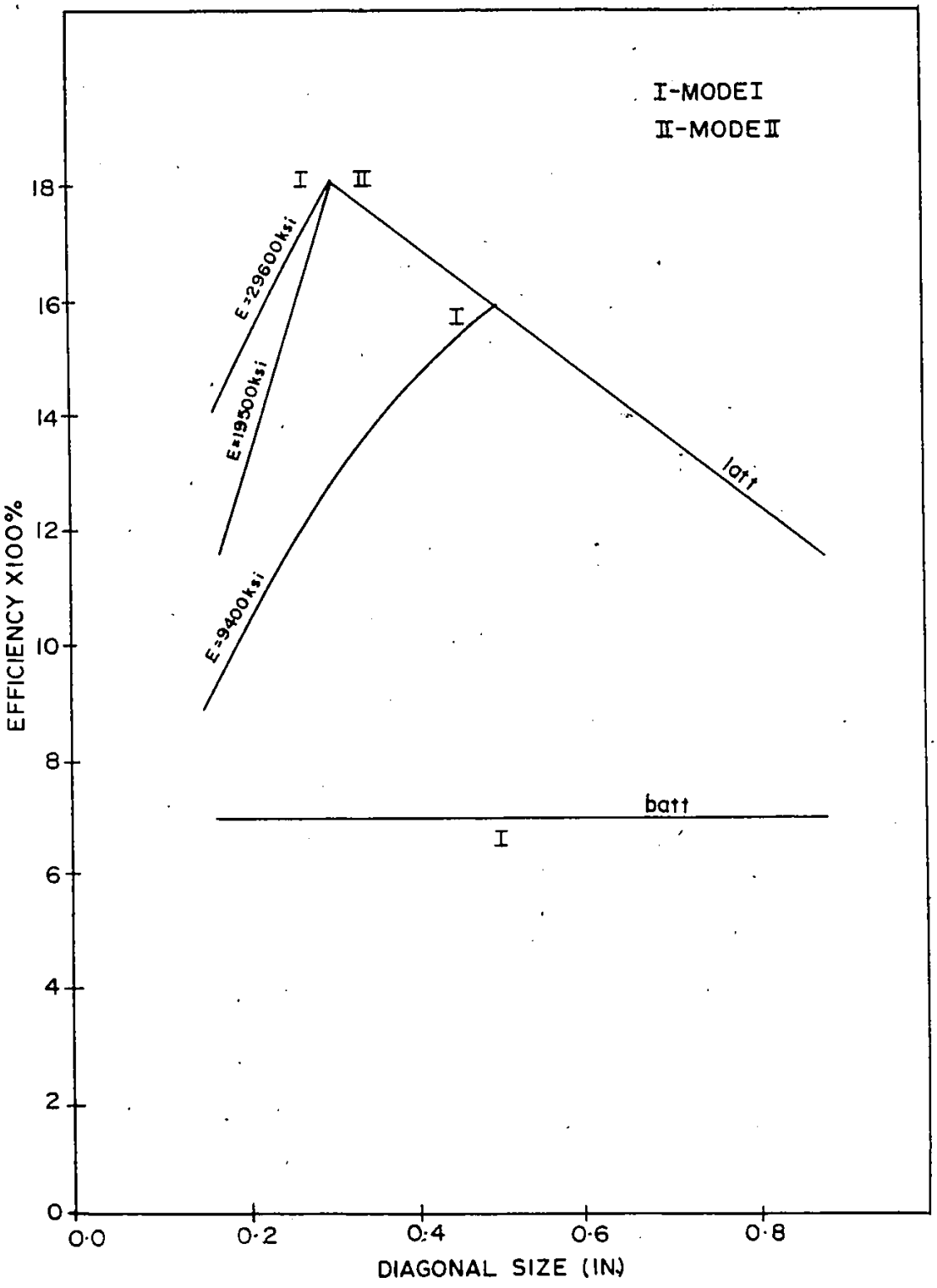

Fig. 4.38 Effect of Diagonal Size on Efficiency for an l/l_{ca} Ratio of five

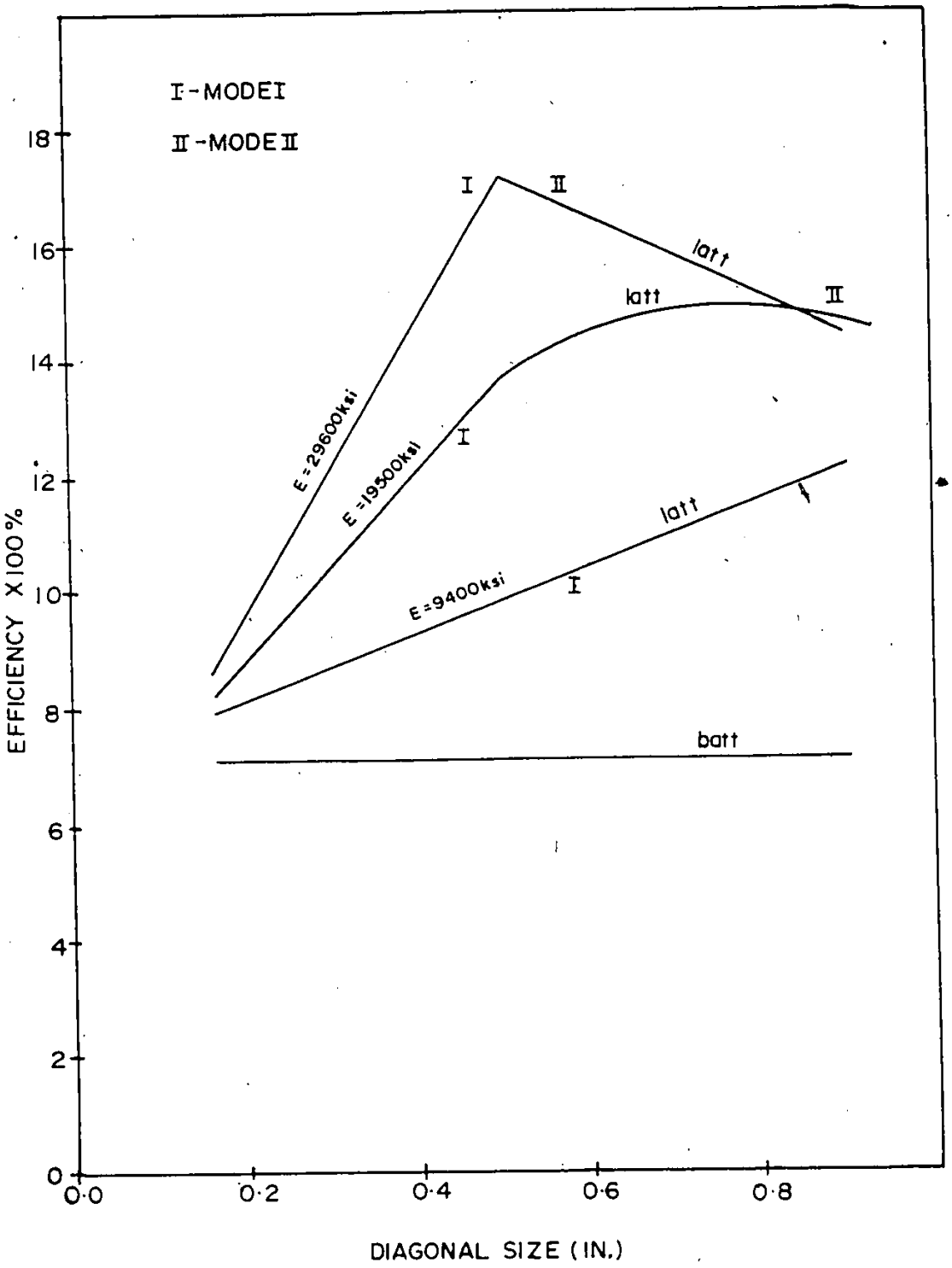

Fig. 4.39 Effect of Diagonal Size on Efficiency for an l/l_{ca} Ratio of ten.

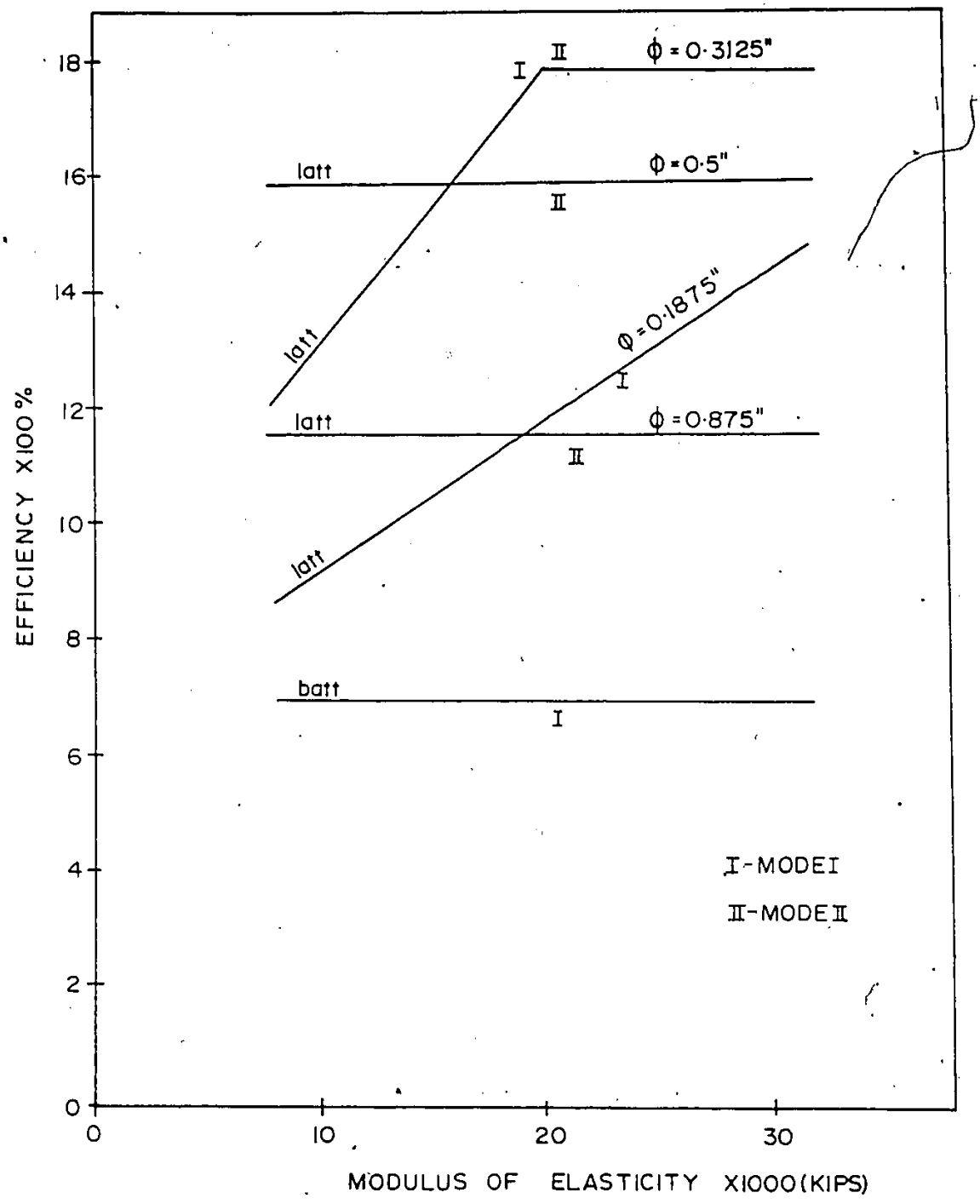

Fig. 4.40 Effect of Diagonal Modulus of Elasticity on Efficiency for an l/l_{ca} Ratio of Five

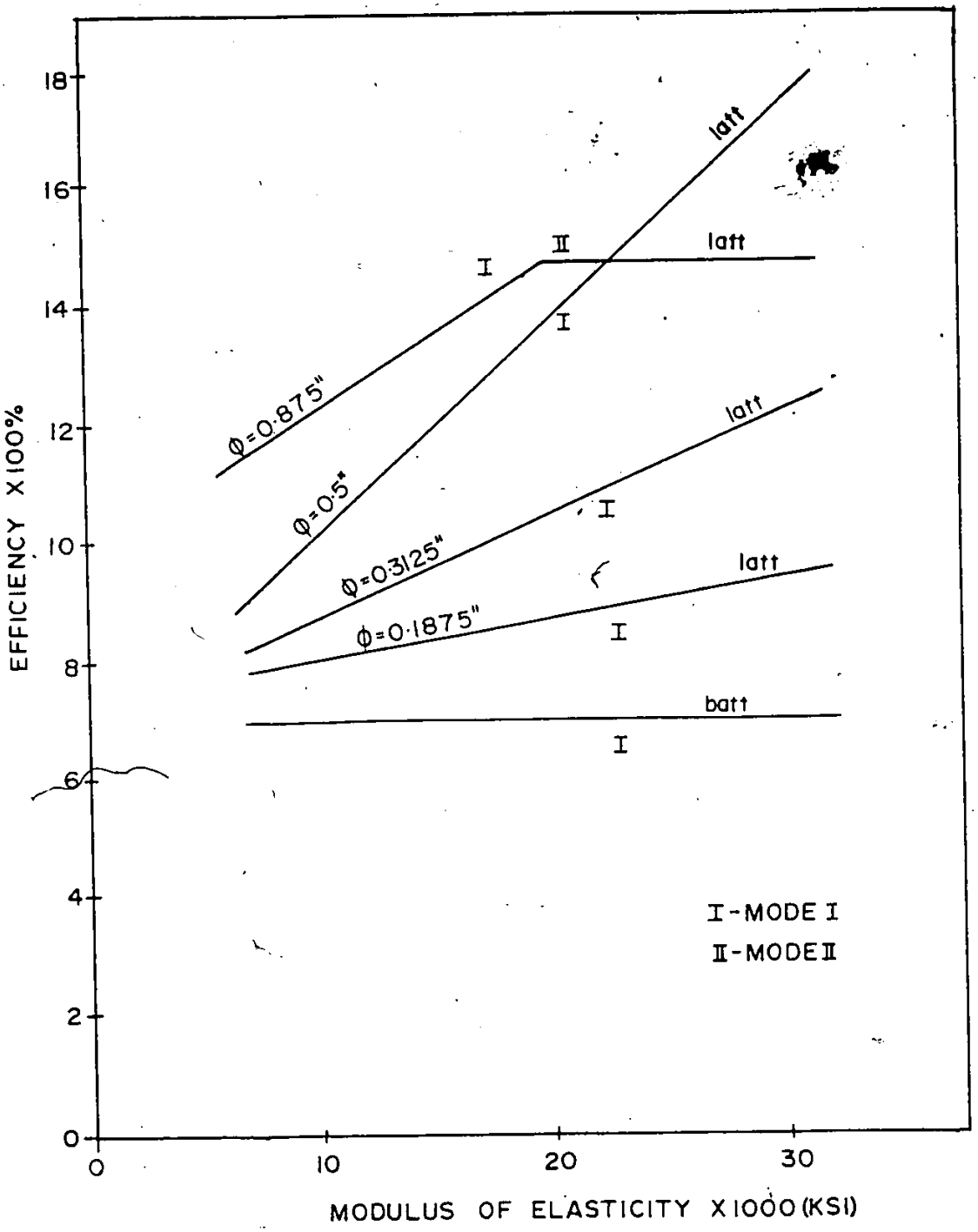

Fig. 4.41 Effect of Diagonal Modulus of Elasticity on Efficiency for an l/l_{ca} Ratio of Ten

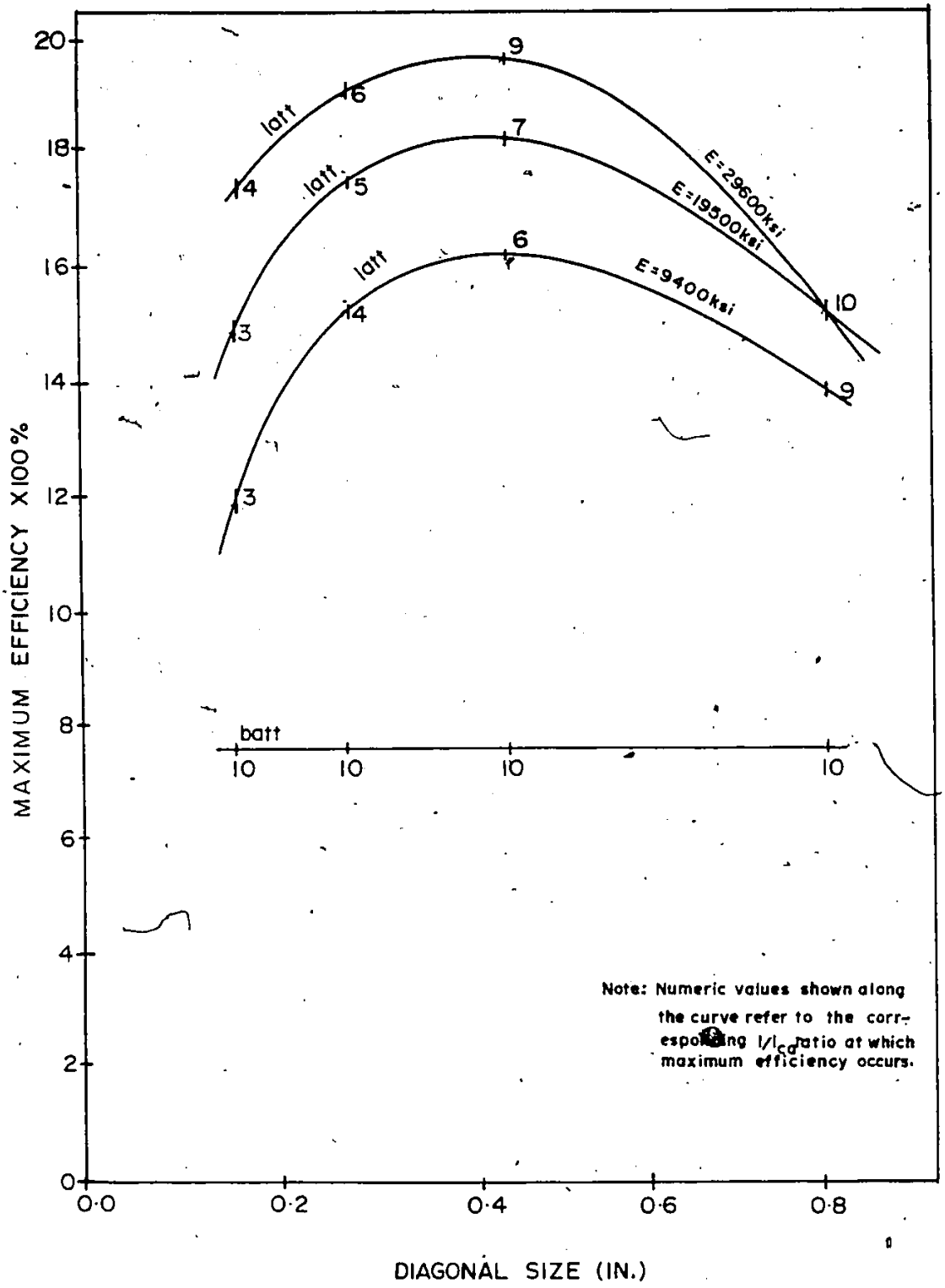

Fig. 4.42 Effect of Diagonal Size on Maximum Efficiency.

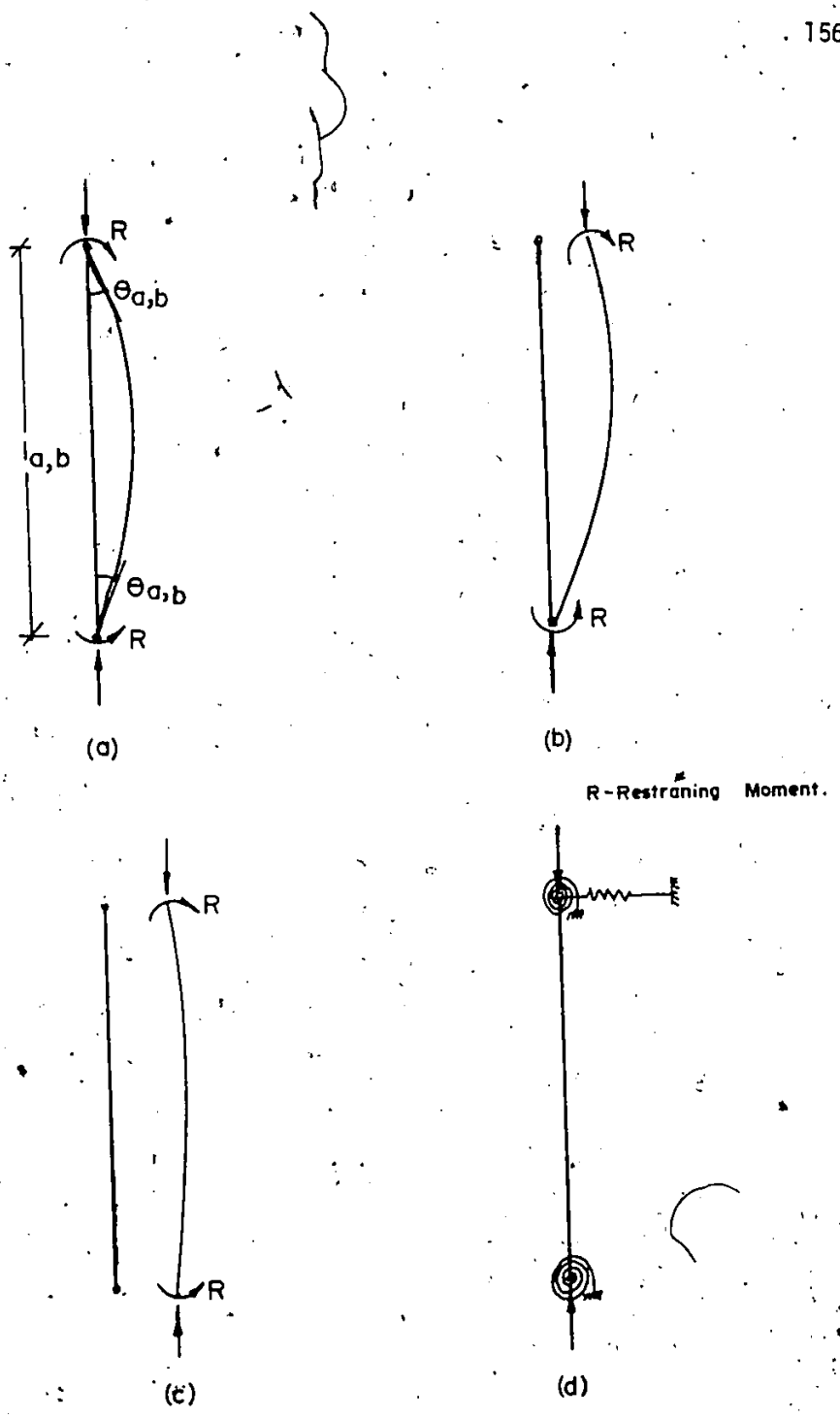

Fig. 5.1 Buckling Shapes of Vertical Members.

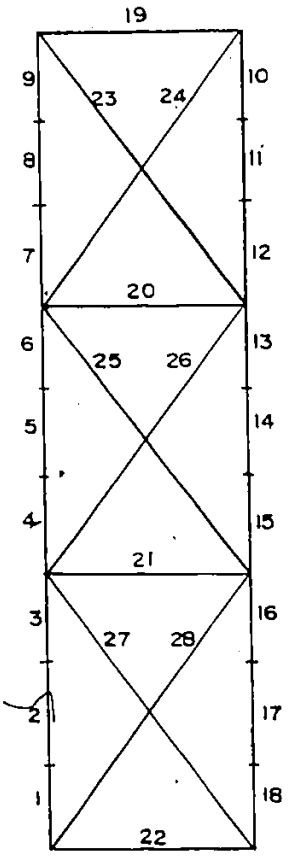

Fig 6.1 Numbering Order for the Elements.

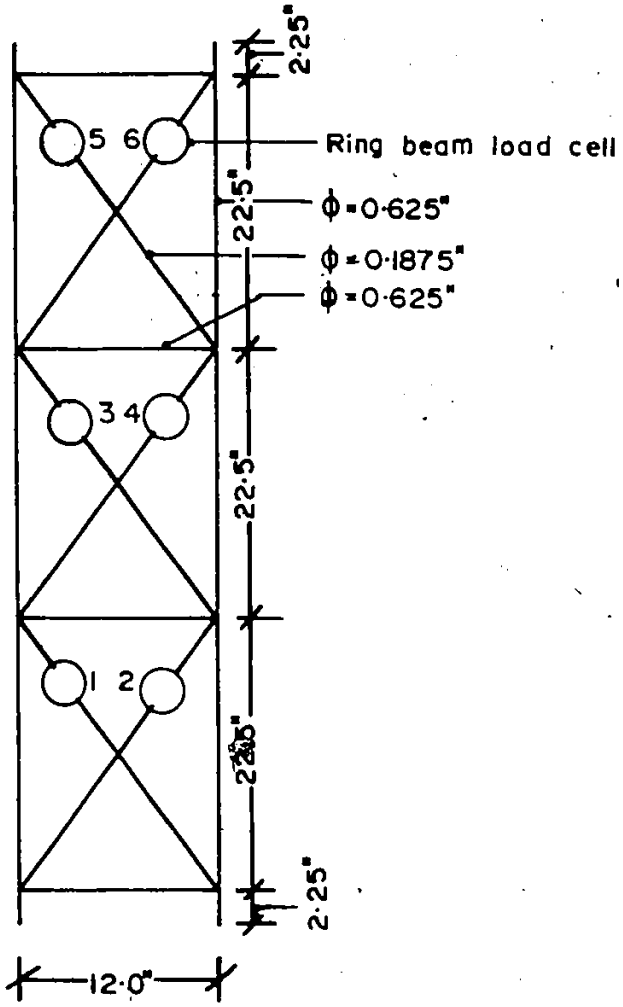

Fig. 7.1 Dimensions of the Model-Frame.

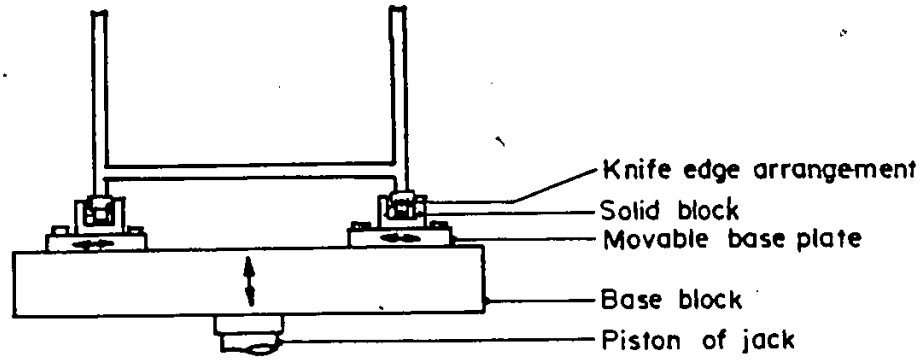

(a)

Bottom Support of Model Frame.

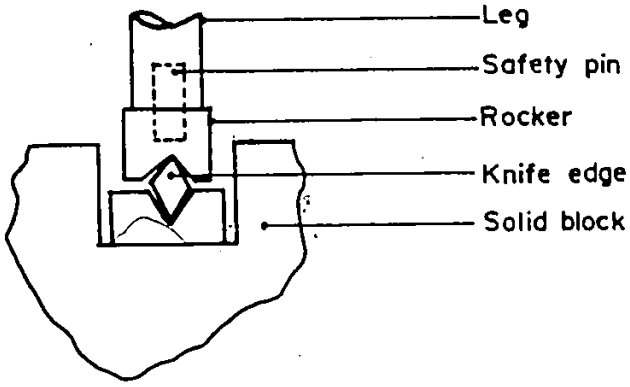

(b)

Knife edge Arrangement.

Fig. 7.2.

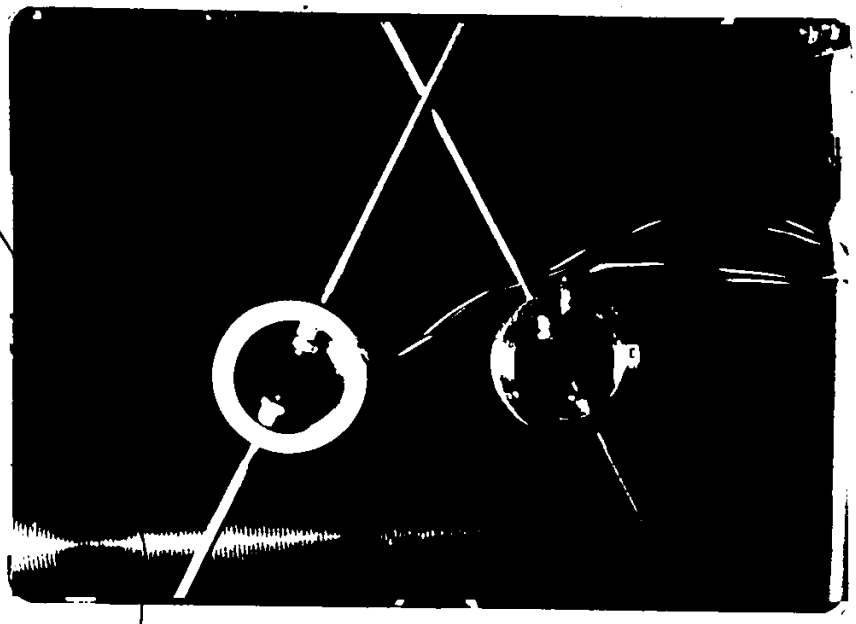

Dimensions of Ring beam load cell:

Mean radius = 1.125 in.

Section = 2/8 X 3/8 in.

Fig. 7.3 Ring beam load cell.

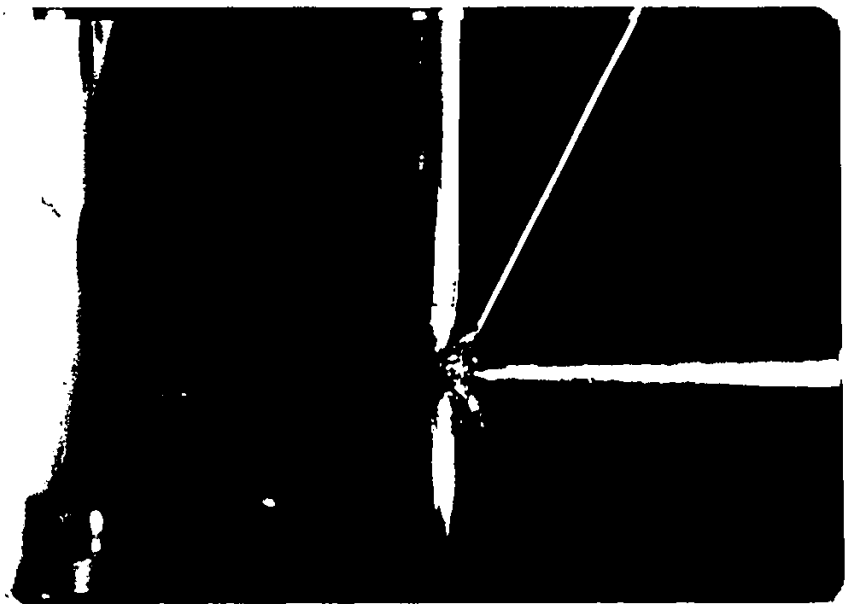

Fig. 7.4 Welded Connection of Members.

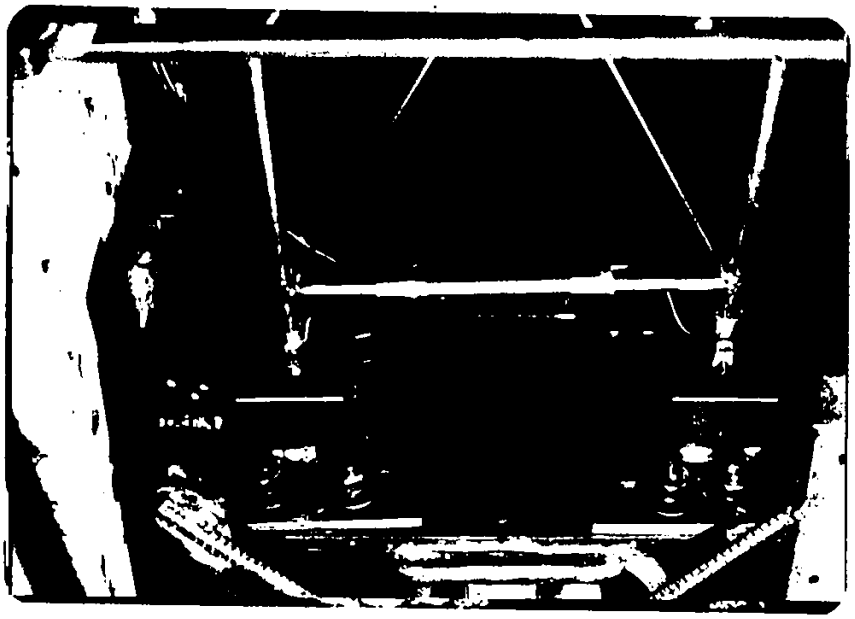

Fig. 7.5 Bottom Support of Model Frame.

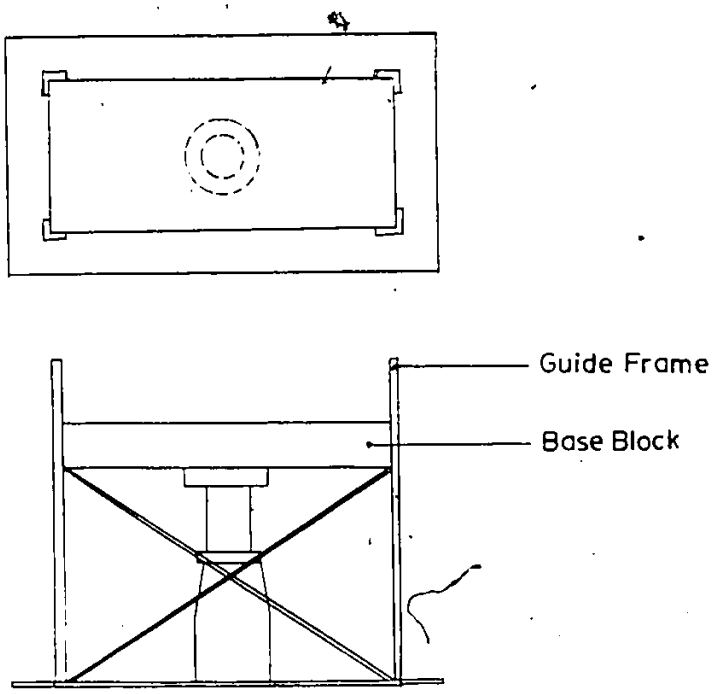

Fig. 7.6 Bottom Support of Model Frame.

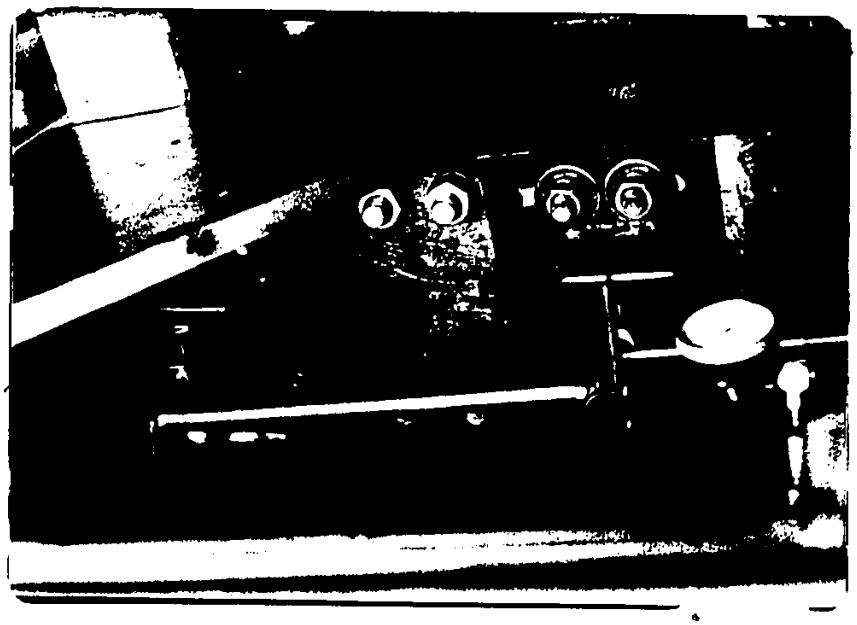

Fig. 7.7 Top Support of Model Frame.

Fig. 7.8 Load cell at the Top Support.

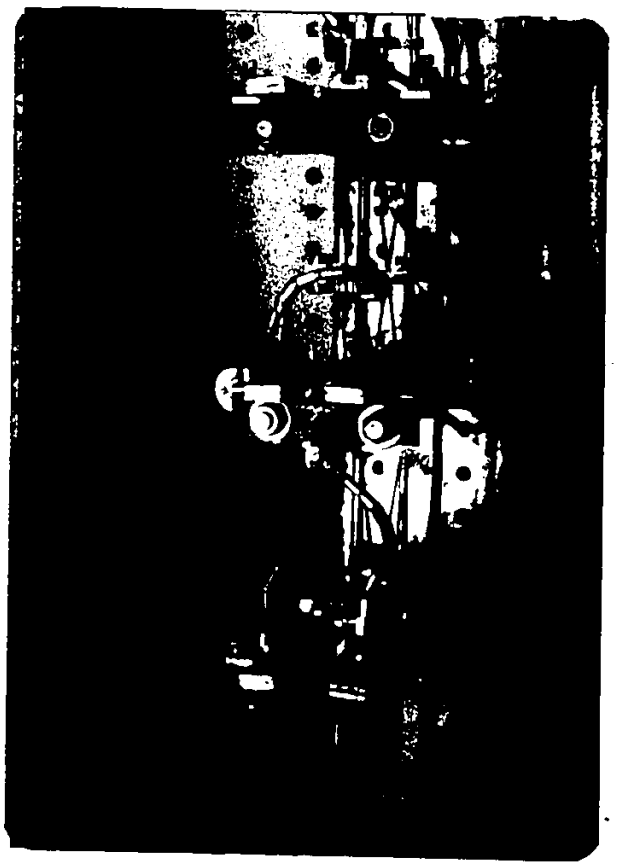

Fig. 7.9 Lateral Support of Model Frame.

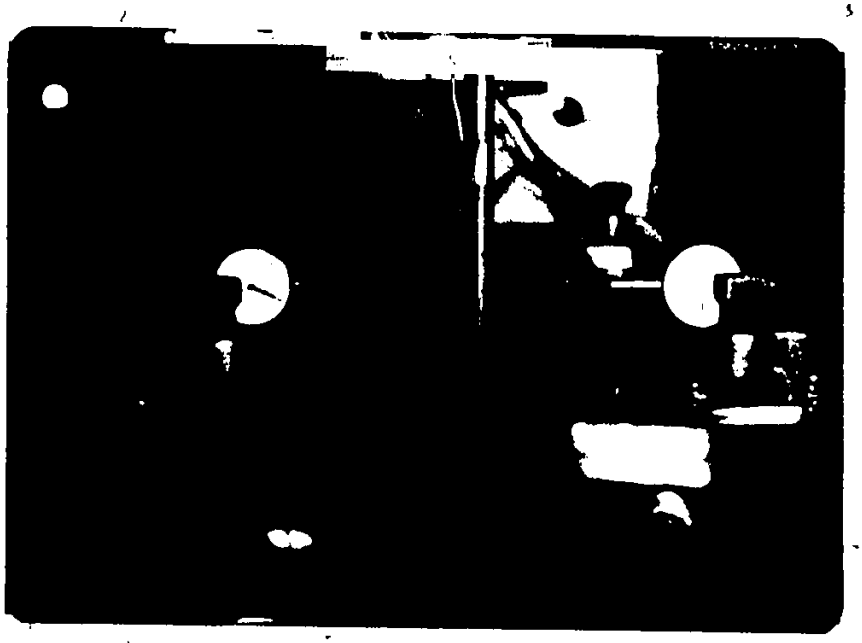

Fig. 7.10 Close View of Lateral Support.

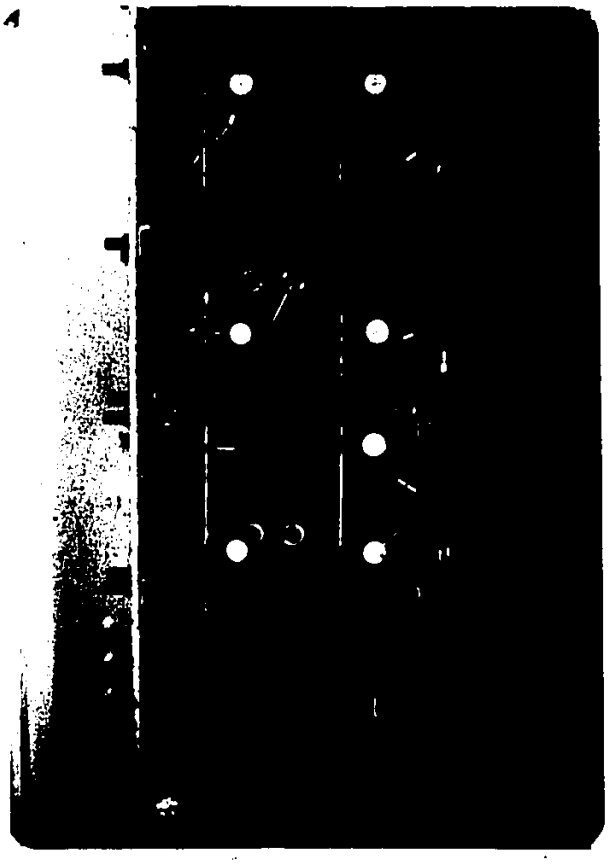

Fig. 7.11 Location of Dial gages in the Model Frame.

Fig. 7.12 Loading Jack at the Bottom Support.

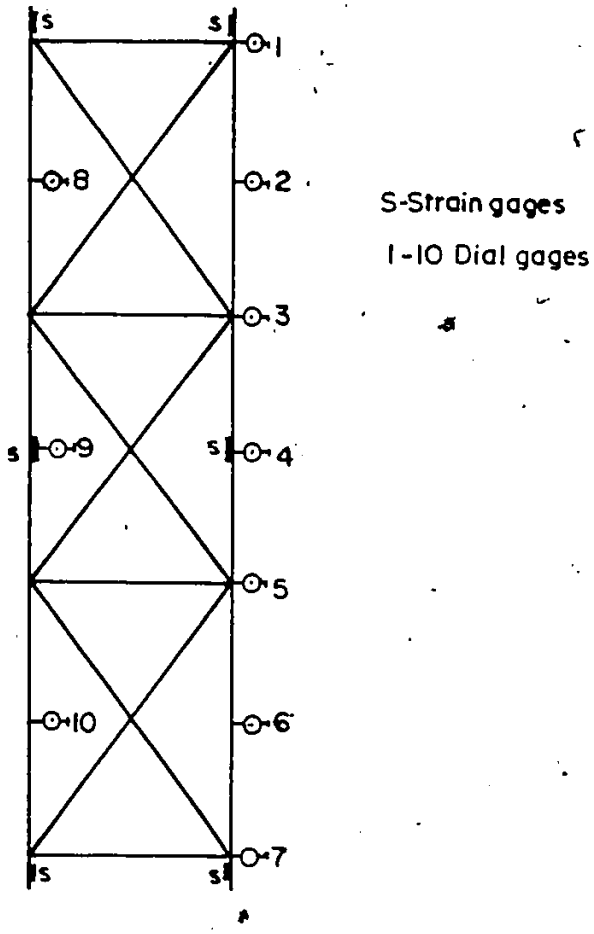

Fig. 7.13 Location of Dial Gages and Strain Gages in the Model Frame.

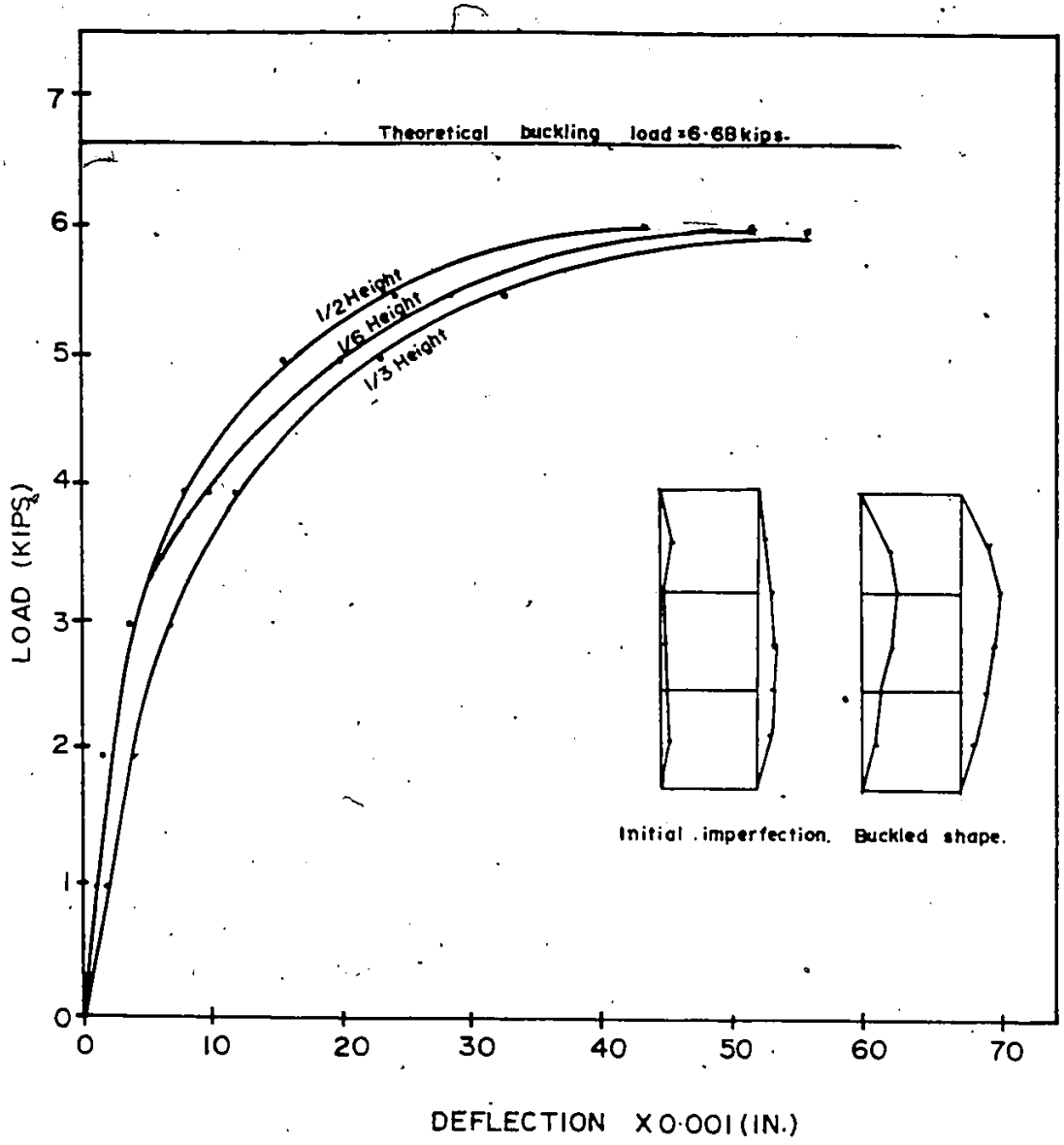

Fig. 8.1 Load Versus Deflection of Battened Frame.

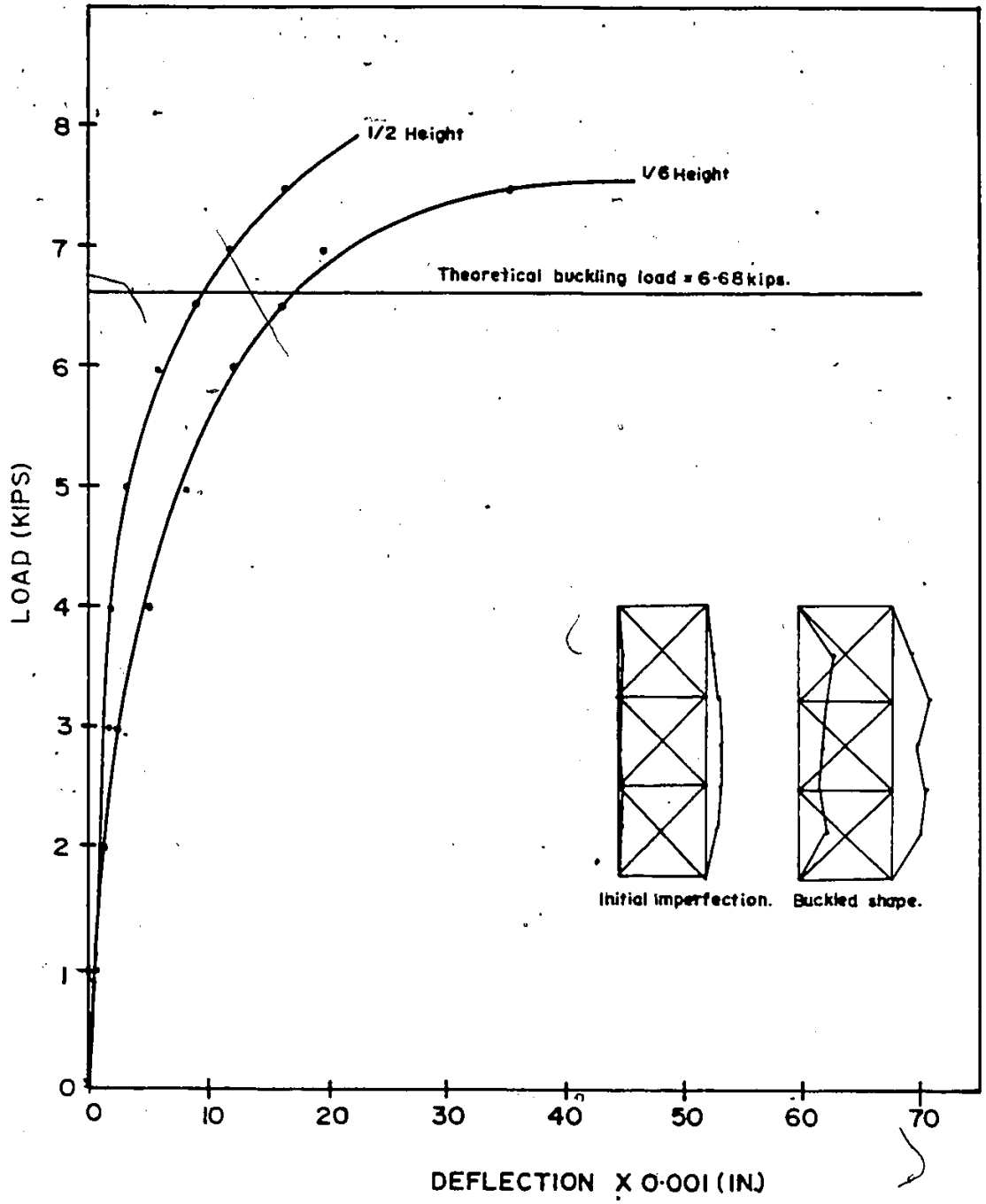

Fig. 8.2 Load Versus Deflection for an Initial Pretension of 50 lbs.

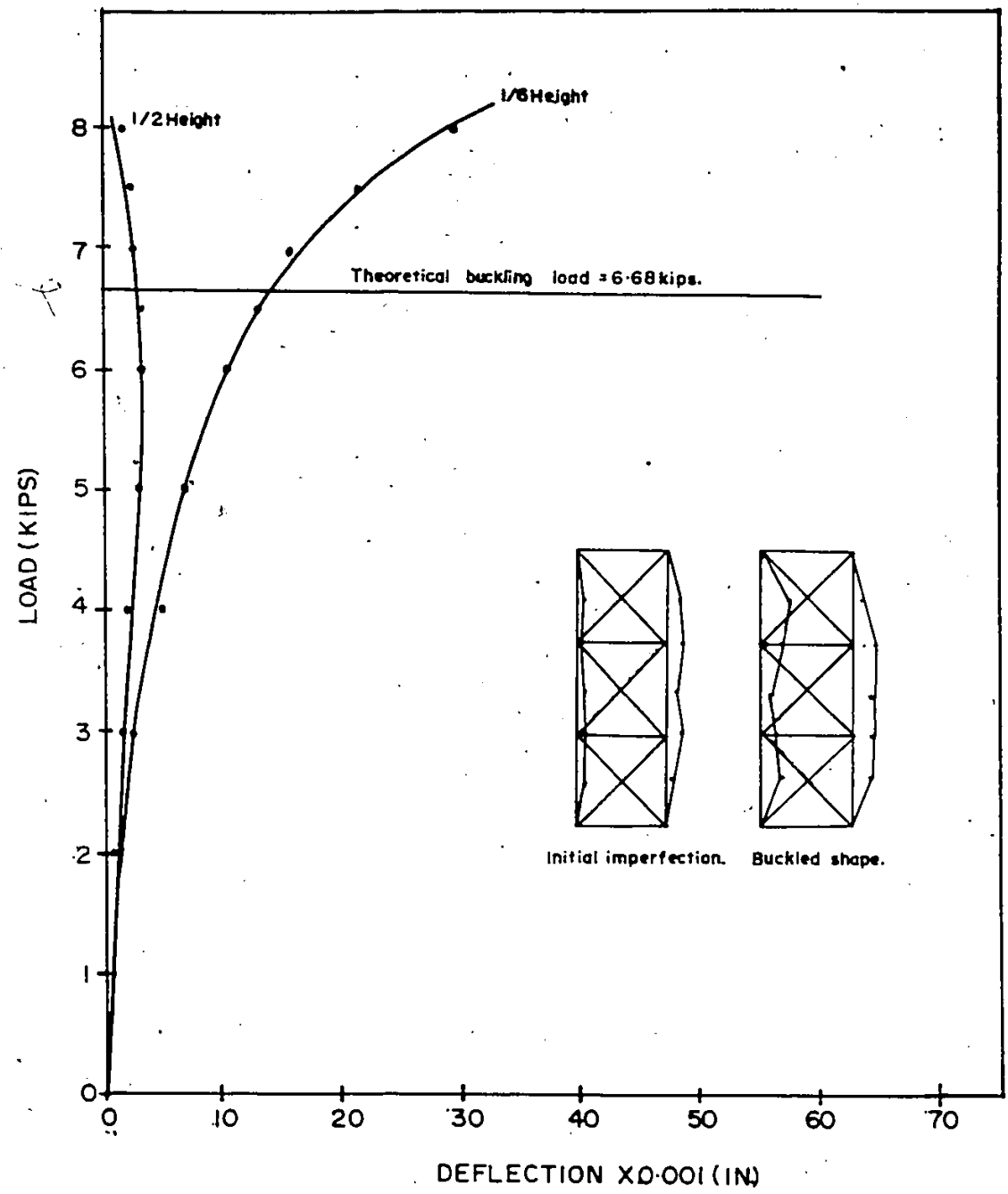

Fig. 8.3. Load Versus Deflection for an Initial Pretension of 100 lbs.

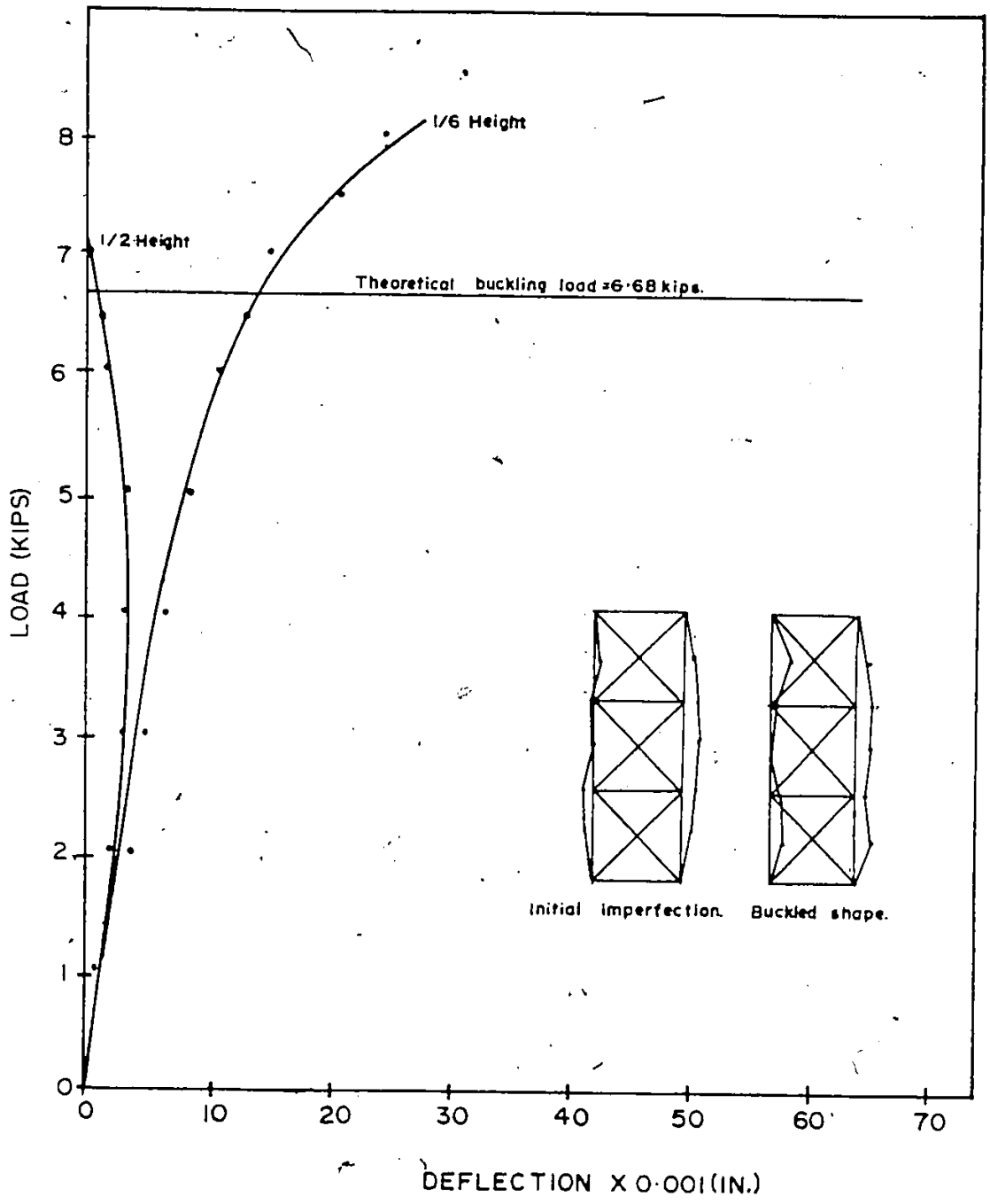

Fig. 8.4 Load Versus Deflection for an Initial Pretension of 150 lbs.

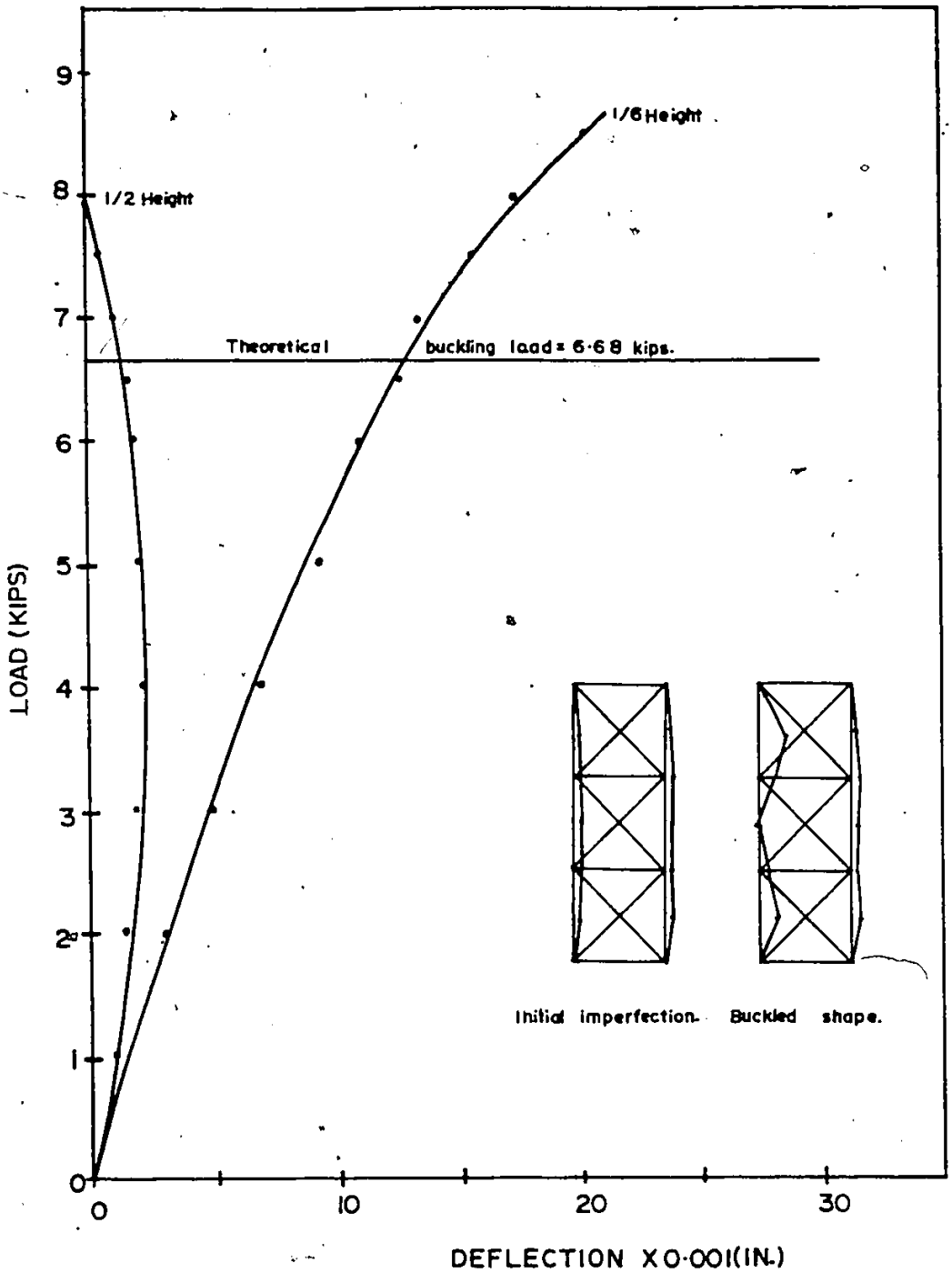

Fig. 8.5 Load Versus Deflection for an Initial Pretension of 230 lbs.

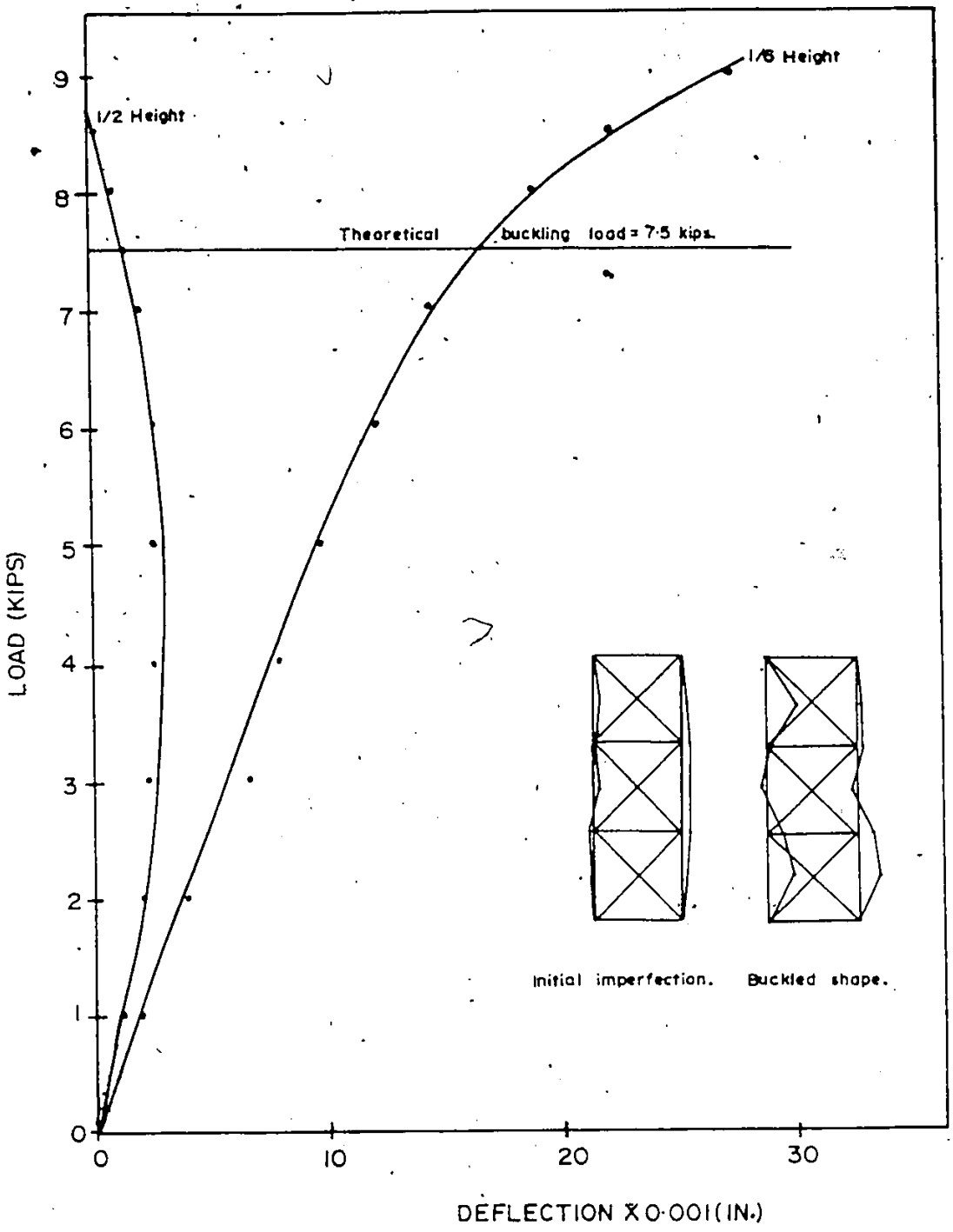

Fig. 8.6 Load versus Deflection for an Initial Pretension of 260 lbs.

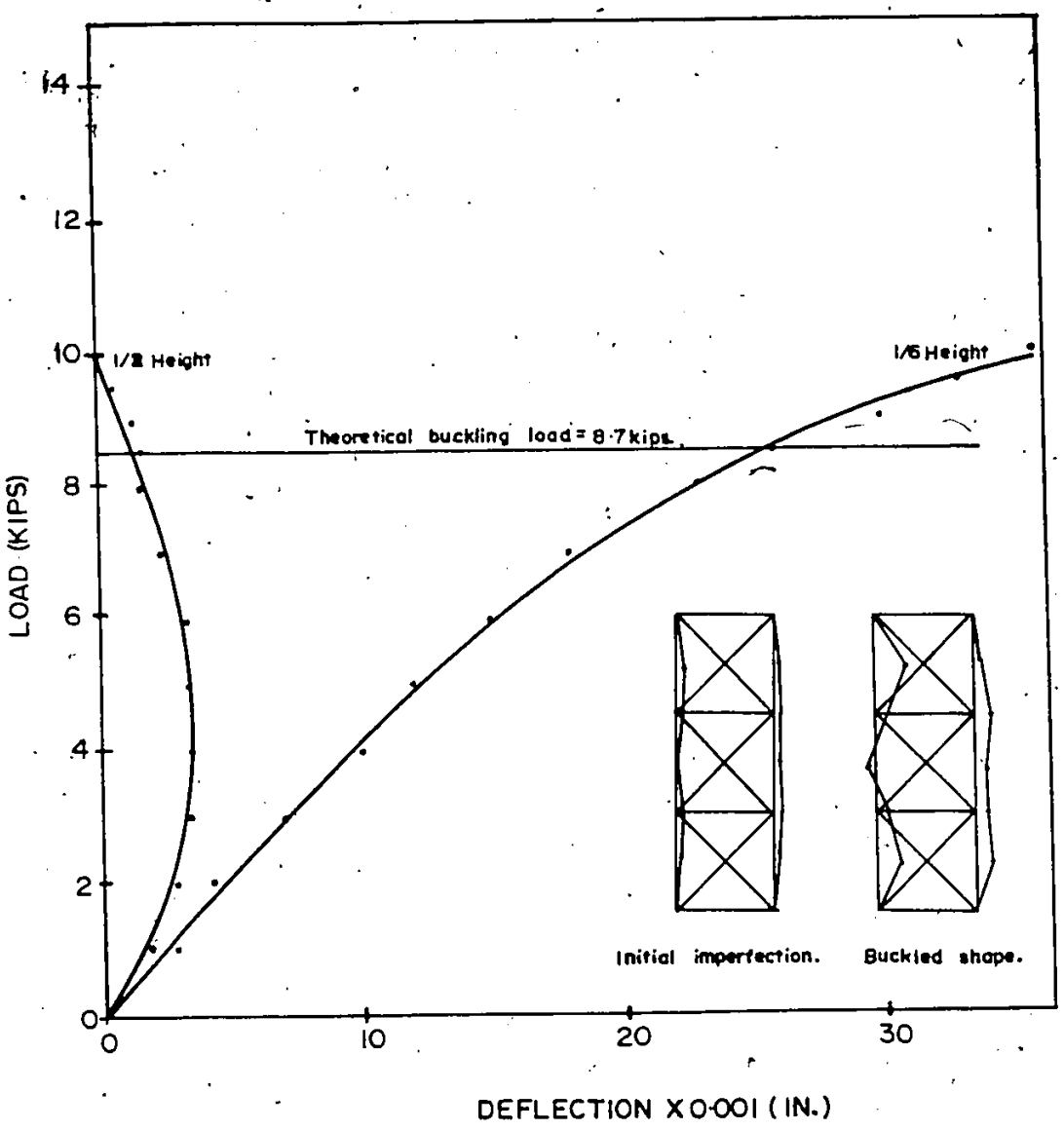

Fig. 8.7 Load Versus Deflection for an Initial Pretension of 300 lbs.

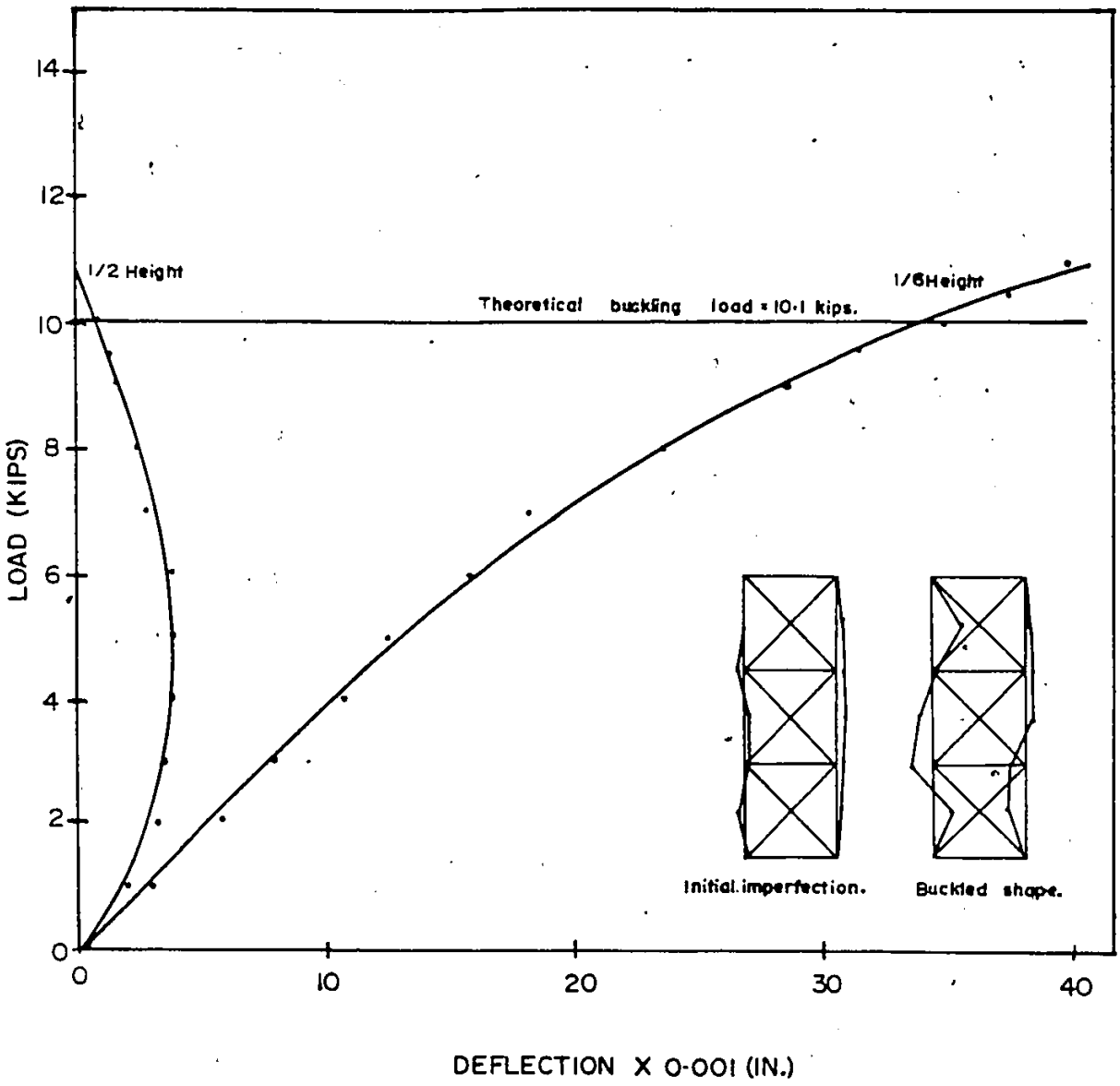

Fig. 8.8 Load Versus Deflection for an Initial Pretension of 350 lbs.

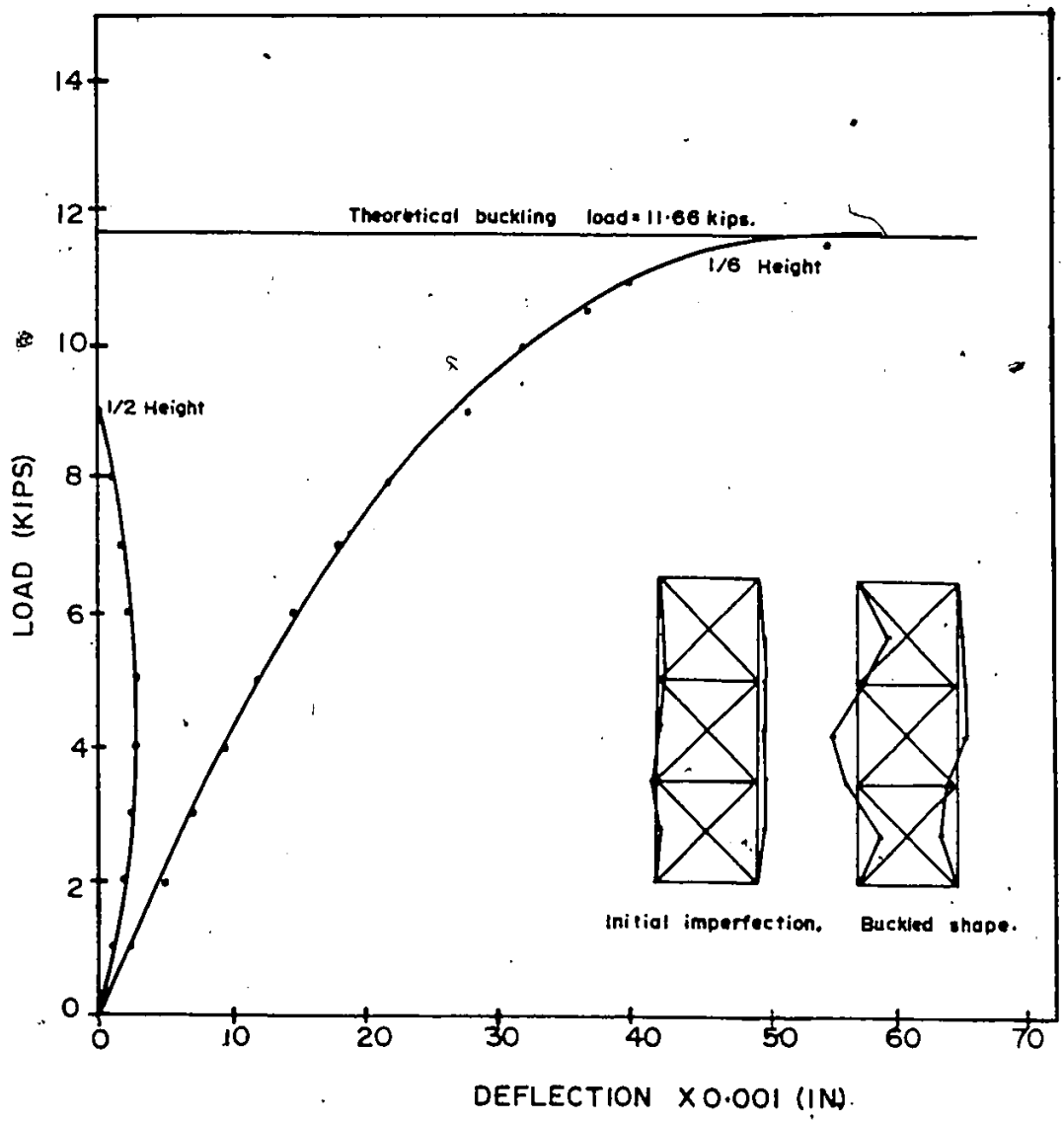

Fig. 8.9 Load Versus Deflection for an Initial Pretension of 400 lbs.

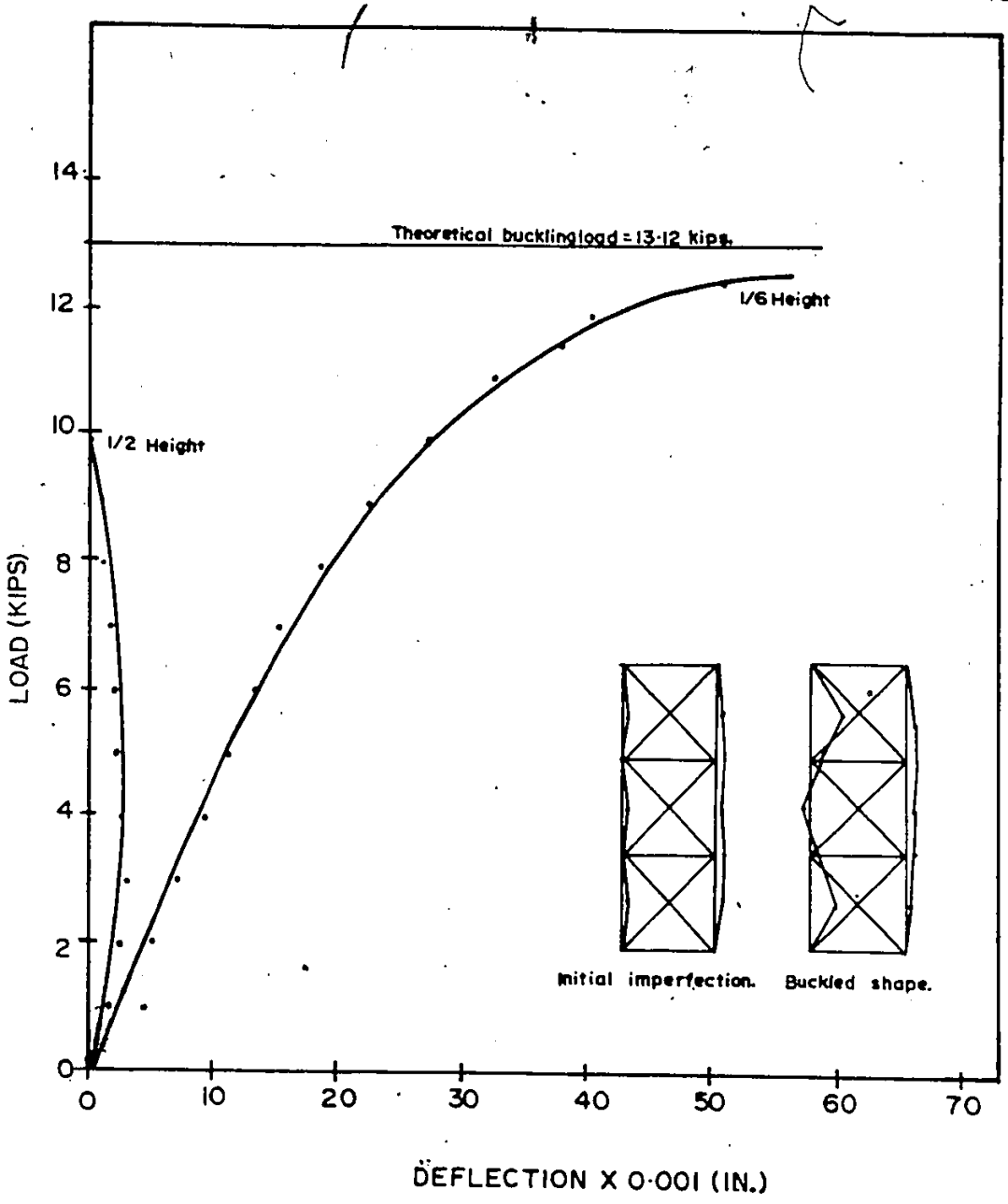

Fig 8.10 Load Versus Deflection for an Initial Pretension of 450 lbs.

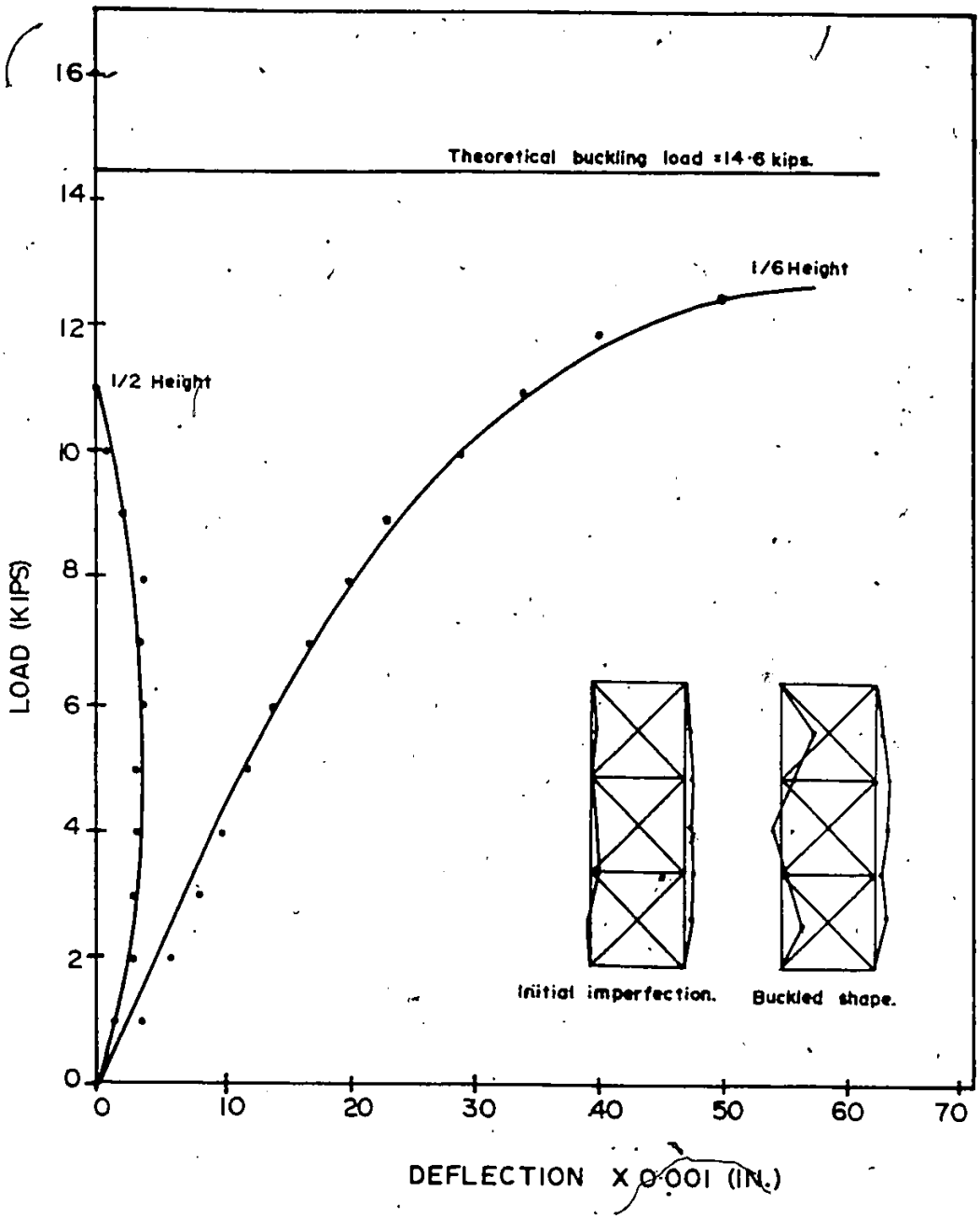

Fig. 8.11 Load Versus Deflection for an Initial Pretension of 500 lbs.

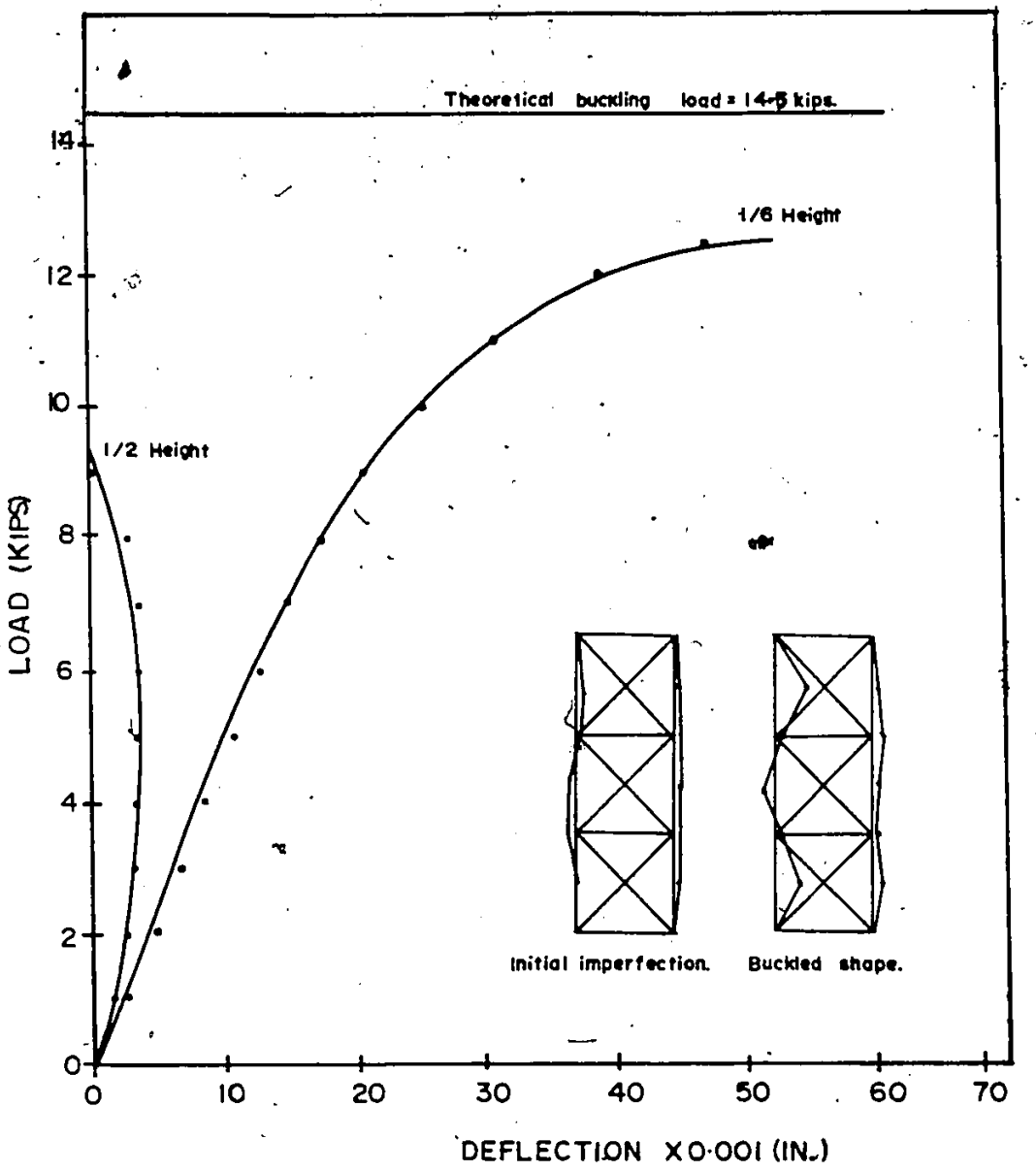

Fig. 8.12 Load Versus Deflection for an Initial Pretension of 550 lbs.

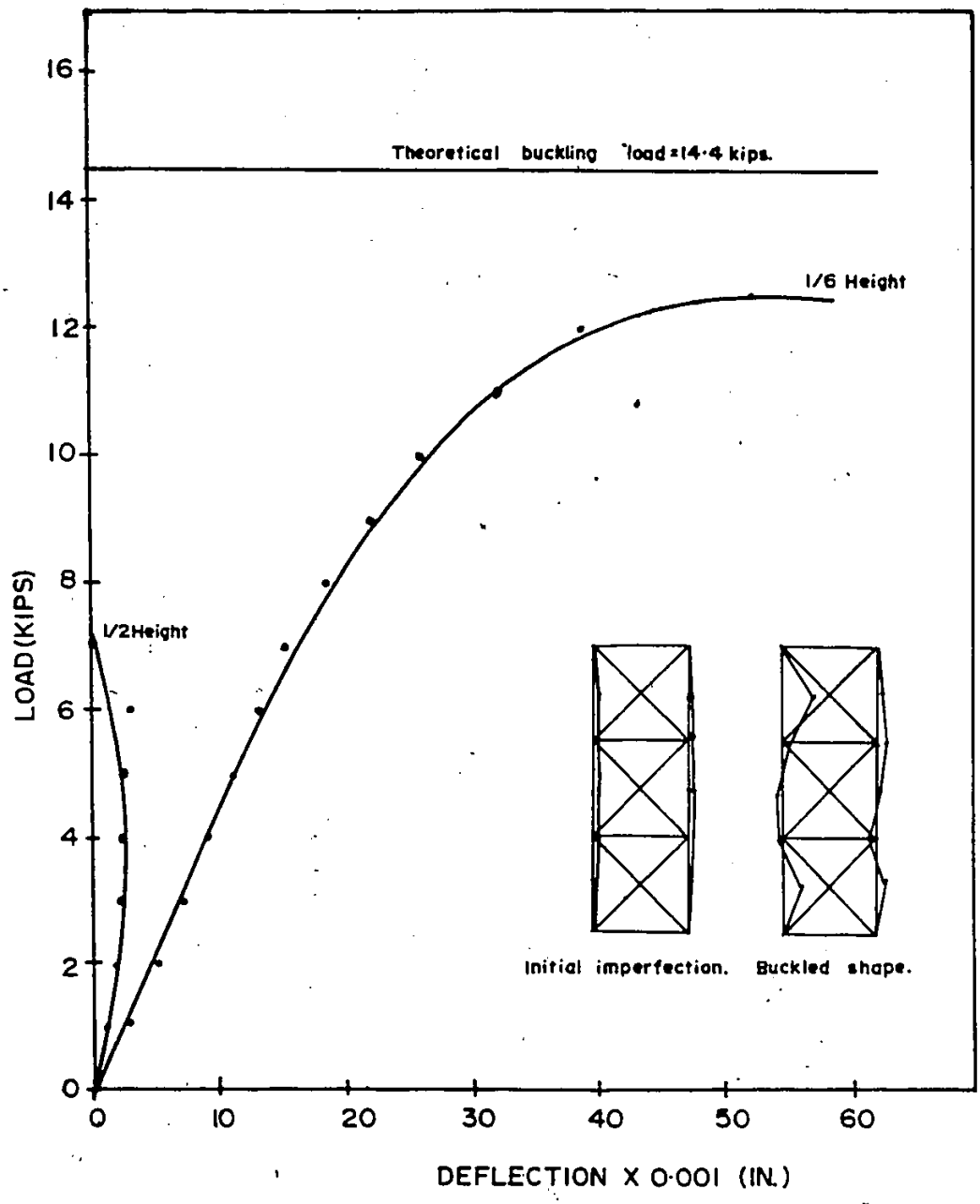

Fig. 8.13 Load Versus Deflection for an Initial Pretension of 600lbs.

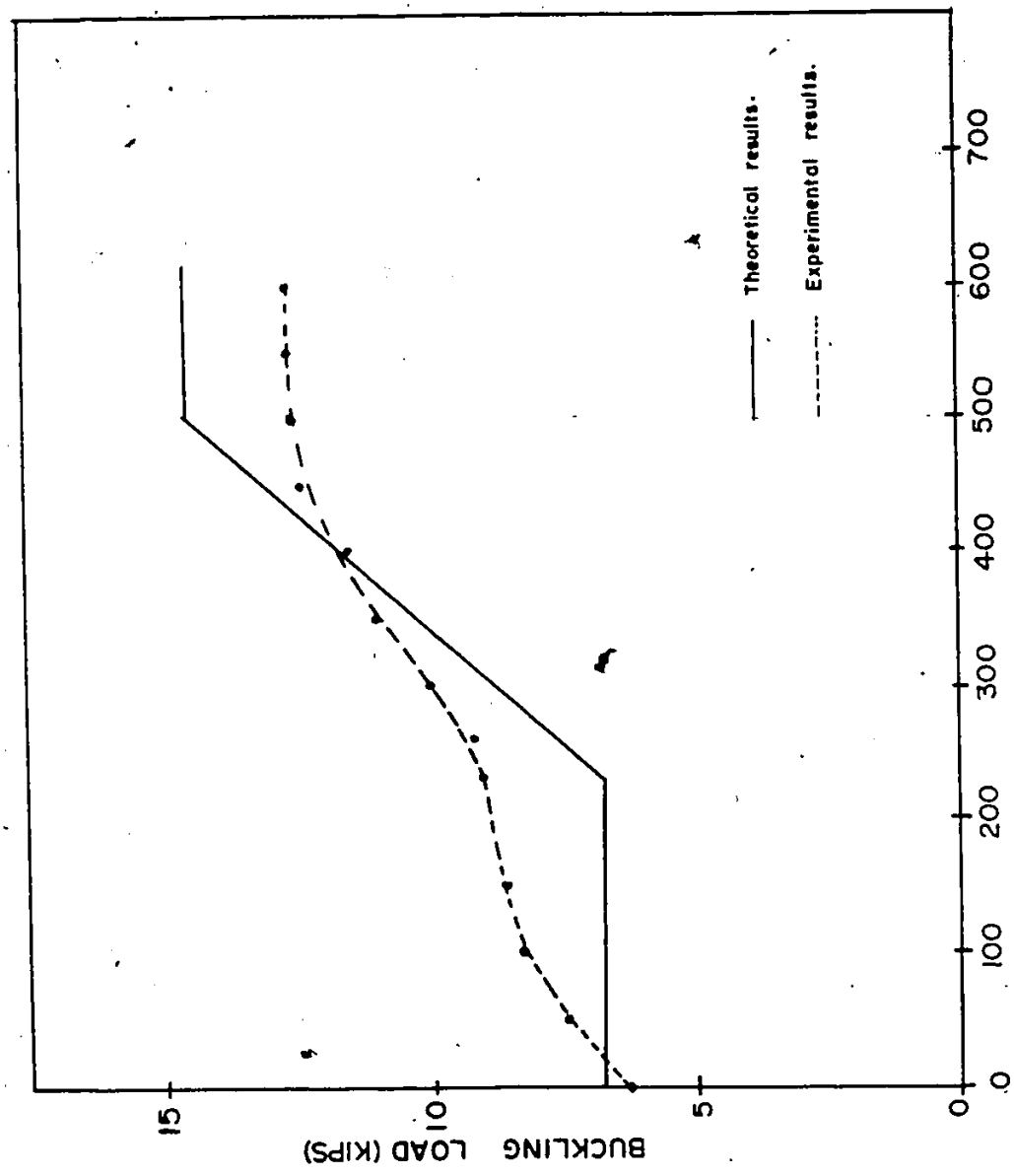

Fig. 8.14 Comparison of Theoretical and Experimental Buckling Loads

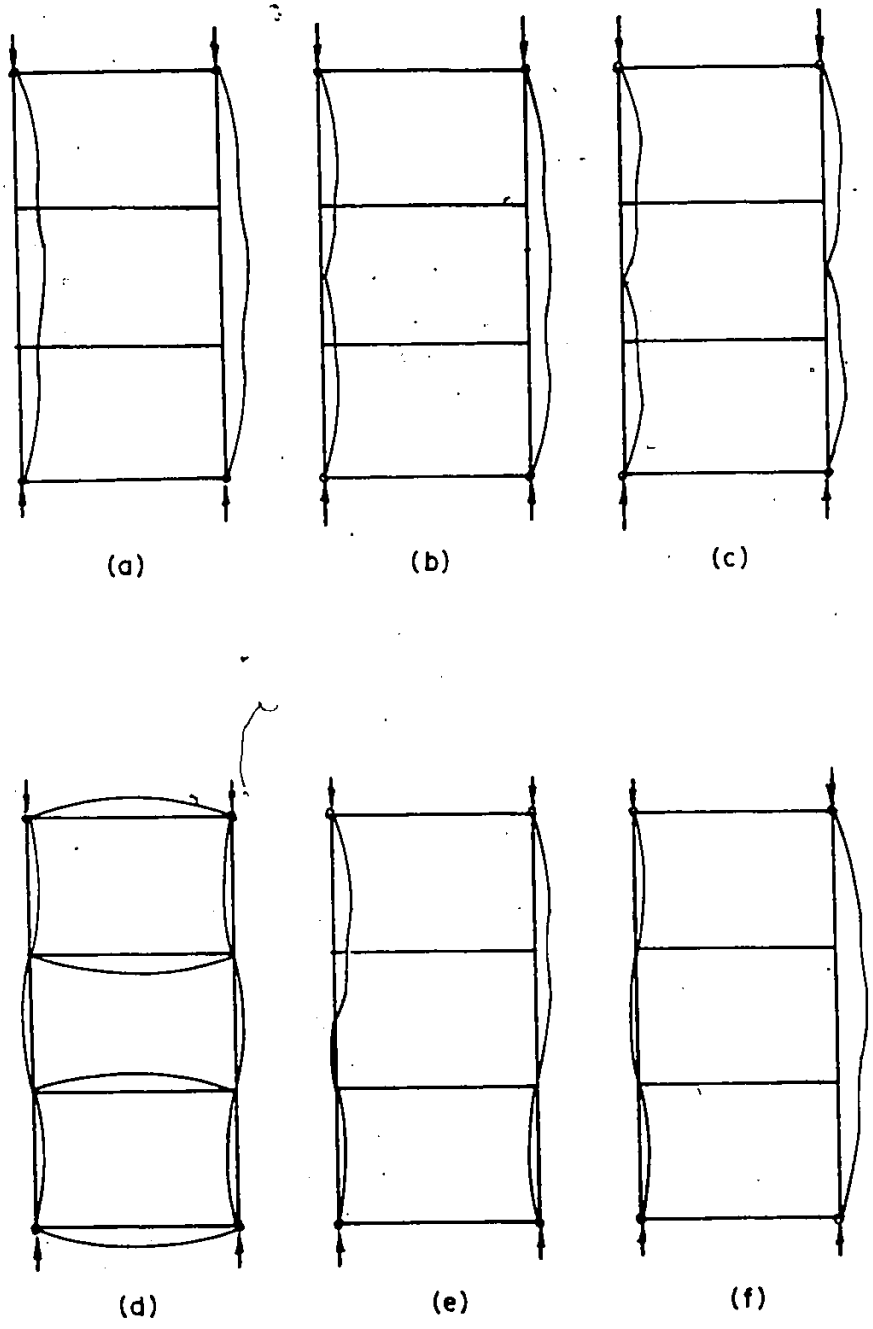

Fig. 8.15 Various Buckling Shapes Due to Imperfections in the Frame

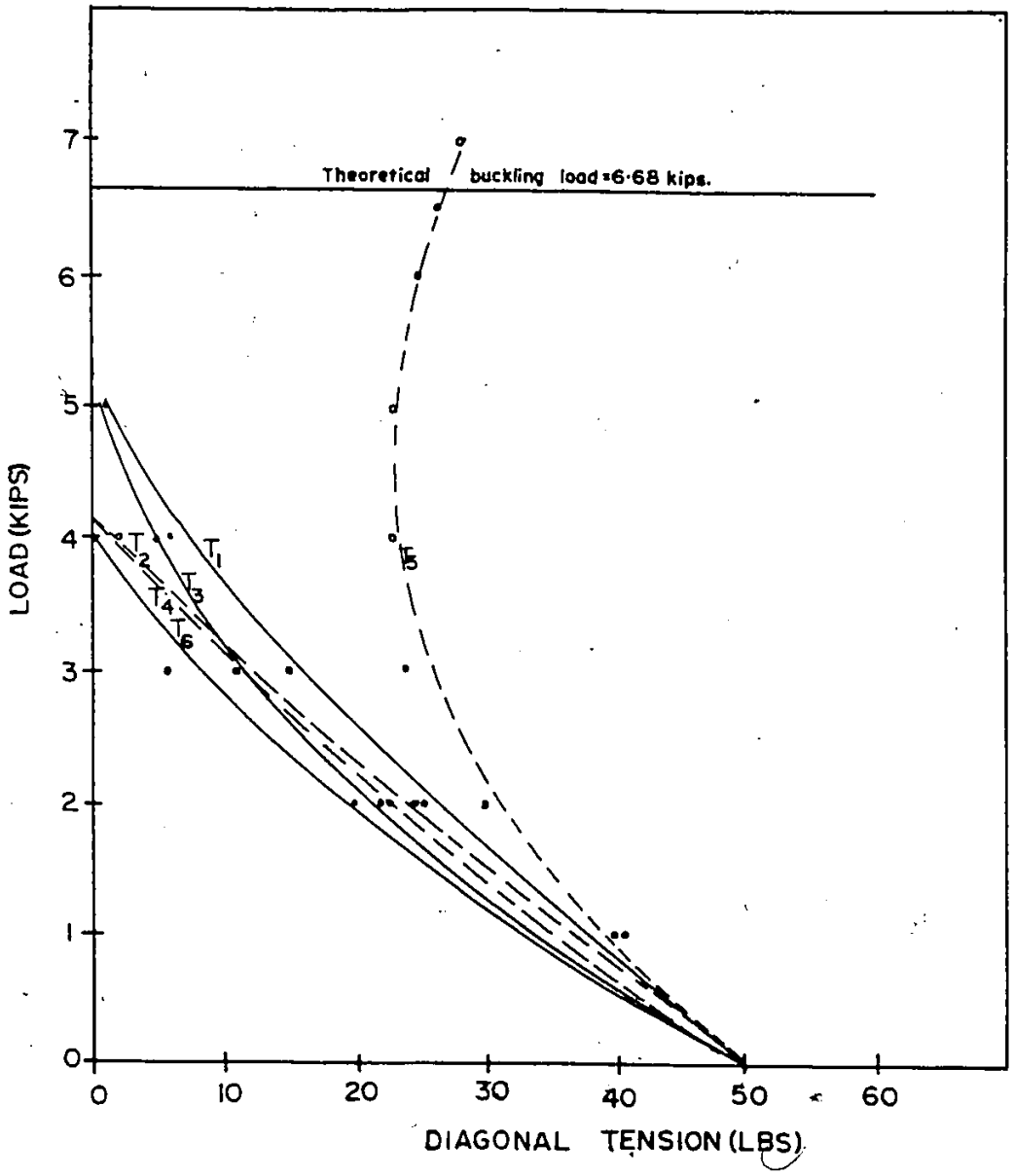

Fig. 8.16 Load Versus Diagonal Tension for an Initial Pretension of 50 lbs.

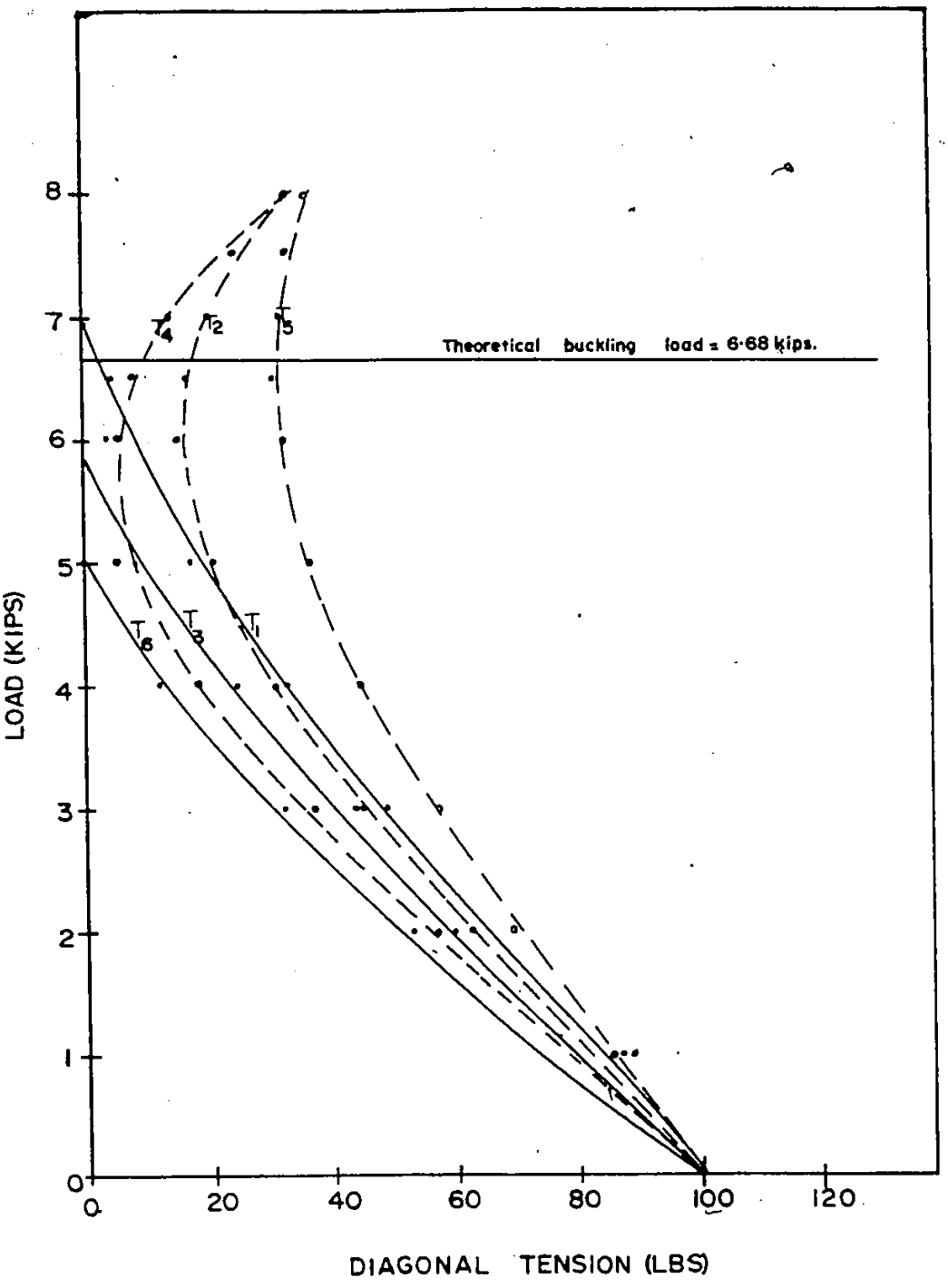

Fig. 8.17 Load Versus Diagonal Tension for an Initial Pretension of 100 lbs.

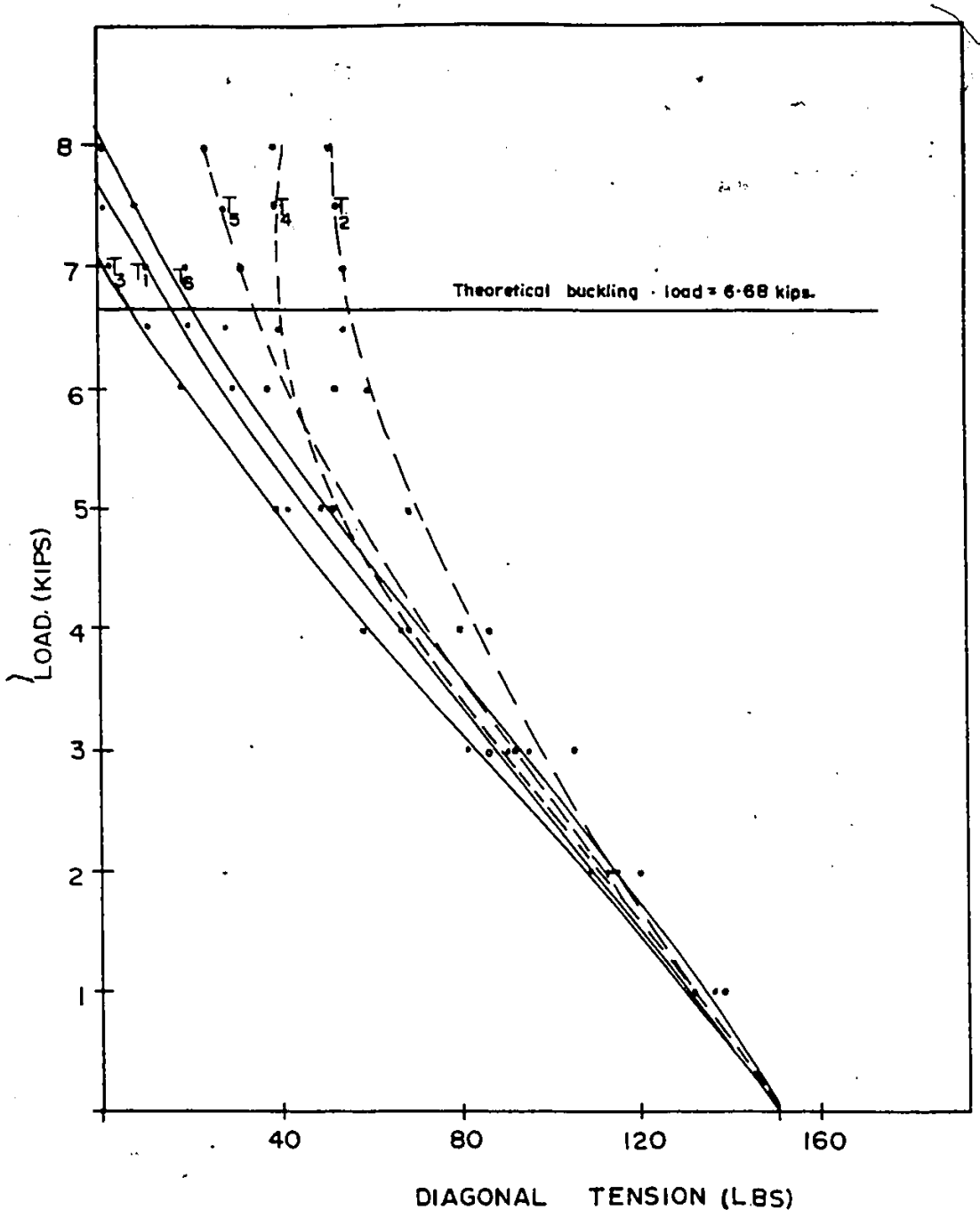

Fig. 8.18 Load Versus Diagonal Tension for an Initial Pretension of 150 lbs.

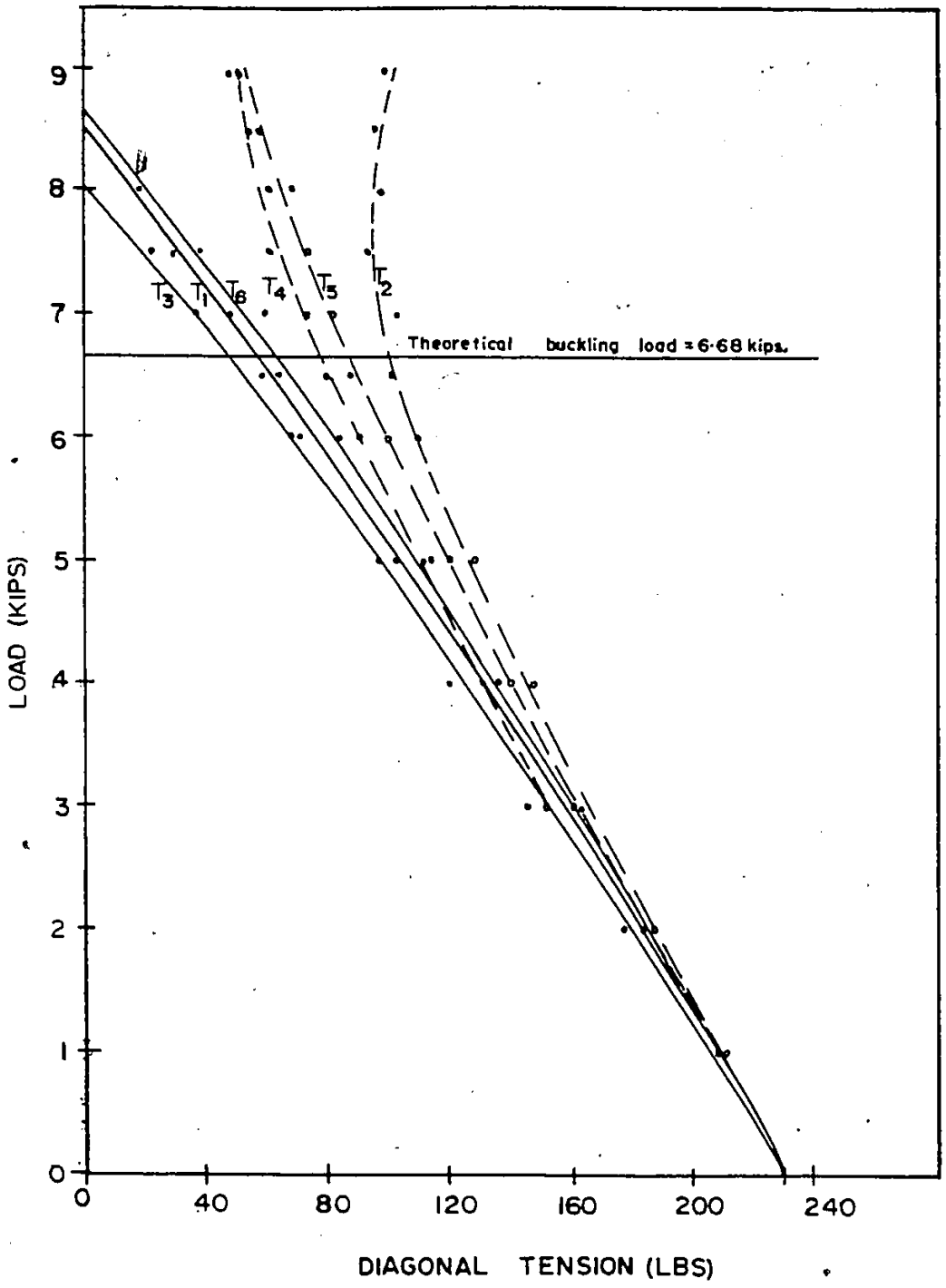

Fig. 8.19 Load Versus Diagonal Tension for an Initial Pretension of 230 lbs.

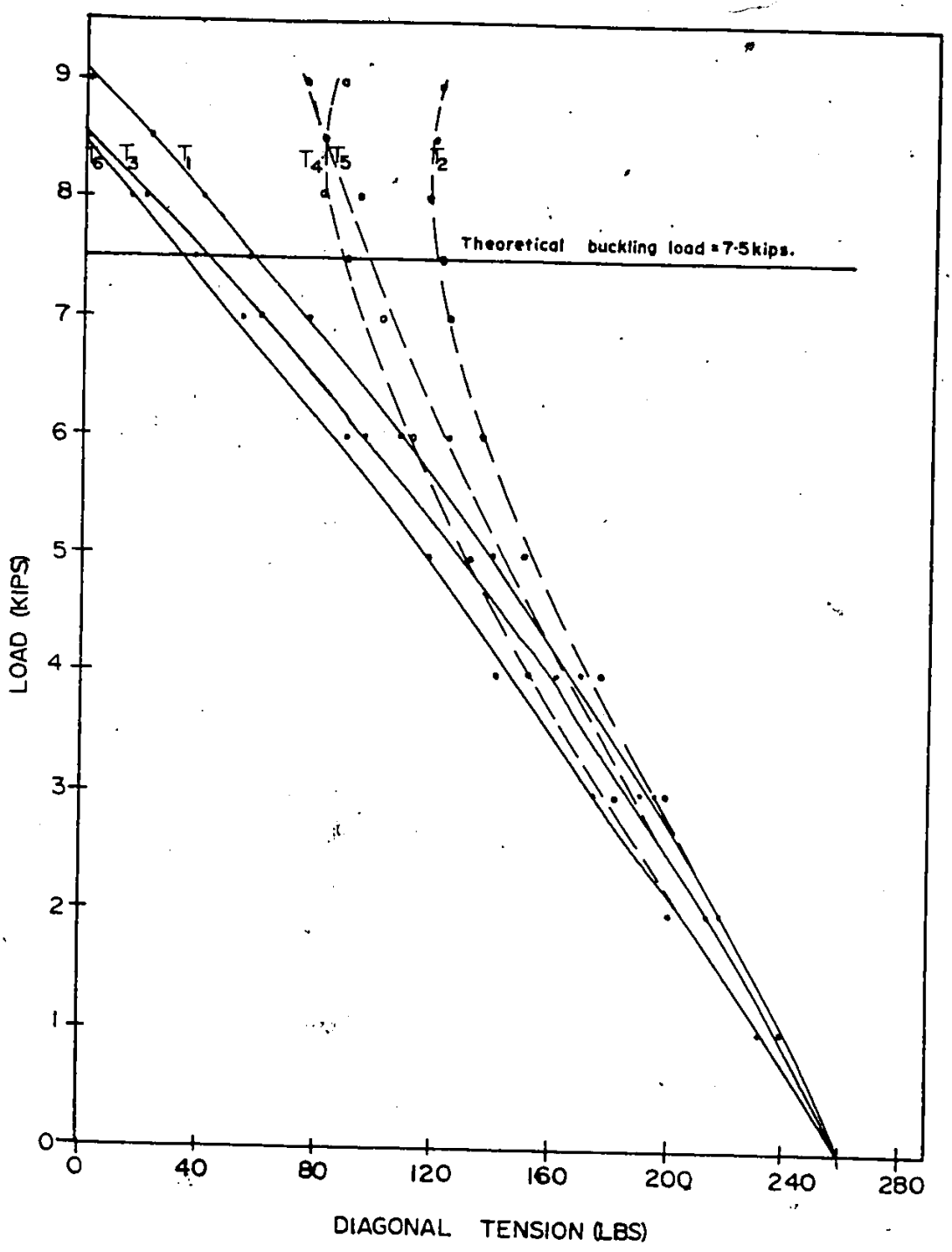

Fig. 8.20 Load Versus Diagonal Tension for an Initial Pretension of 260 lbs.

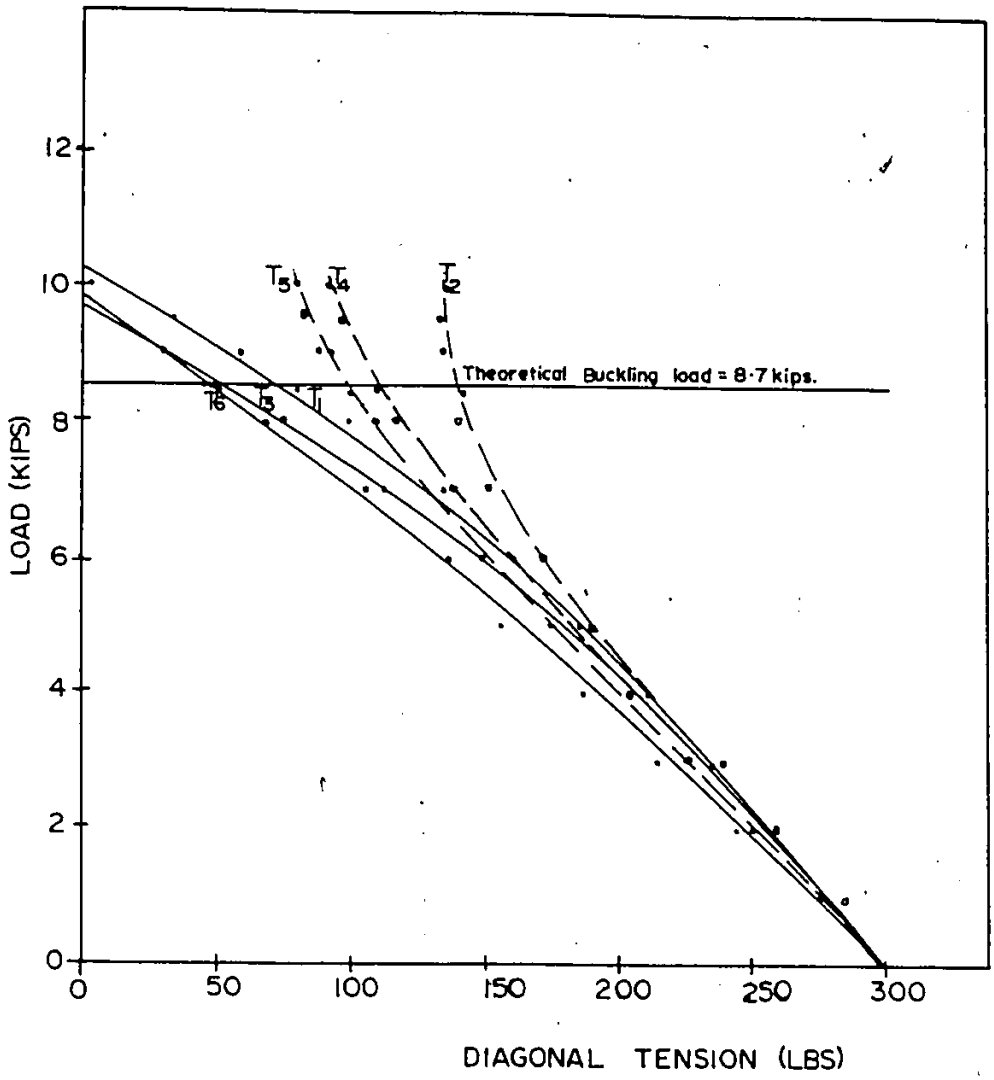

Fig. 8.21 Load Versus Diagonal Tension for an Initial Pretension of 300 lbs.

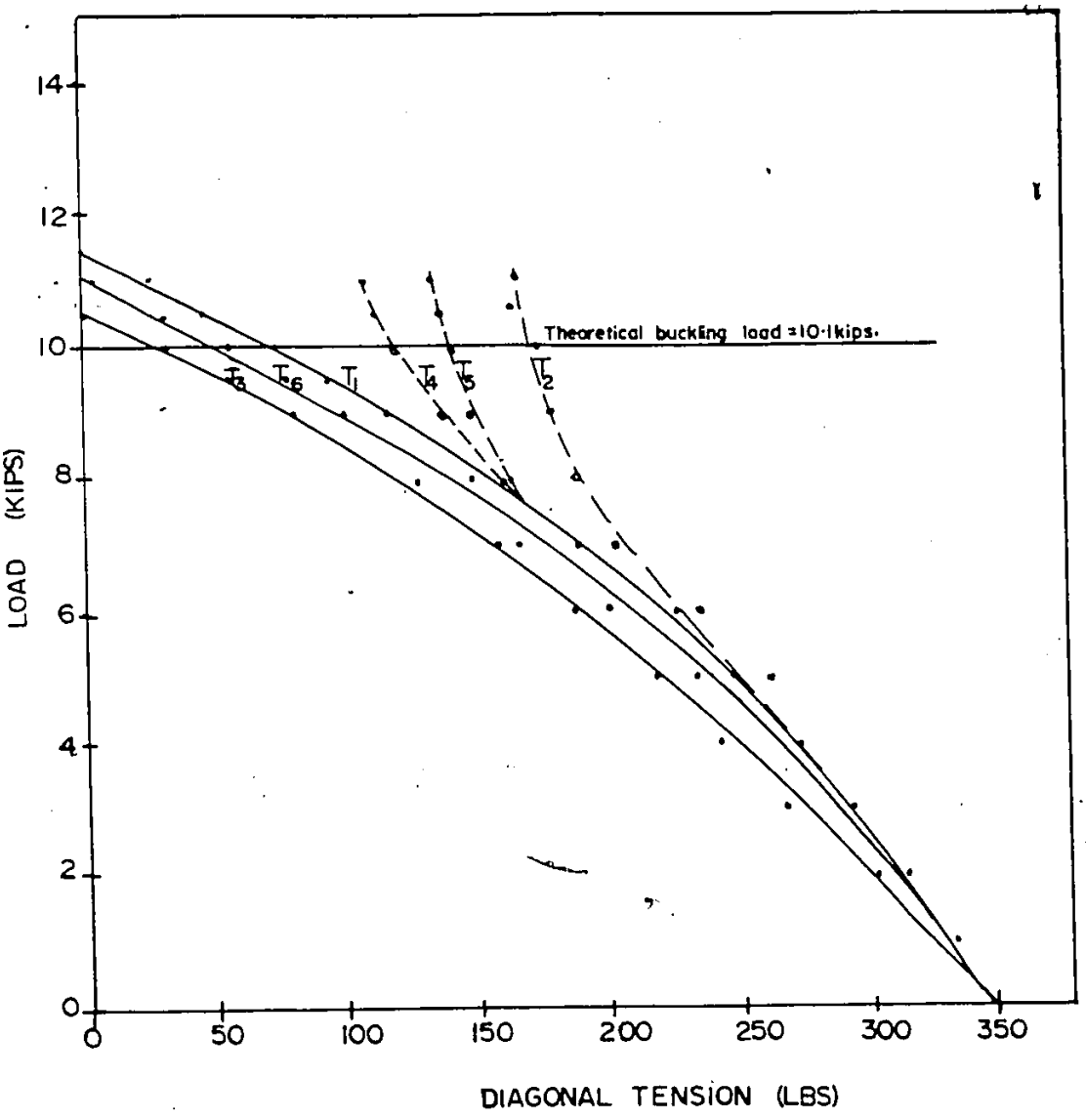

Fig. 8.22 Load Versus Diagonal Tension for an Initial Pretension of 350 lbs.

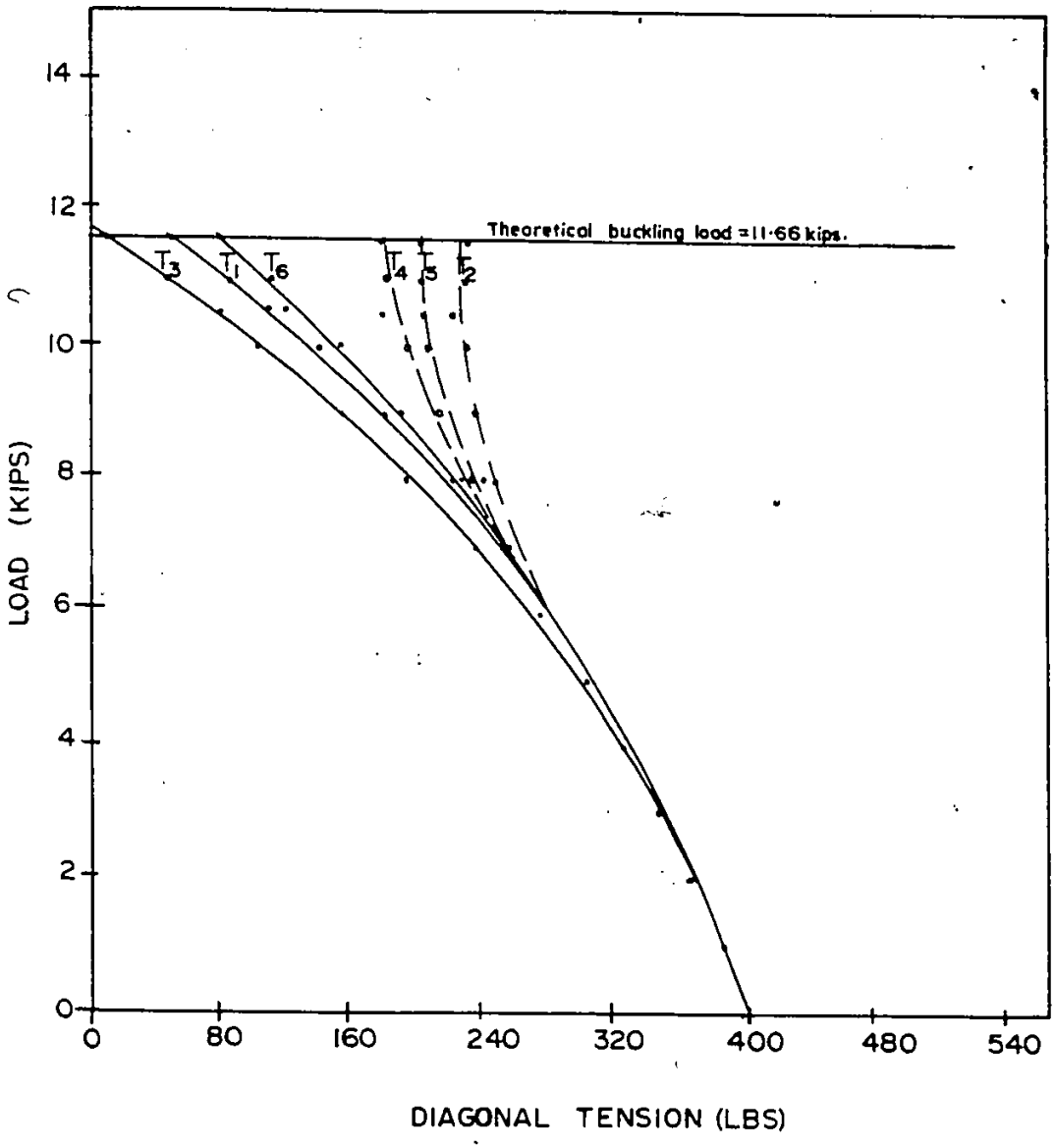

Fig. 8.23 Load Versus Diagonal Tension for an Initial Pretension of 400 lbs.

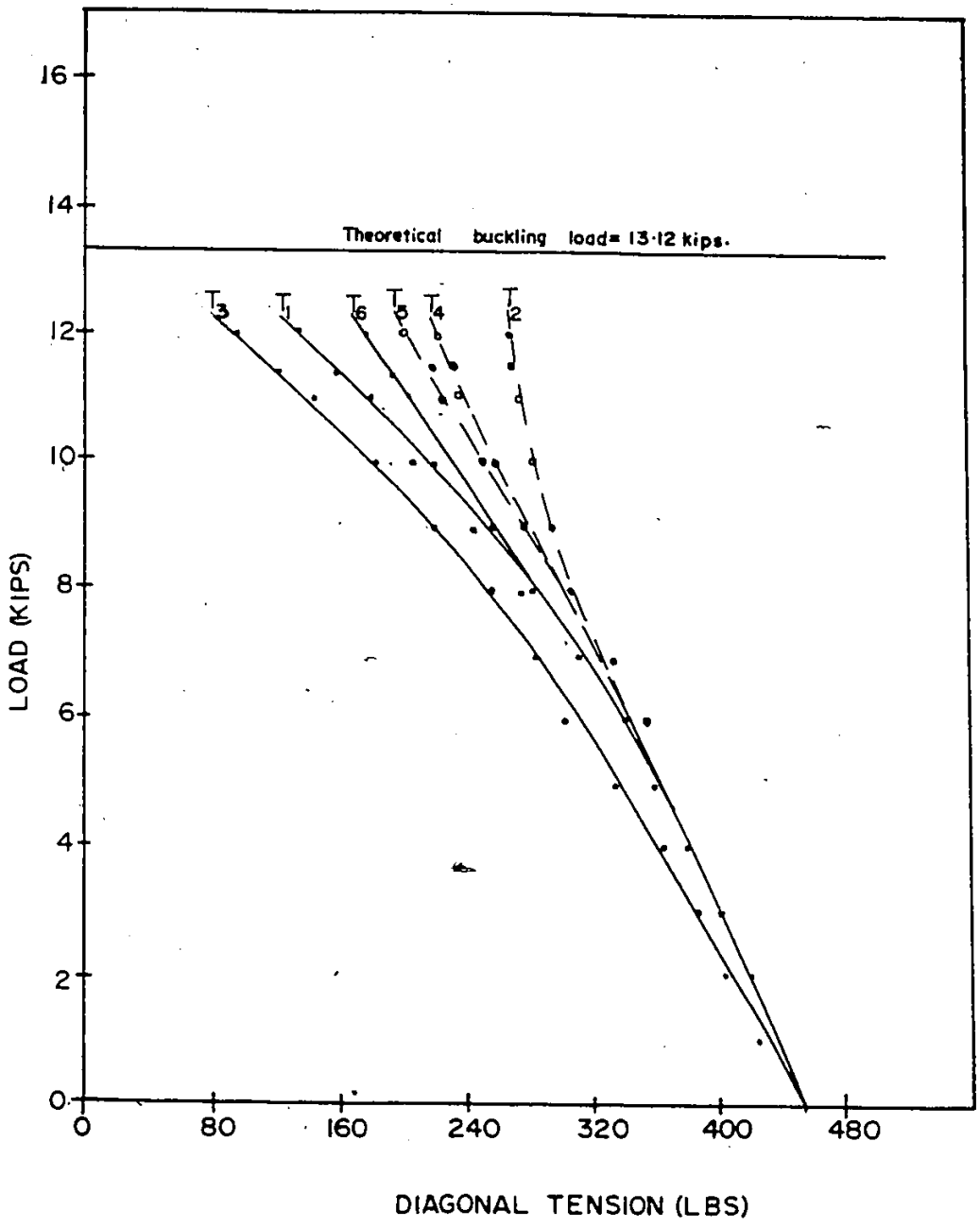

Fig. 8.24 Load Versus Diagonal tension for an Initial Pretension of 450 lbs.

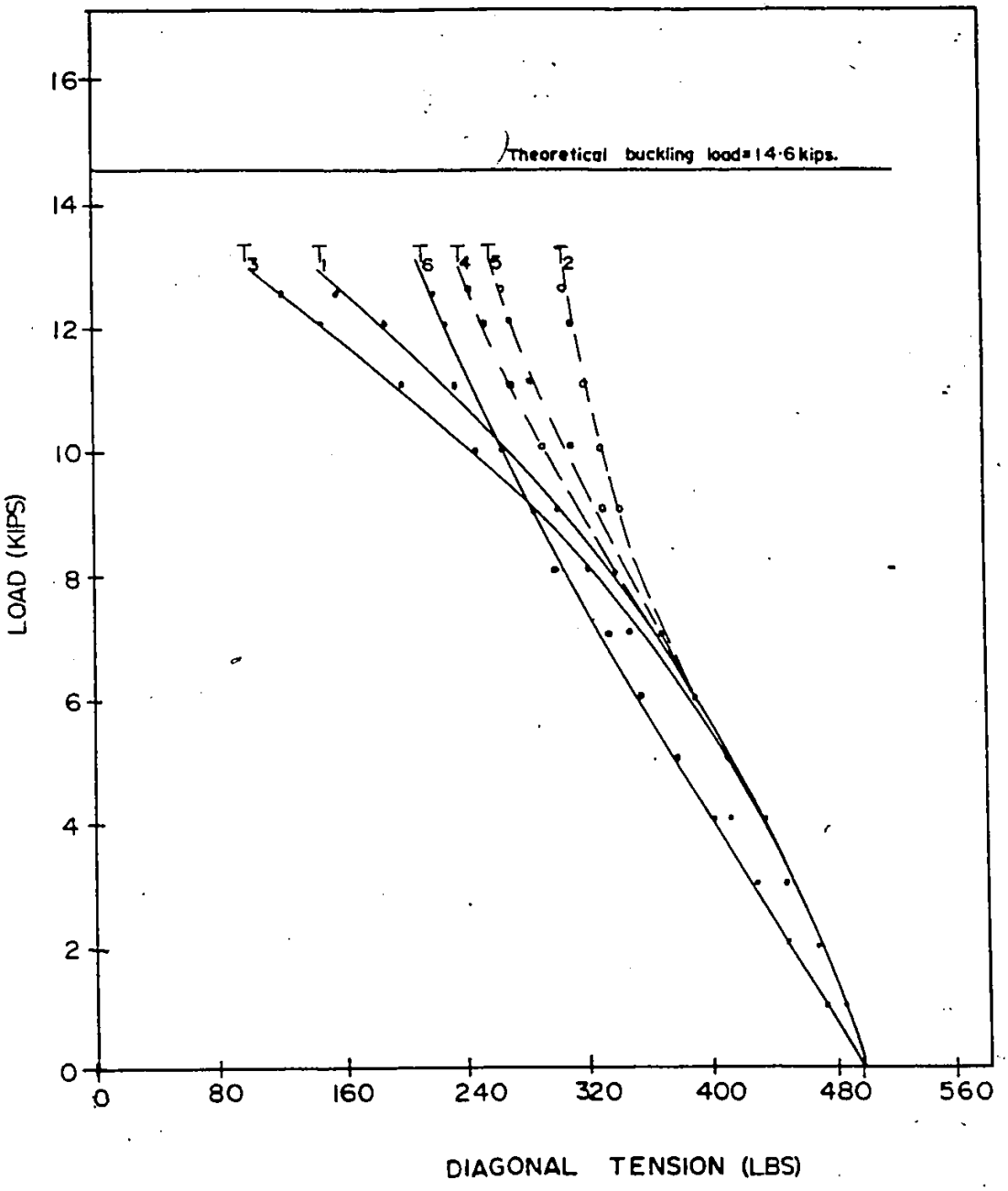

*Fig. 8.25 Load Versus Diagonal Tension for an Initial Pretension of 500 lbs.

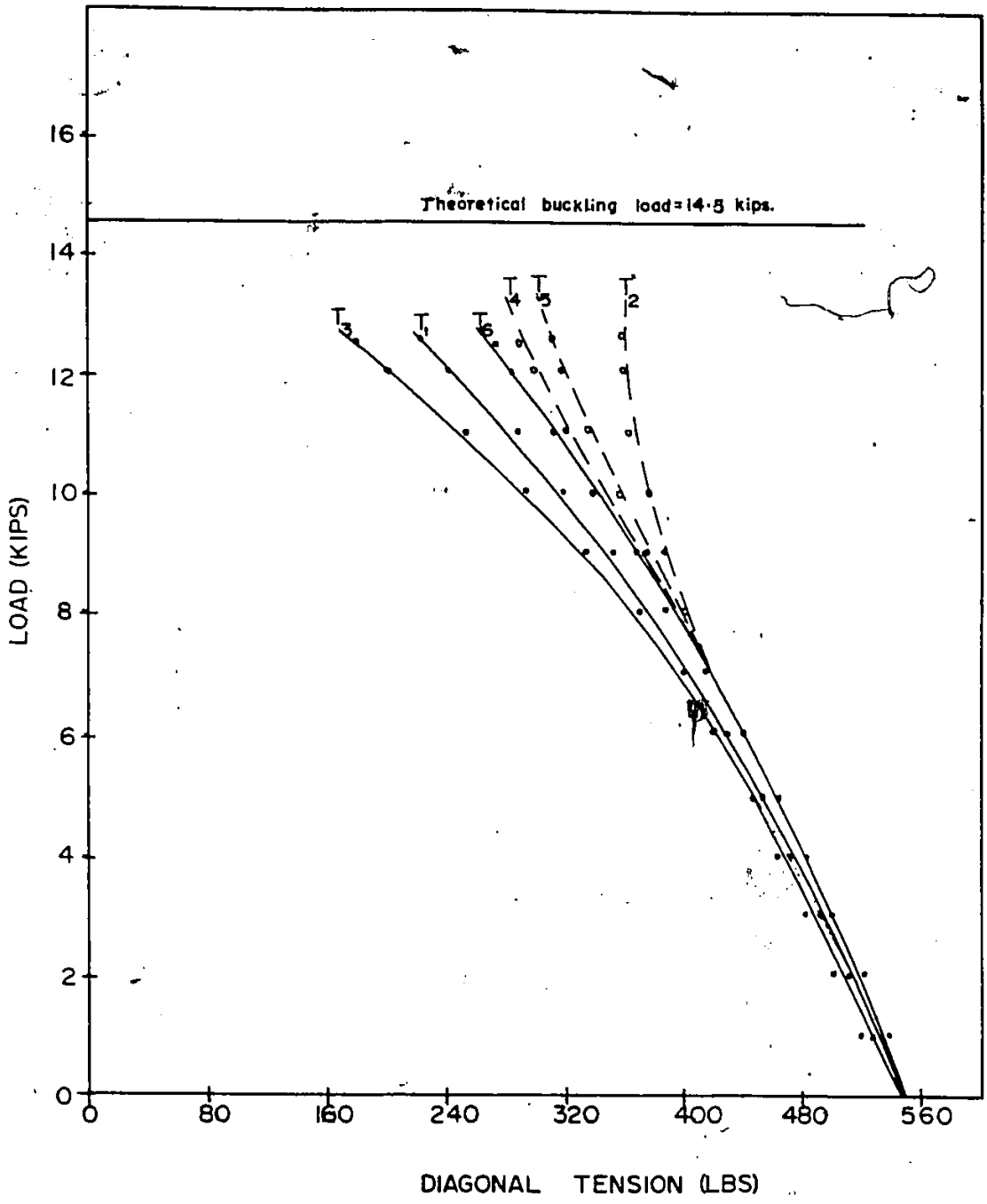

Fig. 8.26 Load Versus Diagonal Tension for an Initial Pretension of 550 lbs.

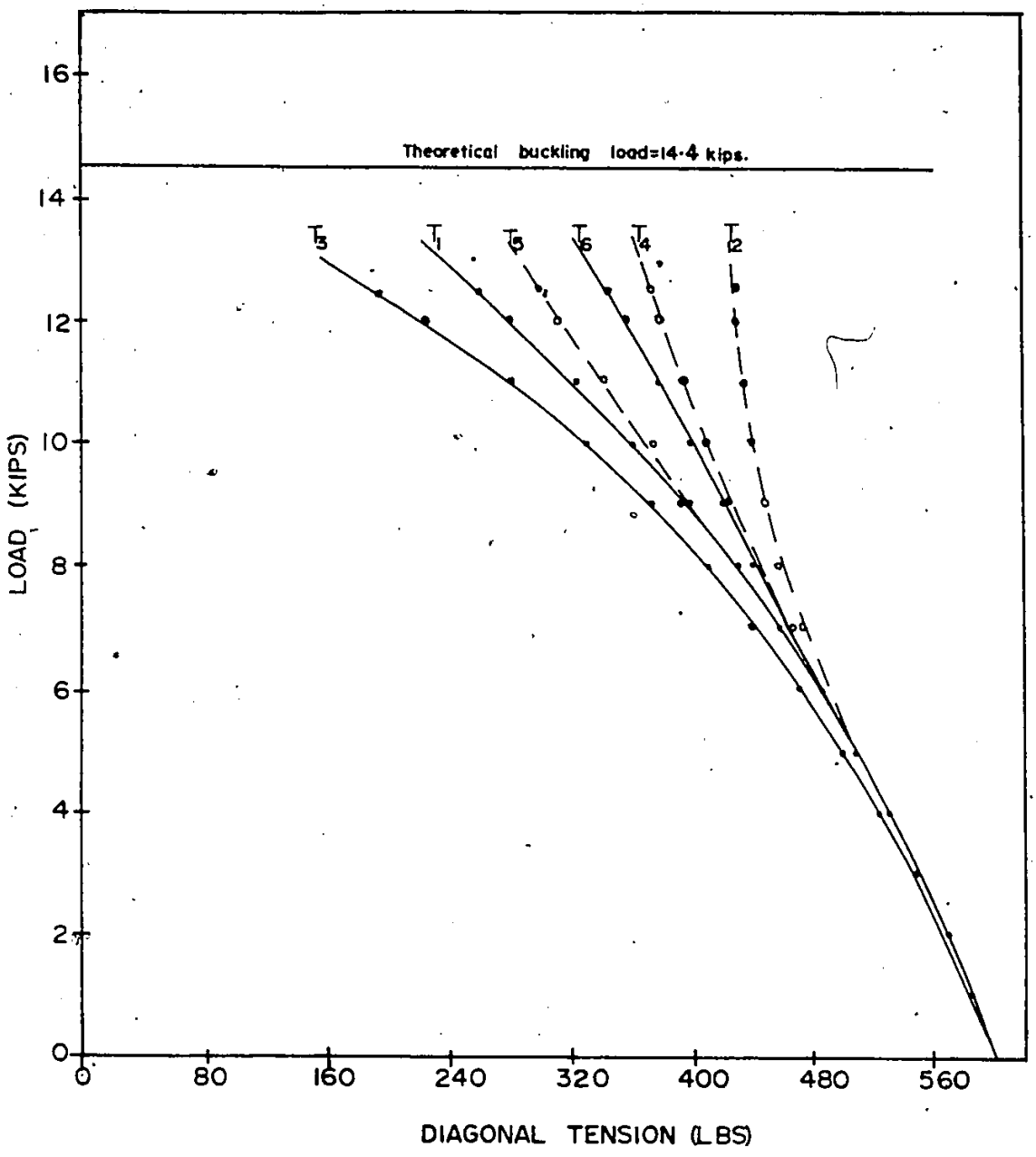

Fig. 8.27 Load Versus Diagonal Tension for an Initial Pretension of 600 lbs.

TABLES

ϕ (in.)	P_{batt} (kips)	P_{latt} (kips)	k_L	W_{batt} (lbs)	W_{latt} (lbs)	Efficiency of battened frame (%)	Efficiency of lattice frame (%)
0.1875	29.623	72.820	0.8269	53.72	55.32	321.26	766.85
0.3125	29.623	72.822	0.8269	53.72	58.17	321.26	729.31
0.5000	29.623	72.819	0.8269	53.72	65.12	321.26	651.51
0.8750	29.623	72.821	0.8269	53.72	88.62	321.26	478.73

Table 5.1

Results for ℓ to ℓ_{ca} Ratio of One

ϕ (in.)	P_{batt} (kips)	P_{latt} (kips)	k_L	W_{batt} (lbs)	W_{latt} (lbs)	Efficiency of battened frame (%)	Efficiency of lattice frame (%)
0.1875	37.037	89.926	0.7441	42.98	44.24	502.08	1184.14
0.3125	37.037	89.925	0.7441	42.98	46.50	502.08	1126.77
0.5000	37.037	89.927	0.7441	42.98	51.99	502.08	1007.79
0.8750	37.037	89.927	0.7441	42.98	70.57	502.08	742.43

Table 5.2

Results for ℓ to ℓ_{ca} Ratio of Two

ϕ (in.)	P_{batt} (kips)	P_{latt} (kips)	k_L	W_{batt} (lbs)	W_{latt} (lbs)	Efficiency of battened frame (%)	Efficiency of lattice frame (%)
0.1875	40.550	103.252	0.6944	39.40	40.59	599.67	1482.00
0.3125	40.550	103.253	0.6944	39.40	42.71	599.67	1408.34
0.5000	40.550	103.254	0.6944	39.40	47.88	599.67	1256.14
0.8750	40.550	103.253	0.6944	39.40	65.41	599.67	919.69

Table 5.3

Results for ℓ to ℓ_{ca} Ratio of Three

ϕ (in.)	P_{batt} (kips)	P_{latt} (kips)	k_L	W_{batt} (lbs)	W_{latt} (lbs)	Efficiency of battened frame (%)	Efficiency of lattice frame (%)
0.1875	42.420	113.937	0.6611	37.60	38.77	657.21	1712.02
0.3125	42.420	113.938	0.6611	37.60	40.85	657.21	1625.00
0.5000	42.420	113.939	0.6611	37.60	45.91	657.21	1445.86
0.8750	42.420	113.939	0.6611	37.60	63.04	657.21	1052.96

Table 5.4

Results for ℓ to ℓ_{ca} Ratio of Four

ϕ (in.)	P_{batt} (kips)	P_{latt} (kips)	k_L	W_{batt} (lbs)	W_{latt} (lbs)	Efficiency of battened frame (%)	Efficiency of lattice frame (%)
0.1875	43.322	93.654	0.7292	36.53	37.69	690.92	1447.82
0.3125	43.322	122.690	0.6371	36.53	39.74	690.92	1798.65
0.5000	43.322	122.689	0.6371	36.53	44.75	690.92	1597.36
0.8750	43.322	122.691	0.6371	36.53	61.70	690.92	1158.56

Table 5.5

Results for ℓ to ℓ_{ca} Ratio of Five

ϕ (in.)	P_{batt} (kips)	P_{latt} (kips)	k_L	W_{batt} (lbs)	W_{latt} (lbs)	Efficiency of battened frame (%)	Efficiency of lattice frame (%)
0.1875	44.110	79.480	0.7915	35.81	36.96	717.55	1252.74
0.3125	44.110	129.967	0.6190	35.81	39.01	717.55	1941.25
0.5000	44.110	129.968	0.6190	35.81	43.98	717.55	1721.54
0.8750	44.110	129.970	0.6190	35.81	60.83	717.55	1244.74

Table 5.6

Results for ℓ to ℓ_{ca} Ratio of Six

APPENDIX

LISTING OF COMPUTER PROGRAM

```
      MAIN                    DATE = 81228        15/51/02

C     M-NUMBER OF MEMBERS
C     N-NUMBER OF NODES
C     NDF-NUMBER OF DEGREES OF FREEDOM
C     NKG-NUMBER OF ELEMENTS WITH GEOMETRIC STIFF MATRIX
C     NDS-NUMBER OF MEMBERS WITH BENDING STIFFNESS
C     PF-FIRST CRITICAL LOAD OF HATT FRAME
C     PS-FIRST CRITICAL LOAD OF LATTICE FRAME
C     NPRC-OUTPUT PRINT CODE
C     LRS-L/LCA START RATIO
C     LRF-L/LCA FINISH RATIO
C     IDI-INNER DIA  VER    MEMBER
C     IDO-OUTER DIA  DIA    MEMBER
C     EBS-YOUNGS MODULUS OF   VER   MEMBER
C     EST-YOUNGS MODULUS OF   DIA   MEMBER
C     NSD-NO  OF   DIA DIA SET
C     NC-NO OF  ELEMENT IN   VER   SEGMENT
C     NSE-NUMBER OF SEGMENTS
C     ------------------------------------------------
      DIMENSION MN(30,2),IVC(30,6),CNO(30,3),DO(30),DI(30),D(30),
     1 MI(30),LGTH(30),DC(30,3),DL1(30),DL1(30),DL2(30),DM2(20),
     1 XL(60),XX(10),X(3600),GLK1(60,60),GLK2(60,90),GLK1V(2*00),
     1 GLK2V(3600),AA(30),TMI(20),TMA(20),GK(6,6),GK(6,6),
     1 PE(15),PET(15),PS(15),PST(15),CNF(10,3),SO(15),
     1 CLF1(15),CLF3(15),WTE(15),WTS(15),
     1 CFFC(15),CFFS(15)
      REAL MK,LGTH,MI
      PI=4.0*ATAN(1.0)
      READ10,M,N,NDF,NKG,NDS,NPRC
   10 FORMAT(6I3)
C     READ MEMBER END NODES
C     ---------------------
      READ15,((MN(I,J),J=1,2),I=1,M)
   15 FORMAT(2I3)
C     READ IVC TABLE
C     --------------
      READ20,((IVC(I,J),J=1,6),I=1,M)
   20 FORMAT(6I3)
C     READ COORDINATES OF NODES
C     -------------------------
C     CO ORDINATES FOR L/LCA=1 ONLY
      READ25,((CNO(I,J),J=1,2),I=1,N)
   25 FORMAT(2F10.0)
      NHP=1
C     -----------------------------
      READ21,LRS,LRF,NSD,NC,NSE
   21 FORMAT(5I3)
C     -----------------------------
      READ22,IDI,IDO,EBS,EST
   22 FORMAT(4F10.0)
      DO16LK=1,NSD
C     -----------------------------
   16 READ17,SO(LK)
   17 FORMAT(F10.0)
      DO1001L=LRS,LRF
      PRINT23,IL
   23 FORMAT(//,T10,'L/LCA=',I3,'=========================
     1 ***************************************************')
      DO300I=1,NSD
      CALL DAT(IL,NE,II,IDI,IDO,EBS,EST,CNO,CLF1,IDI,E,'AA',P,PS,SO)
C     CALCULATE MEMBER PROPERTIES
C     MOMENT OF INERTIA
      DO45I=1,NDS
   45 MI(I)=PI*(DO(I)**4-DI(I)**4)/64.0
      NISS=NDS+1
      DO50I=NDSS,M
   50 MI(I)=0.0
C     AREA,LENGTH,DIRECTION COSINES
      DO55I=1,M
      AA(I)=PI*(DO(I)**2-DI(I)**2)/4.0
      SUM=0.0
      DO60J=1,2
      KS=MN(I,1)
      KF=MN(I,2)
      SUM=SUM+(CNO(KS,J)-CNO(KF,J))**2
   60 CONTINUE
      LGTH(I)=SQRT(SUM)
      DO65J=1,2
```

```
      MAIN                    DATE = 81264          19:53:27
      DC(I,J)=(CN(KE,J)-CN(KS,J))/LGTH(I)
   65 CONTINUE
      DLI(I)=DC(I,1)
      DJI(I)=DC(I,2)
      DI2(I)=-DJI(I)
      DJ2(I)=DLI(I)
   55 CONTINUE
C     ****************************************
C     CALCULATE L/R RATIO
      RESORT(MI(I)/AA(I))
      ELOR=NF*LGTH(1)/R
C     ****************************************
      IF(NNP-1)94,69,94
C     PRINT MEMBER PROPERTIES
   69 PRINT70
   70 FORMAT(T30,'UNITS INCHES AND KIPS',//)
      PRINT75,M
   75 FORMAT(T30,'NUMBER OF MEMBERS',T55,'=',I3,//)
      PRINT80,N
   80 FORMAT(T30,'NUMBER OF NODES',T55,'=',I3,//)
      PRINT85,NDF
   85 FORMAT(T30,'DEGREES OF FREEDOM',T55,'=',I3,//)
      PRINT90,NBS
   90 FORMAT(T10,'NUMBER OF MEMBERS WITH BENDING STIFFNESS'
     1 ,T55,'=',I3,//)
      PRINT91,NKG
   91 FORMAT(T10,'NUMBER OF MEMBERS WITH GIGT AXIAL LOAD'
     1 ,T55,'=',I3,//)
C     ****************************************
   94 PRINT95
   95 FORMAT(//,T10,'MEMBER',T20,'END NODES',T30,'OUTER',
     1 T40,'INNER',T50,'YOUNGS',T60,'AREA',T70,'MOMENT',
     1 T80,'LENGTH')
      PRINT105
  105 FORMAT(T32,'DIA',T42,'DIA',T50,'MODULUS',T68,'OF INERTIA')
      PRINT100
  100 FORMAT(T10,'------',T20,'------',T30,'------',T40,
     1 '-----',T50,'-------',T60,'----',T70,'------',
     1 T80,'-------',/)
      DO110I=1,M
  110 PRINT115,I,MN(I,1),MN(I,2),DO(I),DI(I),E(I),AA(I)
     1 ,MI(I),LGTH(I)
  115 FORMAT(T12,I2,T21,I2,T25,I2,T30,F7.4,T40,F7.4,T50,
     1 F9.1,T60,F7.3,T70,F7.3,T80,F7.2)
C     ****************************************
      IF(NNP-1)128,119,128
  119 PRINT120
  120 FORMAT(//,T10,'MEMBER',T20,'VARIABLE BAND TABLE')
      PRINT125,((I,(IVC(I,J),J=1,6)),I=1,M)
  125 FORMAT(T10,I3,3X,6I3,/)
C     ****************************************
  128 IF(NNP-2)129,129,134
  129 PRINT130
  130 FORMAT(T10,'NODE',T20,'X-COORD',T30,'Y-COORD')
      PRINT135,((I,(CN(I,J),J=1,2)),I=1,N)
  135 FORMAT(T10,I3,T20,F7.2,T30,F7.2,/)
C     ****************************************
C     CRITICAL LOAD OF BATTENED FRAME
  134 MM=NBS
      PRINT136
  136 FORMAT(T20,'BATT FRAME')
      PRINT137
  137 FORMAT(T20,'-----------')
      GOTO 140
C     CRITICAL LOAD OF LATTICE FRAME
  138 MM=4
      PRINT139
  139 FORMAT(T20,'LATTICE FRAME')
      PRINT141
  141 FORMAT(T20,'-----------')
  140 CALL CLKM(MM,MI,AA,E,LGTH,DLI,DJI,DL,DJ,DM,
     1 IVC,BK,SLK1)
      NCC=NKG+1
      CALL CCOKM(MM,NCC,LGTH,DLI,DJI,DL,DJ,DM,IVC,BK,
     1 CLK2)
      CALL ARRAY(2,NDF,NDF,0.0,0.0,SLKIV,SLK1)
      CALL ARRAY(2,NDF,NDF,0.0,0.0,CLKIV,CLK2)
      CALL MRJGT(NDF,CLKIV,SLKIV,XL,X)
```

```
C       CRITICAL LOAD
        PRINT194
  194   FORMAT(2X,120,'CRITICAL LOAD')
        PRINT14,
  195   FORMAT(1X,'----------')
        XX(1)=1./X(1)
        PRINT15,XX(1)
  196   FORMAT(1X,F10.1/)
        IF(NP-1)151,151,152
  151   PC1(1)=XX(1)
        PCT(1)=PC1(1)
        GOTO153
  152   PC1(1)=XX(1)
        PCT(1)=PC1(1)
        GOTO153
C       ***************************************************
  153   IF(NP-1)154,154,170
C       LENGTH VECTORS
  154   PRINT160
  160   FORMAT(1H0,'LENGTH VECTORS')
        PRINT162
  162   FORMAT(1X,'----------')
        DIFF01=1.0E
        I=I+NDF
  170   PRINT17,I,X(I),X(I)
  175   FORMAT(I20,F12.4,E20.4)
  179   PRINT180
  180   FORMAT(//,//)
        IF(I-4)134,175,199
C       MINIMUM AND OPTIMUM WEIGHTS...
  199   NC=NDS+1
        CALPHA=3.*LGTH(1)/LGTH(NC)
        SALPHA=LGTH(NDS)/LGTH(NC)
        CAYC=AA(1)*E(1)/(3.*LGTH(1))
        CAYCA=AA(NDS)*E(NDS)/LGTH(NDS)
        CAYS=AA(NC)*E(NC)/LGTH(NC)
        PRINT200
  200   FORMAT(//,12),'MINIMUM AND OPTIMUM WEIGHTS')
        PRINT205
  205   FORMAT(120,'----------')
        TWI(1)=(PC1(1)*CALPHA)/(CAYC*(1/CAYS)+
     1  (SALPHA**2/CAYCA)+(CALPHA**2/(CAYS)))
        PRINT210,TWI(1)
  210   FORMAT(120,F10.5)
        PRINT212
  212   FORMAT(//,120,'OPTIMUM WEIGHTS')
        PRINT205
        TWA(1)=(PS1(1)*CALPHA)/(CAYC*(1/CAYS)+
     1  (SALPHA**2/CAYCA)+(CALPHA**2/(CAYC)))
        PRINT210,TWA(1)
C       FIND EFFECTIVE LENGTH FACTOR
        ELC=(PI**2)*E(1)*MI(1)/(FSC*LGTH(1)**2)
        SLF1(1)=SQRT(ELC/PS(1))
        SLF2(1)=SQRT(ELC/PC(1))
C       FIND AT WHAT FRAME
        VS=0.0
        DO214JK=1,NDS
        VJC=LGTH(JK)*AA(JK)
        VS=VS+VJC
  214   CONTINUE
        WT(1)=VS*(0.28)
C       FIND AT WHAT LATTICE FRAME
        VS=0.0
        DO215JK=1,1
        VSC=LGTH(JK)*AA(JK)
        VS=VS+VSC
  215   CONTINUE
        WT(1)=VS*(0.28)
        CALCULATE FREQUENCY
        WT1OO2=WT(1)*AA(1)*(1.0)
        PI120=12*(PI**2)*E(1)*MI(1)/((WT1OO2*LGTH(1))**3)
        FF(1)=(PI120*WT(1))*1.0E3/(2*PI)
        FFS(1)=(PI100*ST(1))*1.0E3/(2*PI)
  300   NDP=NDP+C
  305   CONTINUE
        PRINT301,II
  301   FORMAT(//////,T10,'CYCLES',T30,I3,'----------')
        PRINT 302,CLOW
```

```
      MAIN                    DATE = 81292          15/53/32
302   FORMAT(//,T20,'L/B-RATIO=',F7.2)
      PRINT304
304   FORMAT(T20,'--------')
      PRINT305
305   FORMAT(//,T10,'DIASIZE',T30,'PDATT ',T35,'PLATT',T50,'EFFICIENCY',
     1  T65,'TOPTIMUM',3X,'VALUEKDAT',3X,'VALUEKLAT',
     1  3X,'WT(DATT)IDS',3X,'WT(LATT)IDS')
      PRINTJ10
310   FORMAT(T10,'--------',T20,'------',T35,'-----',T50,'---------',
     1  T65,'---------',3X,'-------',3X,'---------',
     1  3X,'----------------',3X'------------')
      DO315 I2=1,NSD
315   PRINT320,SD(I2),PET1(I2),PST1(I2),TNI1(I2),TMA1(I2),ELF3(I2),
     1  ELF1(I2),WTC(I2),WTS(I2)
320   FORMAT(T10,F6.4,T17,F10.3,T30,F10.3,T48,F10.3,T63,F10.3,5X,F6.4,
     1  4X,F6.4,4X,F9.2,4X,F9.2)
      PRINT 325
325   FORMAT(//,T10,'DIA SIZE',T20,'EFF DATT FRAME(%)',T4),
     1  'EFF LATTICE FRAME(%)')
      PRINT 330
330   FORMAT(T10,'--------',T20,'----------------',T30,
     1  '----------------')
      DO 340 I3=1,NSD
340   PRINT 335,SD(I3),EFFE(I3),EFFS(I3)
335   FORMAT(T12,F7.4,T24,F8.2,T44,F8.2)
400   CONTINUE
      STOP
      END
```

```
      ELKM                    DATE = 81232          15/53/32

      SUBROUTINE ELKM(M,MI,AA,E,LGTH,DL1,DM1,DL2,DM2,NDF,
     1 IVC,EK,MK)
      DIMENSION AA(30),E(30),LGTH(30),DL1(30),DM1(30),
     1 DL2(30),DM2(30),IVC(30,6),EK(6,6),MK(60,60),MI(30)
      REAL MK,LGTH,MI
      DO15I=1,NDF
      DO10J=1,NDF
      MK(I,J)=0.0
   10 CONTINUE
   15 CONTINUE
      DO20K=1,M
      EK(1,1)=(DL1(K)**2)*(AA(K)*E(K))/LGTH(K)
     1 +(DL2(K)**2)*(12*E(K)*MI(K))/(LGTH(K)**3)
      EK(1,2)=DL1(K)*DM1(K)*(AA(K)*E(K)/LGTH(K))
     1 +DL2(K)*DM2(K)*(12*E(K)*MI(K))/LGTH(K)**3
      EK(2,2)=(DM1(K)**2)*(AA(K)*E(K)/LGTH(K))
     1 +(DM2(K)**2)*(12*E(K)*MI(K))/(LGTH(K)**3)
      EK(1,3)=DL2(K)*6*E(K)*MI(K)/LGTH(K)**2
      EK(2,3)=DM2(K)*6*E(K)*MI(K)/LGTH(K)**2
      EK(3,3)=4*E(K)*MI(K)/LGTH(K)
      EK(1,4)=-EK(1,1)
      EK(2,4)=-EK(1,2)
      EK(3,4)=-EK(1,3)
      EK(4,4)=EK(1,1)
      EK(1,5)=-EK(1,2)
      EK(2,5)=-EK(2,2)
      EK(3,5)=-EK(2,3)
      EK(4,5)=EK(1,2)
      EK(5,5)=EK(2,2)
      EK(1,6)=EK(1,3)
      EK(2,6)=EK(2,3)
      EK(3,6)=EK(3,3)/2
      EK(4,6)=-EK(1,3)
      EK(5,6)=-EK(2,3)
      EK(6,6)=EK(3,3)
      DO25I=1,6
      DO30J=1,6
   30 EK(J,I)=EK(I,J)
   25 CONTINUE
      DO35I=1,6
      DO40J=1,6
      IL=IVC(K,I)
      IN=IVC(K,J)
      IF(IN*IL.EQ.0)GOTO40
      ILI=IABS(IL)
      INI=IABS(IN)
      JJ=ILI/IL
      KK=INI/IN
      MK(ILI,INI)=MK(ILI,INI)+JJ*KK*EK(I,J)
   40 CONTINUE
   35 CONTINUE
   20 CONTINUE
      RETURN
      END
```

```
      GEOKM          DATE = 81292          15/53/
      SUBROUTINE GEOKM(M,NCC,LGTH,DL1,DM1,DL2,DM2,NDF,
     1  IVC,GK,MK)
      DIMENSION LGTH(30),DL1(30),DM1(30),IVC(30,4),
     1  GK(6,6),MK(60,60),DL2(30),DM2(30)
      REAL MK,LGTH
      DO10I=1,NDF
      DO15J=1,NDF
      MK(I,J)=0.0
   15 CONTINUE
   10 CONTINUE
      DO20K=1,M
      IF(K.GE.NCC)GOTO35
      GK(1,1)=(DL2(K)**2)*6/(5*LGTH(K))
      GK(2,1)=DL2(K)*DM2(K)*6./(5.*LGTH(K))
      GK(2,2)=(DM2(K)**2)*6/(5*LGTH(K))
      GK(3,1)=DL2(K)/10.
      GK(3,2)=DM2(K)/10
      GK(3,3)=2*LGTH(K)/15
      GK(4,1)=-GK(1,1)
      GK(4,2)=-GK(2,1)
      GK(4,3)=-GK(3,1)
      GK(4,4)=GK(1,1)
      GK(5,1)=-GK(2,1)
      GK(5,2)=-GK(2,2)
      GK(5,3)=-GK(3,2)
      GK(5,4)=GK(2,1)
      GK(5,5)=GK(2,2)
      GK(6,1)=GK(3,1)
      GK(6,2)=GK(3,2)
      GK(6,3)=-GK(3,3)/4.
      GK(6,4)=-GK(3,1)
      GK(6,5)=-GK(3,2)
      GK(6,6)=GK(3,3)
      DO25I=1,6
      DO30J=1,6
   30 GK(I,J)=GK(J,I)
   25 CONTINUE
      GOTO50
   35 DO40I=1,6
      DO45J=1,6
   45 GK(I,J)=0
   40 CONTINUE
   50 DO55I=1,6
      DO60J=1,6
      IL=IVC(K,I)
      IN=IVC(K,J)
      IF(IL*IN.EQ.0)GOTO60
      IL1=IABS(IL)
      IN1=IABS(IN)
      JJ=IL1/IL
      KK=IN1/IN
      MK(IL1,IN1)=MK(IL1,IN1)+JJ*KK*GK(I,J)
   60 CONTINUE
   55 CONTINUE
   20 CONTINUE
      RETURN
      END
```

```
      DAF                    DATE = 81298          15/14/32

      SUBROUTINE DAF(IL,NE,II,DDI,DDC,EPS,EST,CN0,CN,DD,DI,E,M,IC,NN
     1  ,NDS,SD)
      DIMENSION CN0(30,3),CN(30,3),DD(30),DI(30),E(30),SD(15)
      N1=NE+1
      LLCA=CN0(N1,2)/CN0(N,1)
      IF(LLCA.EQ.IL) GOTO20
      NL=N/2
      NLE=NL+1
      DO5J=1,NL
      DO10K=1,2
      CN(J,K)=CN0(J,K)
10    CONTINUE
 5    CONTINUE
      DO15JJ=NLE,N
      CN(JJ,2)=CN0(JJ,2)
      CN(JJ,1)=CN0(JJ,1)/IL
15    CONTINUE
      GOTO30
20    DO25JK=1,N
      CN(JK,1)=CN0(JK,1)
      CN(JK,2)=CN0(JK,2)
25    CONTINUE
30    DO35JJ=1,NDS
      DD(JJ)=DDC
      DI(JJ)=DDI
      E(JJ)=EPS
35    CONTINUE
      NS=NDS+1
      DO40KK=NS,M
      DD(KK)=SD(II)
      DI(KK)=0.0
      E(KK)=EST
40    CONTINUE
      RETURN
      END
```

BIBLIOGRAPHY

1. Chu, K.H., and Berge, S.S., "Analysis and Design of Struts with Tension Ties", Journal of the Structural Division, ASCE, Vol. 89, No. ST1, Proc. Paper 3414, Feb., 1963, pp. 127-163.

2. Clarke, J.C., "The behaviour of a Single Stayed Column", Thesis presented to Queen's University, Belfast, Ireland in partial fulfillment of the requirements for the honour degree in Civil Engg. 1972.

3. Ellis, J.S., "The R.M.C. Design-Build-Test Projects", Engineering Education, ASEE, Vol. 62, No. 3, Dec. 1971, pp. 294-296.

4. Ellis, J.S., "Prestressed lattice Beam-Columns with Offset Diagonals", Canadian Journal of Civil Engineering, Vol. 7, No. 4, December 1980, pp. 573-587.

5. Hafez, H.H., "Pretensioning of Single-Crossarm Stayed Columns", Thesis presented to the University of Windsor, Windsor, Ontario, Canada, in partial fulfillment of the requirements for the degree of Master of Applied Science, 1977.

6. Hathout, I.A., "Stability Analysis of Space Stayed Columns by the Finite Element Method", Thesis presented to the University of Windsor, Windsor, Ontario, Canada in partial fulfillment of the requirements for the degree of Master of Applied Science, 1977.

7. Khosla, C.M., "Buckling Loads of Stayed Columns Using the Finite Element Method", Thesis presented to the University of Windsor, Windsor, Ontario, Canada, in partial fulfillment of the requirements for the degree of Master of Applied Science, 1975.

8. Mauck, H.R., and Felton, L.P., "Optimum Design of Columns Supported by Tension Ties", Journal of Structural Division, ASCE, Vol. 93, No. ST3, Proc. Paper 5281, June, 1967, pp. 210-220.

9. Pearson, K.M., "The Behavior of a Stayed Column with Varying Stay Tesnion and Cross Member Length", Thesis presented to the Royal Military College of Canada, Kingston, Ontario, Canada in partial fulfillment of the requirements for the degree of Bachelor of Engineering, 1971.

10. Smith, R.J., McCaffrey, G.T., and Ellis, J.S., "Buckling of a Single-Crossarm Stayed Column", Journal of the Structural Division, ASCE, Vol. 101, No. ST1, Proc. Paper 11071, Jan., 1975, pp. 249-268.

11. System/360 Scientific Subroutine Package, H20-205-3, Version III Programmer's Manual", IBM, Armonk, N.Y.

12. Temple. M.C., "Buckling of Stayed Columns", Journal of the Structural Division, ASCE, Vol. 103, No. ST4, Proc. Paper 12894, April, 1977, pp. 839-851.

13. Timoshenko, S.P., Gere, J.M., Theory of Elastic Stability, Second Edition, McGraw-Hill Book Company Inc., N.Y., 1961, pp. 62-64.

14. Williams, F.W., and Howson, W.P., "Concise Buckling Analysis of Stayed Columns", Int. J. Mech. Sci., Vol. 20, 1978, pp. 299-313.

15. Wong, K.C., "Single-Crossarm Stayed Column with Initial Imperfection", Thesis presented to the University of Windsor, Windsor, Ontario, Canada, in partial fulfillment of the requirements for the degree of Master of Applied Science, 1980.

VITA AUCTORIS

ARUNACHALAM MOHAN

The author was born on May 14, 1956 in Cuddalore, India. In 1965 he completed his primary school education at K.A.P. Viswanathan Primary School, Trichy and in 1971 he has completed his Highschool education at St. Joseph's High School, Trichy, India. Afterwards, he finished one year of study in pre-university course at St. Joseph's College, Trichy. Then he joined at the faculty of Civil Engineering, Regional Engineering College, Trichy. In September 1977 he received his B.E. degree with first class, from the University of Madras. By 1977 he joined at P.S.G. College of Technology, Coimbatore, India and received his M.E. degree in Structural Engineering in 1979.

In 1979 he joined the Civil Engineering Department at the University of Windsor as a teaching and research assistant. The author prepared his thesis in partial fulfillment of the requirements for the degree of Master of Applied Science at that University.

VITA AUCTORIS

ARUNACHALAM MOHAN

The author was born on May 14, 1956 in Cuddalore, India. In 1965 he completed his primary school education at K.A.P. Viswanathan Primary School, Trichy and in 1971 he has completed his Highschool education at St. Joseph's High School, Trichy, India. Afterwards, he finished one year of study in pre-university course at St. Joseph's College, Trichy. Then he joined at the faculty of Civil Engineering, Regional Engineering College, Trichy. In September 1977 he received his B.E. degree with first class, from the University of Madras. By 1977 he joined at P.S.G. College of Technology, Coimbatore, India and received his M.E. degree in Structural Engineering in 1979.

In 1979 he joined the Civil Engineering Department at the University of Windsor as a teaching and research assistant. The author prepared his thesis in partial fulfillment of the requirements for the degree of Master of Applied Science at that University.